Prefabricated Tensile Façade Design and Prototyping

Graduation Report – Sander Bentvelsen – 4851579

Abstract

This research investigates an innovative tensile-based prefabricated façade panel, with the aim of delivering a stiff, lightweight, thermally broken, and highly reconfigurable system within a thin profile. The proposed concept is evaluated through dynamic relaxation simulations, finite element analysis (FEA), and physical prototyping to reveal its structural behaviour and design characteristics.

Beyond assessing the initial concept, the study also explores and analyses alternative configurations, comparing them to conventional light gauge steel framing (LGSF) systems. Expert interviews were conducted to evaluate the façade's feasibility, practical implications, and potential future applications based on industry insights.

The findings indicate that the tensile-based façade panel is unlikely to outperform or compete with established solutions in typical residential or office applications. Key limitations include insufficient stiffness, manufacturing and installation complexity, and higher maintenance requirements.

The research concludes by recommending further exploration into alternative applications that are complimentary to the panels structural characteristics, including integration with ETFE or other membrane-based panels, lightweight overcladding systems, closed cavity façades (CCF), and tent-like all-in-one modular structures.

Key words

Prefabrication – Tensile façade system – Pretensioning – Lightweight construction – Modular design – Out-of-plane stiffness

Acknowledgements

I would like to express my gratitude to everyone who helped me throughout the course of this graduation project.

In particular, I would like to thank my mentors, Dr. A. (Alessandra) Luna Navarro and Prof.dr. M. (Mauro) Overend for their guidance, feedback, and encouragement throughout the process.

I would also like to thank my external advisor, Jacopo Montali, for sharing their expertise during many feedback sessions throughout the process, coming up with the initial ideation of the system and offering practical perspectives that supported the development and evaluation of the system.

Also, I would like to thank Fred Veer with his assistance in calibrating the load cells, as without him the measurements would've been considerately less accurate.

Finally, I am grateful to my friends, family, and colleagues for their ongoing support and motivation during this process.

Contents

1. Introduction

Facades are among the most critical elements of a building, serving as the interface between internal and external environments. Beyond their aesthetic appearance, facades must address a multitude of design criteria (Figure 1). As global temperatures continue to rise, natural resources grow increasingly scarce, and societal expectations for comfort remain high, meeting these design criteria is becoming progressively more complex.

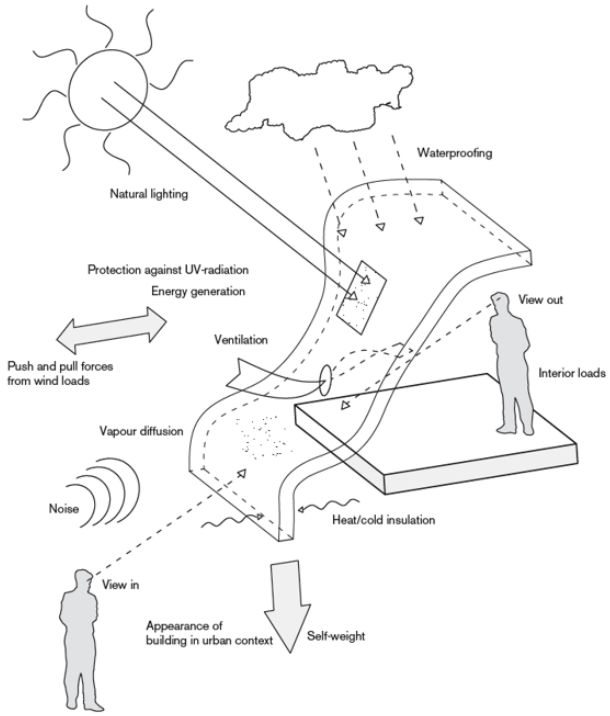

Figure 1: Facade design criteria (Knaack, 2007).

In recent decades, the development of prefabrication has brought significant innovations to facade design and construction. Prefabricated facades are manufactured off-site in controlled environments, ensuring consistency and precision while remaining unaffected by weather or on-site constraints. Additional benefits include faster installation, reduced costs, better cost estimates, greater scalability, and enhanced sustainability through optimized resource use. Furthermore, prefabricated facades can alleviate challenges posed by site constraints, such as limited urban space or difficult site access. As these advantages align with the increasing complexity and performance demands of modern buildings, prefabrication has become a cornerstone of contemporary facade design (Rammig et al., 2023; Sah et al., 2024).

However, even prefabricated facade systems have their limits. These constraints underscore the need for innovative solutions that can address these gaps and meet the growing challenges of modern construction. Such solutions should enable more sustainable designs, provide architects with greater design freedom, help investors achieve their targets, and ensure users can enjoy comfortable living environments.

1.1 Introduction to the tensile-based facade concept

This thesis introduces such an innovative solution, a tensile-based facade concept, that addresses some limitations of conventional facade systems. It explores the structural performance and potential application of such a system and assesses its competitiveness within the context of modern prefabricated construction.

The proposed invention aims to overcome the typical trade-off between structural rigidity and lightweight design by enabling the fabrication of facade elements that are both lightweight and stiff (Montali, 2021).

At the core of this system is a configuration comprising three main components: an inner frame, which may for instance include an opening for windows; an outer frame, which defines the unit's perimeter and interfaces with the primary building structure; and a set of four tensioned cables that connect the two frames (Figure 2).

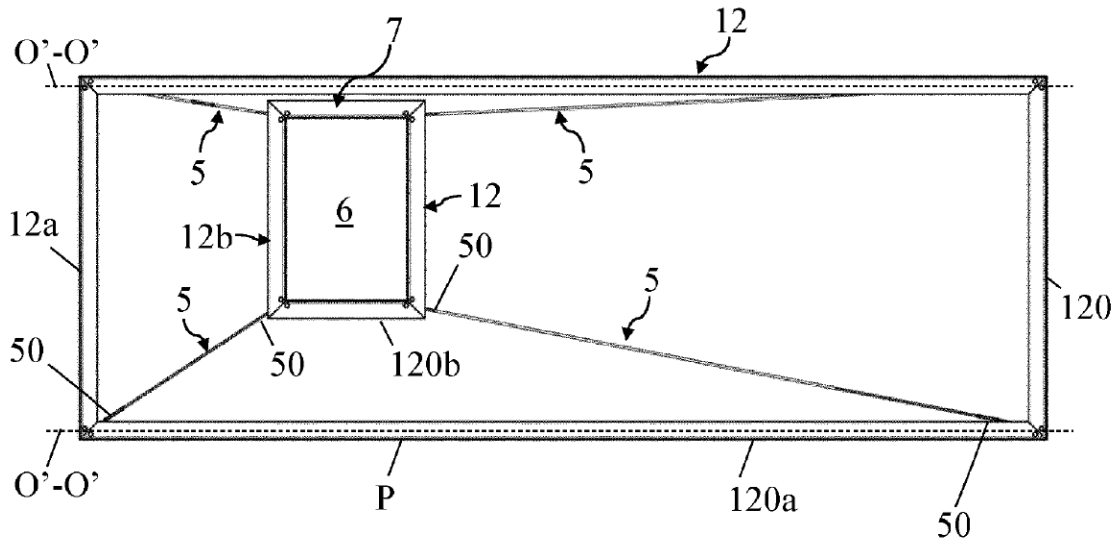

Figure 2: Tensile based facade panel (Montali, 2021)

These cables transform the assembly into a tensile structure, where stiffness can be dynamically adjusted by modifying the tensioning force, thus avoiding the need for potentially heavy stiffening elements.

Moreover, the system integrates thermal insulation between the frame layers, improving energy performance without compromising structural integrity in a thin package (Figure 3). Collectively, the system aims to advance the field of facade engineering by offering an adaptable, efficient, and thermally optimized prefabricated facade solution.

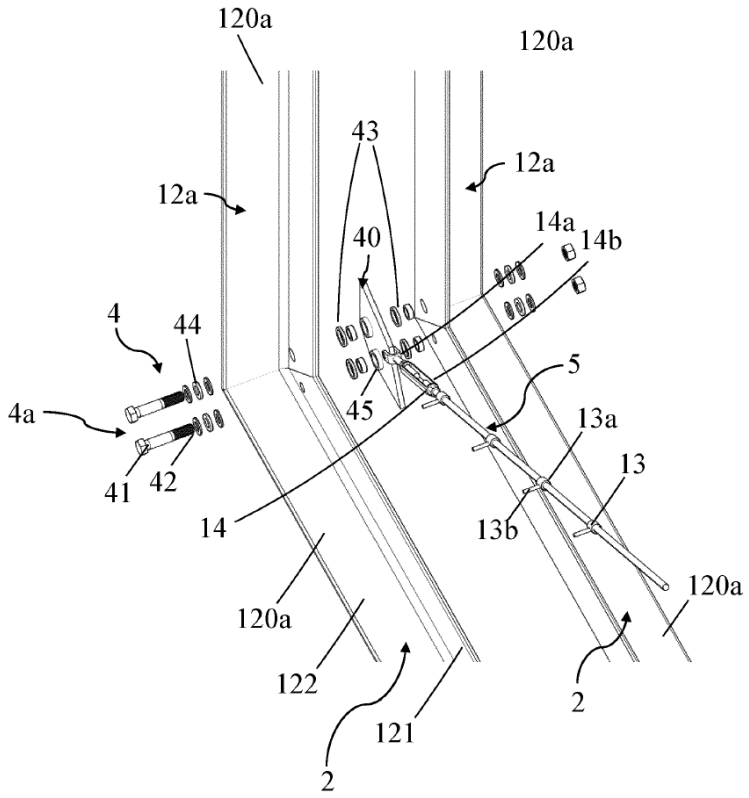

Figure 3: Corner detail of the tensile based facade system (Montali, 2021)

1.2 Research aim and scope

The aim of this research is to evaluate the structural behaviour of the proposed system and assess its feasibility as a prefabricated façade panel.

It expands to address the central research question: *How can the principle of a tensile based system be utilized to create a more effective prefabricated facade solution?*

Based on the insights gained, potential configurations of tensile-based façade panels are developed and assessed, with the objective of evaluating their performance and application range.

2. Background and Theoretical framework

2.1 Structural Engineering Principles

To understand the structural behaviour of a tensile-based system, it is important to first explore several relevant structural theories and principles. These concepts apply both to specific components of the panel and to the system as a whole. The following chapter provides the necessary contextual knowledge to support the interpretation of the models and simulations presented later.

2.1.1 Equilibrium and Stability

In structural engineering, equilibrium refers to the condition in which all forces and moments acting on a structure are perfectly balanced. For a structure to be in equilibrium, the sum of forces in all directions ($\sum F_{x,y,z} = 0$) and the sum of all moments ($\sum M = 0$) must equal zero. This ensures that the structure, or any part of it, is neither accelerating nor rotating under applied loads. Equilibrium is a fundamental requirement for structural analysis and forms the basis for solving internal forces and reactions in both simple and complex systems.

While equilibrium ensures that forces and moments are balanced, it does not guarantee that a structure will remain safe or functional when subjected to real-world conditions. This is where stability comes into play. A structure may be in equilibrium but still unstable, meaning that small disturbances, such as slight geometric imperfections or changes in loading, can lead to large, uncontrolled displacements or failure. A helpful analogy is that of a ball resting on a surface: a ball in a bowl (stable equilibrium) returns to its original position when disturbed, while a ball balanced on top of a hill (unstable equilibrium) may be in equilibrium, but any small disturbance causes it to roll away (Figure 4).

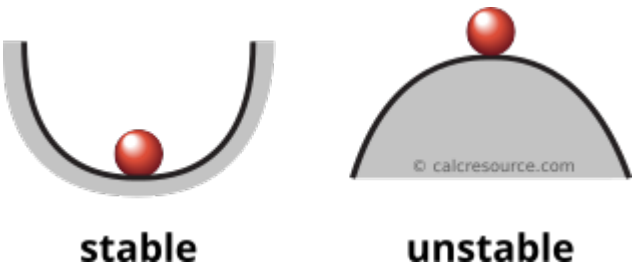

Figure 4: Ball on a hill analogy (Dr. Minas E. Lemonis, 2024)

In essence, equilibrium ensures a structure is at rest, while stability ensures it remains at rest in the face of disturbances.

2.1.2 Static and Kinematic (in)Determinate Structures

Building on the concepts of equilibrium and stability, structures can be further classified based on their static and kinematic determinacy. A statically determinate structure is one in which all support reactions and internal forces can be found using only the equations of static equilibrium.

In contrast, statically indeterminate structures have more unknown forces than the number of available equilibrium equations. Solving these requires additional relationships based on material behaviour and deformation compatibility, methods such as the force method, displacement method, or modern computational techniques like finite element analysis are typically employed (*Intro to Nonlinear Solver — Lesson 2*; Obinna, 2024).

Separately, a structure is kinematically determinate if it is sufficiently constrained to prevent motion under load; if not, it is kinematically indeterminate (unstable) and may deform without resistance.

2.1.3 System (non)Linearity

Structural systems can behave in either a linear or nonlinear manner, depending on the magnitude of deformations and the material response under loading. Tensile structures often exhibit nonlinear behaviour due to large displacements and the changing geometry of their load paths. Understanding the distinction between linear and nonlinear analysis is essential when evaluating the performance of such systems, as it directly affects the accuracy of internal force predictions and deformation behaviour. The subsections below outline the key concepts involved.

First-Order Theory (Linear Elastic Analysis)

This approach assumes small deformations that do not significantly alter the structure's geometry. Material behaviour is considered linear elastic, meaning stress is directly proportional to strain. Equilibrium equations are based on the original, undeformed configuration, simplifying calculations.

Second-Order Theory (Geometric Nonlinearity)

Second-order analysis accounts for deformations that modify the structure's geometry, affecting internal forces and overall stability. By considering equilibrium in the deformed state, this method captures effects such as global and local deformations. This approach is particularly relevant for slender or flexible structures where deformations significantly influence internal forces and moments.

Material Nonlinearity

Material nonlinearity considers the behaviour of materials beyond the elastic range, including yielding, plastic deformation, and cracking. Although designs are usually kept within the elastic limit of a material, it is important to understand the difference between geometric and material nonlinearity.

In the tensile-based façade system, incorporating second-order theory into the design process is crucial. As the cable elements experience increased deflection, their geometry adjusts, leading to a change in force components and an increase in tensile forces that both enhance the structure's out of plane stiffness.

2.1.4 Buckling

In structural design, buckling is a critical and mostly sudden instability phenomenon that occurs when compressive stresses cause a structural member to deform laterally or torsionally, often well before the material's yield strength is reached. It typically affects slender or thin members with low lateral stiffness or torsional and warping resistance, where even minor imperfections, such as geometric misalignments or residual stresses, can initiate lateral or torsional movement. As the load increases, these imperfections amplify deflection, reducing the member's ability to carry additional load and potentially leading to sudden failure. A simple analogy is a BBQ skewer: when compressed from both ends, it doesn't crush but rather bends sideways, illustrating how instability, not material failure, governs the response.

While flexural instability, also referred to as Euler buckling, is widely recognized, it represents only one of several possible buckling modes. In practice, buckling behaviour can become more complex when looking for instance at cold formed steel sections, it can then be categorized into three fundamental types: global, local, and distortional buckling (Mon et al., 2023). These modes differ in terms of the scale, location, and mechanism of the deformation involved.

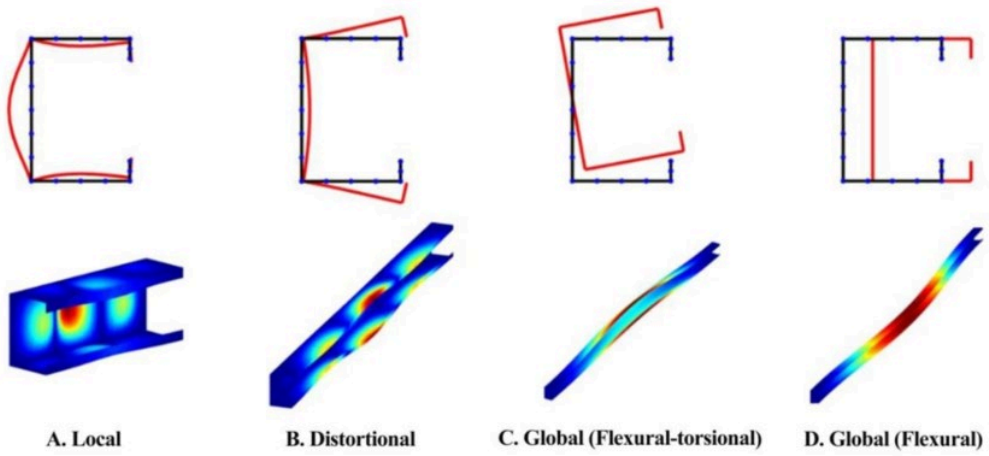

Figure 5: Types of buckling in cold rolled steel sections (Mon et al., 2023)

Global buckling

Global buckling modes involve deformation of the entire member and are primarily influenced by the member's geometry, slenderness, and boundary conditions. These can be further divided into flexural (Euler), torsional, and flexural-torsional buckling.

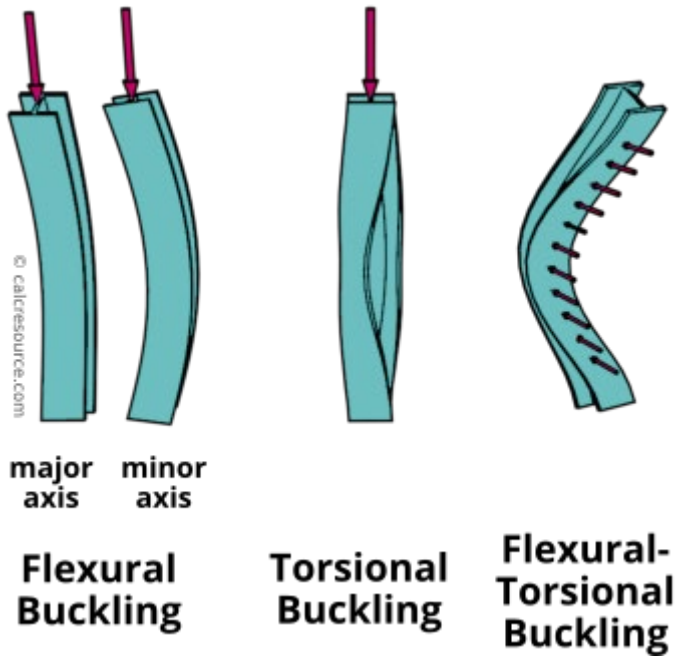

Figure 6: Types of global buckling modes (Dr. Minas E. Lemonis, 2024)

Flexural buckling (Euler buckling)

In flexural buckling, the entire member undergoes lateral deflection about one of its principal axes, typically the weaker one, under axial compression. This

commonly occurs in slender columns, including solid or built-up compression members with symmetrical cross-sections.

Torsional buckling

Torsional buckling, on the other hand, is a mode in which the entire cross-section twists along its longitudinal axis without significant lateral displacement. This typically happens when the member has low torsional rigidity and is highly symmetric. Though relatively rare, pure torsional buckling can occur in highly symmetric profiles with low torsional stiffness, such as cruciform columns (Figure 7).

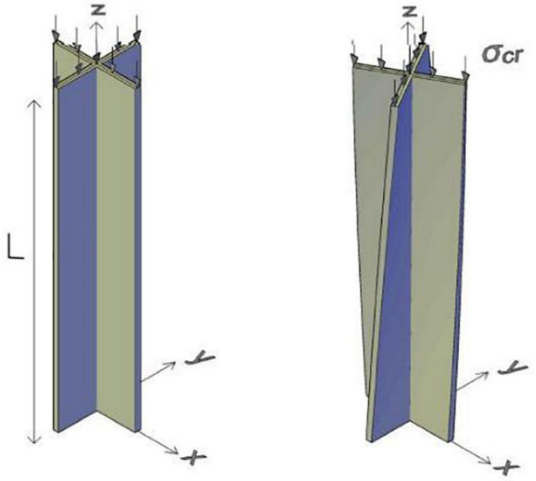

Figure 7: Torsional buckling inside a cruciform column (Shamass, 2020)

Flexural-torsional buckling

Flexural-torsional buckling is a combined instability mode involving both lateral displacement and twisting. When a member is subjected to axial compression and has an open or singly symmetric cross-section, such as angles, channels, or T-sections, flexural-torsional buckling often occurs due to the offset between the centroid and the shear centre, causing simultaneous bending and torsion.

Under bending conditions, this coupled behaviour manifests as lateral-torsional buckling (LTB), typically seen in beams with unbraced compression flanges. As the beam bends, the compression flange tends to displace laterally and twist, leading to a sudden, out-of-plane failure.

Flexural-torsional buckling under axial load is common in slender compression members with unsymmetric or open sections, while LTB under bending is particularly relevant to open-section beams such as I-beams, H-sections, and wide-flange shapes, especially when lateral support is insufficient.

Local buckling

Local buckling refers to deformation confined to individual flat elements within the cross-section, such as the flange, web, or lip, while the global geometry of the member remains unchanged. This mode is caused by compressive or shear stresses acting on thin-walled components, leading to wave-like deformation between the element's boundaries (Figure 5). Local buckling often occurs when flat plate elements, such as flanges or webs, are slender and loaded in compression. It is especially common in cold-formed steel sections that feature flat, unsupported components like channels, Z-sections, and box profiles. In beams, local buckling may also occur in webs under high shear (shear buckling), or in flanges under compressive or bending stress (Figure 8).

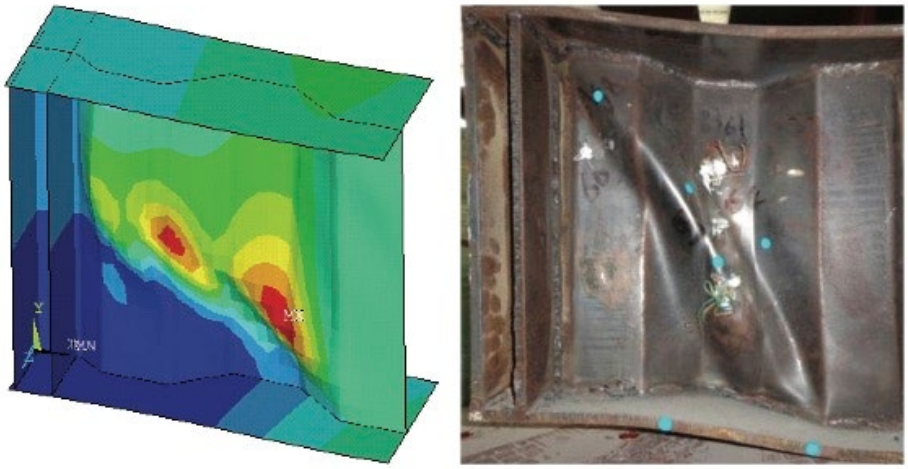

FIGURE 27: Deformation of C3H in FEM and experiment.

Figure 8: Shear buckling of corrugated web (Cao et al., 2015)

Distortional buckling

Distortional buckling is a failure mode that visually involves a combination of local and global deformations. It is characterized by a partial distortion of the cross-section, particularly around the flange-lip or flange-web junction, without full-body displacement. Unlike local buckling, where individual flat plates (like a flange or web) bend independently, distortional buckling causes these components to rotate or translate relative to each other, leading to a change in the cross-sectional shape (Hancock, 1997).

2.1.5 Vibrations

Façade panels can be subjected to vibrations from a variety of sources, not only from sound, but also from wind actions and seismic events, all of which must be considered in the design process.

Acoustic vibrations are sound pressure waves and are typically generated by external sources such as traffic, subways, or industrial activity. While these vibrations are not likely to cause structural damage, they can lead to noticeable sound transmission through the building envelope, resulting in reduced occupant comfort.

Wind-induced vibrations on building façades arise from several dynamic aerodynamic phenomena, including flutter, galloping, vortex shedding, torsional divergence, and gust loading (Mendis et al., 2007). Each of these mechanisms is complex and can affect different components and scales of a façade system, from individual panels to the entire envelope. To simplify things, designers can refer to the wind power spectral density graph provided in the Eurocode (Figure 9), which illustrates how wind-induced forces predominantly occur within the 0.01 to 10 Hz frequency range (Spjuth & Åkesson, 2016).

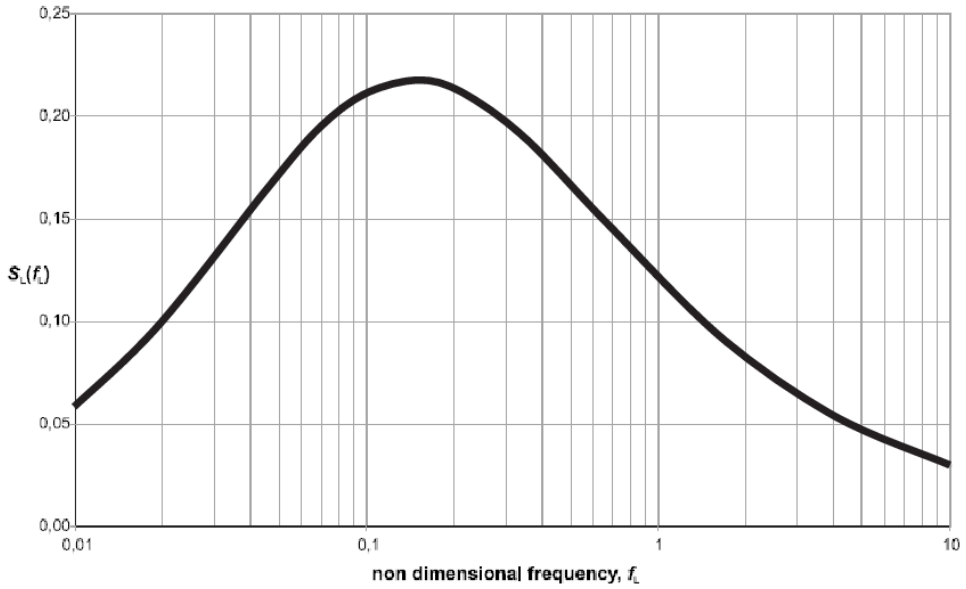

Figure 9: The wind power spectral density according to Eurocode ("Eurocode 1: Actions on structures - Part 1-4: General actions - Wind loads," 2012)

Façade systems with natural frequencies within this range are particularly vulnerable to wind induced resonance, which can lead to excessive deformation, occupant discomfort, and even structural damage. Similarly, mechanical systems such as HVAC units and elevators can introduce low-frequency vibrations, and if these align with the natural frequency of a façade panel, they too can lead to similar problems.

While avoiding the 0.01–10 Hz frequency band is a useful design guideline, it is not sufficient on its own to ensure safety and occupant comfort. For larger or more wind-sensitive projects, detailed dynamic analysis, using tools such as finite element analysis (FEA), computational fluid dynamics (CFD), or wind tunnel testing, is typically required to accurately assess and mitigate vibration risks.

However, during early design stages, it is good practice to aim for natural frequencies outside this critical range. This can be achieved by increasing the system's stiffness or changing its mass to shift its dynamic response (Jafari & Alipour, 2021).

Seismic vibrations differ in that they are driven by ground acceleration, often affecting the entire building. Façade design for seismic conditions focuses not on resonance, but on flexibility, accommodating drift, and robust anchorage, ensuring panels can move without detaching or cracking under relative story displacements. (Moeinadini et al., 2023).

2.1.6 Fatigue

Fatigue is a critical consideration in steel structures subjected to dynamic loading. In the tensile-based system, the cables are exposed to variations in tensile force due to fluctuating wind loads over the system's lifespan. It is therefore essential to incorporate fatigue considerations into the design to ensure long-term structural integrity and performance.

Fatigue refers to the progressive and localized damage that occurs when a material is subjected to repeated cyclic loading, even at stress levels well below its ultimate strength. Over time, this can lead to the initiation and growth of small cracks, which may ultimately result in sudden, brittle failure if not properly addressed. This phenomenon is especially critical in tensile members, where applied stresses tend to open and propagate cracks (SIMSCALE, 2023).

Fatigue can generally be classified into two types: low-cycle fatigue (LCF) and high-cycle fatigue (HCF). The distinction lies in both the magnitude of stress and the number of load cycles leading to failure. In low-cycle fatigue, the component is subjected to high stress levels, often causing plastic deformation, and failure typically occurs in fewer than 10.000 cycles. In contrast, high-cycle fatigue involves lower stress amplitudes, within the elastic range of the material, and failure occurs over a much larger number of cycles, typically greater than 10.000 (SIMSCALE, 2023). Ferrous alloys and titanium alloys can have a fatigue limit below which the material can have infinite life without failure, this point is also known as the endurance limit (Xin, 2013).

Estimating the fatigue life of a component in the high cycle regime is commonly done using an S-N curve (or Wöhler curve), which plots stress range or amplitude (S) against the number of cycles to failure (N) on a logarithmic scale (Figure 10).

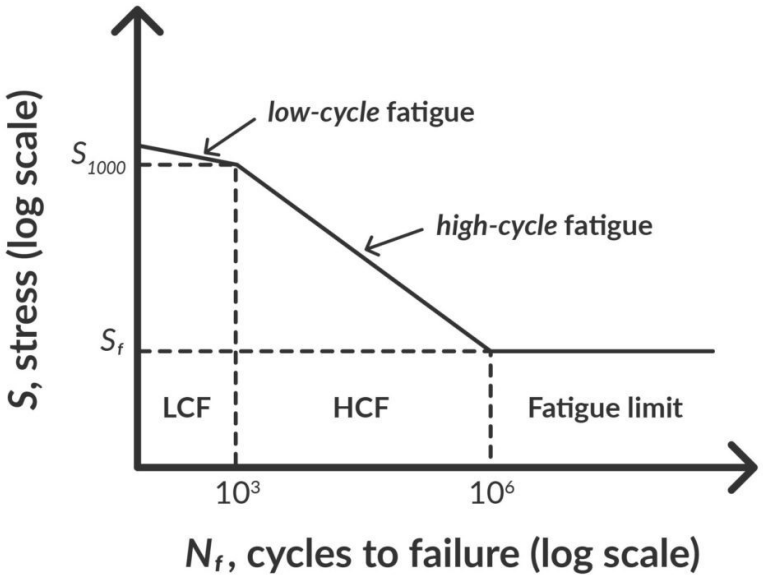

Figure 10: S-N curve showing the low-cycle and high-cycle regions (SIMSCALE, 2023)

A key characteristic of the S-N curve is its slope, which determines how rapidly fatigue life decreases with increasing stress amplitude. This slope, often denoted as m, varies depending on the material and type of loading. A higher slope means the fatigue life drops sharply with small increases in stress, while a lower slope implies the material is more tolerant to stress variation. In steel, the slope is commonly taken as m = 3 in the high-cycle regime, which is the basis for many standardized fatigue assessments, such as those in Eurocode EN 1993-1-9.

S-N curves are derived from experimental data and usually represent the material's behaviour under fully reversed loading conditions, where tensile and compressive stresses are equal in magnitude but opposite in direction, or in other words, where the mean stress (σ_m) is 0 (Figure 11). If the stress range or amplitude in a component is known, the corresponding S-N curve can be used to estimate the number of cycles the material can endure before fatigue failure occurs.

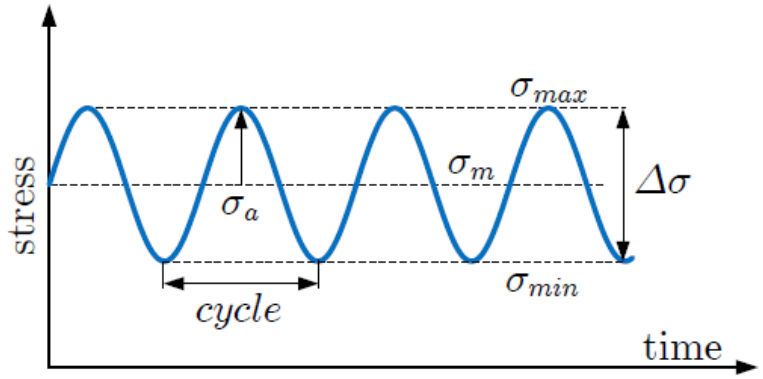

Figure 11: Mean stress, stress amplitude, and stress range (figure: https://fatigue-life.com/what-is-fatigue-life/)

However, real-world loading is rarely fully reversed. Many components experience fluctuating loads that are primarily tensile, with a non-zero mean stress (σ_m). A tensile mean stress reduces fatigue resistance because it keeps existing cracks open longer during each cycle, promoting crack growth. Conversely, a compressive mean stress can inhibit crack propagation and improve fatigue life.

To account for the effect of mean stress, engineers often apply correction models such as the Goodman, Gerber, or Soderberg diagrams (Figure 12). These models adjust the allowable stress amplitude based on the mean stress and the material's ultimate or yield strength.

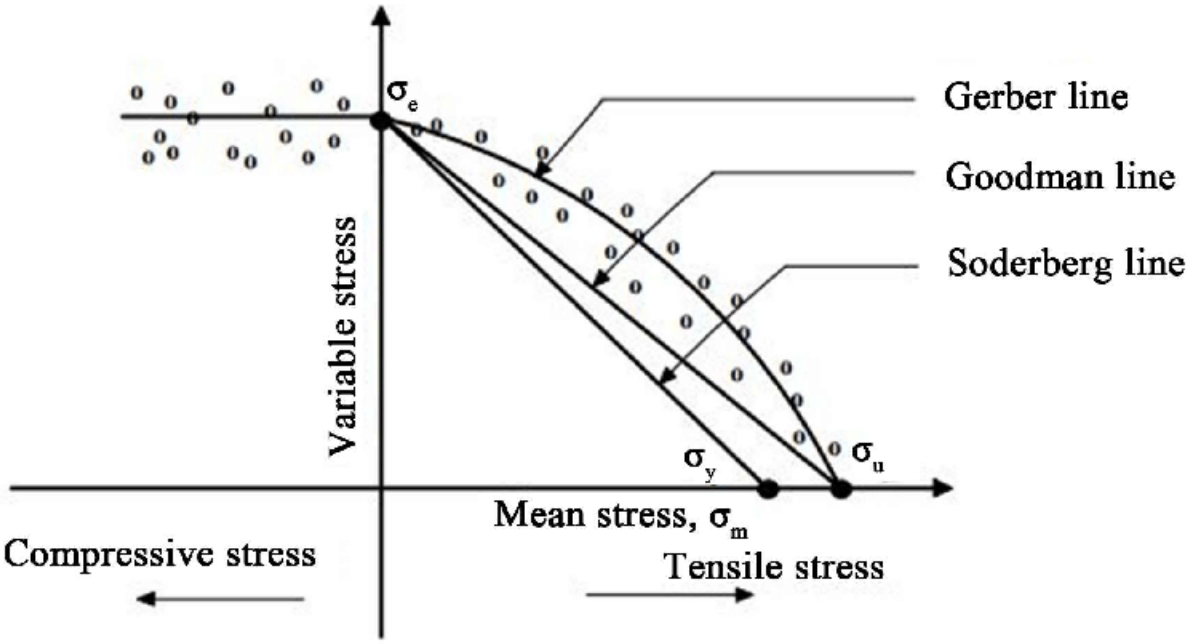

Figure 12: A typical schematic showing Gerber, Goodman and Soderberg lines and relation between the variable stress and the mean stress in an ideal fatigue test (Santhosh et al., 2017)

The Goodman relation, for example, provides a linear approximation and is commonly used:

$$\frac{\sigma_a}{\sigma_e} + \frac{\sigma_m}{\sigma_u} = 1$$

σ_a : Stress amplitude

σ_e : Fatigue limit (determined experimentally)

σ_m : Mean stress

σ_u: Ultimate strength

To summarise, as a design guideline, an effective way to improve the fatigue life of a tensile-based system is through pre-tensioning. This approach reduces stress

fluctuations by maintaining a controlled tension level, keeping stress cycles within a desired range and within safe limits. As a result, it helps prevent premature fatigue failure by limiting crack initiation and growth under cyclic loading.

2.1.7 Pretension losses

The tensile façade system contains cables that must remain under tension to ensure sufficient component stiffness. Once the required pretension is achieved, it is also necessary to maintain it at a similar or sufficiently high level, or to know when checks should be performed to reapply tension. This is why it is important to understand what might cause pretension losses in such a system.

Several factors can contribute to pretension losses in a pretensioned system. These can be categorized into immediate (short-term) effects and long-term factors.

Short-term effects

One short-term effect is elastic shortening. A common example occurs in prestressed concrete beams: when the prestress force from a tendon is transferred to the concrete, the beam itself shortens slightly due to compression. As a result, the tendon also shortens, leading to a small but measurable loss of pretension. (Hsiao, Jan 2017).

Additional short-term effects that can lead to pretension losses in for instance reinforced concrete beams are anchorage slip and friction losses. Anchorage slip, or slippage at the connection point, occurs when a prestressed tendon experiences a slight movement at the anchorage during or after the release of the tensioning force. This can lead to a minor but measurable loss in pretension. One effective method to minimize this effect is to slightly over-tension the elements during installation. This ensures that any expected slippage does not significantly reduce the final tension and allows the connection joints to fully seat or embed themselves under load (Walter Podolny, October 1969).

Friction losses arise when a tendon or cable rubs against the surrounding materials, leading to additional resistance that must be overcome during tensioning. These losses are influenced by factors such as the curvature of the tendon path and the surface characteristics of the duct (Walter Podolny, October 1969).

For the tensile-based façade system, short-term pretension losses are unlikely to present significant issues. Elastic shortening can be accounted for during the design phase by incorporating expected deformations into the dimensioning of the cables and struts. Anchorage slip can be minimized, depending on the type of connection joint, and can be verified during installation by ensuring proper embedment and seating of the components. Friction losses are not anticipated, as the cables are arranged in straight

lines without contact with other structural elements, thereby removing any potential for friction along their length.

Long-term effects

Long term effects could pose significant problems however as these occur after the cables are installed and tensioned. Potentially requiring access to the cables and regular maintenance if losses are great enough to reduce panel stiffness significantly.

Potential long-term effects in the tensile based façade system are creep or relaxation and temperature effects.

Creep is the gradual, time- and temperature-dependent deformation of a material under constant load or stress. It results in permanent deformation, as the material does not return to its original shape once the load is removed. Different materials exhibit varying creep rates depending on environmental conditions. For example, in an experimental study on low-alloy structural Q345 steel, a wide range of creep behaviour was observed across different temperature ranges (Wang et al., 2016).

Under room temperatures however, creep poses less of a problem to structural steels and is usually negligible. For materials such as polymers and woods, creep can however pose a large problem for sustained loads. For woods for instance creep is even moisture and load-to-grain angle variable and is heavily regulated in structural design (Granello & Palermo, 2019). Generally speaking polymers too exhibit significant creep in room temperatures and can even rupture due to creep, resulting in a sudden mechanism of failure (Spathis & Kontou, 2012). Concrete too shows creep behaviour at room temperature, but it's rates are more moderate (Vandamme & Ulm, 2009).

Relaxation differs from creep primarily in the context of the applied loading conditions. Generally, creep refers to an increase in strain under constant stress, while relaxation involves a decrease in stress under constant strain. Despite this difference, the underlying material mechanisms are largely the same. Both phenomena arise from the time-dependent internal rearrangement of the material's microstructure. As noted in Technical Tidbits, an intuitive example is the behaviour of a rubber band (Gedeon, December 2009). In the case of creep, the rubber band is stretched under a constant load and, when the load is removed, it exhibits a slight permanent elongation (Figure 13). In the case of relaxation, the rubber band is stretched to a fixed length and held; over time, the internal stress decreases, and when the elongation is released, the rubber band again shows a small, irreversible deformation (Figure 14).

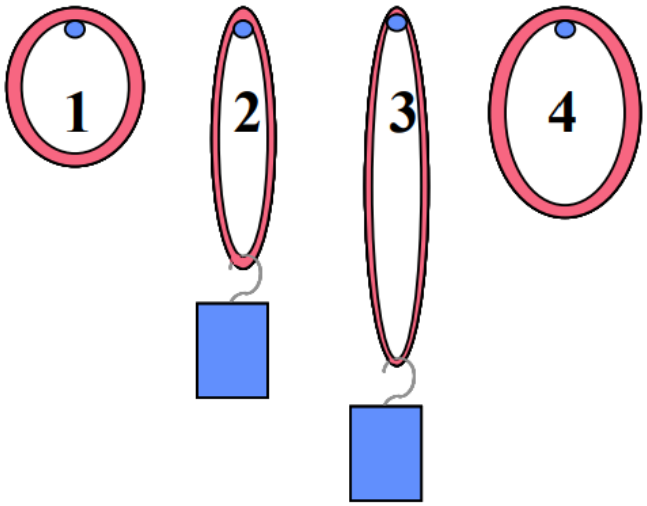

Figure 13: Creep example in a rubber band (Gedeon, December 2009)

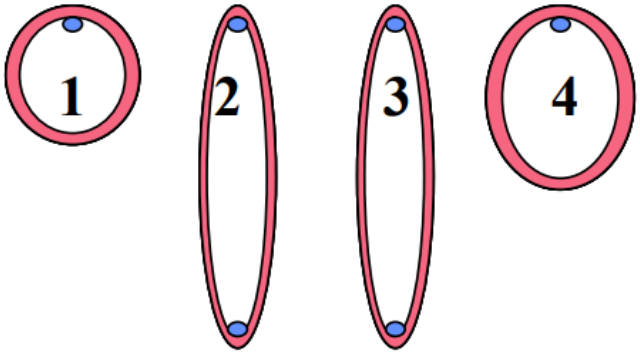

Figure 14: Relaxation example in a rubber band (Gedeon, December 2009)

Temperature effects can significantly influence pretension in a cable system, as both the cables and the supporting structure expand or contract with temperature fluctuations.

This behaviour is governed by the principle of thermal expansion, which describes how materials change in length in response to temperature changes. The extent of this expansion is defined by the material's linear thermal expansion coefficient (α), typically expressed in units of 1/°C. For example, steel has a coefficient of approximately 12×10^{-6} /°C, meaning it expands 1.2 mm per 10 m of length for every 10°C increase in temperature (*Linear Thermal Expansion Coefficients of Materials*).

For the tensile system, when temperatures rise, the cables expand, which may reduce cable tension if the anchor points are fixed and do not allow for adjustment. However, if the supporting frame expands more than the cables, it can instead increase pretension, depending on the relative thermal expansion coefficients and stiffness of the components. Conversely, in colder conditions, the opposite might happen. These

interactions must be considered in the design to ensure that pretension levels remain within safe and functional limits throughout expected temperature ranges.

2.1.8 Structural Design Criteria

Substructures of facades are structurally dimensioned to meet two primary criteria: the Ultimate Limit State (ULS) and the Serviceability Limit State (SLS).

Ultimate Limit State (ULS):

ULS pertains to the safety and stability of structures under maximum expected loads, ensuring they do not reach a point of collapse. The foundational document for ULS is EN 1990, Basis of Structural Design, which outlines principles and requirements for safety and serviceability. This standard is implemented in the Netherlands under NEN-EN 1990 (2019). ULS checks are typically performed under factored combinations of permanent and variable loads, including wind, snow, and self-weight, with partial safety factors applied to account for uncertainties in load estimation and material performance. For façade substructures, this involves verifying that structural components such as brackets, anchors, and cable systems can withstand extreme loading scenarios without failing.

Serviceability Limit State (SLS):

Serviceability Limit States (SLS) relate to the performance and comfort of structures under normal usage conditions, focusing on aspects such as deflections, vibrations, and cracking. For glass for example, specific deflection limits under SLS are clearly defined. According to the Dutch standard NEN 2608, allowable deflection limits for glass elements are established and remain consistent under both permissible stress and limit state design approaches (RNSI, 2014). However, for most other materials, the Eurocodes do not specify strict deflection limits for all structural elements, including most façade components. Instead, they offer general guidance, leaving the definition of specific SLS criteria to be determined through agreement between designers, manufacturers, and clients, based on the specific requirements of the project (JRC, 2008).

This flexibility presents significant potential for the development of tensile façade systems. Even if such systems do not limit deflections as effectively as traditional rigid solutions, their inherent flexibility allows them to accommodate and manage larger deformations without compromising structural integrity or performance. This principle is already applied in many cable-stayed façades, which are intentionally designed to tolerate significantly higher deflection limits (Schlaich et al., 2005).

2.2 Prefabrication and Façade Typologies

2.2.1 Prefabrication classifications

Prefabricated construction, also known as off-site construction (OSC), off-site manufacturing (OSM), off-site fabrication (OSF), or industrialized building systems (IBS), is a construction method where building components or entire structures are designed, manufactured, and partially or fully assembled in a controlled factory environment before being transported to the construction site for final installation. They can be categorized into Volumetric Prefabricated Construction (VPC) and Non-Volumetric Prefabricated Construction (NVPC) (Sah et al., 2024).

VPC involves off-site assembly of complete 3D modules, including beams, columns, floor panels, and wall panels. These modules are delivered fully finished, potentially with electrical wiring, plumbing, and interior finishes, ready for installation on-site. This approach minimizes on-site work and is ideal for projects prioritizing speed and standardization (Sah et al., 2024).

NVPC, on the other hand, focuses on off-site fabrication of individual components, such as load-bearing walls, floor panels, beams, and columns, which are assembled on-site. Variants include panelised NVPC, where walls and floors are joined on-site, and framed NVPC, where prefabricated beams and columns are combined with floor panels and facade elements. NVPC offers greater flexibility and customization but requires more on-site work compared to VPC (Sah et al., 2024).

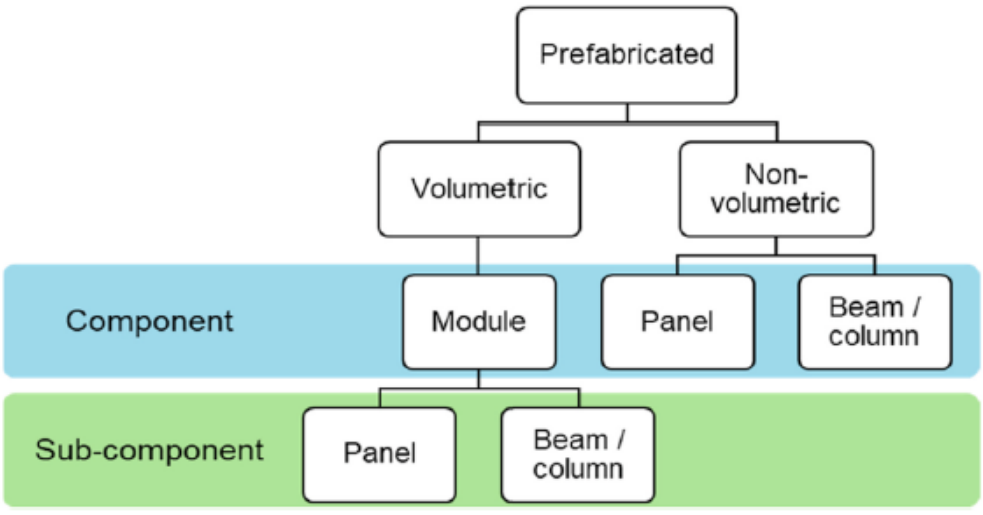

Figure 15: Classification of prefabricated construction (Sah et al., 2024)

2.2.2 Comparable prefabricated façade systems

Although it would be possible to fabricate volumetric modules using the proposed façade system or ship it as a collection of its constituent parts, the system is inherently panelised in its functional state. Given this, here are some other types of panelised systems that are widely used in the construction industry. These systems include:

(source: https://www.structuraltimber.co.uk/timber-systems/timber-frame/)

Light Timber Framing (LTF) Panels and Component Systems:

> *Comprised of a framework of small timber members that form studs, plates, and braces, these panels rely on sheathing materials for additional stiffness and structural integrity. The system creates a lightweight structure capable of carrying vertical and lateral loads.*

(source: https://www.np5.eu/manufacturer-of-lgsf)

Light Gauge Steel Framing (LSF or LGSF) Panels and Component Systems:

> *Made from cold-formed steel sections, LSF panels consist of thin steel studs and tracks that are connected to form a rigid framework. Like LTF, structural strength can be derived from sheathing materials or additionally from the steel members itself and additional bracing elements.*

(source: https://buildingdynamics.nl/)

Cross-Laminated Timber (CLT) Panels:

Engineered from layers of solid-sawn timber boards arranged perpendicular to each other, CLT panels form a rigid, monolithic structure. The cross-lamination provides strength and stiffness in both longitudinal and transverse directions, which in turn make the panels act as solid shells.

(source: https://susanwardre.com/blog/sb9-manufactured-homes-success)

Structural Insulated Panels (SIP):

Composed of a rigid insulating core sandwiched between two structural facing materials, typically oriented strand board (OSB), although steel and other metals are also common. These panels derive their strength from the composite action between the core and the facings and require prober bonding between the two.

(source: https://leimro.com/elematic_category/walls/)

Precast Concrete Sandwich Panels (PCSP):

Constructed with two outer layers of reinforced concrete separated by an insulating core, which is bonded or tied together with connectors. These panels can be designed to take heavy loads using singular or composite action of one or both concrete layers.

(source: https://www.mornglass.com/unitised-curtain-wall-introduction-installation.html)

Unitized Curtain Wall (UCW):

> *Constructed from thermally broken aluminium transoms and mullions rigidly connected to form a solid panel, unitized curtain wall systems are typically characterised by large, glazed openings and a tighter, grid pattern.*

2.2.3 Cable-stayed façades

Another façade type worth mentioning is the cable-stayed façade, not for its prefabricated or panelised qualities, but due to their structural similarity. These systems feature an array of pretensioned cables, with glazing panels hung between them to achieve a highly transparent appearance.

The primary load-bearing system typically consists of straight tension members, such as cables or rods, arranged in parallel. These elements efficiently transfer the dead load of the glazing to the supports. Under wind loads, single layer cable net facades experience significant deflections, which in turn activate their lateral stiffness. A striking example of such a cable net façade is of the Markthal in Rotterdam, which can deform by up to 70 cm under high wind conditions over a 35 m span, approximately span/50 (Figure 16). This level of movement requires innovative detailing to accommodate large deflections while maintaining structural integrity (Sobek et al., 2010).

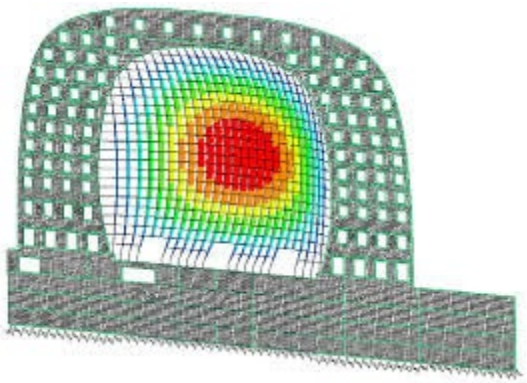

Figure 16: Deformation of the cable net facade of the Markthal in Rotterdam(Octatube).

To prevent excessive deflections, structural designers have developed alternative configurations for cable-stayed façades. By introducing an initial out-of-plane curvature to the cable system, the façade gains stiffness without requiring significant deformation, allowing it to more effectively resist forces such as wind loads from the outset (Figure 17).

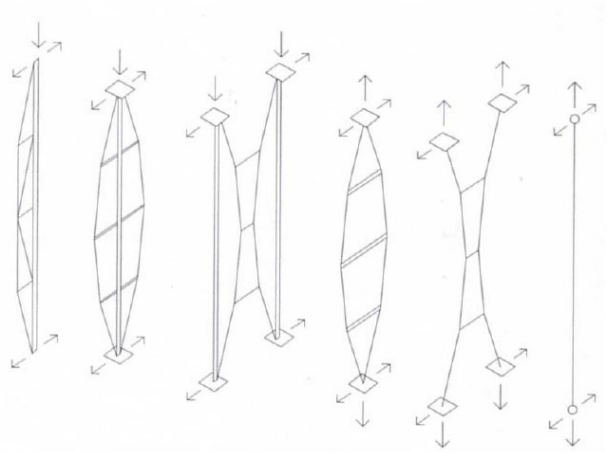

Figure 17: Principle primary structural systems of cable-stayed façades (Sobek et al., 2010)

Similarly, the single-layer tensile-based façade panel described in the patent relies on a certain degree of deformation to become structurally effective, potentially requiring large deflections before sufficient lateral resistance is achieved. As with cable-stayed systems, the design could benefit from introducing initial out-of-plane curvature, which may enhance stiffness earlier in the loading process and reduce the extent of deflection required for the system to engage effectively.

2.3 Manufacturing context

The prefabrication of façade panels offers numerous advantages over traditional on-site construction. It ensures greater consistency and precision, while also being less affected by weather conditions. Additional benefits include faster installation, improved cost control, enhanced scalability, and more sustainable resource use. Prefabricated solutions are particularly effective in overcoming urban constraints such as limited space or restricted site access. (Rammig et al., 2023; Sah et al., 2024).

While these advantages represent significant progress in façade engineering over the past decades, the increased regularization of elements also introduces a specific set of rules and constraints, primarily related to manufacturing limitations and logistical requirements.

Starting at the design phase and continuing through to on-site installation, façade panels undergo a tightly integrated, digitally managed process. Advanced Building Information Modelling (BIM) and parametric design tools can be employed to define panel geometry, integrate performance requirements, and coordinate interfaces with structural and service systems. With modern parametric tools enabling mass customization, designers can efficiently adapt panel designs to varied building geometries without sacrificing manufacturing efficiency (Abdelmohsen & Hassab, 2020). In the factory, panels are fabricated under controlled conditions, where standardized procedures and even robotic assembly lines can help maintain quality and reduce material waste (Loh et al., 2019; Tish et al., 2020).

Once completed, panels are prepared for logistics, often designed within strict dimensional and weight constraints to ensure efficient stacking and safe transport, typically via flatbed trucks or modular containers. These constraints become especially critical when navigating narrow urban streets or coordinating international shipments where different size constraints might apply. For example, the recommended maximum vehicle height on UK roads is 4.93 m. As illustrated by the 2012 Explore Manufacturing's design guide for precast cladding (Figure 18), this overall limit must account not only for the panel itself but also for the trailer height and any additional clearance required for packing and support systems. Consequently, the choice of transport vehicle imposes specific dimensional limitations on prefabricated façade panels, influencing their maximum height, length, and configuration.

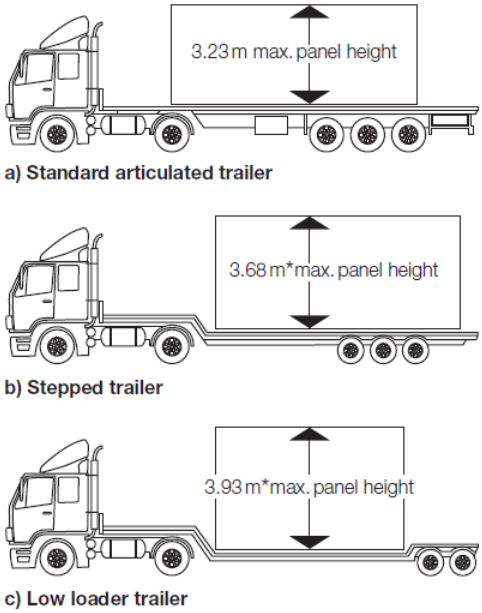

Figure 18: Panel height limitations on different types of vehicle trailer ("Precast Cladding Design Guide," 2012)

Upon arrival at the construction site, installation methods vary depending on level of prefabrication, building height, and site constraints. On low- to mid-rise buildings, mast

climbing platforms or scaffold-based systems may be used for manual placement, while high-rise projects typically rely on tower cranes or mobile cranes for lifting (Figure 19).

Figure 19: (left) mast climbing platforms and (right) tower crane installation (image sources: https://alimak.com/nl/product-category/mast-climbing-work-platforms/ & https://popsfacades.co.uk/unitised-curtain-wall-installation/)

Theoretical systems even go as far to propose fully robotic assembly mechanisms for panelised and curtain wall facades (Iturralde et al., 2022; Iturralde et al., 2016).

Especially for systems hoisted in place using tower cranes attention must be given to the connection points of the façade panel. As during the assembly phase structural loads likely differ from those compared to the final installed condition.

Regardless of the installation method, the primary objective is to achieve a safe and rapid connection to the building frame. For unitized façade panels in concrete structures for instance, this is typically accomplished using a range of fastening systems, including cast-in-place anchors, post-installed mechanical fixings, and powder-actuated fasteners (Figure 20).

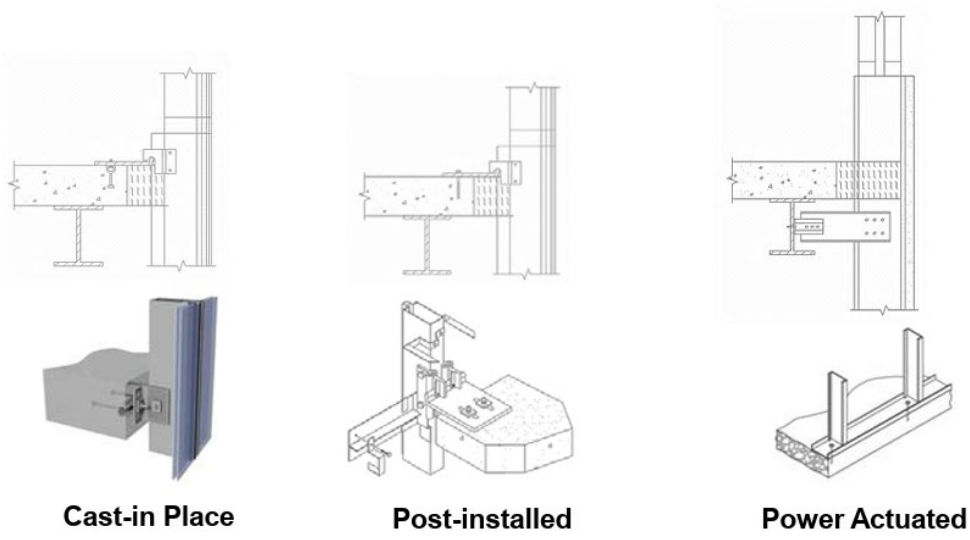

Figure 20: Facade fastening systems in concrete buildings (HILTI, July 2019).

At the same time, these connections must accommodate necessary movement to prevent damage caused by various factors, including assembly tolerances, thermal expansion, wind-induced sway, and seismic activity as depicted in Figure 21.

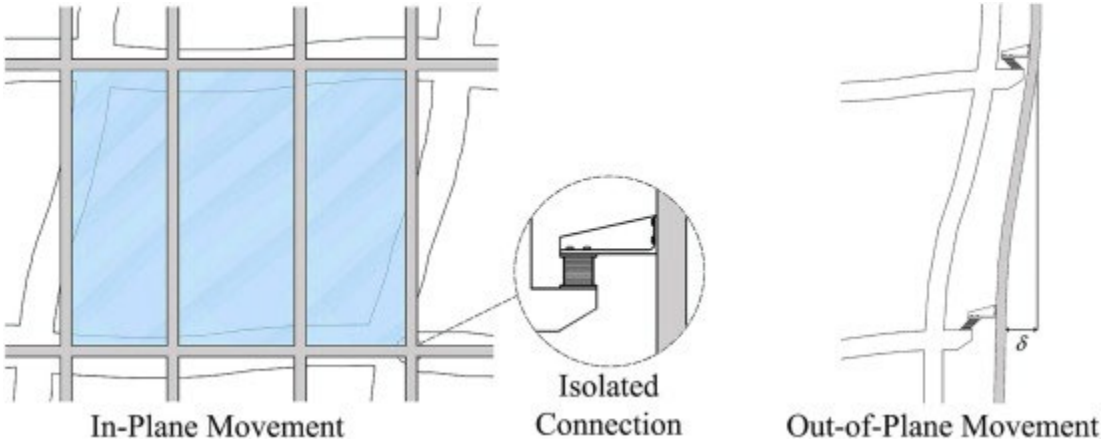

Figure 21: Facade isolation in seismic design of tall buildings (Moeinadini et al., 2023)

To address these challenges, connection detailing often incorporates slotted holes, flexible brackets, or isolated bearing points, allowing for controlled movement without compromising the system's structural performance or long-term durability.

2.4 Façade Performance Criteria

As outlined in the introduction of this thesis, modern façades should aim to integrate a wide range of functionalities to support more sustainable building designs, provide architects with greater creative freedom, help investors meet performance and cost targets, and ensure comfortable living environments for users. To assess the effectiveness of a façade system, a broad set of performance indicators can be considered.

From a physical and architectural standpoint, façades should meet constraints related to weight, minimum and maximum dimensions, and manufacturing tolerances, while also offering customizability, potential transparency, and finish applications. These

attributes impact not only the structural integrity but also the architectural possibilities of the system.

In terms of functional performance, façades must deliver reliable thermal and acoustic insulation, maintain weather tightness, and ensure appropriate fire resistance to uphold safety and comfort standards.

Installation and adaptability are next with considerations including the level of prefabrication, installation time, demountability and compatibility with access equipment such as mast climbing platforms or tower cranes, all of which affect construction speed and site logistics.

The durability of façade panels must be ensured through resistance to weather exposure, corrosion, biological factors, and seismic forces, ensuring long-term reliability.

There is a rising focus on the environmental credentials of materials. Factors such as initial and lifecycle carbon footprints, circularity potential (CPI), and the use of critical raw materials (CRMs) are important criteria to evaluate products, including façade systems. (Domaracka et al., 2022; Saidani et al., 2024; Saidani et al., 2019).

Finally, economic considerations such as the initial investment and the total cost of ownership (TCO) play a decisive role in selecting façade solutions that offer both immediate and long-term value (Tam et al., 2018).

Taken together, evaluating these factors provide valuable insight into which façade solutions are best suited for specific locations, design constraints, and performance requirements, enabling informed, context-sensitive decision-making in both design and construction.

3. Concept development

3.1 Exploring structural principles

Before engaging in complex numerical modelling or simulation of potential design configurations, it is valuable to first reason through some of the fundamental structural engineering principles that will govern the system. This early-stage assessment can already highlight likely challenges and opportunities within the design.

3.1.1 The influence of asymmetries

A logical starting point is the equilibrium of forces in the tensile system, understanding how these forces are resolved in various configurations already highlights the importance of symmetry in the system.

To recap, when tensioning the cables in the system, the structure must remain in a state of equilibrium, meaning that all internal and external forces and moments are balanced.

If the force in a single cable and the geometry of the frame is known, and assuming that only axial forces act within the frame elements, tensile forces act in the cables, and all connections are pinned, the system is statically determinate and is easily solvable using basic principles of statics Figure 22.

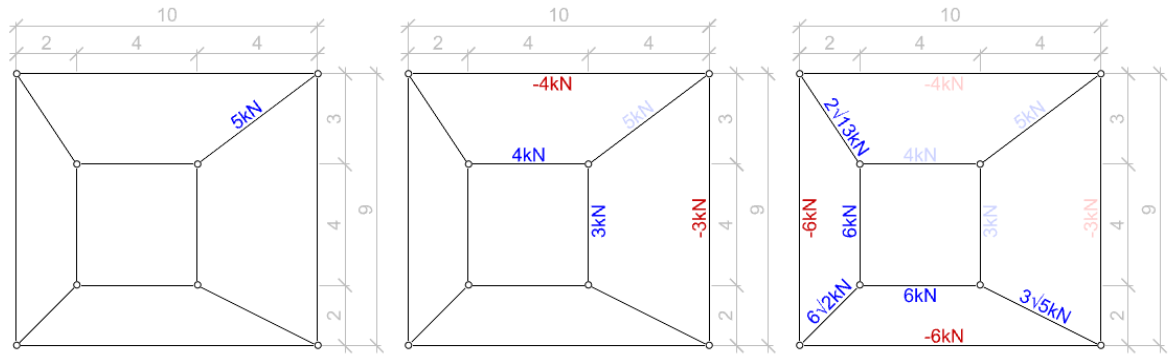

Figure 22: Example calculation of axial forces in the system

To accelerate the analysis of other configurations, the Karamba3D plugin for Rhino/Grasshopper was used. (Karamba3D, 2024). Using this solver, a parametric framework was created to easily evaluate a wide range of design variations. Parameters include the height and width of the inner and outer frames, as well as the inner frame's offset from the centre point.

This visual method makes it intuitively clear how symmetry or asymmetry influences the system. Introducing an arbitrary pretension now demonstrates how asymmetry can negatively impact the system's adaptability in design (Figure 23).

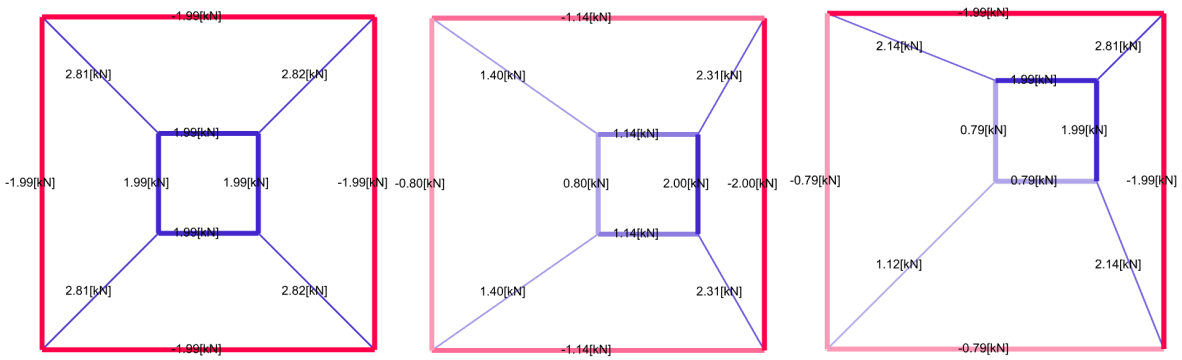

Figure 23: The influence of asymmetries on axial forces within the system

What can be observed is how an asymmetry causes the axial forces in the system to become uneven, reaching high axial forces near the edges where the inner and outer frame closely meet.

This becomes a negative effect when lateral loads such as wind loads are considered, because this directly influences the stability of the tensile based system in those, and more importantly, in opposing regions.

For instance, in a symmetrical configuration, the outer frames can be designed with consistent sizing and a maximum compressive capacity of around 2 kN axially (Figure 23). However, maintaining a maximum compressive force of 2kN, when the frame is shifted into an asymmetrical layout, the tensile forces in the opposing cables drop significantly. This reduction leads to lower out-of-plane stiffness in those regions, which now additionally face an increased surface area exposed to wind, produces a double negative effect. Both reduced stiffness and higher loading on the façade's opposing side.

This also implies that designing a frame for multiple asymmetric configurations would require excessive, mostly unused, strength in the outer compressive struts, as compressive forces would skyrocket in individual struts in order to maintain sufficient tensile forces on the opposing side, ultimately reducing the system's overall efficiency.

There is, however, also a beneficial structural effect of the asymmetry that should be acknowledged. In an asymmetric configuration, the compressive strut subjected to increased axial load is now also exposed to a smaller wind-facing surface area. Consequently, depending on the remaining load path, this member will likely experience lower lateral loads and therefore a reduced bending moment, making it less susceptible to buckling. This effectively increases the axial load-bearing capacity of the compressive member compared to a symmetrical configuration. The exact opposite will also be true for the opposing member facing lower axial force, but greater bending moments.

Since the balance between increased axial load and decreased bending moment is unlikely to perfectly offset one another, asymmetry will have a net negative impact on the

overall stiffness of the façade panel. The precise extent of this effect will be further explored in the numerical modelling presented in later sections.

3.1.2 Exploring system stability

To intuitively assess the system's stability, another interactive model was created using the Rhino Grasshopper plugin Kangaroo. Kangaroo operates by minimizing the total energy of a system. Users can define various goals, each corresponding to specific energies that are minimized under certain geometric conditions. The solver iteratively adjusts the positions of points in the model to achieve a state where the sum of these energies is as low as possible. For instance, the 'Length' goal functions analogously to a spring, adhering to Hooke's law, where the energy is minimized when the spring reaches its rest length (Piker, 2024).

Modelling the system with set lengths for the inner and outer frame and a shortened length for the cables can mimic the real-world scenario of pretensioning the cables. Even if the ‘real’ pretension is unknown, the location of forces and their directions are similar.

When the corners of the frames are not rigid but are instead modelled as eight pinned connections, the system's inherent instability can be revealed (Figure 24).

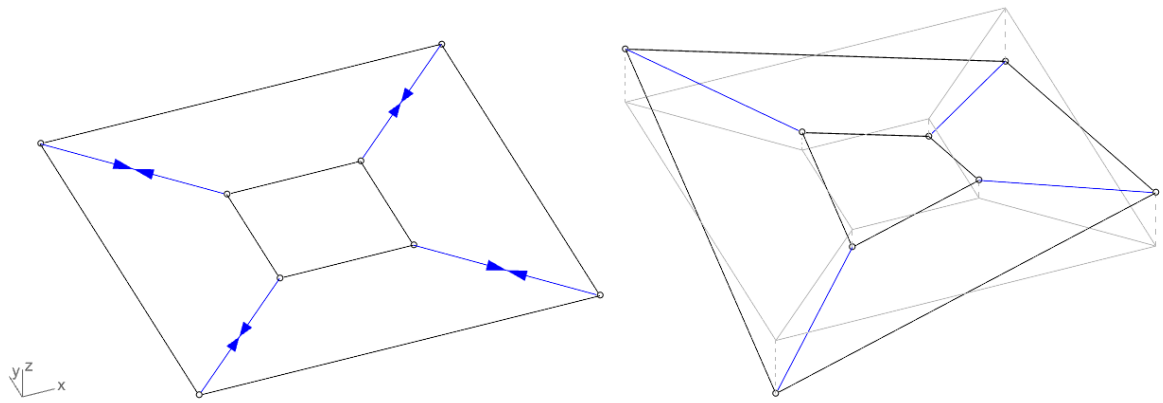

Figure 24: The tensile system's inherent geometric instability

Imagine the nodes of the tensile-based frame lying on the X & Y plane. With all eight nodes on the plane, the system remains balanced and in equilibrium. However, as soon as one of the nodes is disturbed and moves slightly out of plane in a positive or negative Z direction, the tensile forces in the cables create an out-of-plane component. This component continues pulling the frame further out of the X & Y plane until the cables reach a length at which they are no longer in tension, causing the system to warp. This instability persists across all geometric configurations, regardless of size, offset, or the aspect ratio of the inner or outer frame. This effect can be confirmed by measuring the

deformed geometry. With this change in shape the length of the inner and outer frame stays the same, but the cables get shorter.

Restricting out of plane movements of the inner and/or outer frame

Continuing the exploration, restraints were independently applied to the inner and outer frames to simulate a stiff inner and/or outer frame. This is where the system's behaviour becomes more complex. When the outer frame is restricted to in-plane movement (X and Y directions), the system consistently remains stable. In contrast, when similar restraints are applied to the inner frame, the structural response become dependent on geometric configuration, specifically, the size and aspect ratio between the inner and outer frames, but not on the offset of the inner frame.

Plotting the results for configurations where the system remained stable, limiting out of plane movement of the inner frame, whilst keeping the outer four nodes as unrestricted pin joints yields the following results (Figure 25). From this, a pattern begins to emerge, tracing on the second row a diamond shape boundary where equilibrium occurs.

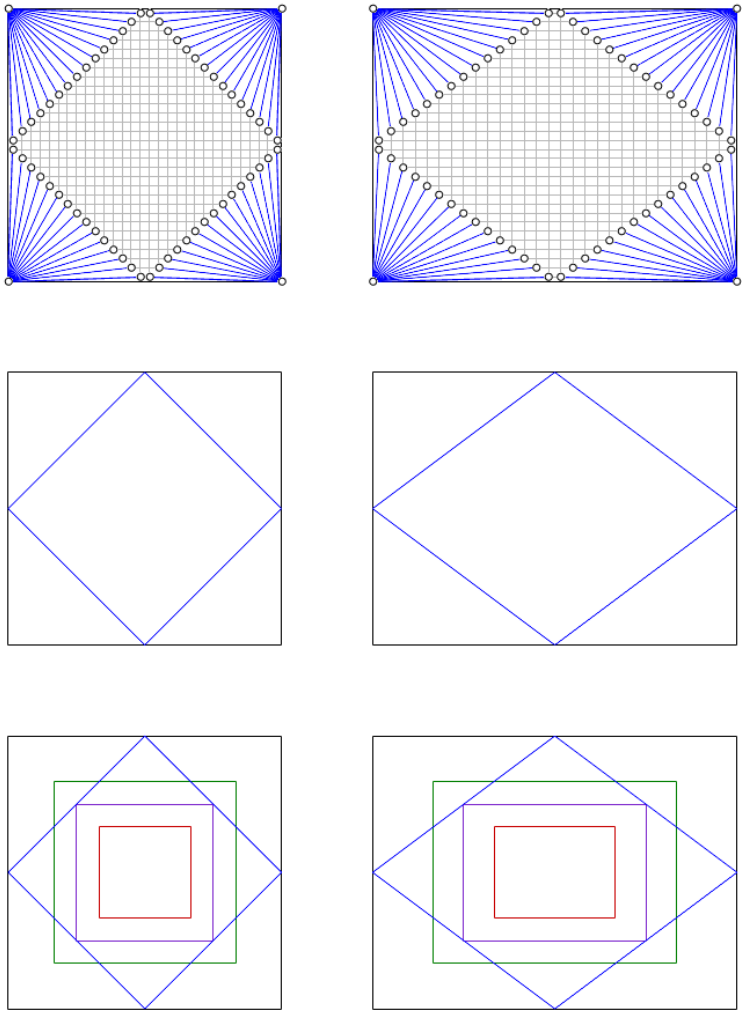

Figure 25: Stable and unstable configurations of the tensile based system when limiting out of plane deformations of the inner frame

In the bottom row of Figure 25 three sizes of inner frames are shown: red, smaller than the blue boundary diamond being unstable; purple right on the boundary exactly stable but taking a while for the system to regain its shape after an out of plane excitation is applied; and the green frame larger than the boundary, easily regaining stability after an out of plane excitation.

Doing a 2D geometric analysis of the square configuration confirms this stability. Tilting the frame by 45 degrees and plotting the projected deformation of the outer frame. Lines can be drawn in the exact plane as the tensile cables. This reveals the shortening of the cables in the unstable configuration (red), the lengthening of the cables in the stable configuration (green) and the cables remaining of similar length right on the boundary (purple). The circles representing the undeformed cable lengths serve as a reference, with the deformed states deviating from these radii, seen as the magenta curves that trace the deformation of the outer frame nodes (Figure 26).

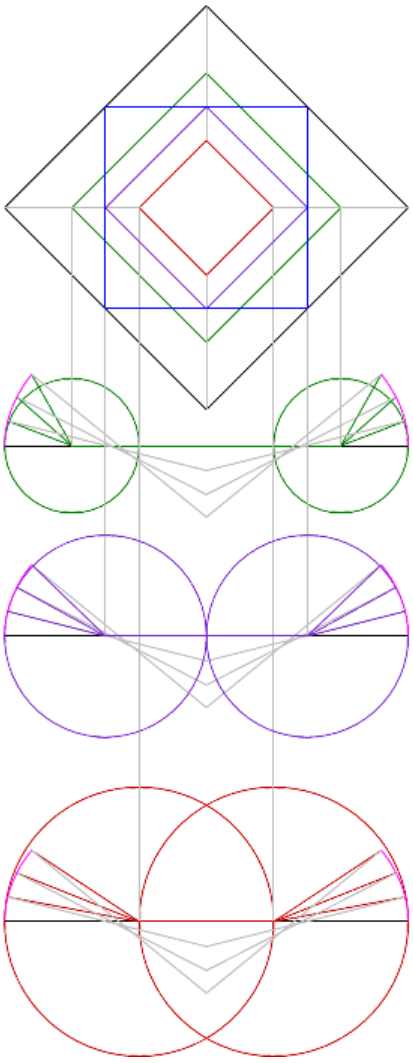

Figure 26: 2D Geometric analysis of inner frame (in)stability, showcasing the lengthening or shortening of tensile cables.

This observation also holds true for the rectangular frame and can be confirmed using the same 2D method or through a 3D geometric analysis (Figure 27). The deformed endpoints of the outer frame are again traced in magenta, while an orange cylinder is created around one of the axes of the blue equilibrium diamond. This visualization demonstrates how multiple green inner frames placed on the equilibrium diamond that correspond to the purple circles of equal radii, *all share the same tangent* as the traced magenta curve at the orange points when viewed along the normal of the orange cylinder (Figure 28). This implicates that for inner frames dimensioned along the axes of the equilibrium diamond, the cables neither shorten nor elongate when the outer frame warps and are therefore right on the boundary of being stable.

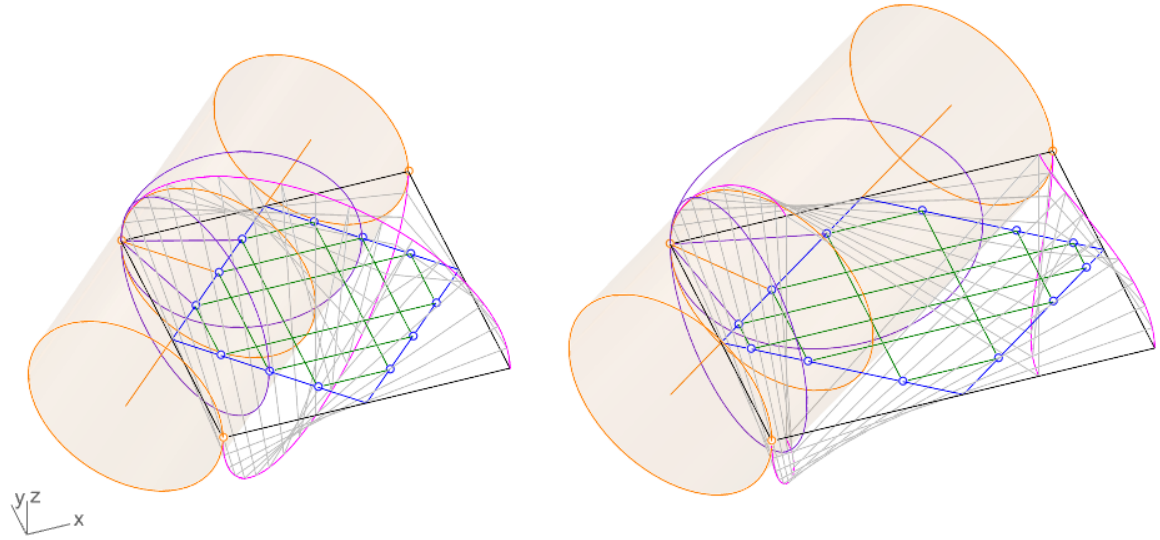

Figure 27: 3D analysis of square or rectangular inner frame (in)stability, showcasing the lengthening or shortening of tensile cables

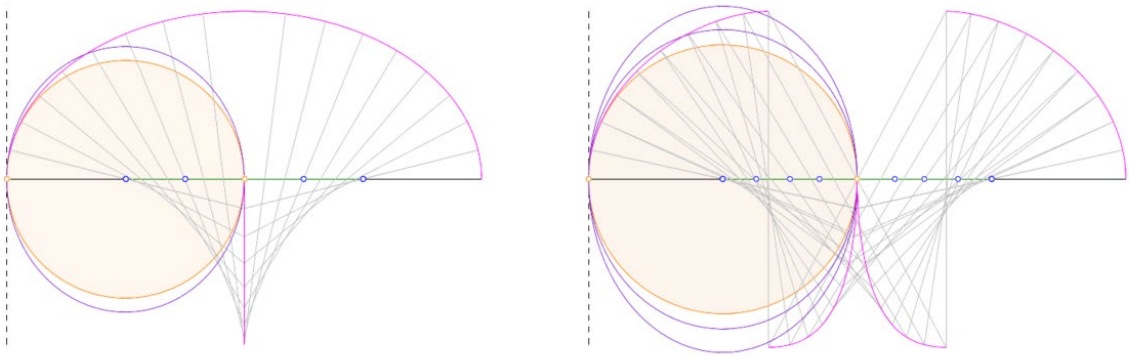

Figure 28: Projected 3D to 2D analysis of square or rectangular inner frame (in)stability, showcasing the lengthening or shortening of tensile cables

Offsetting the inner frame is where the system displays an interesting effect. The placement of the rigid inner frame has no effect on the system's stability whatsoever, only its size does. For example, a 1.6x1.6m rigid inner frame within a 3x3m panel with pin joints at the four outer corners is always stable, even if the inner frame is placed off-centre. This is better illustrated in Figure 29, which displays stable configurations in green and unstable configurations in red for both the left and right panels. The sizes of the frames remain unchanged; only their placement varies.

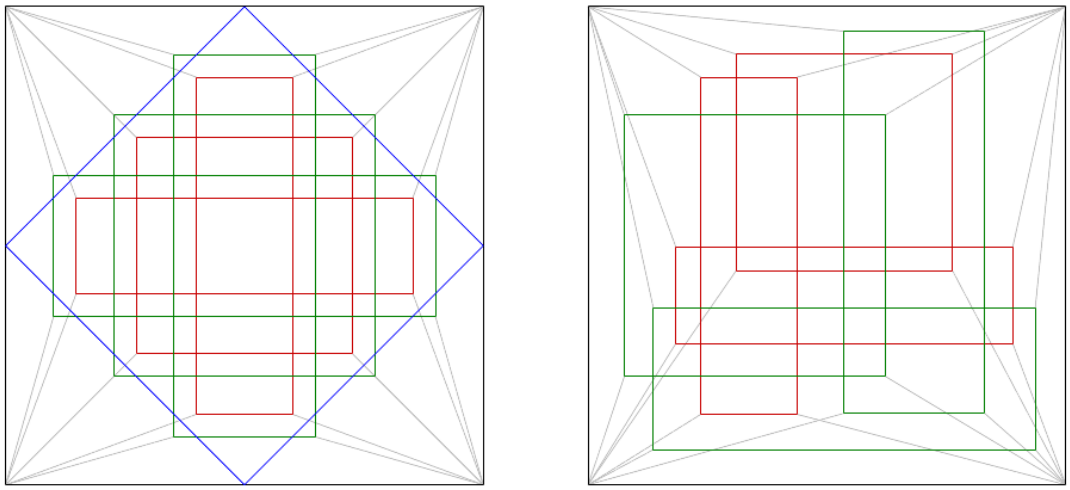

Figure 29: Potential stable and unstable configurations of the tensile system where only the inner frame's out of plane deformation is restricted

This effect can be understood through the average elongation or shortening of the cables and their potential movement toward a higher or lower energy state. Analysing the stable configurations necessitates an average elongation of the cables toward a higher energy state to deform the outer frame, while unstable configurations show the opposite, with average cable length shortening and moving toward a lower energy state when the outer frame warps.

In conclusion, the inner frame can contribute to the system's stability if, during the sizing process, its corners are positioned outside the equilibrium diamond (Figure 25). The further the corners are from the diamond, the greater the stability the inner frame can contribute to the systems overall stability. However, the subsequent placement of the inner frame has no effect on stability in the simplified model.

From a design perspective, this means that warping of the system can be prevented by either restricting out of plane movement of the corners of the outer frame, or of the inner frame if the inner frame is dimensioned correctly.

Corner and profile requirements

This analysis does not yet resolve how out-of-plane movement of the inner or outer frame can be effectively prevented. The most straightforward solution is to anchor the outer frame to the building's substructure using brackets at each corner. However, this approach may pose challenges when considering seismic activity or wind-induced

movement of the substructure, as a fully rigid connection between the unitized frame and the building may not cause damages to the façade finish.

An alternative approach is to design a fully rigid outer and potentially inner frame that can maintain its structural integrity independently of the substructure. To investigate this possibility, an exaggerated deformation model of the façade panel was created, illustrating how both the inner and outer frames may warp under load. The model underscores the need for corner connections and profile sections capable of resisting both torsion and bending.

In the following figures, the left side presents a perspective view of the deformed system, while the right side shows a view along the normal axis of a pair of inner and outer struts. The undeformed configuration, projected onto the X and Y plane, is shown in grey for reference. While the illustrations show the bending and torsional behaviour of the outer frame, the same principles can be applied to the inner frame, as it is geometrically similar and essentially a scaled version of the outer frame.

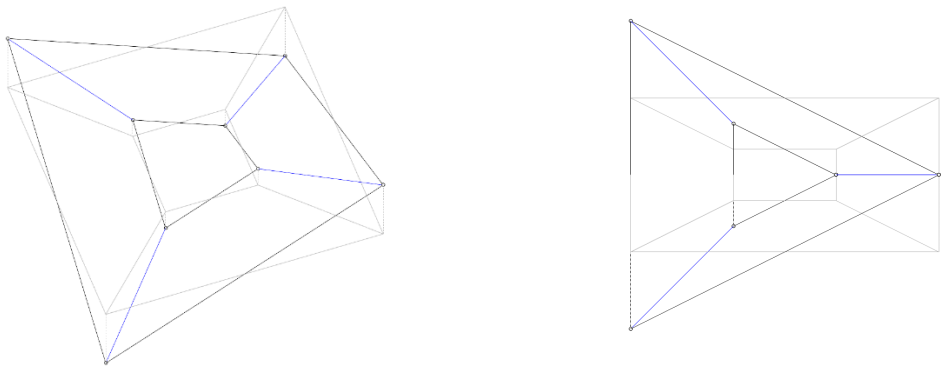

Figure 30: Exaggerated deformation of a symmetrical tensile façade panel. The left image shows a perspective view, while the right displays a view along the normal axis of a pair of inner and outer struts.

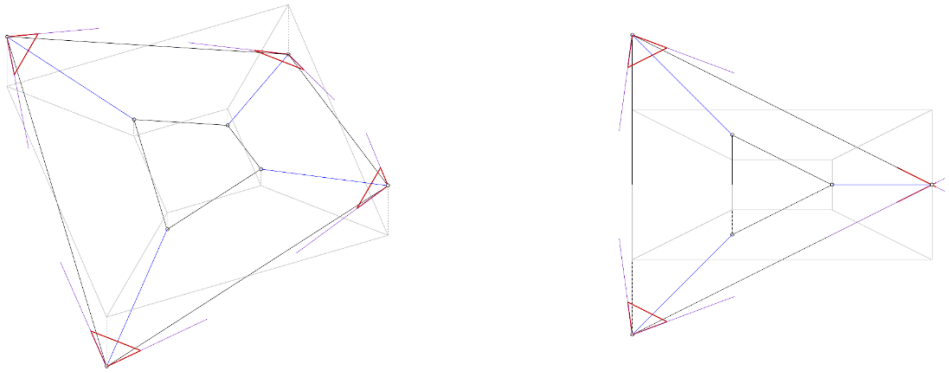

Figure 31: A change in angle at the corners is visible, and along the normal direction, a noticeable change in rotation as well.

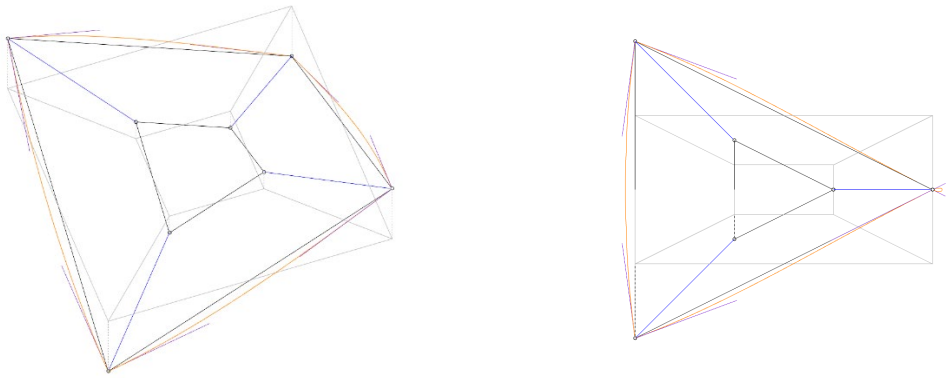

Figure 32: An orange line is drawn tangential to the 90-degree corners, simulating rigid corner profiles, this now indicates bending in the profiles will occur.

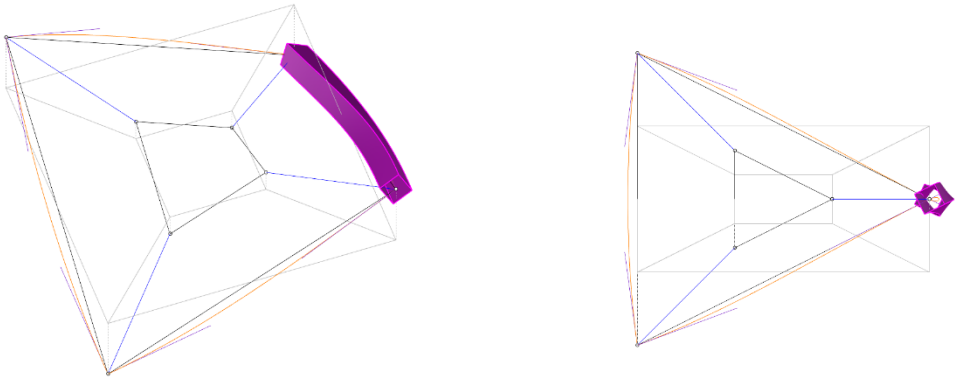

Figure 33: Extruding a profile along the orange line now clearly illustrates how the profiles will be subjected to bending and torsion.

3.1.3 Exploring pretensioning sequences and the use of pullies

As revealed by the system equilibrium simulations, symmetrical configurations result in equal tensile forces across corresponding cables. In cases of horizontal, vertical, or full symmetry, at least two, if not all, cables exhibit identical pretension, assuming the self-weight of the inner frame is neglected. This opens up an interesting opportunity: the potential use of pulleys or mechanical linkages to distribute tension evenly throughout the system. Such an approach could simplify the pretensioning process, potentially requiring only a single connected cable to be actively tensioned to achieve the desired tension levels across all cables, thereby reducing installation or manufacturing time.

Once again, the Kangaroo plugin in Grasshopper is used to simulate pretension by modelling the cables as artificial springs. In the following figures shown, unless otherwise stated, only the right-most cables are tensioned, indicated in green in (Figure 34). The red geometry represents the deformed frame, while the grey lines show the initial,

undeformed configuration. As before, the tension values have been intentionally exaggerated to amplify movement for illustrative purposes and to clearly demonstrate the structural behaviour under partial pretensioning.

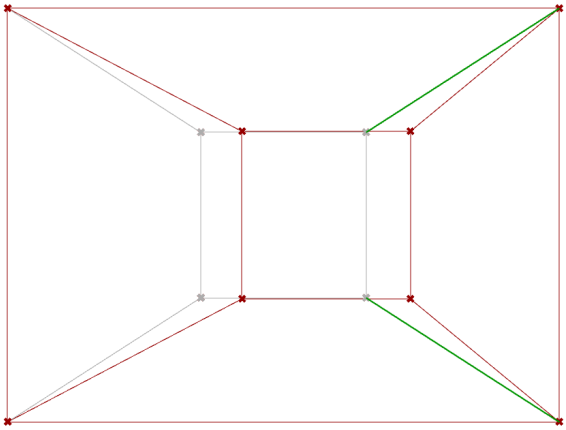

Figure 34: Tension is applied to the right most cables, shown in green.

When the cables are tensioned equally, simulating a pulley system shared between the two right-most cables, the inner frame begins to rotate as soon as it is positioned off-centre along the axis of the tensioning cables (Figure 35). This behaviour is expected, as equilibrium cannot be maintained in such a setup, since the cables are assumed to carry only axial loads.

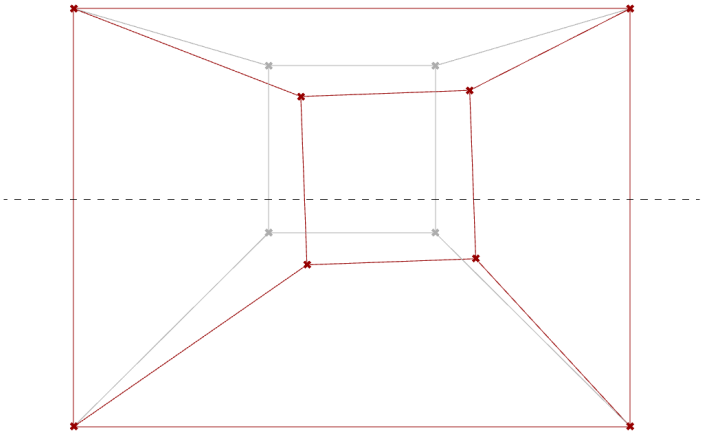

Figure 35: Rotation of the inner frame when placed off-centre in a pully setup.

Adjusting the pretension in the left-most cables does not resolve the observed rotation, unless of the forces happen to balance out to the exact middle of the frame (Figure 36). Indicating that only the distance from the symmetry axis in a pully system governs the rotation of the inner frame.

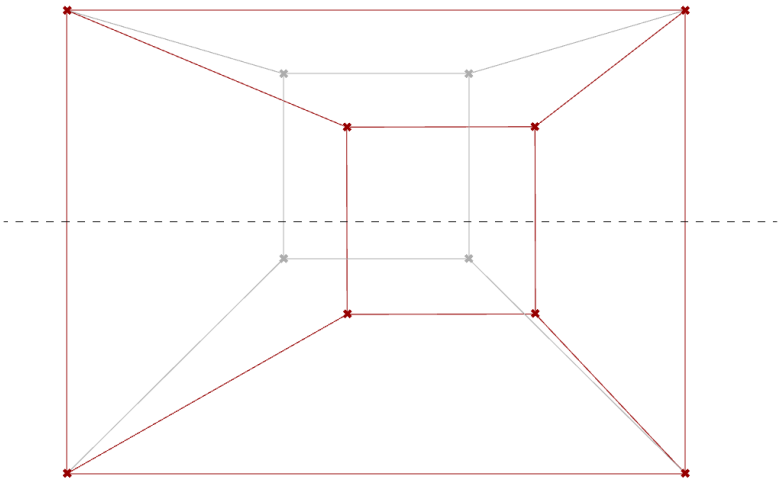

Figure 36: Changing the forces of the other cables to equalize the frame along its symmetry axis.

Similarly, adding a weight to the inner frame now highlights the asymmetry from the vertical axis, now that a vertical component acts on the system, a rotation is observed in a pully system where the right most cables are in equal tension (Figure 37).

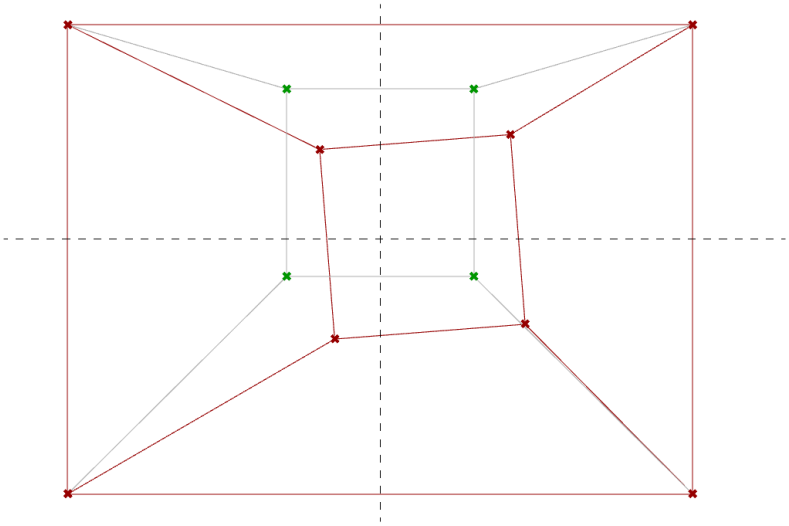

Figure 37: Adding a weight to the inner frame highlights how vertical symmetry also plays a role when a vertical force is applied.

Thus, the only viable pulley configuration that avoids unwanted rotation of the inner frame is one in which either the top or bottom pair of cables is tensioned, with the inner frame centrally aligned along the system's vertical symmetry axis. This arrangement ensures that the tension forces remain balanced even with an applied weight to the inner frame, preventing rotational moments. However, the pulleys would preferably need to be locked in place after pretension is applied, as any force along the facade could otherwise cause the inner frame to slide along the pulley system, reducing overall stability (Figure 38). Additionally, when two of the cables are connected continuously,

effectively forming a single longer cable, the stiffness of the system decreases. This is because a longer cable requires less force to the produce the same amount of strain.

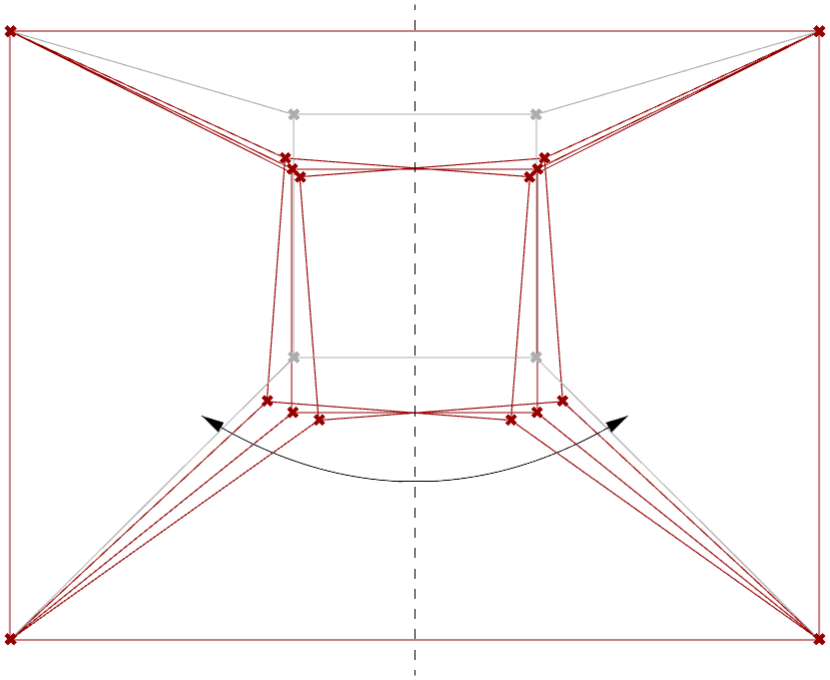

Figure 38: A frame setup where the bottom two cables are connected via a pully setup, highlighting the potential sliding during a sideways excitation of the façade.

To conclude, in practice, the most feasible and reliable solution is likely one in which all cables are tensioned individually, allowing pretension to be applied incrementally to each cable, either sequentially or simultaneously, provided that tension levels or the deformation of the inner frame can be accurately monitored or is managed with sufficient design tolerances. This approach minimizes the risk of unwanted deformations, which could introduce stress into components not designed to carry the tensile forces. Additionally, the use of pulleys is generally inadvisable, as that would cause significant rotation of the inner frame. Even in symmetrical configurations it is inadvisable, as the cables should be locked in place after tensioning to prevent potential movement and a decrease in stiffness, which is likely difficult and expensive to detail.

3.1.4 Designing for durability

To ensure that the façade panel remains structurally sound and effective in resisting out-of-plane deformations, it is important to consider the effects of vibrations, fatigue, and other factors that can lead to pretension losses.

Vibrations

As discussed earlier, a common design guideline is to avoid natural frequencies below 10 Hz for façade systems, as the panel is more likely to be excited by wind-induced vibrations.

In tensile systems, the natural frequency can be adjusted in three primary ways:

- Increasing the pretension in the cables,
- Reducing the mass of the inner frame and cables,
- Altering the overall size (length) of the frame and cables.

This relationship is reflected in the equation for the fundamental natural frequency of a tensioned string, as seen in systems like musical instruments (Greminger, March 12, 2023).

$$f = \frac{1}{2 \cdot L} \cdot \sqrt{\frac{T_0}{\mu}}$$

f : Frequency

L : Sting length

T_0 : Tension applied to the string

μ : Mass per unit length

From the formula can be derived that increasing the string length or mass per unit length decreases the natural frequency, whilst increasing the tension will increase the natural frequency.

Combined, these factors imply that for larger panel sizes or when using heavier cladding and glazing systems, certain design options may become infeasible. Alternatively, such configurations would require the application of higher pretension forces to effectively counteract the increased span and weight, which in turn may impose additional demands on the structural frame and anchorage system leading to high material demand.

Fatigue

Next consider fatigue, which occurs more rapidly when there is a high variability in forces, primarily in tensile members or connection points that exhibit tensile forces. While it is inherently impossible to eliminate tensile forces in a tensile-based system, it is advisable from a design perspective to minimise their fluctuation. One effective strategy is to apply a high initial pretension, which helps stabilise the system and reduces the second-order

effect of increases in cable tension, when the façade is subjected to lateral wind loads throughout its service life. By doing so, the system maintains a more consistent internal force distribution, thereby improving long-term fatigue resistance. For the same reasons, preventing resonance from external factors also improves fatigue life.

Pretension losses

When addressing pretension losses, whether they result from short-term effects or long-term mechanisms, the possible design strategies can be distilled into three clear approaches:

- Over-tension the system during prefabrication or installation, anticipating predictable losses so that the system remains sufficiently pretensioned throughout its service life.
- Design for accessibility and maintenance, enabling periodic inspection and re-tensioning of the cables to ensure that structural performance is maintained over time.
- Prevent tension losses from occurring in the first place, through careful detailing, minimizing the usage of viscoelastic materials or through usage of constant tension anchorage systems.

While over-tensioning and designing for accessibility are relatively straightforward, the third strategy, preventing tension losses, warrants further elaboration.

A primary approach to preventing these losses is to avoid the use of viscoelastic materials that are prone to long-term deformation. Steel, for instance, is often preferred due to its stable elastic properties over time, making it highly reliable for maintaining pretension.

In contrast, wooden components, present more challenges. Their creep behaviour is strongly influenced by grain orientation and moisture content. While engineered timber products such as glulam and LVL significantly reduce these effects, creep or relaxation can still occur, potentially leading to noticeable losses in pretension.

If wooden elements remain a design preference, for aesthetic, environmental, or other reasons, a practical mitigation strategy is to integrate a soft spring element into the system. This can help maintain pretension over time by absorbing slow deformations and compensating for tension losses.

This approach can sometimes be seen in post-tensioned concrete anchorages, where large steel coil springs are visibly installed around tendon bundles to ensure ongoing force retention despite time-dependent material behaviour (Figure 39).

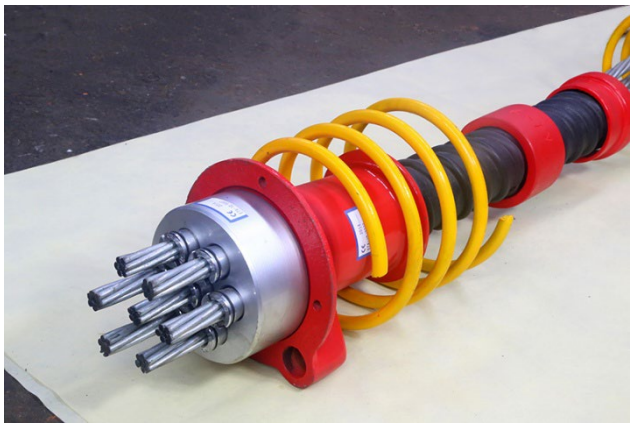

Figure 39: Multi Strand Round anchor (image source: https://beta-technical.com/post-tension-anchorages/)

The principle on why this works can be identified when 2 springs are placed in series. The equivalent spring constant of 2 springs in series is as follows:

$$\frac{1}{k_{eq}} = \frac{1}{k_1} + \frac{1}{k_2}$$

k_{eq} : The equivalent spring constant

k_1: Spring constant 1

k_2: Spring constant 2

If one of the two springs in a series system has a low spring constant, the resulting equivalent spring stiffness for the system will also be low. Applied to the context of a tensile façade, this means that when the outer frame is constructed from wood, prone to relaxation and creep, the introduction of softer springs at the cable anchor points could help mitigate pretension losses over time.

However, this reduction in system stiffness also dampens second-order effects, particularly the increase in pretension that typically results from cable elongation under loading. While this can reduce peak force spikes, it may also diminish the system's ability to self-stiffen under deformation. As a result, it could have a negative impact on the overall out of plane resistance of the system.

Each of these strategies involves trade-offs between reliability, constructability, and long-term maintenance requirements, and the appropriate choice will depend on the specific application and performance demands of the system.

3.1.5 Designing for material efficiency

From a structural perspective, there are two primary strategies to improve the material efficiency of the system when subjected to out-of-plane wind loads. The first is to permit larger deflections of the façade panel, thereby increasing the out-of-plane component of the tensile members and reducing the internal force required to maintain structural equilibrium. The second is to employ geometrically efficient profiles for the compression elements, optimised to resist axial and bending and potentially torsional forces in configurations where the panel is not secured to the substructure at all four corners.

Focusing first on deflection, designing for larger allowable displacements can be challenging and requires careful detailing to avoid serviceability issues. In line with common serviceability criteria used in façade engineering, deflection is typically limited as a function of the element's spanning length. This is often expressed as a ratio such as l/360, span/360, or 1/360 of the span, depending on the standard referenced. For example, a façade panel with a height of 3.6 m that is permitted to deform by 10 mm corresponds approximately to l/360.

In practice, acceptable deflection limits typically range from l/500 to l/50, with the appropriate value depending on factors such as the type of surface finish, tolerance for visual movement, and overall design intent. Chapter 16 of the 2018 International Building Code (IBC) provides specific guidance:

- l/360 for finishes like plaster and stucco
- l/240 for other brittle finishes
- l/120 for flexible finishes

While Eurocode EN 1991-1-4 does not prescribe exact deflection thresholds, it highlights the importance of establishing project-specific serviceability criteria as part of the design process.

As described in Section 2.2.3, cable-stayed façades typically take advantage of large deflections to activate the lateral stiffness of the cable net system. These systems are intentionally designed to deform significantly under load and often operate at deflection limits as high as l/50, far exceeding those used for more rigid façade systems.

Applying this knowledge to the unitised tensile façade panel, similar deflection limits may need to be considered, as imposing stricter deflection limits could necessitate very high pretension forces. This, in turn, would require heavier and more robust compression elements, potentially undermining the material efficiency and practicality of the system.

That brings us to the second key aspect of designing a material-efficient system: selecting compressive members that are effective at resisting buckling and bending, and additionally, in some cases, torsion in unsupported frame conditions where global stability must be ensured through rigid members and connections.

While these compressive elements can be manufactured from wood, steel, or even reinforced concrete, some cross-sectional shapes inherently perform better under combined actions like axial compression, bending, and torsion. This is especially evident in the case of steel profiles, which are often specifically engineered for optimal performance under particular loading scenarios.

If the goal is to resist pure axial compression while minimising material use, the most important factors to consider are the slenderness ratio and the minimum moment of inertia. In such cases, circular or square (CHS SHS) sections are highly efficient due to their symmetrical geometry, offering equal stiffness in all directions and a high resistance to global buckling.

For axial compression and uniaxial bending, I-sections (such as IPE or HEA profiles) can be highly efficient. These shapes offer a high second moment of inertia about their strong axis, making them ideal for uniaxial bending with efficient material use. However, they are less suitable for bi-axial bending and possess low torsional rigidity. In the context of the tensile façade system, where compression elements are likely to be slender and unbraced, lateral-torsional buckling becomes a significant concern. In such cases, I-sections may become prone to instability, even under moderate loading. An alternative is to use rectangular hollow sections (RHS), which provide higher torsional stiffness and a more uniform resistance to bending in both principal directions, offering a more robust solution for unrestrained compression members.

When designing for axial compression, bending, and torsion simultaneously, the profile must resist complex interactions between these forces. In such cases, closed sections, like rectangular hollow sections (RHS) or circular hollow sections (CHS), are preferred, due to their high torsional rigidity and uniform stiffness in all directions.

This, in turn, raises a great challenge for the design of the thermally broken struts proposed in the patented system, particularly in cases where high torsional resistance is required. Closed sections, such as rectangular or circular hollow sections, are

significantly more effective at resisting torsion than open profiles like I-beams when the centre of twist is within the profile. In fact, the torsional stiffness of closed sections is approximately two orders of magnitude greater than that of open sections with comparable area (Figure 40). This means that, for similar profile lengths and applied torsional moments, open sections will experience around 100 times more rotational deformation compared to closed sections of comparable cross-sectional area.

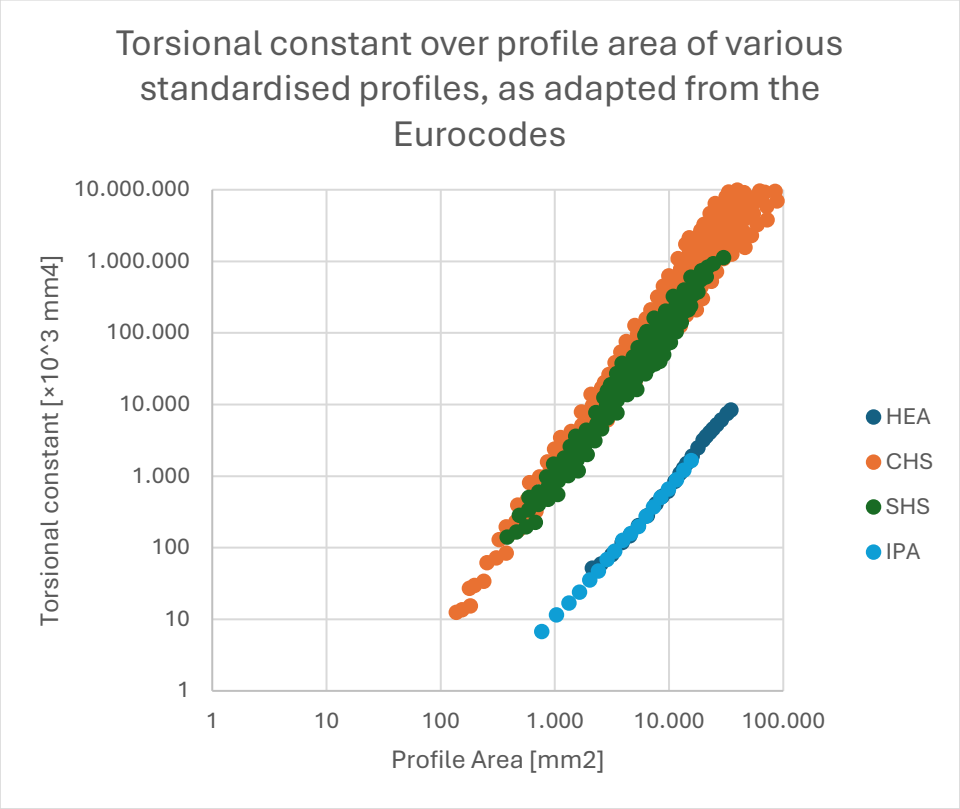

Figure 40: Torsional constant over profile area of various standardised profiles, as adapted from the Eurocodes

As a result, designing a thermally broken profile that preserves both the mechanical continuity and thus torsional capacity of a hollow section presents a significant engineering challenge. Even when using two symmetrical hollow sections on either side of the thermal break, the resulting assembly may still exhibit poor torsional rigidity, as the centre of twist lies outside the combined profile.

3.2 Potential benefits of the system

As stated in the patent, the proposed invention seeks to overcome the conventional trade-off between structural rigidity and lightweight design by enabling the fabrication of façade elements that are both lightweight and resistant to out-of-plane forces such as wind. Additionally, it aims to achieve high thermal performance within a thin construction through the integration of a thermal break (Montali, 2021).

However, based on exploring some of the structural principles, it appears that the tensile system may not inherently provide high out-of-plane stiffness while maintaining a lightweight profile. Similar structural systems, such as cable net façades, typically require large deformations before developing significant resistance to out-of-plane loads.

Nonetheless, if deflection limits are relaxed, the system could remain lightweight while achieving high load-bearing capacity at larger deformations. This aspect requires further detailed analysis.

Beyond structural efficiency, the system presents several additional potential advantages:

- Reconfigurability: The cable configuration allows for repositioning or reconfiguration of the internal frame during the panel's lifecycle, enabling significant portions of the structural system to be reused at end-of-life.
- Remanufacturability: Since the outer frame geometry is uniform, standardized or existing profiles could be employed, enhancing reuse potential and contributing to sustainability goals.
- Prefabrication potential: The frame could be detailed similarly to other unitized curtain wall systems, with gaskets around the perimeter, enabling a high degree of prefabrication and reduced on-site installation time.
- Space efficiency: The integration of a thermal break could allow the façade panel to be thinner than conventional solutions, potentially increasing usable floor area, a key factor of interest to developers and investors seeking to maximize rentable space.

These potential benefits must be critically assessed against the system’s drawbacks before a holistic evaluation of the façade panel’s performance can be completed.

4. Structural Modelling and Simulations

4.1 Excel Model Predictions

To predict the deformation of the tensile-based façade system under perpendicular wind loads, an Excel model was constructed. This model can analyse the theoretical deformation of a single cable or, when the system is configured symmetrically, the overall behaviour of the tensile-based façade. This model assumes that the height and width of the inner and outer frames are equal, and that the inner frame is placed perfectly centrally.

4.1.1 Background information for the Excel model

The model is based on Hooke's Law and Pythagoras's Theorem, which together are used to calculate the force reaction resulting from the elongation of the cables.

Pythagoras's Theorem is used to determine the elongation of the cable when subjected to an out-of-plane deformation. By comparing the original and deformed lengths of the cable, the model calculates the change in length (ΔL).

Hooke's Law describes the linear relationship between force and deformation in elastic materials. It states that the force F needed to stretch or compress an object is proportional to the change in length ΔL, as long as the material stays within its elastic limit. For a structural element under axial load, stress σ is defined as force over area $\sigma = F/A$, and strain ϵ is the relative deformation $\epsilon = \Delta L/L$. According to Hooke's Law, $\sigma = E \cdot \epsilon$, where E is Young's Modulus. Substituting these definitions gives $F/A = E \cdot (\Delta L/L)$. Multiplying both sides by A leads to the derived formula:

$$F = \frac{\Delta L \cdot A \cdot E}{L}$$

In the model, the force is explicitly modelled as acting on only half of the cable, effectively treating the cable as being "cut in half." In practice, if a cable setup such as the one depicted in Figure 42 were to deform, twice the modelled force would be required.

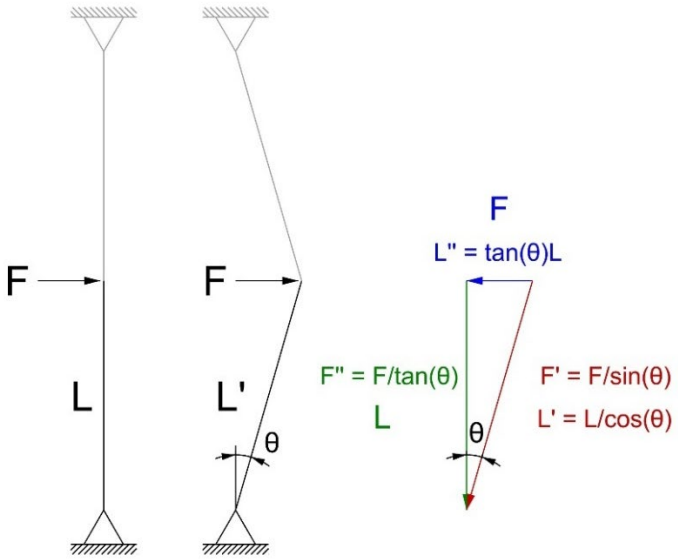

Figure 41: Elongation of the cable caused by force F

This simplification is valuable because, in a tensile façade system, a symmetrical setup can be effectively represented by four half-length cables. It is assumed that both the inner and outer frames are sufficiently stiff, such that they do not experience significant elongation or contraction under load. So, the connection points in the Excel model are treated as rigid.

Even if minor shortening of the outer frame does occur, it would primarily affect the overall spring stiffness of the cable system, without significantly altering the position of the connection points.

This modelling approach allows for quick and effective analysis of the influence of key variables, including cable cross-sectional area, Young's modulus, pretension, and deformation behaviour.

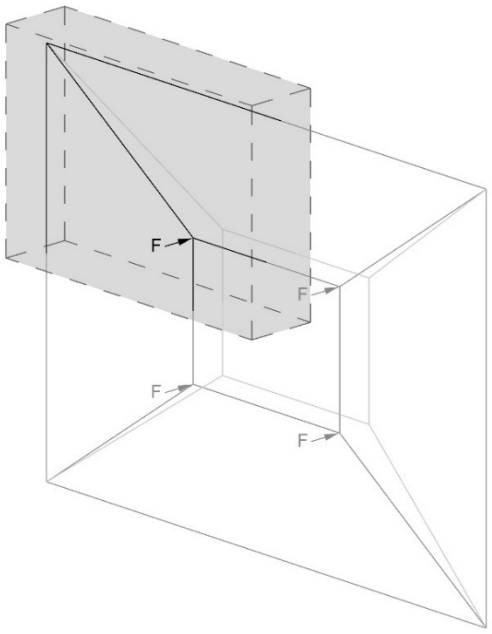

Figure 42: Representation of a fully symmetrical system consisting of 4 half cut cables

For all subsequent diagrams, a symmetrical system is assumed, with an outer frame size of 3x3 m and an inner frame size of 1x1 m. This configuration results in a cable length of $\sqrt{2}$, or approximately 1,414 m.

To improve clarity in the diagrams, all half-length cables will now be referred to as spokes, and the point at which the force is applied, i.e., the inner frame, will be referred to as the hub, drawing an analogy to the structure of a bicycle wheel.

Additionally, to some of the graphs, orange dots have been added to further improve readability. These markers indicate specific levels of system deformation, expressed relative to the overall span. For example, a deformation level of span/100 (or l/100) in a 3x3 m system corresponds to a total displacement of 30 mm.

To determine the wind pressure the facade will be exposed to, one can again refer to the EN 1991-1-4 guidelines. According to these, typical wind pressure values range from 0.5 to 2.5 kPa, depending on factors such as building height, location, and terrain category (Figure 43 & Figure 44).

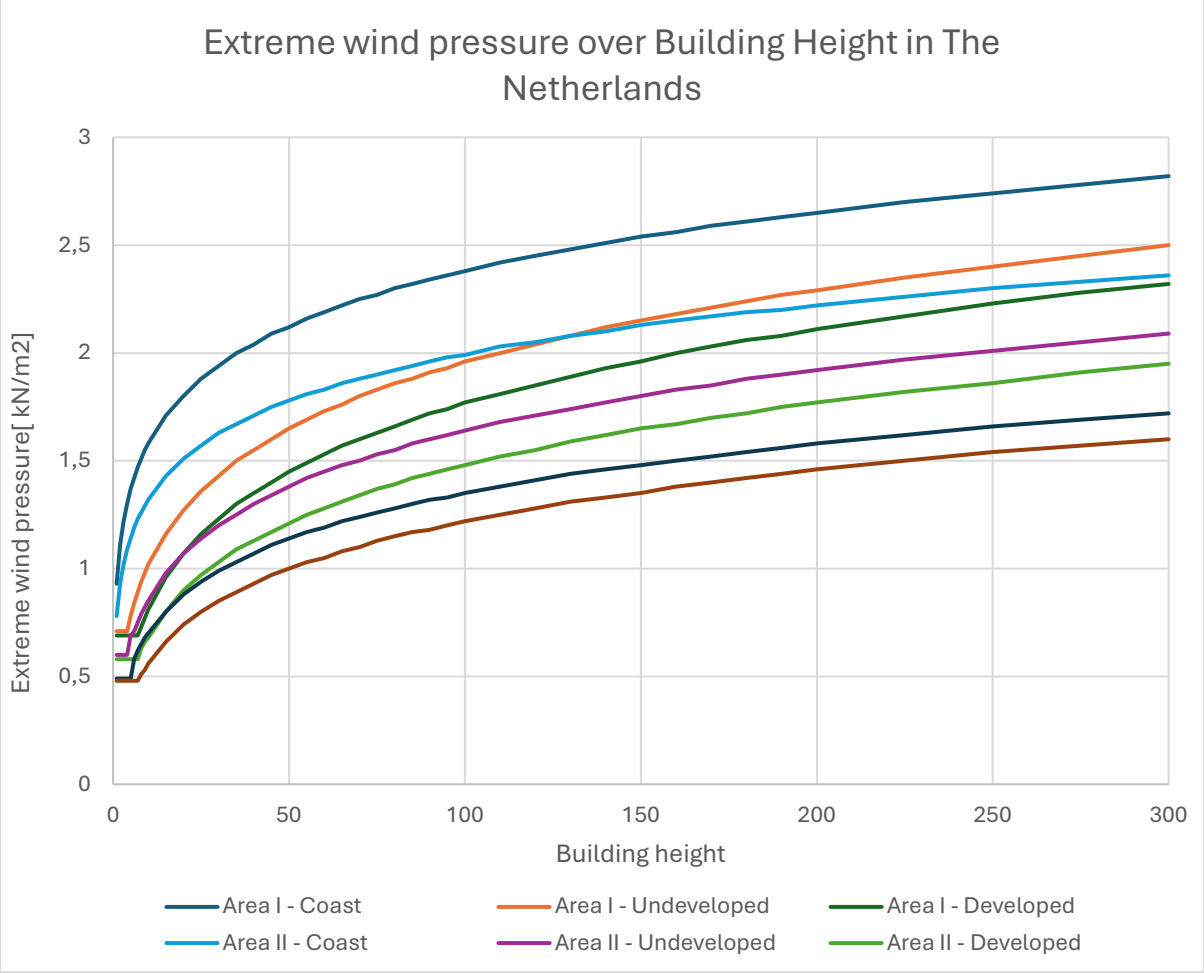

Figure 43: Extreme wind pressure values in The Netherlands (EN 1991-1-4)

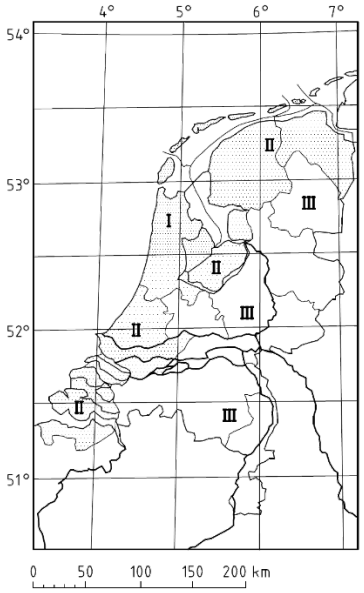

Figure 44: Wind areas in for determining extreme wind pressure in The Netherlands (EN 1991-1-4)

As a reference case for the remainder of this section, a wind load of 1 kPa is used. This value corresponds to conditions for a building approximately 15 m in height, situated in an open, undeveloped area in Area II.

Assuming each spoke corresponds to a facade area of roughly 1 m^2 in the 3x3 m system, each spoke must therefore be capable of resisting a maximum perpendicular force of approximately 1 kN under these conditions.

4.1.2 Understanding the effects of Spoke area, Young's modulus, pretension, and deformation

With the model setup and explained, and the exemplary force that each spoke must resist established, the model can be used to explore the influence of key parameters, spoke diameter, Young's modulus, pretension, and deformation, and demonstrate how these factors can be balanced to achieve the required perpendicular resistance of 1 kN.

Firstly, the relationship between spoke elongation and hub deformation is purely geometric and can be easily determined using Pythagoras's theorem. This relationship is illustrated in Figure 45.

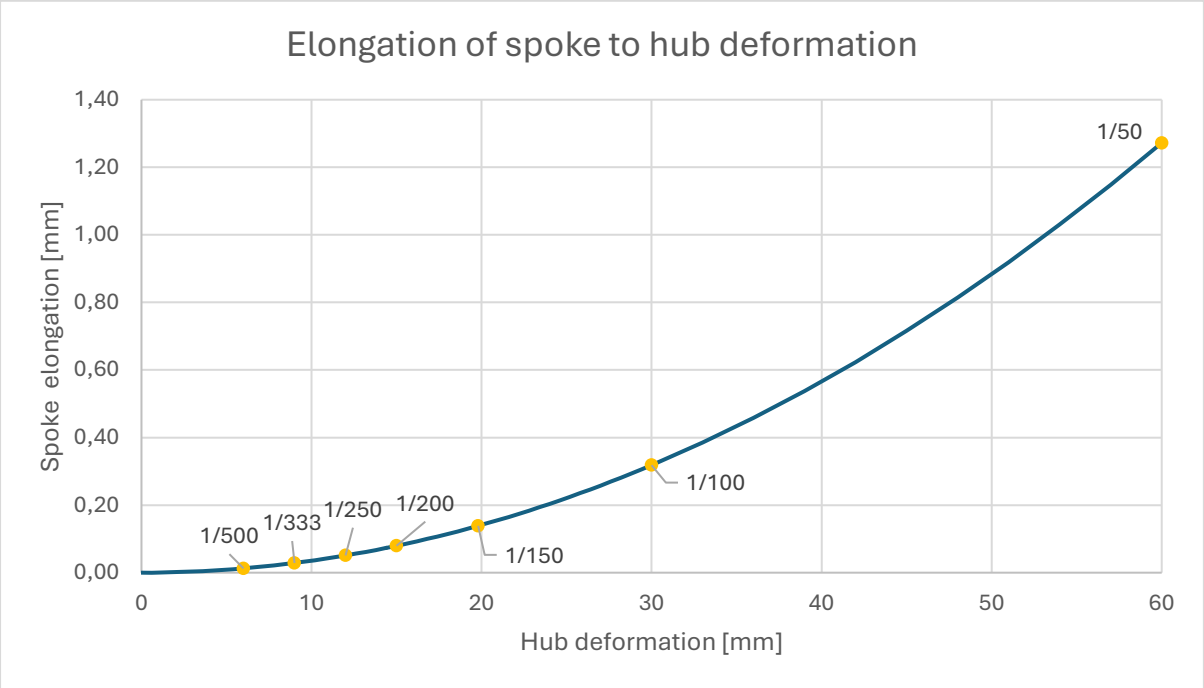

Figure 45: Elongation of spoke to hub deformation

Secondly, the relationship between spoke cross-sectional area and Young's modulus is examined for systems without pretension. According to the formula, both parameters have a linear influence on the resulting force, which becomes evident when analysing the results shown in Figure 46 & Figure 47. The force can be understood as the elongation of

the cable multiplied by a constant factor, determined by the product of the cable's cross-sectional area and its Young's modulus.

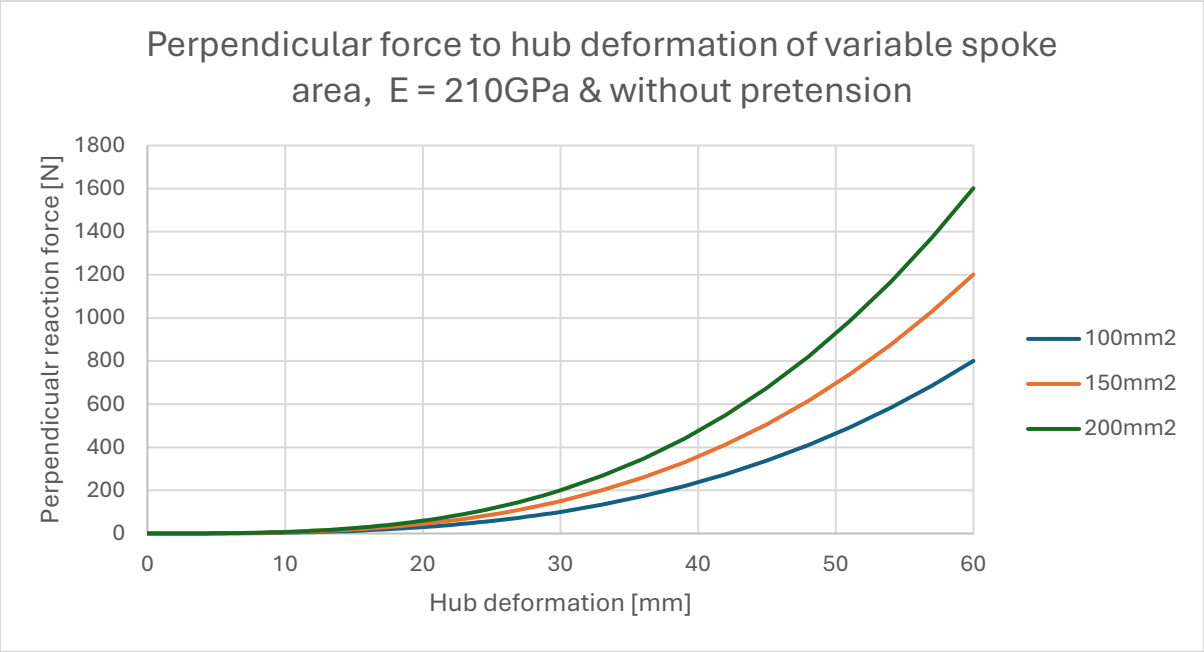

Figure 46: Perpendicular force to hub deformation of variable spoke area, E = 210GPa & without pretension

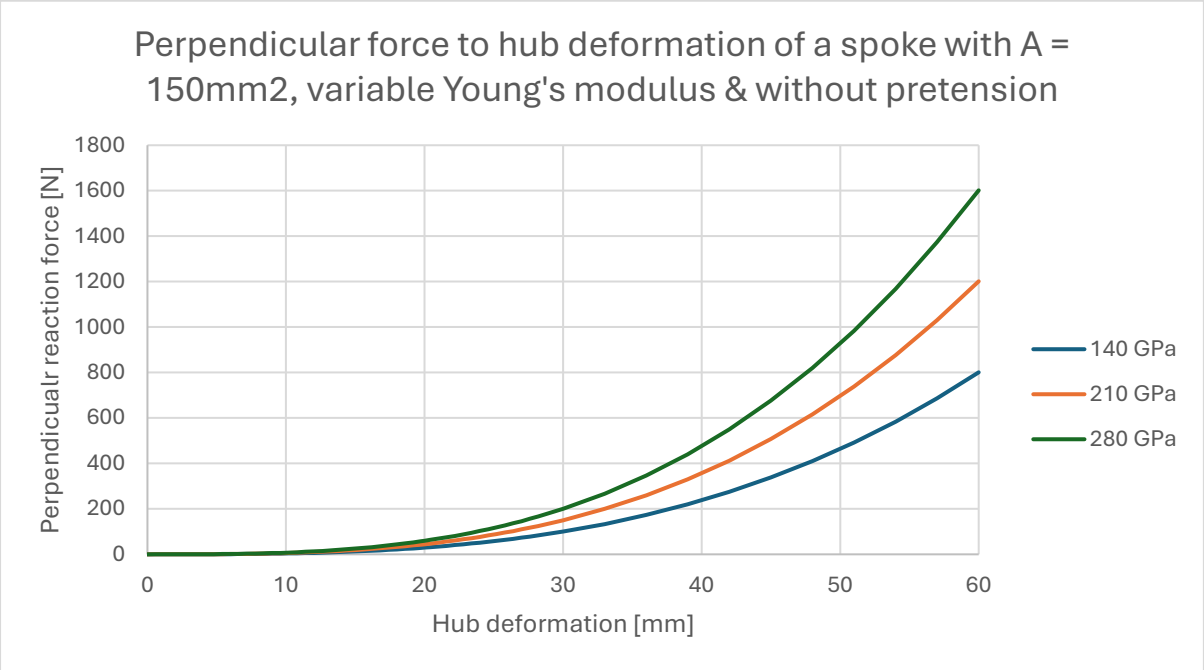

Figure 47: Perpendicular force to hub deformation of a spoke with A = 150mm2, variable Young's modulus & without pretension

Next, pretension can be applied to the system. Starting with a cable cross-sectional area of 150 mm^2 and a Young's modulus of 210 GPa, the following values can be obtained for various levels of pretension (Figure 48).

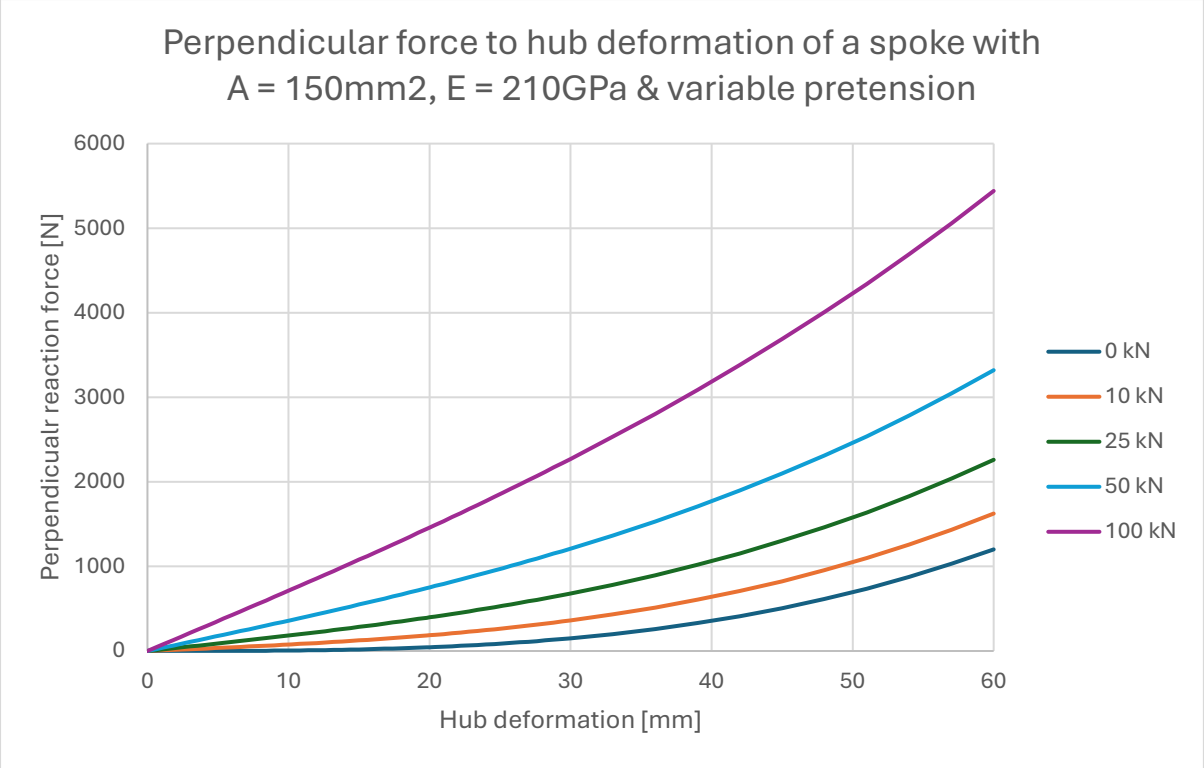

Figure 48: Perpendicular force to hub deformation of a spoke with A = 150mm2, E = 210GPa & variable pretension

An interesting observation is that at higher levels of pretension, the relationship between force and deformation becomes increasingly linear, and the influence of the product AE (Area x Young's Modulus) becomes less significant in determining system behaviour. This is because the pretension now dominates the response, effectively reducing the relative impact of the cable stiffness.

For instance, even when the cable elongates by 1.2 mm at a hub deformation of 60 mm, the tension in the cable remains relatively unchanged. This effect is especially noticeable at low deformation levels, where the additional strain in the spoke is minimal.

To illustrate this, the following comparison shows the behaviour of three cables subjected to a pretension of 100 kN, each with a different cross-sectional area, while maintaining a constant Young's modulus of 210 GPa. Additionally, a theoretical cable is included with an effective AE=0, further reinforcing the idea that increasing cable area at high pretension levels has a negligible impact on overall system stiffness. This highlights that, beyond a certain point, adding material is an inefficient strategy for improving structural performance under high pretension conditions (Figure 49).

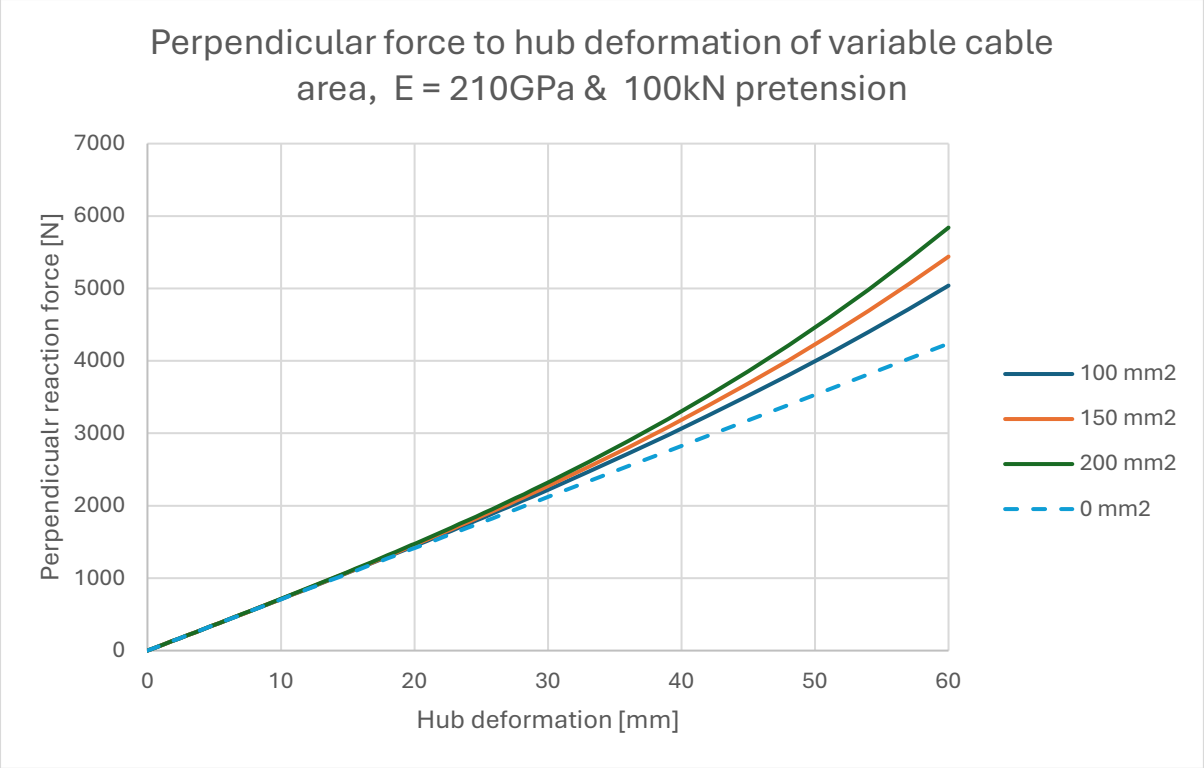

Figure 49: Perpendicular force to hub deformation of variable cable area, E = 210GPa & 100kN pretension

4.1.3 System material efficiency

In reality, no material could withstand the stresses implied by an $\lim_{A \to 0} AE$ condition, but the model highlights an important principle: at high levels of pretension, minimizing cable diameter is generally the most material-efficient strategy. As the increase in spoke tension is minimal at high prestresses and low deformation levels.

The most significant factor in determining overall material efficiency of the frame, however, is the ratio between the perpendicular (wind) forces and the horizontal (strut) forces transferred to the inner and outer frames. In practice, the spokes are supported by struts within the inner and outer frames, with the outer frame struts in particular acting as slender, compression-loaded elements. Due to their susceptibility to buckling, these components are by far the most material-intensive to manufacture. Consequently, minimizing the forces transmitted to these struts is critical for maximizing the material efficiency of the entire system.

To elaborate, refer to Figure 50 & Figure 51. These figures illustrate the behaviour of a spoke with a cross-sectional area of 150 mm^2, a Young's modulus of 210 GPa, and a pretension force of 100 kN. Figure 50 shows the relationship between hub deformation and the resulting perpendicular force in the spoke, while Figure 51 presents the corresponding horizontal force, i.e., the force experienced by the struts in the inner and outer frames, plotted against the same hub deformation. It's important to note that in

practice, the horizontal force will be shared between two struts at the connection point. In the current symmetrical configuration, this force could therefore be divided by $\sqrt{2}$ to reflect the distribution to the inner and outer frame struts. However, for simplicity, the values shown represent the full horizontal component aligned with the cable, without accounting for this division.

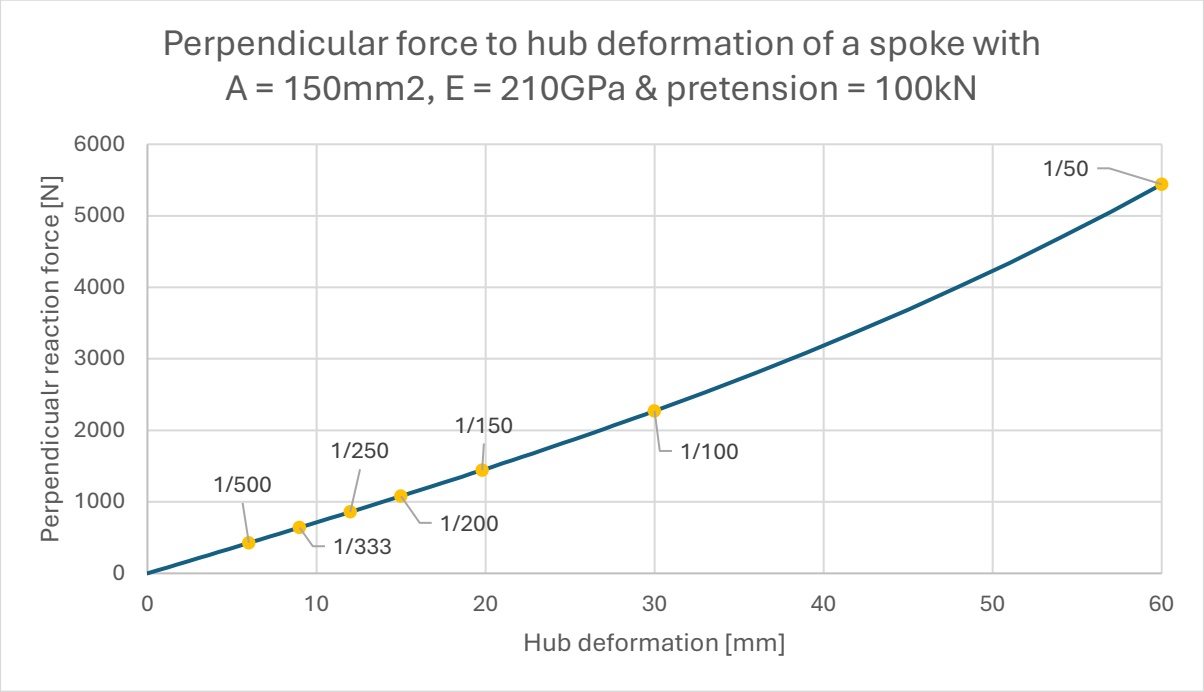

Figure 50: Perpendicular force to hub deformation of a spoke with A = 150mm2, E = 210GPa & pretension = 100kN

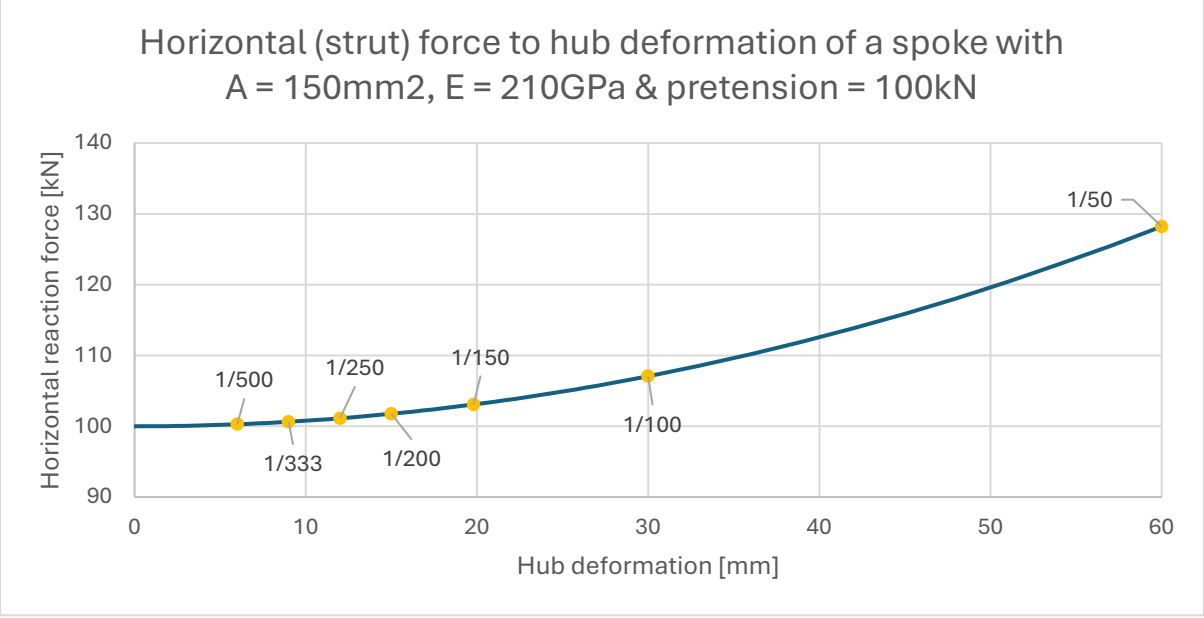

Figure 51: Horizontal (strut) force to hub deformation of a spoke with A = 150mm2, E = 210GPa & pretension = 100kN

A system using this configuration, designed to resist a load of 1 kN per spoke, would therefore deform by approximately 14 mm, corresponding to a deformation ratio

somewhere between span/200 and span/250. In this scenario, the forces in the struts would increase from roughly $\frac{100}{\sqrt{2}}$kN to $\frac{102}{\sqrt{2}}$kN, or approximately 70.7 kN to 72.1 kN.

To evaluate the material efficiency of this system, one can examine the ratio between the horizontal and perpendicular forces. This ratio is determined purely by the geometric configuration of the system and remains completely independent of pretension, cross-sectional area, or Young's modulus. As illustrated in Figure 52, the force distribution is only governed by the angle of the spokes, making the level of allowable deformation a critical factor in assessing the material efficiency of the entire system.

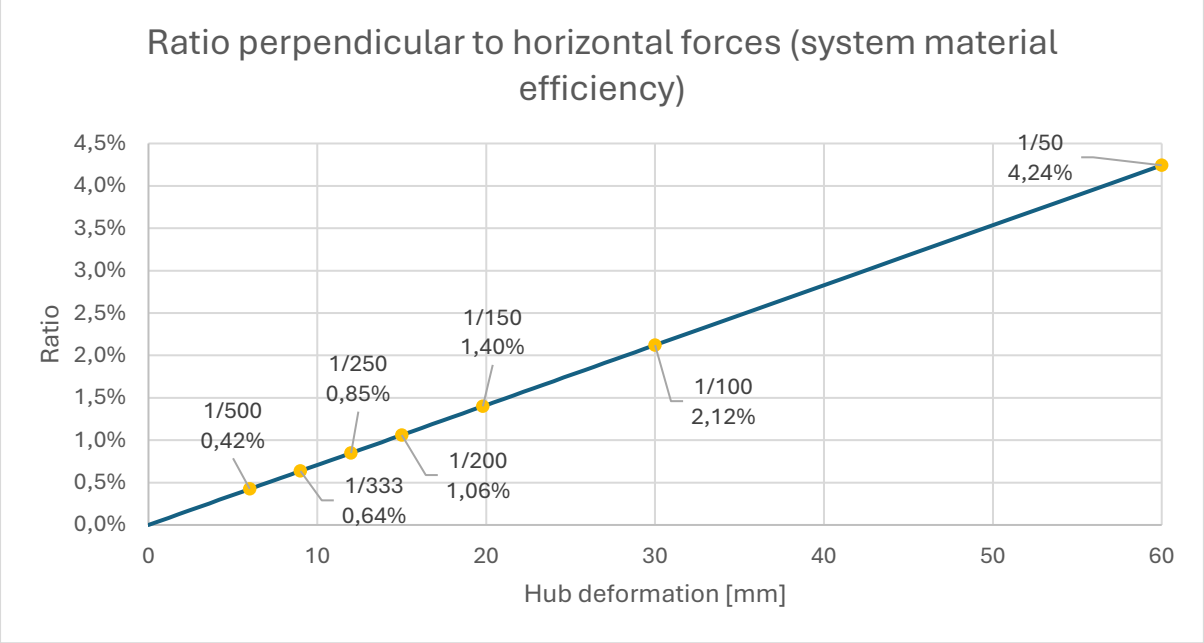

Figure 52: Ratio perpendicular to horizontal forces (system material efficiency)

Continuing the example, lowering the pretension of the system depicted in Figure 50 and Figure 51 from 100kN to 40 kN results in a hub deformation of 30 mm to achieve a perpendicular reaction force of 1 kN, or around span/100 (Figure 53). Correspondingly, the horizontal force increases from approximately $\frac{40}{\sqrt{2}}$kN to $\frac{47}{\sqrt{2}}$kN, or from roughly 28.3 kN to 33.2 kN. This illustrates how reduced pretension results in a greater deformation and depending on $A \cdot E$, a steeper increase in the horizontal load carried by the struts. Notice how it likely also leads to improved material efficiency, as the struts in the inner and outer frames are now required to resist less than half the force compared to the higher pretension scenario. This effect can again be observed by comparing the system's 'efficiency' at deformation levels around span/250 to span/200 and contrasting it with the 'efficiency' at span/100.

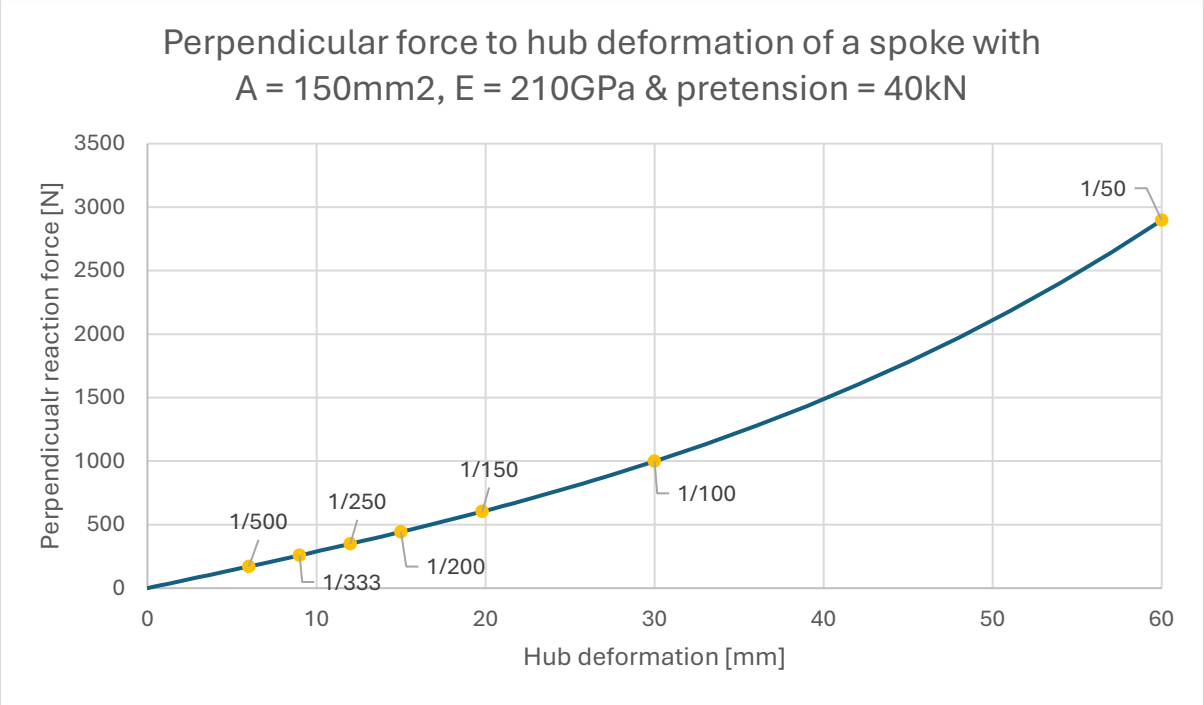

Figure 53: Perpendicular force to hub deformation of a spoke with A = 150mm2, E = 210GPa & pretension = 40kN

4.1.4 Potential system improvements by offsetting the spokes

It is now evident that increasing the angle of the spokes within the system is an effective strategy for reducing compressive forces in the outer frame, thereby enhancing the overall material efficiency. Based on this principle, an alternative configuration can be proposed: a system consisting of two symmetrical spokes. In such a setup, when a load is applied, one spoke would elongate while the other would shorten (Figure 54).

To maintain stability, the spokes would require an initially balanced pretension to prevent any displacement of the hub. Moreover, the pretension should be sufficiently high to ensure that the shortening spoke does not go slack during deformation, to prevent an unwanted change in the systems stiffness.

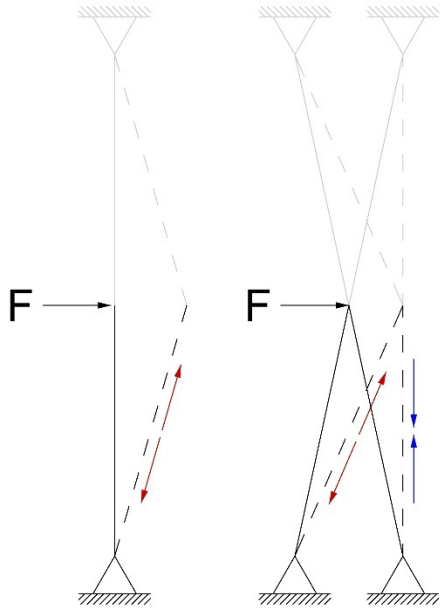

Figure 54: A potential system with two opposing spokes

An interesting aspect of such a system is that it can be optimized to achieve a desired out-of-plane resistance before one of the cables goes slack. This can be accomplished by adjusting key parameters such as the initial offset or angle of the cables, the level of pretension, and the cable stiffness ($A \cdot E$).

As an example, the following graphs assume that the connection points of the spokes are completely rigid (Figure 55, Figure 56, Figure 57). While this assumption does not fully reflect real-world conditions, it nonetheless provides a useful basis for understanding how the system can be optimized and highlights its potential advantages in terms of material efficiency and structural performance.

In this scenario, consider again the system with a 3 m span and a spoke length of $\sqrt{2}$m. Now with sets of spokes again required to resist a wind load of 1 kPa over an area of 1 m^2, corresponding to a necessary perpendicular resistance of 1 kN. In this variation, each spoke is duplicated and offset laterally by 10 cm to either side, resulting in an initial spoke angle of approximately 4,03 degrees.

Each spoke is pre-tensioned to 6 kN, with a cross-sectional area of 50 mm^2 and a Young's modulus of 210 GPa. Based on these parameters, the following three graphs illustrate the system's behaviour and performance under lateral load (Figure 55, Figure 56, Figure 57).

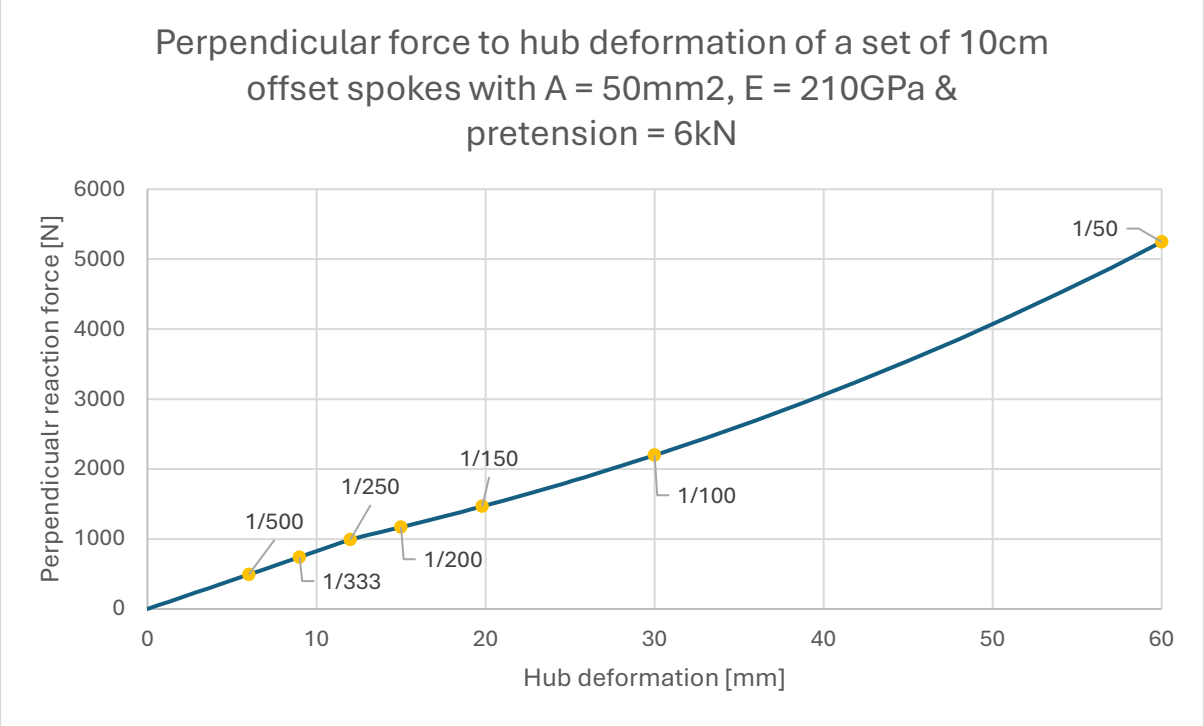

Figure 55: Perpendicular force to hub deformation of a set of 10cm offset spokes with A = 50mm2, E = 210GPa & pretension = 6kN

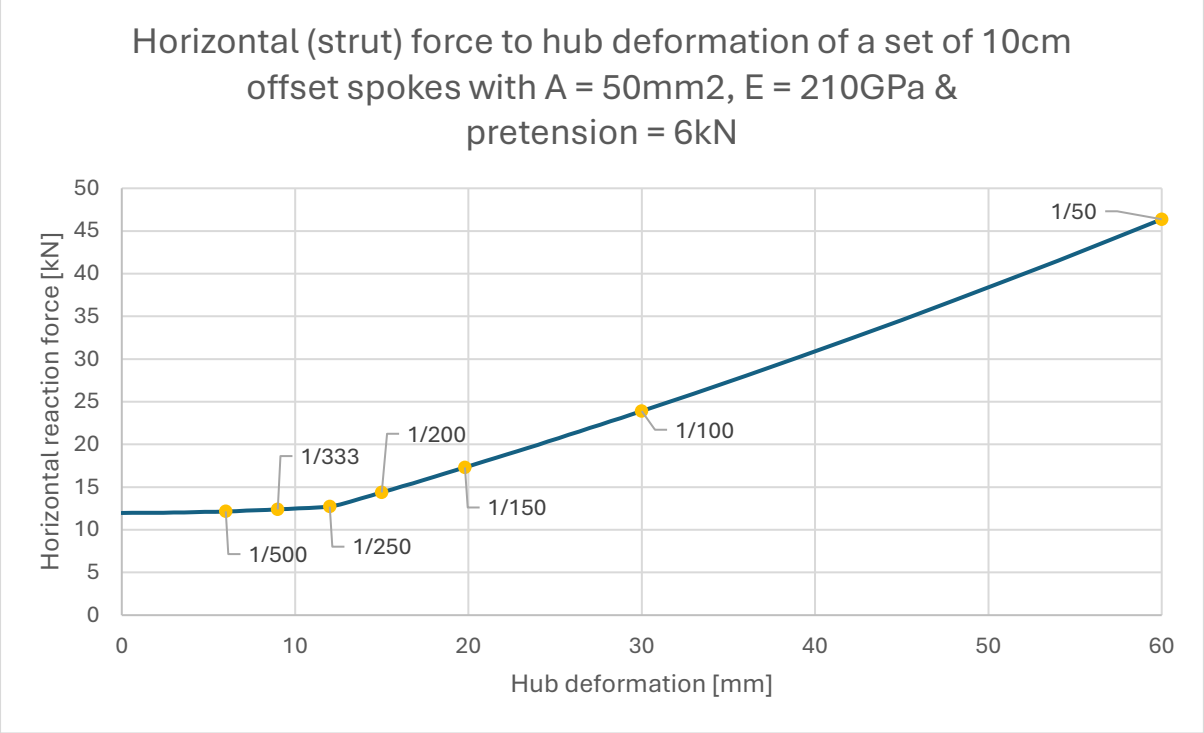

Figure 56: Horizontal (strut) force to hub deformation of a set of 10cm offset spokes with A = 50mm2, E = 210GPa & pretension = 6kN

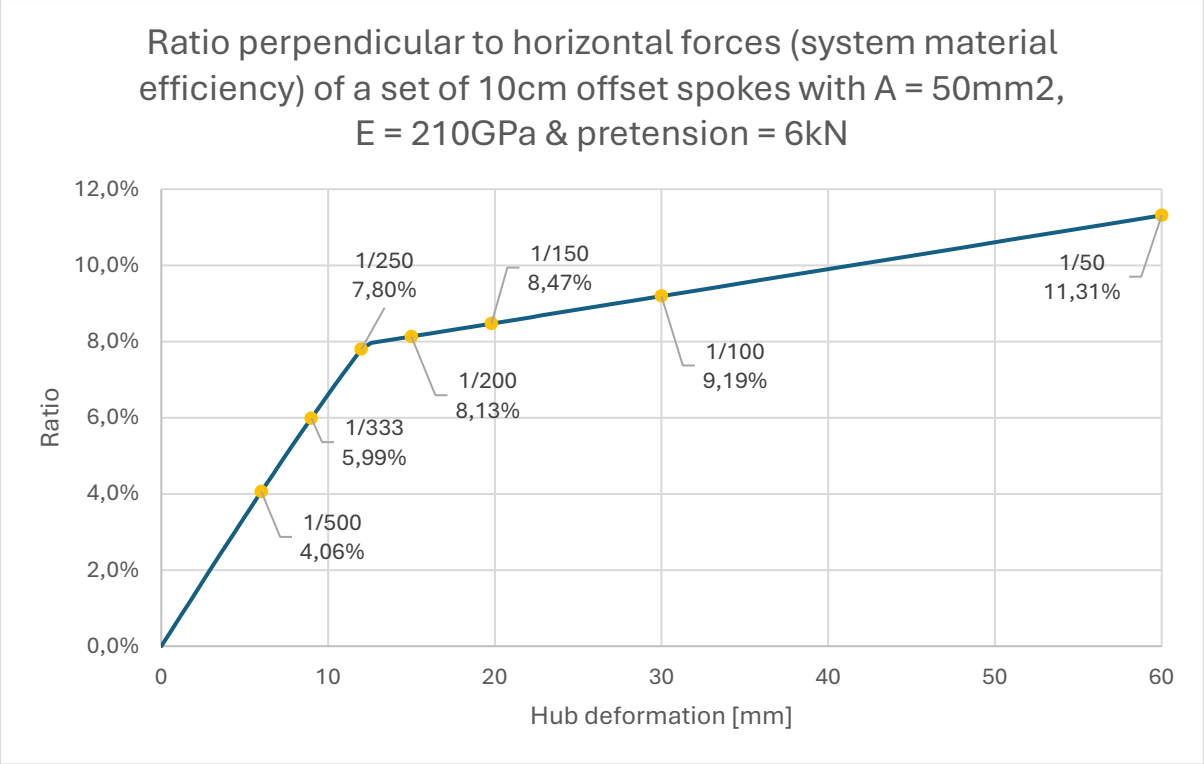

Figure 57: Ratio perpendicular to horizontal forces (system material efficiency) of a set of 10cm offset spokes with A = 50mm2, E = 210GPa & pretension = 6kN

A key observation from these results is the noticeable drop in the ratio between perpendicular and horizontal forces at approximately 12 mm of deformation, corresponding to a deflection of span/250. This marks the point at which one of the two spokes, specifically, the one that shortens under deformation, goes slack. Prior to this point, both spokes actively contributed to the system's out-of-plane resistance: one increasing in tension with its out-of-plane force component opposing the applied load, and the other decreasing in tension with its component oriented in the opposite direction.

What is particularly noteworthy is the substantial improvement in the system's potential overall 'material efficiency'. At a deformation level of span/250, the system achieves a perpendicular resistance of 1 kN with a total horizontal reaction in the struts of approximately 12.7 kN. This results in a perpendicular-to-horizontal force ratio of about 7.8%, compared to just 0.85% in the single-spoke configuration at the same deformation level.

Exploring variations in the system parameters provides valuable insight into how a double-spoke configuration can be effectively designed. One of the most influential parameters is the lateral offset of the spokes. Adjusting this offset impacts both the absolute perpendicular resistance and the ratio of perpendicular to horizontal forces,

while also slightly shifting the point at which one of the spokes goes slack (Figure 58 & Figure 59).

These effects can be fully attributed to the underlying geometric configuration of the system. As the initial angle of the spokes increases, the system demonstrates improved mechanical performance, with larger offsets resulting in greater lateral resistance and distribution and overall efficiency. Additionally, changes in the initial angle affect the extent to which each spoke elongates or shortens under deformation, which in turn explains the variation in the transition point at which one of the spokes goes slack.

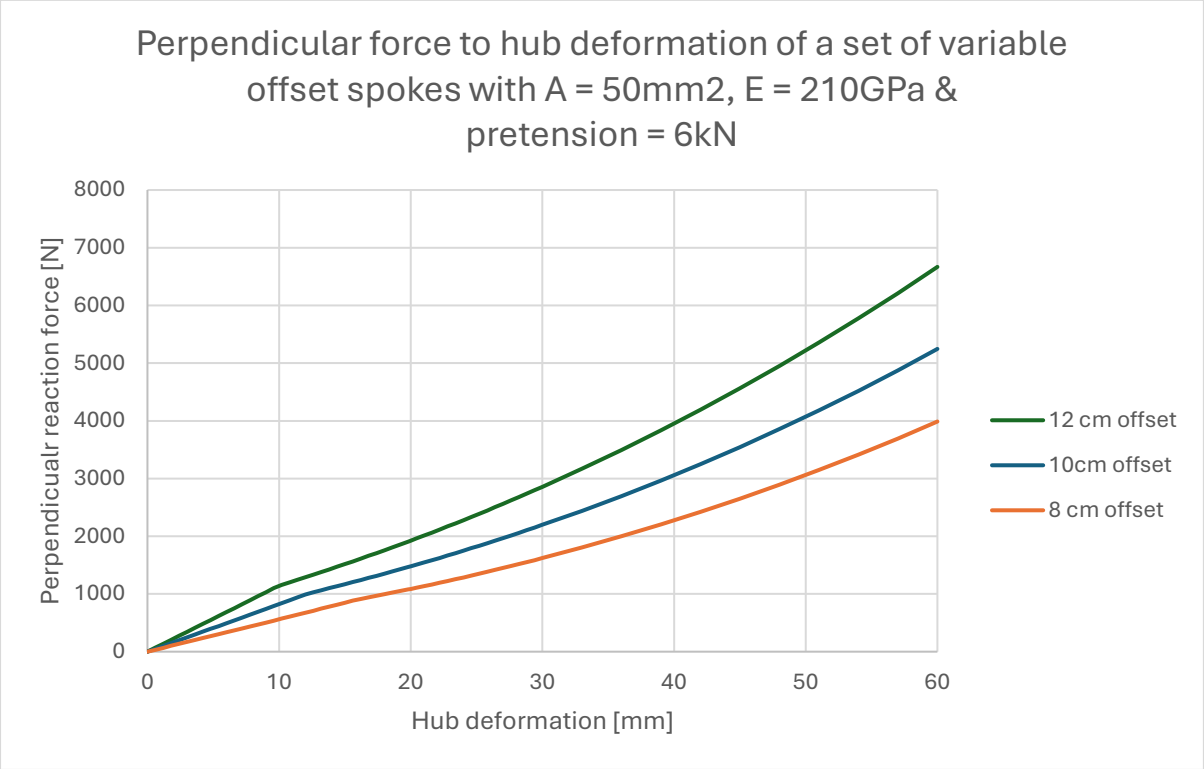

Figure 58: Perpendicular force to hub deformation of a set of variable offset spokes with A = 50mm2, E = 210GPa & pretension = 6kN

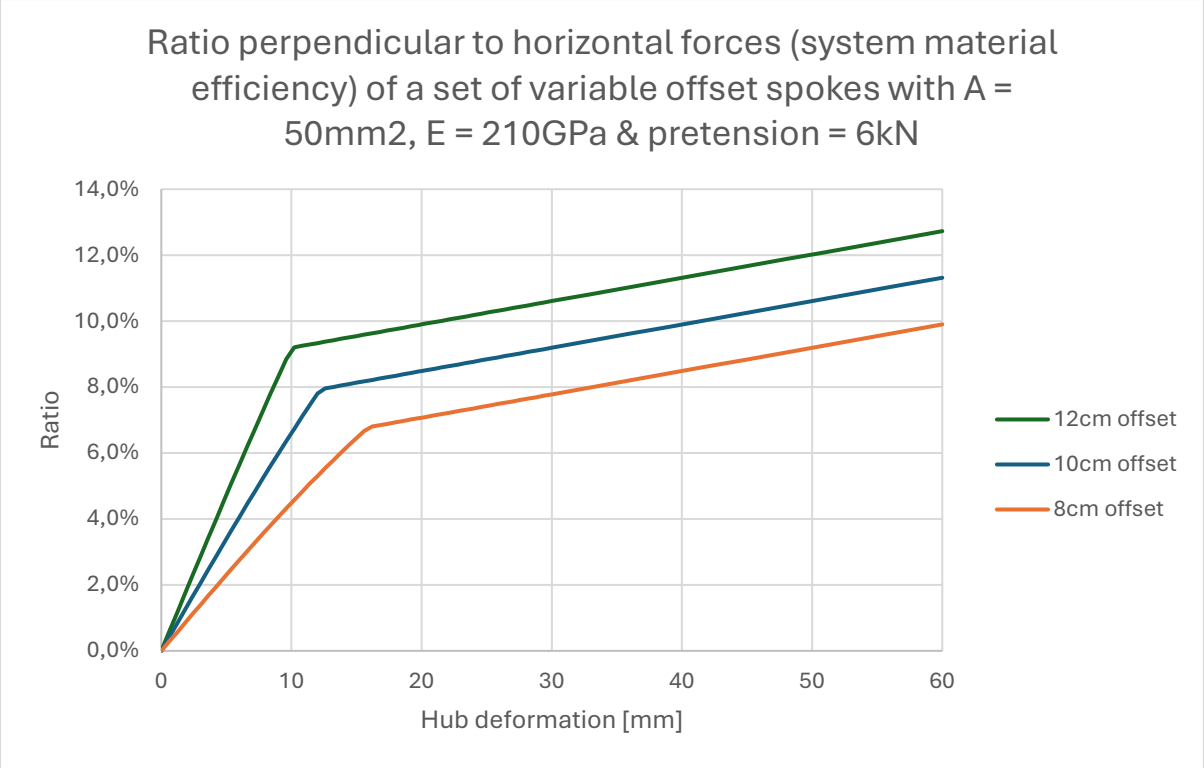

Figure 59: Ratio perpendicular to horizontal forces (system material efficiency) of a set of variable offset spokes with A = 50mm2, E = 210GPa & pretension = 6kN

Secondly, varying the pretension reveals that higher pretension levels increase the system's overall resistance to lateral loads (Figure 60). More importantly, pretension directly influences the point at which one of the cables goes slack (Figure 61). Lower pretension values cause this transition to occur earlier in the deformation process. As a result, the system achieves improved material efficiency at lower lateral load levels, since it more rapidly shifts to a state where the counteracting spoke that turns slack is fully relieved of tension and its perpendicular component no longer aligns with the wind load.

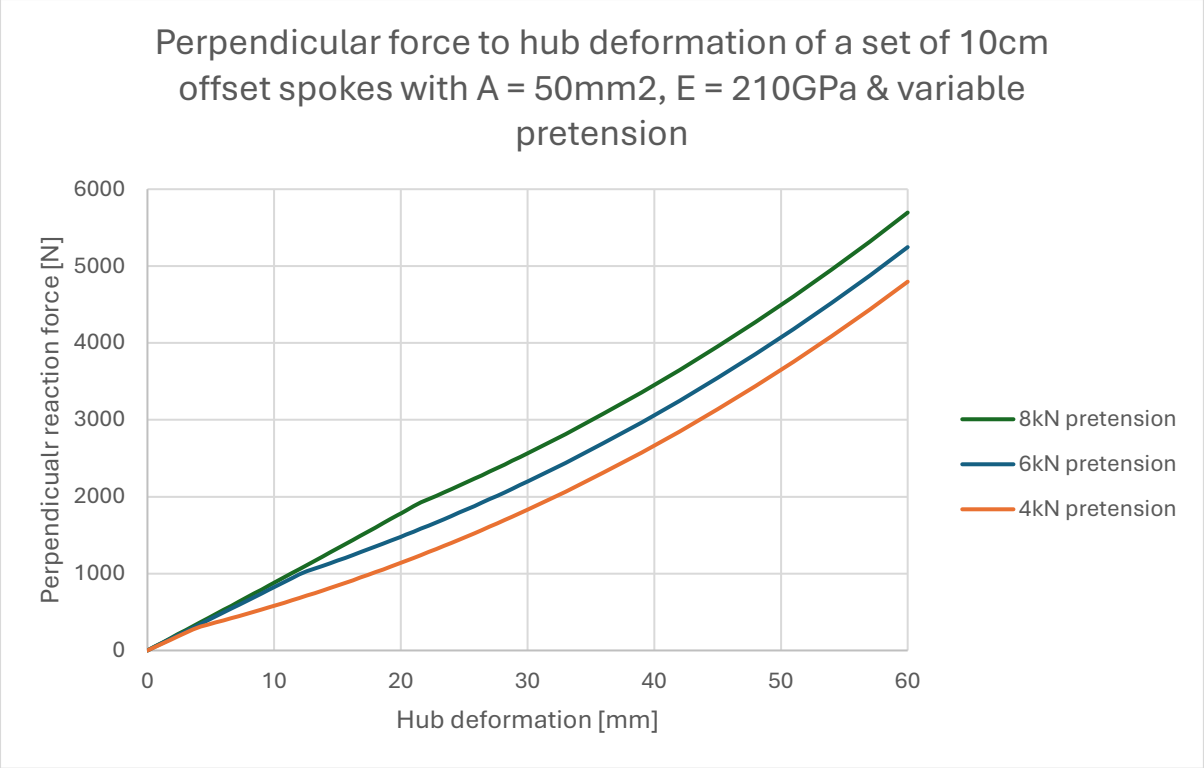

Figure 60: Perpendicular force to hub deformation of a set of 10cm offset spokes with A = 50mm2, E = 210GPa & variable pretension

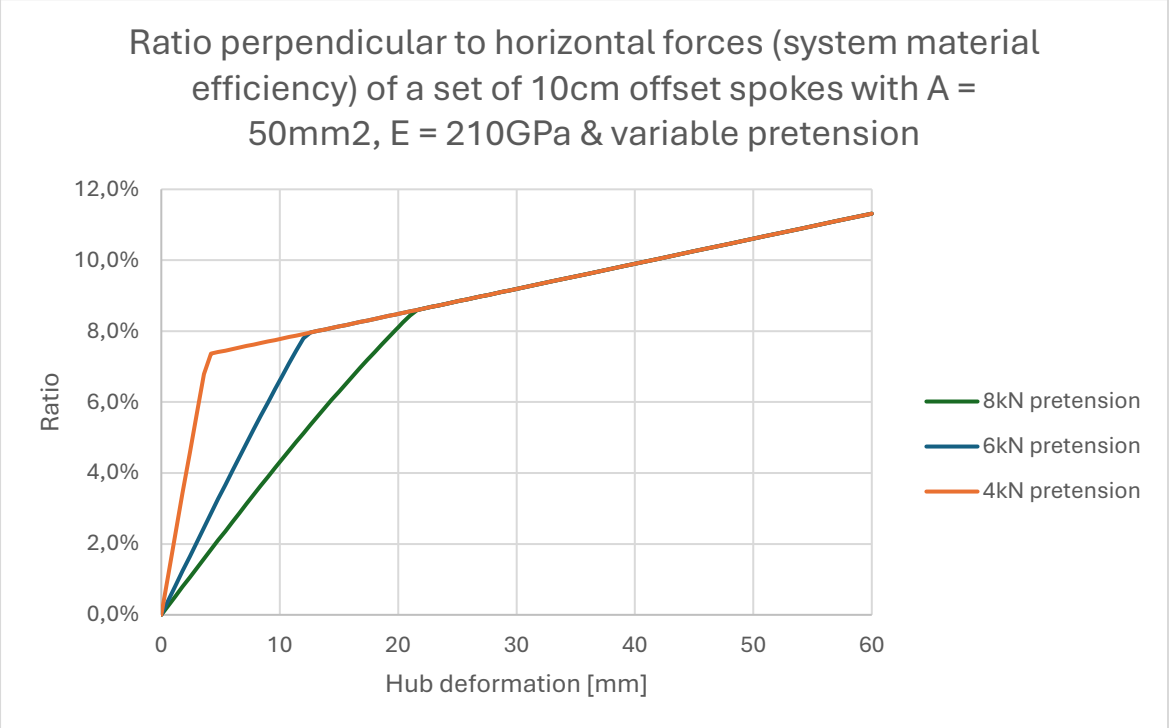

Figure 61: Ratio perpendicular to horizontal forces (system material efficiency) of a set of 10cm offset spokes with A = 50mm2, E = 210GPa & variable pretension

Finally, varying the stiffness, in this case with the cross-sectional area, of the spokes reveals a trend like the one observed with increased pretension: greater area leads to increased lateral resistance of the system (Figure 62). However, unlike changes in pretension, increasing the area also reduces the deformation required for one of the spokes to go slack (Figure 63). This outcome aligns with expectations, as a stiffer spoke reaches a given tension level with less elongation, causing the transition to occur earlier in the deformation process.

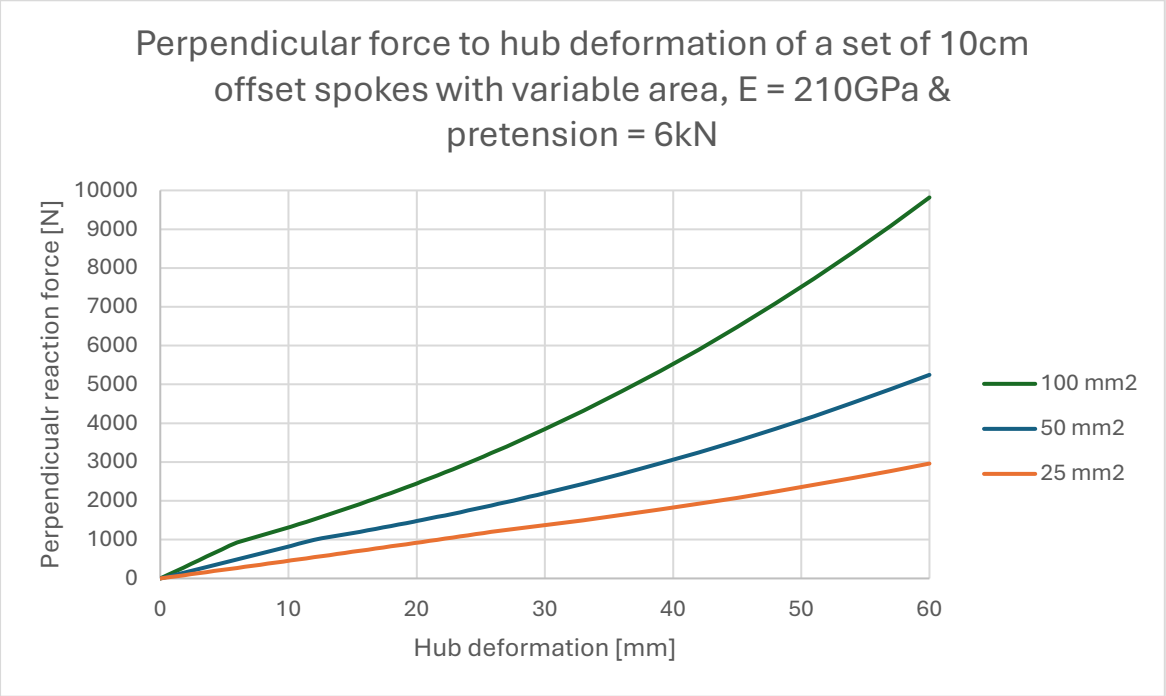

Figure 62: Perpendicular force to hub deformation of a set of 10cm offset spokes with variable area, E = 210GPa & pretension = 6kN

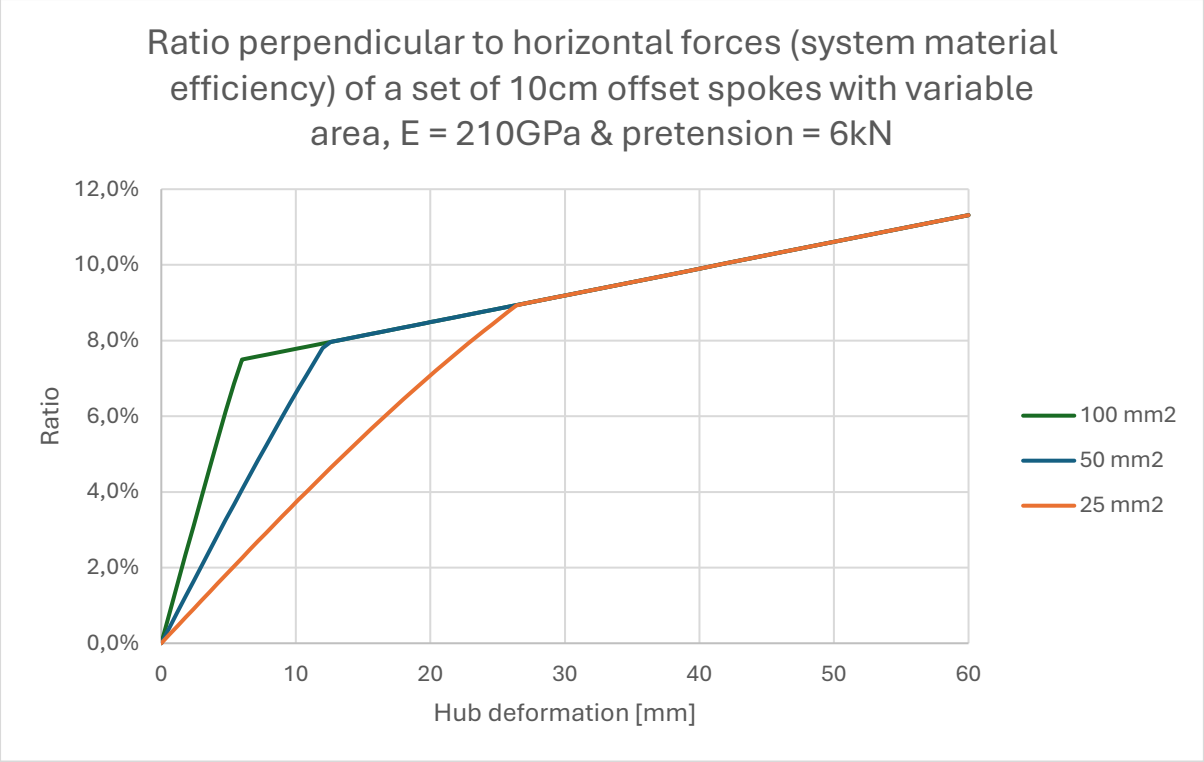

Figure 63: Ratio perpendicular to horizontal forces (system material efficiency) of a set of 10cm offset spokes with variable area, E = 210GPa & pretension = 6kN

With this understanding, it should now be more intuitive how variations in cable offset, pretension, and stiffness influence the behaviour of the system, and how these parameters can be strategically optimized to achieve a desired level of lateral resistance. Importantly, such optimization can significantly reduce the forces transferred to the outer frame struts, thereby enhancing the overall material efficiency of the system.

4.2 FEA model predictions

Using the Excel model, the fundamental principle behind the out-of-plane resistance of the tensile façade system was revealed. A potential improvement was identified by offsetting the cables. However, these initial simulations did not account for the asymmetric placement of the inner frame, nor did they analyse the frame's inherent instability.

To address these complexities, Ansys Mechanical was employed to both validate the Excel calculations and to assess the influence of asymmetry and potential instability within the system. The finite element analysis (FEA) simulations conducted prior to the prototype phase can be divided into four main parts:

1. Validation of the Excel model: An identical scenario was modelled to verify that the FEA results matched the analytical Excel results.
2. Assessment of asymmetry: The influence of asymmetric placement of the inner frame on the overall stiffness of the façade panel was evaluated.
3. Stability analysis: The stability of the outer frame under variable out of plumbness is analysed

4.2.1 Validation of the Excel model

To begin, the Excel model was validated by constructing a similar symmetric FEA model for both the single-spoke and double-spoke setups. The connection points to the outer frame were modelled as rigid supports, replicating the boundary conditions used in the Excel calculations. Identical forces were applied, and the cables were modelled with the same cross-sectional properties as assumed in the analytical model. The FEA simulations produced results that matched the Excel calculations precisely, for the single and double cable setups, indicating that the Excel model was likely set up correctly and that its assumptions were valid for the symmetric case (Figure 64).

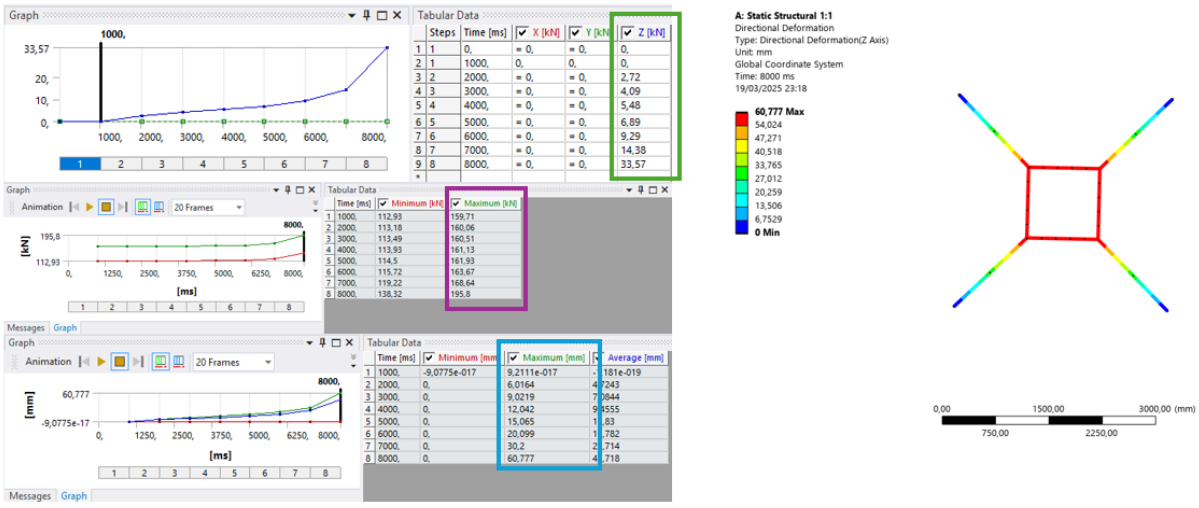

	Deformation [mm]	Perpendicular force [N]	Force Cable 1 [kN]	Force Cable 2 [kN]	Total compressive force in struts	Ratio Perpendicular force to force in struts	Perpendicular force x4 [kN]
undeformed	0,00	0	160,00	0,00	160,00	0,00%	0,00
1/500	6,00	680	160,38	0,00	160,38	0,42%	2,72
1/333	9,00	1023	160,86	0,00	160,85	0,64%	4,09
1/250	12,00	1370	161,52	0,00	161,51	0,85%	5,48
1/200	15,00	1722	162,37	0,00	162,37	1,06%	6,89
1/150	20,00	2322	164,22	0,00	164,21	1,41%	9,29
1/100	30,00	3594	169,50	0,00	169,46	2,12%	14,38
1/50	60,00	8392	197,98	0,00	197,81	4,24%	33,57

Figure 64: Results of the Excel model (below) and the FEA model (above)

4.2.2 Assessment of asymmetry

With the simulation correctly set up, the next step was to assess the effects of incremental asymmetry on the out of plane rigidity of the facade. Three potential configurations were analysed, where the inner frame was gradually displaced from its centred position. The outer frame measured 3x3 meters, and the inner frame measured 1x1 meter, with the inner frame being offset by 0,3 meters at each step. All of the cables in the simulations had an 8mm radius and every component had a Young's modulus of 210GPa.

To control the system's behaviour under increasing asymmetry, cable pretensions were independently adjusted for each configuration to minimize deflections of the entire system. Additionally, the outer struts were selected from square hollow sections (SHS), which are effective at resisting bending in both principal axes, mimicking an indicative optimized profile. The profile sizes were minimized to balance the bending stiffness of the outer frame and the movement of the inner frame, aiming to ensure similar deformation behaviour for both elements.

The first step in the analysis involved identifying the loads applied to both the inner and outer frames. This was accomplished using a simple Grasshopper script, which modelled the panels as two-way spanning elements. The script allowed for the approximate area exposed to each individual strut to be quickly and systematically estimated (Figure 65).

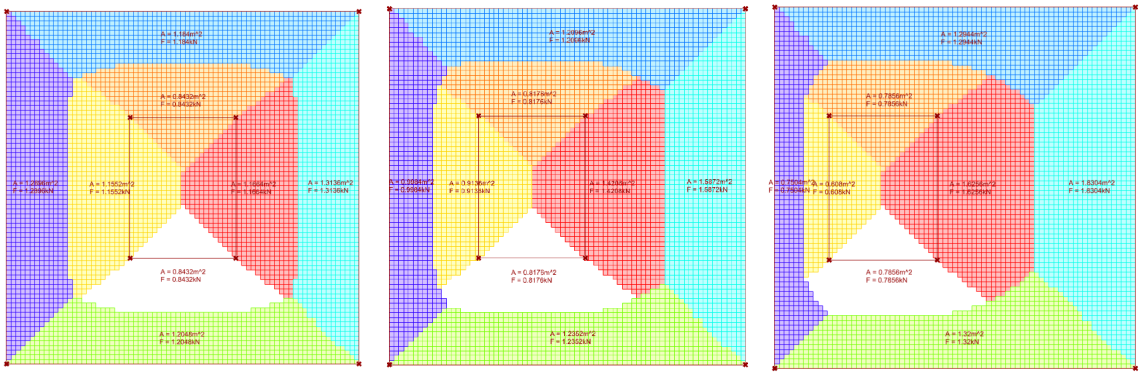

Figure 65: Force distribution of 2-way spanning cladding

These surface areas were subsequently converted into individual line loads based on a wind pressure of 1 kN/m^2 and applied directly to each profile within the FEA model (Figure 66). This simplification does not capture the exact load distribution but was considered sufficiently accurate to provide indicative results for analysing the effects of asymmetries in the system's behaviour.

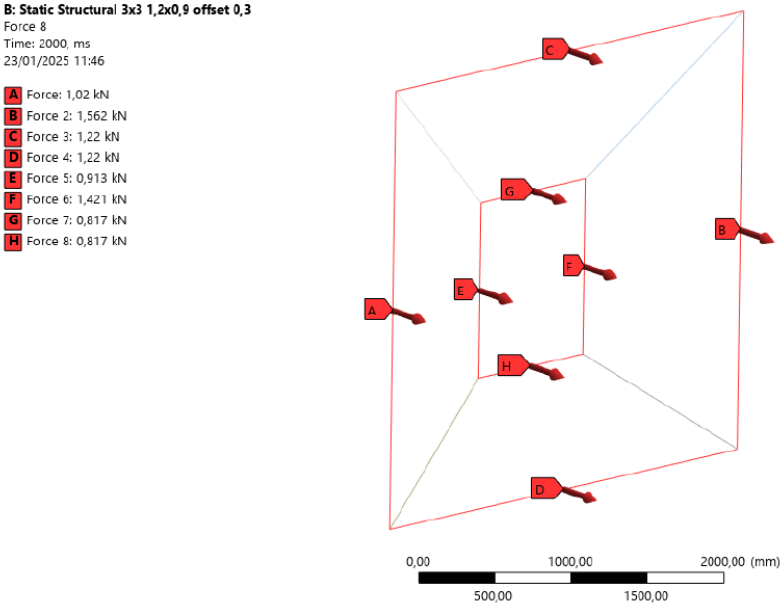

Figure 66: Applied forces onto the FEA model

The first configuration was designed using SHS 80x80x4 profiles for the outer struts. By applying a high pretension of 230 kN to each cable, the system achieved a deformation of approximately 6 mm in its symmetrical state, corresponding to a Span/500 limit (Figure 67).

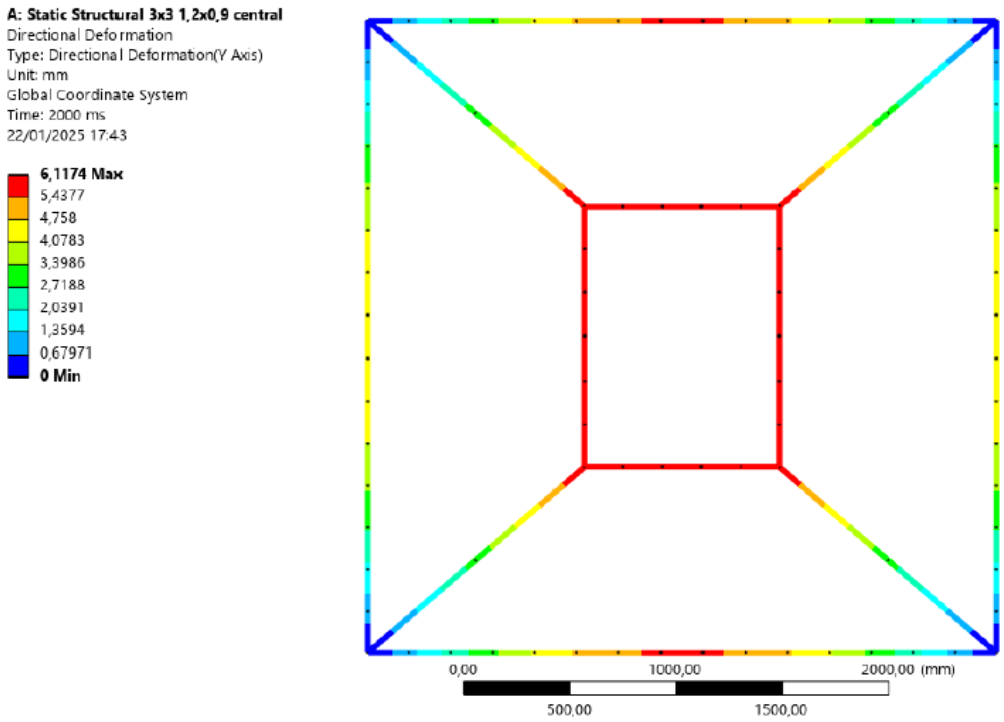

Figure 67: FEA deformation analysis of a symmetrical system

Maintaining the same SHS 80x80x4 profiles, the impact of asymmetry on the system's out-of-plane stiffness became evident. When the inner frame was offset by 0.3 meters and 0.6 meters, the maximum deformations increased to approximately 6.7 mm and 8.7 mm, respectively, assuming no limit was imposed on the compressive forces in the struts (Figure 68).

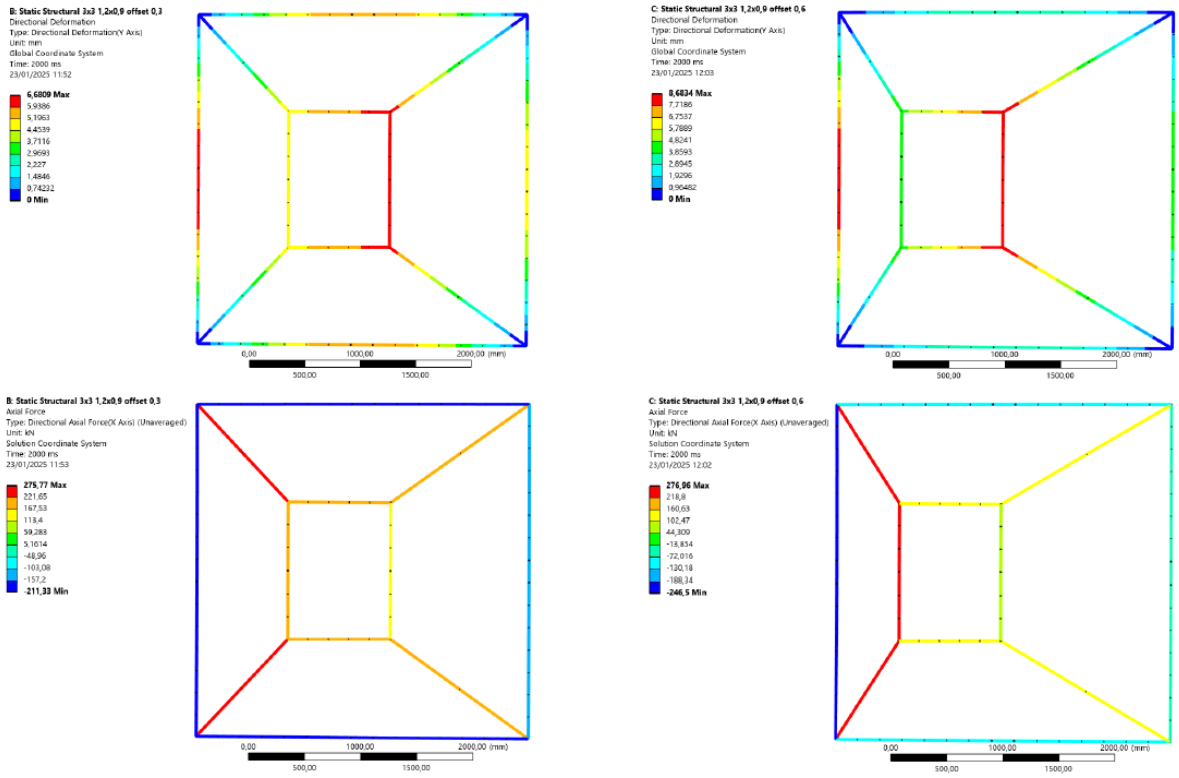

Figure 68: Deflection increase due to asymmetric placement of the inner frame, no limit on the compression of the outer stuts

However, when the axial forces in the struts were limited to the design compressive resistance of the profiles, 174 kN, based on strut capacity curves, the deformations further increased to 7.8 mm for the 0.3 m offset and 12.3 mm for the 0.6 m offset. This effectively doubled the deformation of the façade panel with only a marginal offset of the inner frame (Figure 69).

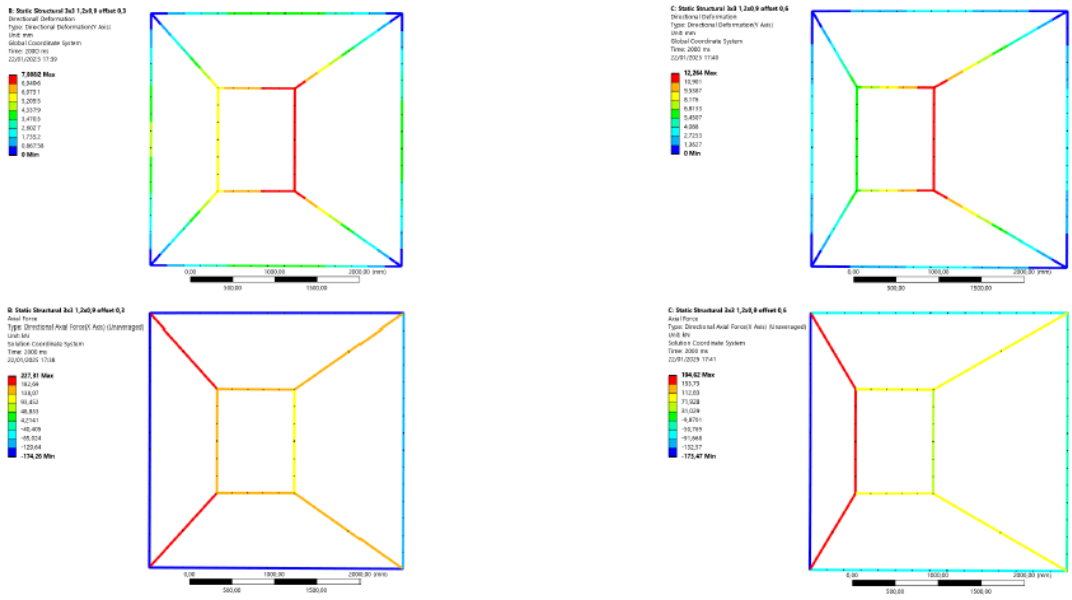

Figure 69: Deflection limits when NRd is governing

Similar trends were observed when the panel was detailed using 60x60x4 and 60x60x2 SHS profiles.

In the case of the 60x60x4 SHS profiles, under a symmetrical configuration, the panel reached a maximum deflection of 15 mm. When the design compressive resistance of the outer struts (91 kN) was applied as a limit, the deformation increased to 16.2 mm for the 0.3 m offset and 23.5 mm for the 0.6 m offset.

For the 60x60x2 SHS profiles, the system showed an initial deformation of 26.7 mm in the symmetrical setup. Upon limiting the maximum compressive force in the outer struts to 48 kN, the deformations rose to 30.7 mm and 44.9 mm for the 0.3 m and 0.6 m offset cases, respectively.

These results indicate that model asymmetry is highly detrimental to system stiffness. As the inner frame becomes increasingly offset, the axial forces in the strut closest to the inner frame rise significantly, resulting in increased bending of the profile. The reduction in wind pressure acting on this strut does not compensate for the corresponding increase in precompression, ultimately leading to greater out-of-plane deformation and a notable loss in overall system rigidity.

Simultaneously, on the opposite side of the frame, the decrease in cable tension, combined with an increase in wind loading, causes further deformation. This dual effect reduces the overall stiffness of the façade panel, highlighting the importance of maintaining symmetry for efficient designing of the frames.

4.2.3 Stability analysis

The next step was to assess the stability of the system. It was already understood that the system is intrinsically unstable in its basic form. To achieve stability, two main strategies were identified:

- Corner connections must be attached directly to the substructure, providing external restraint; or
- The frame and its connections must be designed to resist bending and torsion sufficiently, with the inner frame potentially contributing to overall stability if appropriately sized and stiffened.

This understanding guided the subsequent FEA simulations, focusing on evaluating how different design choices influence the system's ability to resist instability.

Having identified the likely modes of instability in the structure, three geometric configurations were modelled with varying levels of initial out-of-plumbness to assess sensitivity to imperfections. Out-of-plane displacements were introduced by moving two opposing corners of the frame by the corresponding amounts, simulating initial geometric imperfections. The levels of imperfection modelled were:

- 1/500 of the span
- 1/1000 of the span
- 1/2000 of the span

The corner connections were modelled as fully rigid, capable of transferring both bending and torsion without allowing relative deflection between the connected struts. As a starting point, a 3x3m frame with a 1x1m inner opening was analysed, again using SHS 80x80x4 profiles for the outer struts. At various levels of cable pretension, the total deformation of the frame was evaluated by subtracting the minimum from the maximum deformations across the structure.

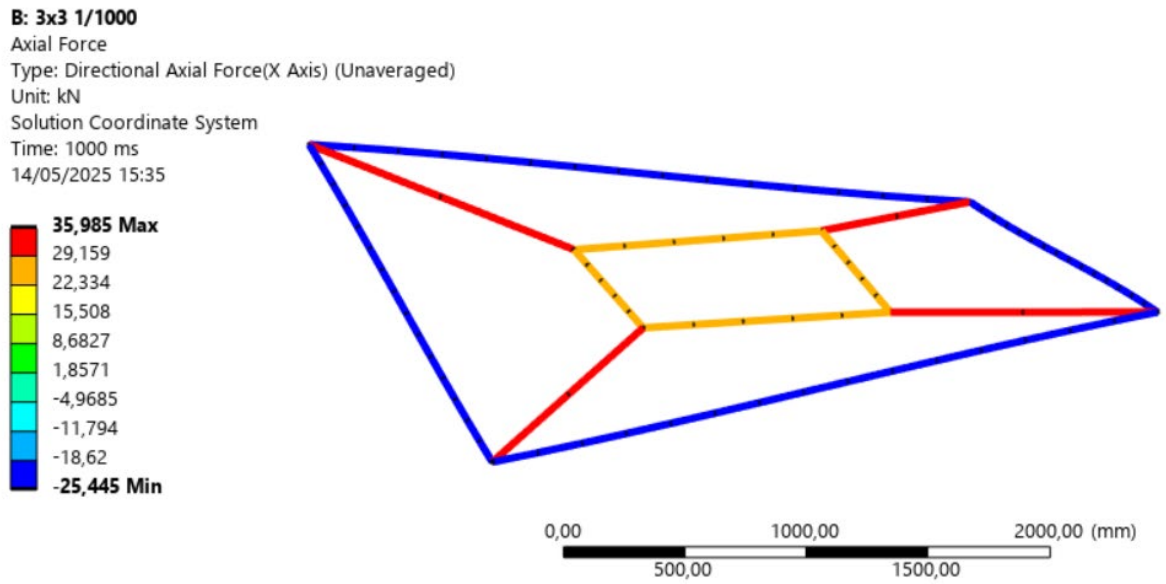

Figure 70: Axial forces in a stiffened 3x3m outer frame and centralized stiffened 1x1m window, SHS80x80x4, 1/1000 out of plumbness

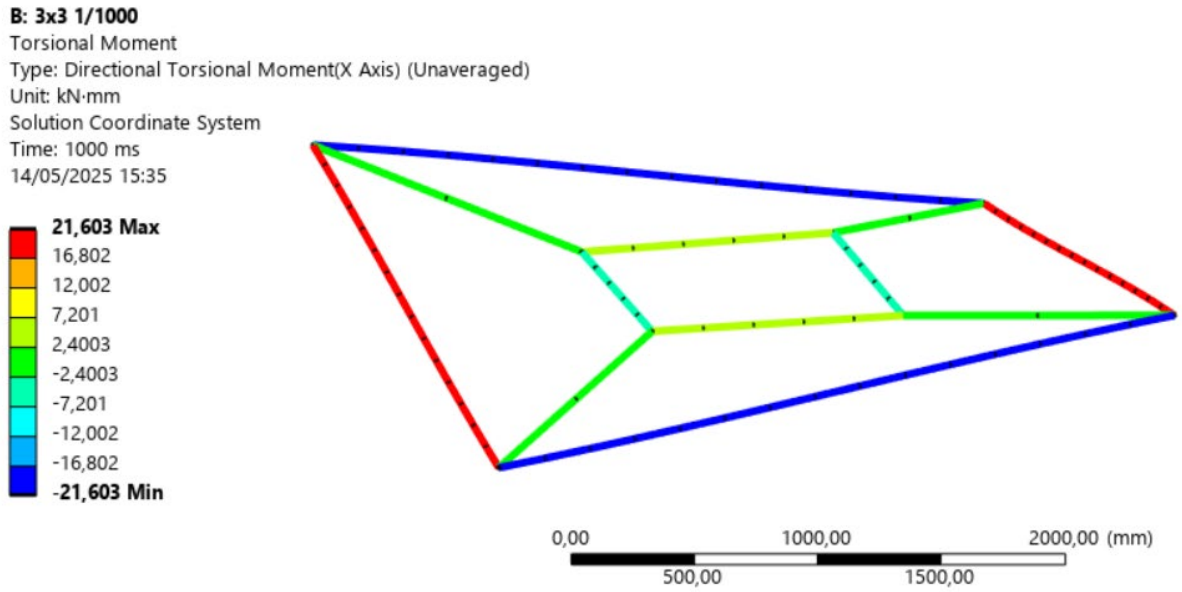

Figure 71: Torsional moments in a stiffened 3x3m outer frame and centralized stiffened 1x1m window, SHS80x80x4, 1/1000 out of plumbness

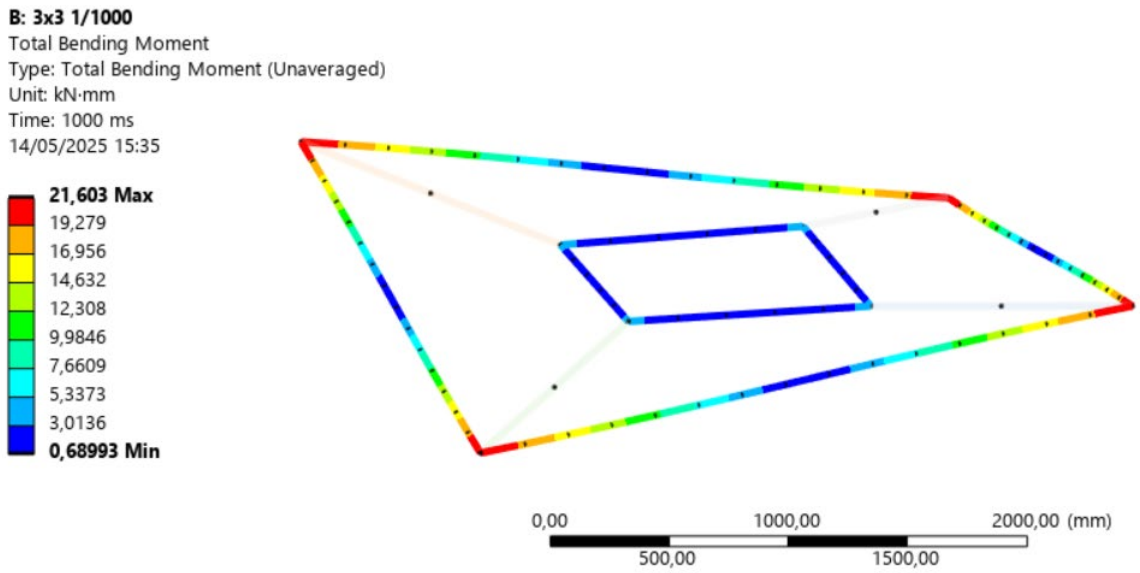

Figure 72: Bending moments in a stiffened 3x3m outer frame and centralized stiffened 1x1m window, SHS80x80x4, 1/1000 out of plumbness

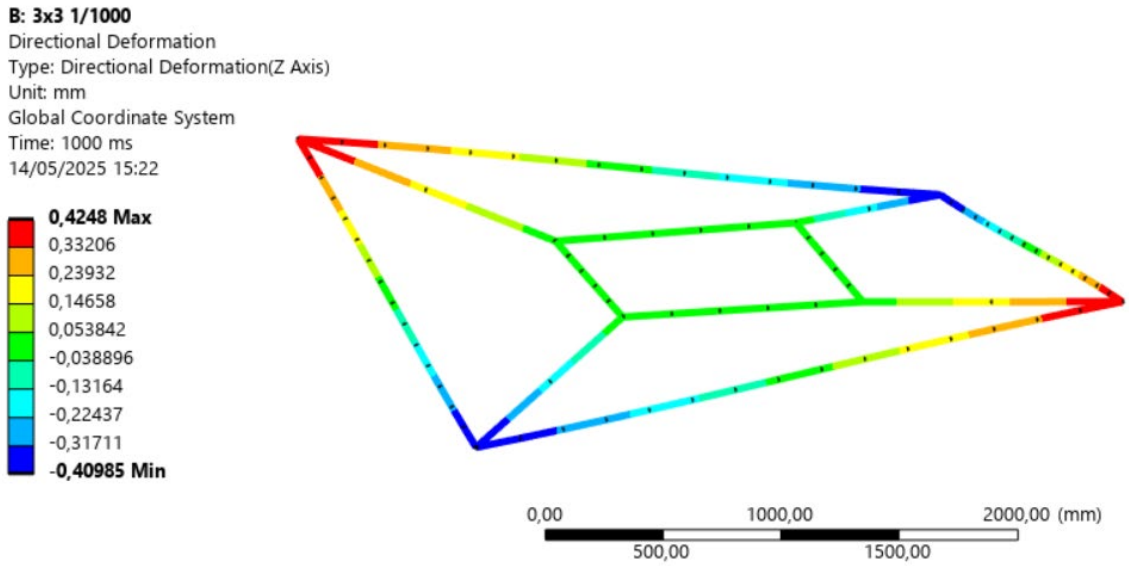

Figure 73: Deformations in a stiffened 3x3m outer frame and centralized stiffened 1x1m window, SHS80x80x4, 1/1000 out of plumbness

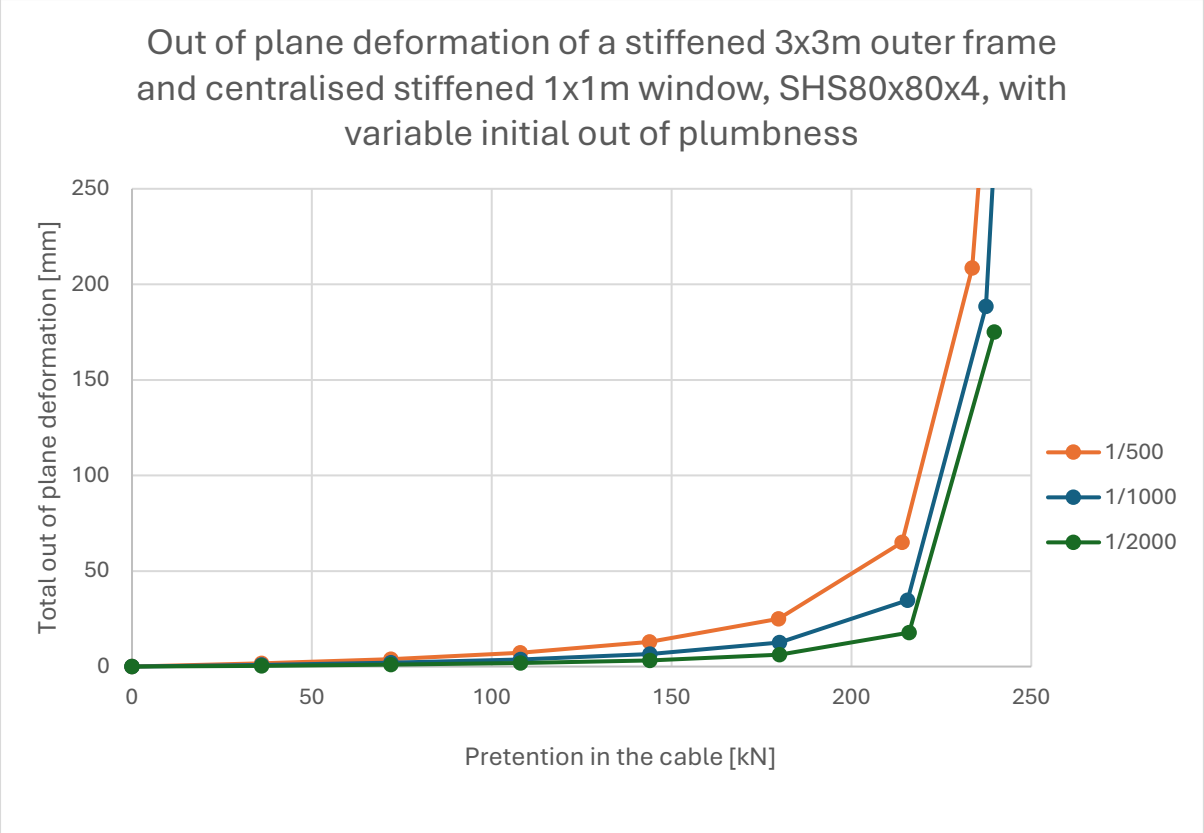

Figure 74: Out of plane deformation of a stiffened 3x3m outer frame and centralized stiffened 1x1m window, SHS80x80x4, with variable initial out of plumbness

From Figure 74, it can be observed that initial out-of-plumbness directly translates into increased out-of-plane deformations during pretensioning. This highlights the critical importance of maintaining high manufacturing and assembly tolerances. Frames assembled with lower initial imperfections will experience less deformation during cable tensioning.

Furthermore, the results illustrate that tensioning the cables leads to an exponential increase in frame deformation. As the cables are pretensioned, the frame deforms slightly more out of plane; this deformation increases the out-of-plane component of the cable forces, which in turn pulls the frame further out of plane, creating an exponential self-reinforcing effect. However, as long as all the materials stay in their elastic limit, this effect is incremental and therefore safe, even at high levels of deformation.

Additionally, the figures reveal that the bending moment is directly proportional to the torsional moment experienced in the struts. This relationship is logical: as the frame warps, the structural elements undergo a slight rotation, which, due to the rigid corner connections, is fully transferred into a bending moment in the adjoining struts.

However, it is important to note that the previous example was based on a closed SHS section, which inherently provides high torsional resistance. In contrast, sections such as I-beams, or assemblies of two opposing profiles (even if they are two enclosed sections), exhibit much lower torsional stiffness because the centre of rotation is not contained within a fully enclosed section.

To investigate this effect, the same simulation was repeated using a hat section, dimensioned to mimic two thermally broken L-profiles with a similar cross-sectional area to the SHS profile (Figure 75). This comparison revealed a significant problem: the system's stability completely deteriorated when using the open-section configuration.

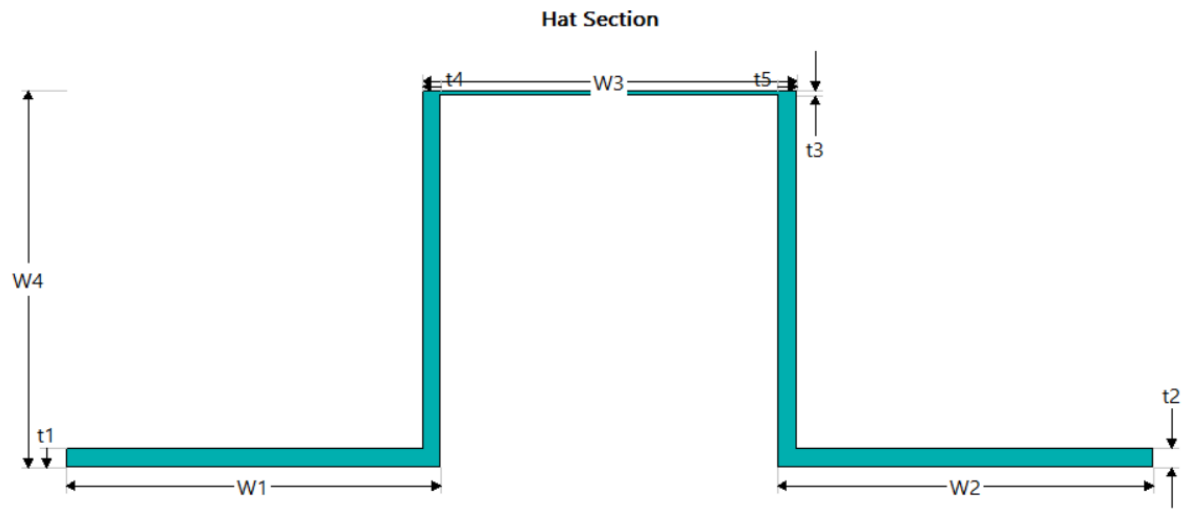

Figure 75: Hat section with a similar cross-sectional area as the SHS 80x80x4

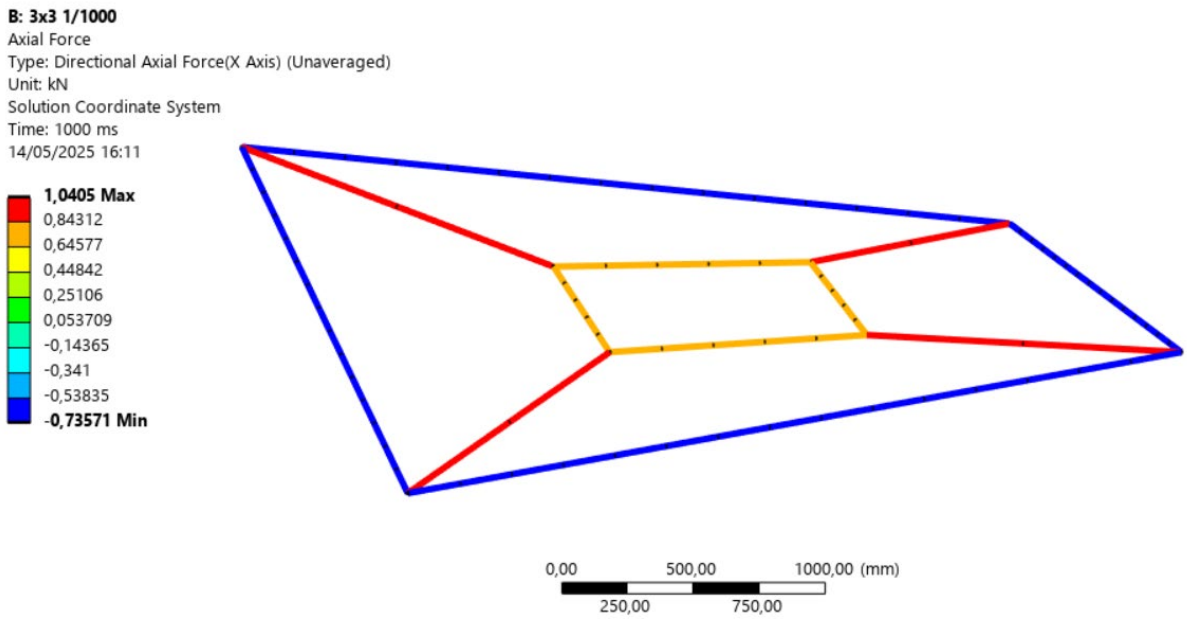

Figure 76: Axial forces in a stiffened 3x3m outer frame and centralized stiffened 1x1m window, Hat section, 1/1000 out of plumbness

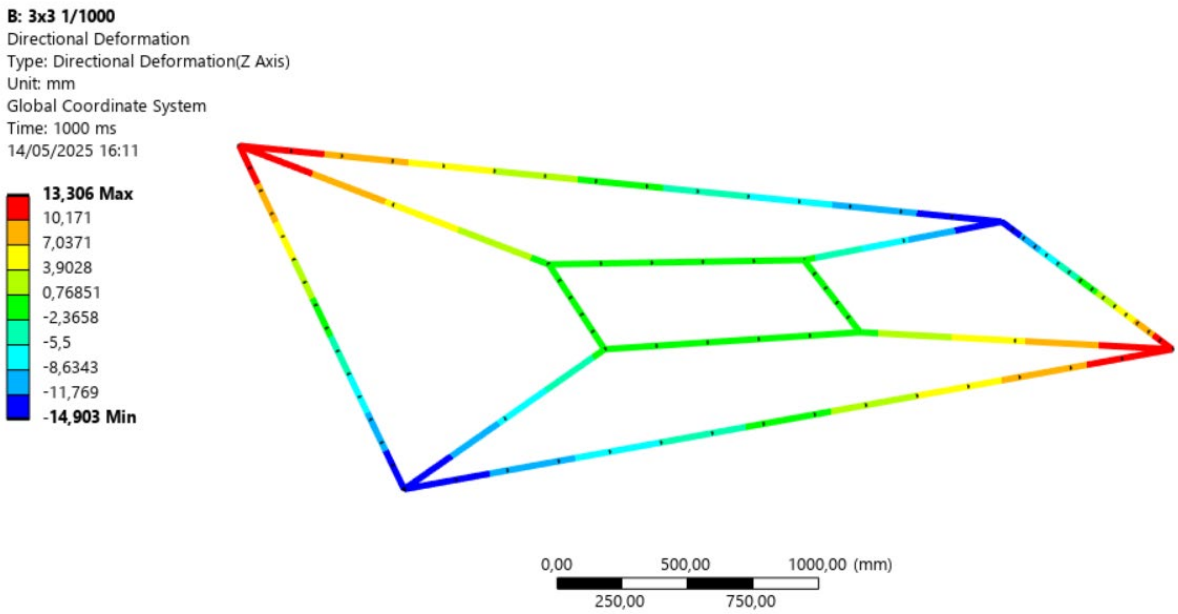

Figure 77: Deformation in a stiffened 3x3m outer frame and centralized stiffened 1x1m window, Hat section, 1/1000 out of plumbness

When applying only 1 kN of pretension, the frame with the hat section already deformed by over 13 mm, with an initial out-of-plumbness of 1/1000. This level of instability makes it completely unviable to achieve the required pretension levels in the prefabricated panel before it is attached to the supporting structure.

As a result, for thermally broken profiles, or any other profiles that lack high torsional rigidity, it becomes virtually impossible to apply high pretensions during prefabrication. Additional checks and careful design measures would be necessary even to achieve moderate pretension levels potentially required for the initial manufacturing stage in the factory.

5. Prototype Development and Tests

To evaluate the out-of-plane stiffness of the system, it was deemed necessary to develop a physical prototype to verify the numerical models. For the prototype, four tests were conducted. The first three were based on the configuration outlined in the original patent, focusing on the effects of varying the position of the inner frame. The first test featured a fully symmetrical setup, while the second and third introduced increasing levels of asymmetry to analyse how off-centre positioning of the inner frame affects the system's behaviour. The fourth test served as a validation of an alternative design concept, utilizing eight cables instead of four. With these cables already intentionally positioned slightly out of plane.

5.1 Prototype Development and Assembly

The prototype design went through several iterations before reaching its final form. Below is an overview of the key components and the rationale behind their selection.

Load Cells and forces

For logistical reasons the Pushton PSD-S1 load cells were initially selected as the foundation for the system's measurements. As these load cells were available through the faculty for the duration of the project, and the force range they support was considered safe for testing purposes. The PSD-S1 is an S-shaped load cell with a measurement range of 0–300 kg (Figure 78).

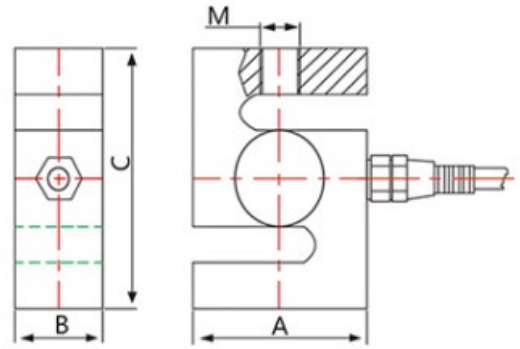

Capacity	Size mm				Weight (kg)
t	A	B	C	M	
0.05-0.3t	50.8	19	76.2	M12X1.75	0.6
0.5t	50.8	25.4	76.2	M12X1.75	0.6
1-2t	50.8	25.4	76.2	M16X2	0.6
3-5t	76.2	25.4	108	M18X1.5	1.3
10t	127	50	178	M30X2	8.9
(20)30t	160	60	190	M39X2	15

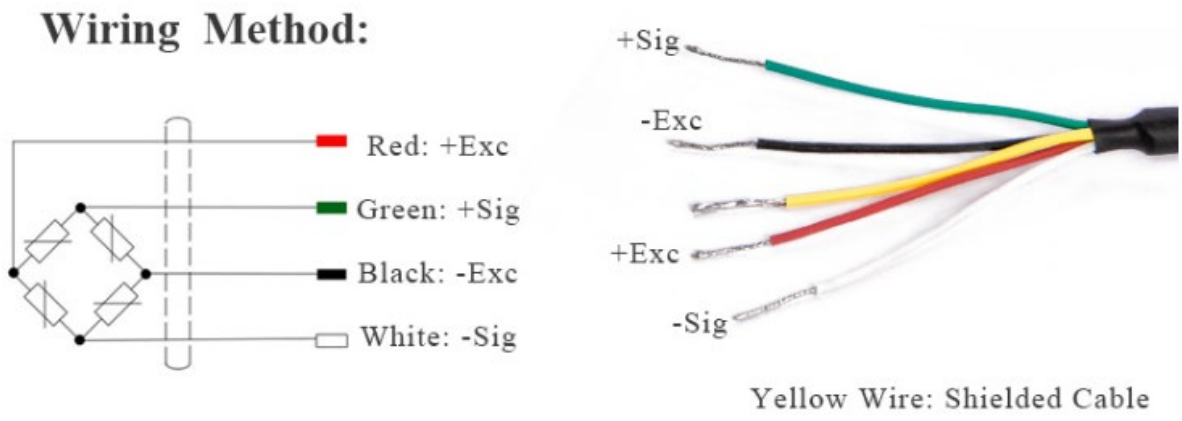

Figure 78: PSD-S1 load cells (PUSHTON)

To obtain usable readings from the load cells, additional circuitry was required, as the load cells output only analogue signal and excitation wires. To address this, four HX711 modules were used as intermediaries between the load cells and an Arduino UNO R3 board. These modules amplify and convert the analogue signals into digital data readable by the Arduino. The Arduino was programmed to collect the measurements, and a corresponding Python script was used to interpret the data transmitted from the board. Both the Arduino and the Python scripts are uploaded to the graduation repository.

The load cells were initially calibrated on March 14th, 2025, at the MSE Lab in the Mechanical Engineering department. To ensure their accuracy, a follow-up test was conducted on March 27th. In this test, an identical weight of 12,451 g ±10 g was applied to each load cell (Figure 79).

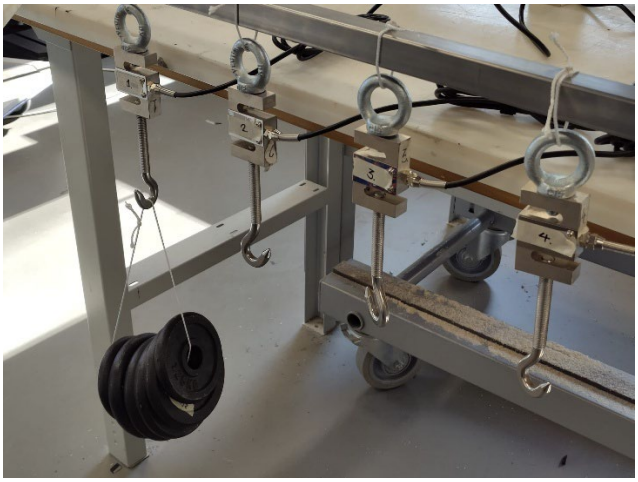

Figure 79: Load applied to the load cells

Using a conversion factor of 9,807N/kg, they all came in within 1% accuracy. Which was deemed sufficient for the remainder of the tests (Table 3).

Table 1: Load cell calibration test values

	Load cell accuracy	
	Measured force [N]	Accuracy [%]
1	121,9	99,83%
2	121,8	99,75%
3	121,6	99,58%
4	121,4	99,42%

Since the load cells would be integrated directly into the system, their presence had the potential to influence the overall stress-strain behaviour of the cable assembly. To evaluate this impact, a simplified Finite Element Analysis (FEA) model was developed in Ansys to assess the stiffness of the load cells. The results indicated that the load cells were at least 2-3 times stiffer than the 4 mm cable selected for the system. This difference in stiffness was considered acceptable for the intended application (Figure 80).

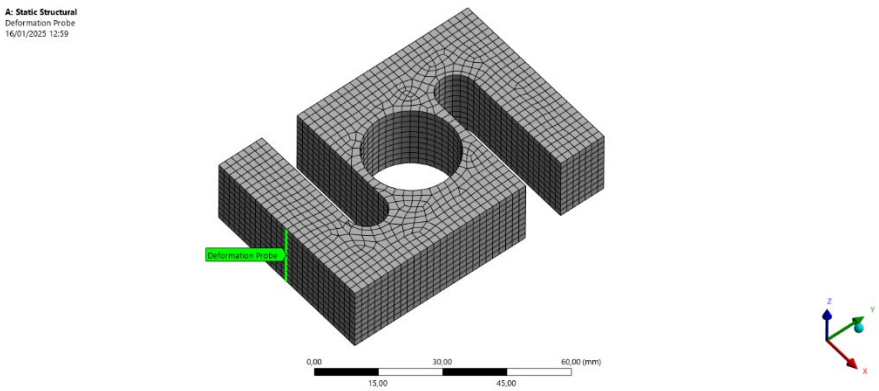

Figure 80: FEA setup for the load cell

Frame size

For the outer frame, the first major decision involved determining the overall size of the assembly. Two key factors influenced this choice.

The first was the maximum measurable force in the cables, which was limited by the load cells to 300 kg, or approximately 3 kN.

Since constructing a full-scale model was not feasible, a scaled-down version needed to be developed while maintaining realistic behaviour. To achieve this, Froude scaling factors were applied. Although typically used in hydrodynamic simulations, the force scale factor (λ^3) from Froude scaling was relevant in this context, as it provided a method to estimate the maximum tension expected in the spokes of the full-scale system (Table 2).

Where: $F_{Full} = F_{model} \cdot \lambda^3$

Table 2: Froude scaling factors (Samuel, 2019)

Variable	Unit	Scale factor
Length	[m]	λ
Wave height	[m]	λ
Wavelength	[m]	λ
Water depth	[m]	λ
Time	[s]	$\sqrt{\lambda}$
Wave period	[s]	$\sqrt{\lambda}$
Force	[N]	λ^3
Structural mass	[kg]	λ^3
Pressure	[Pa = N/m^2]	λ
Moment	[Nm]	λ^4

By applying the maximum pretension of 3 kN into the Froude scaling formula across various potential scale factors, the corresponding pretension values for the full-scale (1:1) model were calculated as follows (Table 3).

Table 3: Scled forces from smaller scales to the 1:1 model

Scale	Force in the 1:1 model [kN]
1:2	24
1:3	81
1:4	192

Initial FEA simulations and Excel-based calculations indicated that, for a 3x3 m frame with a centrally positioned 1x1 m window opening, to withstand a standard wind load of 1 kPa in its serviceability range, while keeping deformations within the commonly accepted limit of L/250, a pretension of approximately 117 kN (±3) would be required. The exact value varies depending on the thickness of the cables used and the stiffness of the outer frame.

To achieve similarly low deformations while limiting the maximum pretension to 3 kN, a scale model between 1:3 and 1:4 was therefore considered ideal. This would correspond to strut lengths of approximately 75–100 cm, effectively representing a 3×3 m frame at scale.

However, this reduced size introduced practical challenges during detailing. The force gauges, tensioners, and other hardware components were relatively large in comparison to a 1x1 m frame, leaving little to no room between components. As a result, the 75 cm (1:4) frame was already deemed unfeasible.

Ultimately, the second key factor, and the one that determined the final prototype size, was the potential for real-world testing at the MATE Lab in the Green Village at TU Delft. The lab features standardized openings measuring 1430×2380 mm, which could accommodate the prototype and allow for practical façade testing under realistic conditions. As a result, a prototype size of 1430×1430 mm was selected. While this scale would exhibit relatively greater deformation at a maximum pretension of 3kN, it still allowed for feasible assembly and ensured that key components could be reused in the potential installation at the MATE Lab.

Detailing of the frames

With the frame size and expected loading conditions established; the detailing process could begin. The design work started with the corners of the outer frame, as these were expected to be the most complex to realize. Each corner needed to function as a moment-resistant connection while also being disassemblable for practical assembly and transport. Additionally, the corners had to accommodate three force directions, the two frame struts and the cable, ideally converging at a single central point to ensure efficient load transfer and structural clarity. This was particularly difficult as there would be different configurations of the inner frame in which the cable could come from various angles. As seen in Figure 81, this could lead to eccentricities of forces. Modelling this in Ansys with pretensions of up to 3kN, this could lead to premature buckling of the outer struts.

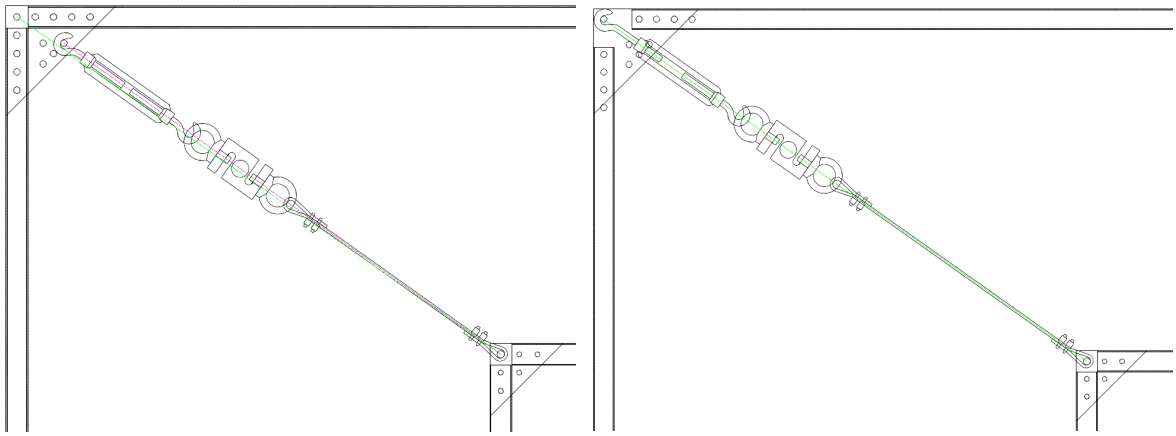

Figure 81: Off centred and centred cable attachment points

Ultimately, this required the cable connection point to be positioned precisely at the intersection of the two struts. To achieve this, the design incorporates a solution where the steel struts are wedged between two solid steel plates measuring 150×150×6 mm. These plates are off-the-shelf components with pre-cut holes for M8 bolts, which would further simplify the assembly process.

The use of the corner plates necessitated selecting a steel profile no wider than 30 mm for the struts. To maximize the stiffness of the outer frame within this constraint, two square hollow section (SHS) profiles, 30x30x2 mm and 30x30x3 mm, were evaluated based on availability. Ultimately, the 2 mm thick option was selected, as it provided sufficient structural capacity. Specifically, the 30x30x2 mm SHS offers a design compressive resistance of 15,09 kN for a 1,43 m long strut, and 6,03 kN for a 2,38 m long strut, both calculated using a safety factor of 1,5 (see Appendix). These values exceeded the expected loading, eliminating the need for a thicker profile.

For the inner frame, a similar connection detail was developed, but with a more lightweight approach. Since the inner frame is subjected only to tensile forces, buckling is not a concern. Moreover, reducing the weight of the inner frame allows for greater loads to be applied before reaching the 300 kg tension limit in the cables. This increases the possible range of movement and therefore also the range of measurements.

As a result, smaller off-the-shelf 100×100×4 mm triangular steel wedge plates were used for the inner frame, paired with smaller M6 bolt holes. For the struts, 30x15x1,5 mm rectangular hollow section profiles were then selected. This profile still provided sufficient contact surface between the strut and the wedge plate, helping distribute load at the connection point while keeping the overall frame lightweight.

Bolt pretension

As previously stated, it was important to prevent slippage at the interface between the struts and the wedge plates. This was achieved by applying pretension to the bolts, clamping the wedge plates against the struts. Based on hand calculations the potential configurations, the maximum sliding force expected at the ends of the inner and outer struts was 2,6 kN in total.

Depending on the condition of the steel, the coefficient of friction can vary, but a rough estimate of clean and dry steel on steel would be μ ≈ 0.3.

To prevent slippage the following formula can be solved: $F_{friction} = \mu \cdot N \geq F$

Solving this yields a required normal force of approximately 8.67 kN. When distributed across two bolts, this equates to about 4.34 kN per bolt. Including a safety factor of 1.15, a pretension of approximately 5 kN per bolt was deemed sufficient.

While this was the theoretical target, in practice, a mistake was made when assembling the prototype. Initially a torque calculation was made to estimate the required tightening torque for both the galvanised 8.8 M8 and M6 bolts. However, mistakenly, the bolts were installed without lubrication, resulting in a significantly higher coefficient of friction at the threads and under the bolt heads than the assumed value of 0,15. Consequently, the strut and wedge plates slipped in the initial tests.

What ended up happening was that the bolt pretensions were incrementally increased to the point where it was known not to strip the bolt and before deforming the steel hollow struts. Specifically, the 30x15x1,5 SHS were prone to deformation under high pretensions.

The second time, loading the frame beyond test loads and checking the markings showed no slippage taking place. A success when it came to making the model, but not as ideal of a solution as using the calculations.

At this stage, the frame was also checked for squareness prior to final bolt tightening. Using a laser distance meter, the diagonals were measured, revealing a 1 mm discrepancy between the two corner-to-corner distances, 1819 mm and 1820 mm (Figure 82). Based on this minimal deviation, the frame was deemed sufficiently square for the purposes of testing.

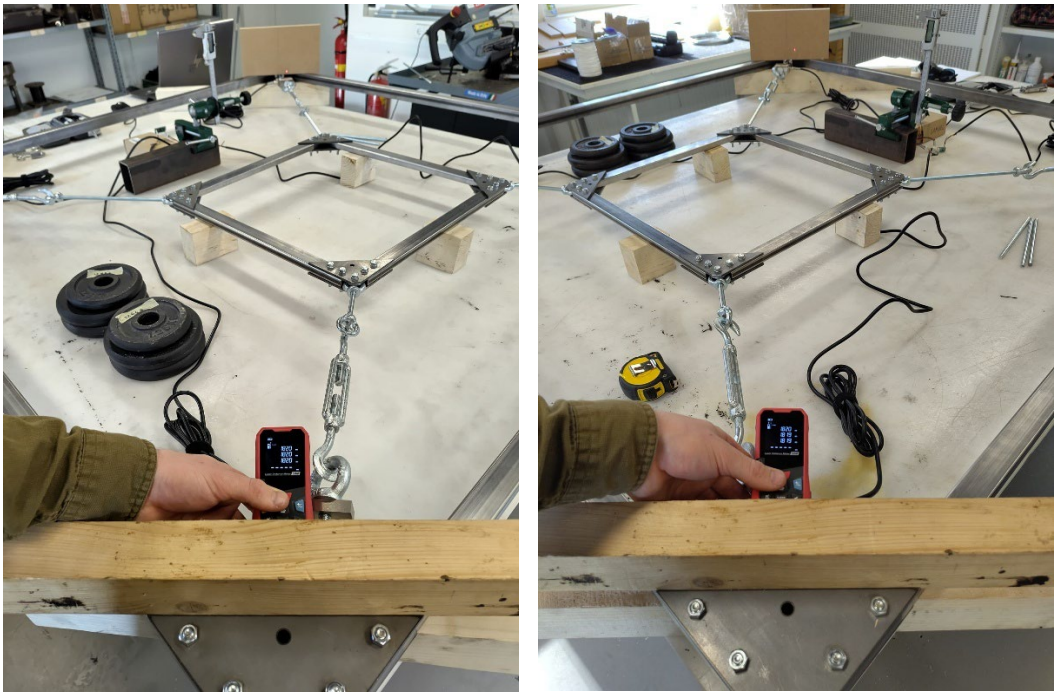

Figure 82: Checking the corner-to-corner distance

Cable configuration

With both the inner and outer frames completed, the next step was to configure and install the cables connecting the two. Prior modelling of the prototype indicated that the cables would be subjected to tensile forces ranging from approximately 2 to 3 kN. Based on this loading range, a 4 mm diameter cable was selected. According to its test report, this cable exhibits a relatively linear elastic response within the expected force range, while still maintaining a sufficiently high safety factor for safe operation. (Figure 83).

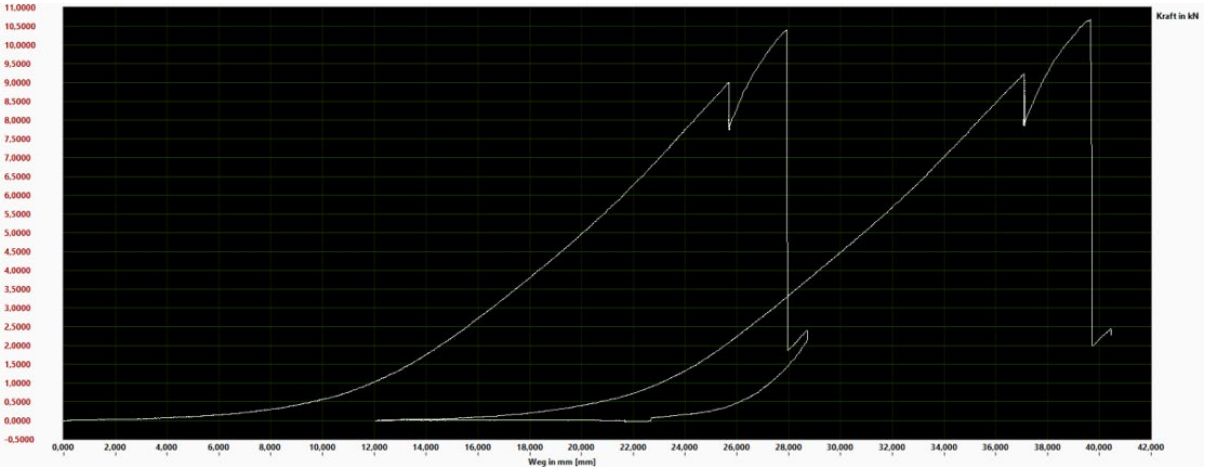

Figure 83: Test rapport 4mm cable (Drahtseile24, 2021)

Other hardware such as the eyebolts, tensioners and links were chosen based on size compatibility or a minimum safety factor of 2.

Throughout the handling of all the additional hardware, it became apparent their weight could potentially influence the measurements (Figure 84). To check this effect additional FEA models were created to check their potential effect on the overall deformation of the inner frame.

Figure 84: Weight of individual hardware components

In the initial model, a setup was created which, according to Excel-based hand calculations, was expected to deform by 4,00 mm under a load of 18,5 N applied at each corner. Finite Element simulation confirmed this predicted deformation when the system was modelled without the weight of the force gauge. However, once the mass of the force gauge was incorporated into the simulation, the predicted deformation increased to 4,24 mm (Figure 85). This discrepancy, though seemingly minor, highlighted a critical consideration, especially given that the weight and influence of additional hardware components had yet to be accounted for.

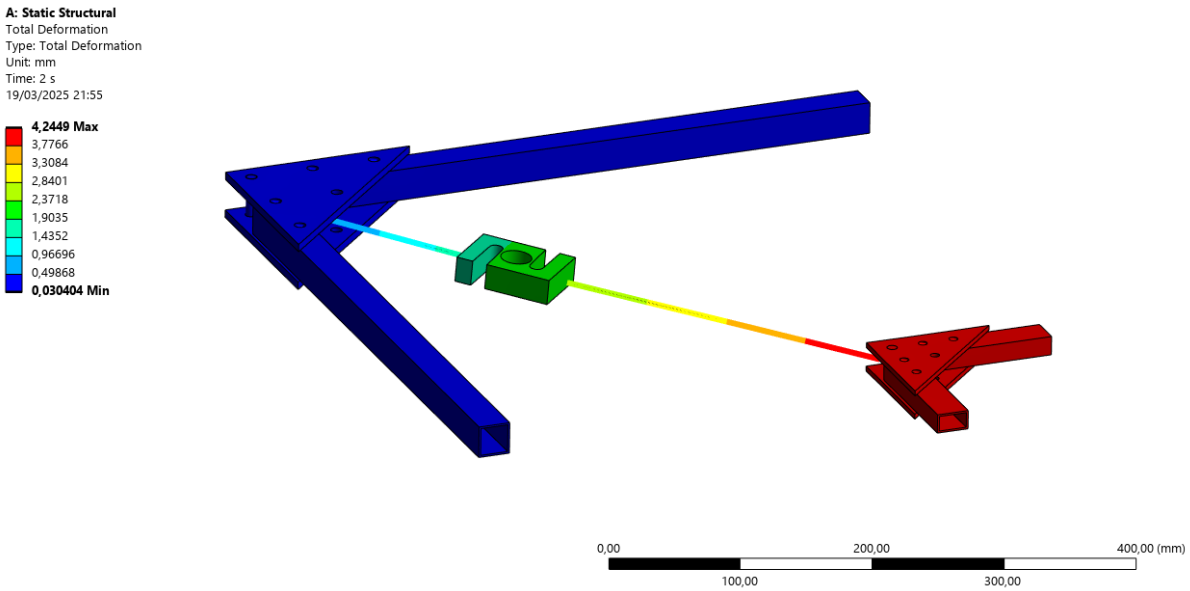

Figure 85: Initial FEA test including self-weight of the cables and force gauge

This outcome prompted the development of an additional FEA model aimed at identifying the optimal configuration for placing the force gauges and other hardware, while also validating whether modelling the additional hardware was necessary.

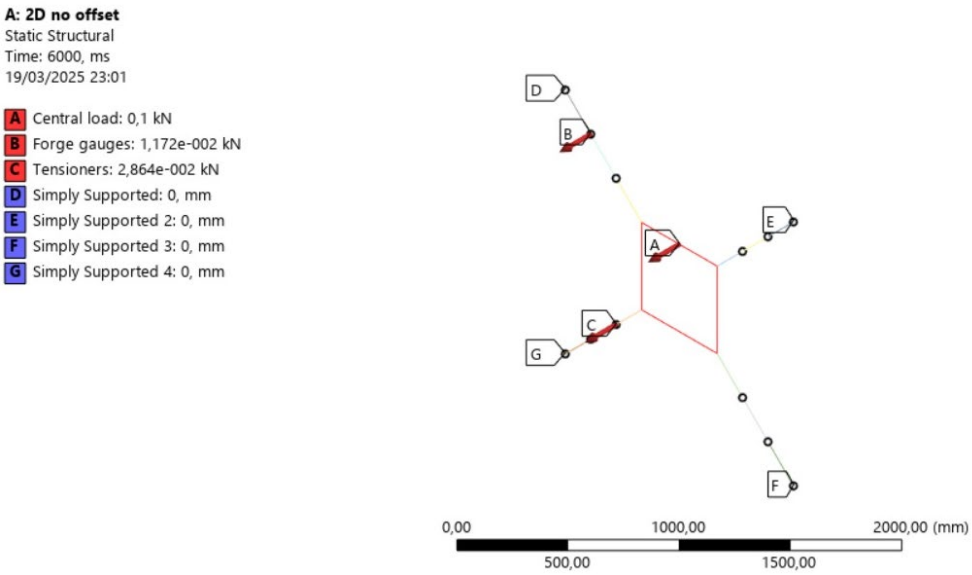

Figure 86: Geometric configuration of the FEA model, to determine the best placement of the force gauges and other hardware

Geometrically, the model represents the inner portion of the frame, with the corners simplified as rigid supports. To facilitate the application of point loads, each cable was divided into three segments (Figure 86). The model was then subjected to six incremental load steps, designed to test various placements of the tensioners, force gauges, and additional loads acting on the inner frame. This approach allowed for a detailed analysis of how different hardware configurations influence the system's overall deformation.

The results revealed a notable increase in deformation when the weight of the force gauges and other hardware was included in the model. Deformation rose from an initial 5,47 mm to 6,27 mm and 6,54 mm, depending on the specific configuration (Figure 87). The greatest displacement occurred when the heaviest components were positioned closer to the centre of the frame, an outcome that aligns with intuitive expectations, as a centrally placed load on a beam causes greater deformation than an off centred one of similar magnitude.

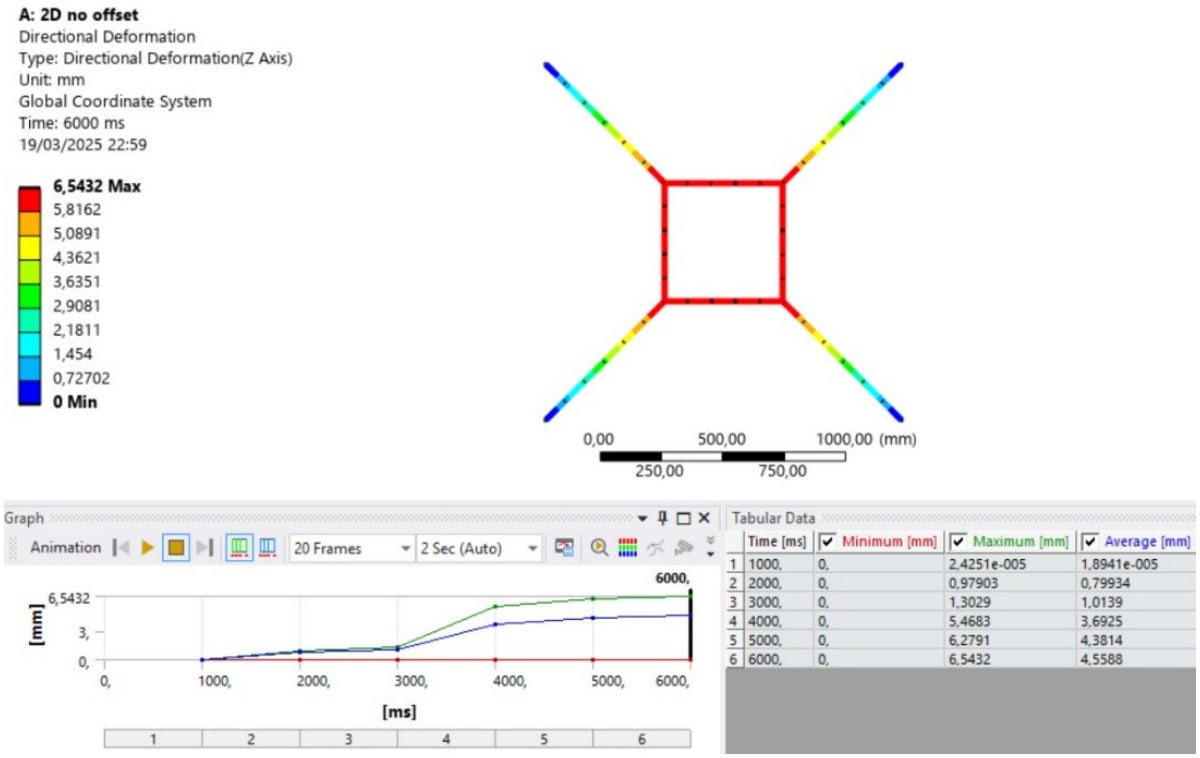

Figure 87: Deformations in the FEA model caused by various configurations of the force gauges and other hardware

Based on these findings, the final configurations for the first three prototypes were decided (Figure 88). Each setup includes specific overall layouts and corner details, designed to ensure that all forces converge along a common axis at the corners (Figure 89). Additionally, the heavier hardware components, such as the cable tensioners and force gauges, were strategically placed closer to the outer edges of the frame to minimize their influence on deformation. Despite this placement, each cable was still equipped with its own tensioner to allow for precise adjustment and positioning of the inner frame.

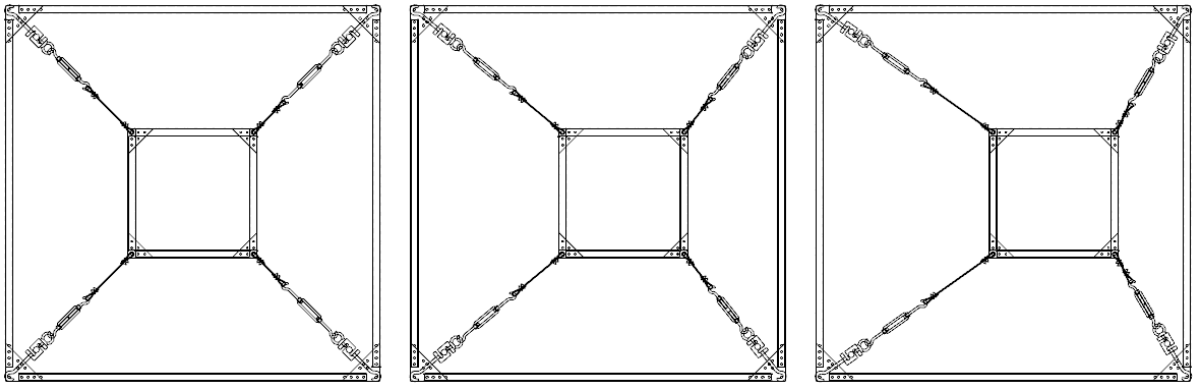

Figure 88: Final configuration of the first three prototypes

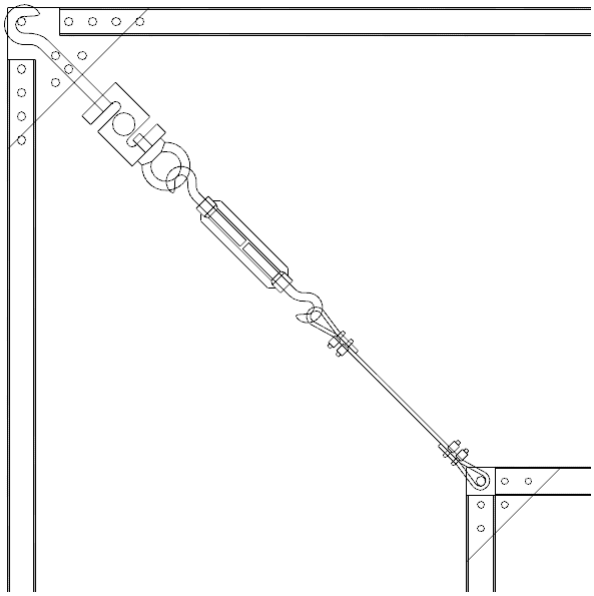

Figure 89: Corner detail of the final configuration of the prototype

Before moving on to the test results, one final modification to the prototype was implemented during the testing phase: the replacement of the cables with M8 threaded rods. Initially, the frame was pre-tensioned using cables; however, it soon became apparent that the cables were losing pretension at an unexpectedly high rate, dropping approximately 5, 10% of the total pretension within just 5 to 10 minutes. Marking the cable ends showed no visible signs of slippage, yet the pretension loss persisted. Even after adding three cable clamps per cable, the issue remained when pretensions approached 2800 N.

A possible explanation for this phenomenon was minute slippage at the cable ends, too small to detect visually, yet significant enough to cause a rapid decline in pretension forces. Another possibility was the reordering of cable strands around corners relaxing at a greater rate than normally observed in steel. A possible solution to this would have been to pre-tension the cables to a higher load and then reduce the tension to the target level

for testing. However, this approach was not feasible, as the load cells were rated for a maximum of 3000 N. Exceeding this limit risked damaging the sensors and made controlled implementation of the method impractical.

Instead, the chosen solution was to replace the cables with M8 threaded rods. This change proved effective: when subjected to comparable loads, the pretension loss was significantly reduced and stabilized after the initial few minutes (Figure 90). Specifically, the threaded rod-based system exhibited a pretension drop of only 0,43% in the first 5 minutes, followed by an additional 0,14% over the next 40 minutes (Figure 91). This confirmed the rods as a more reliable and stable solution for maintaining consistent pretension during testing.

While the high levels of relaxation were now largely resolved in the prototype, this issue highlights a critical design challenge that must be addressed in real-world applications.

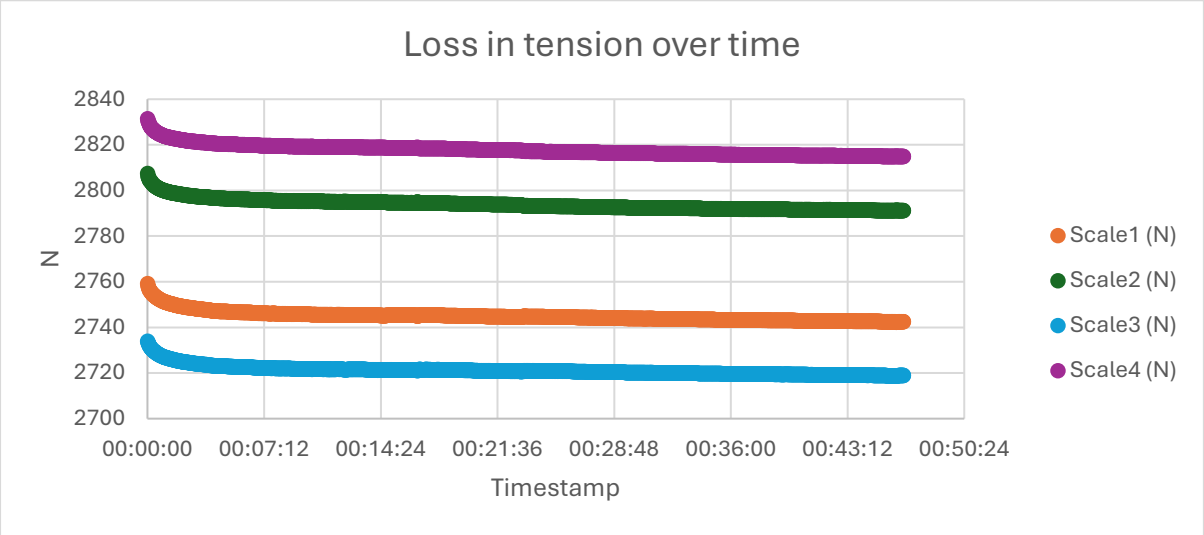

Figure 90: Loss in tension in the load cells over time

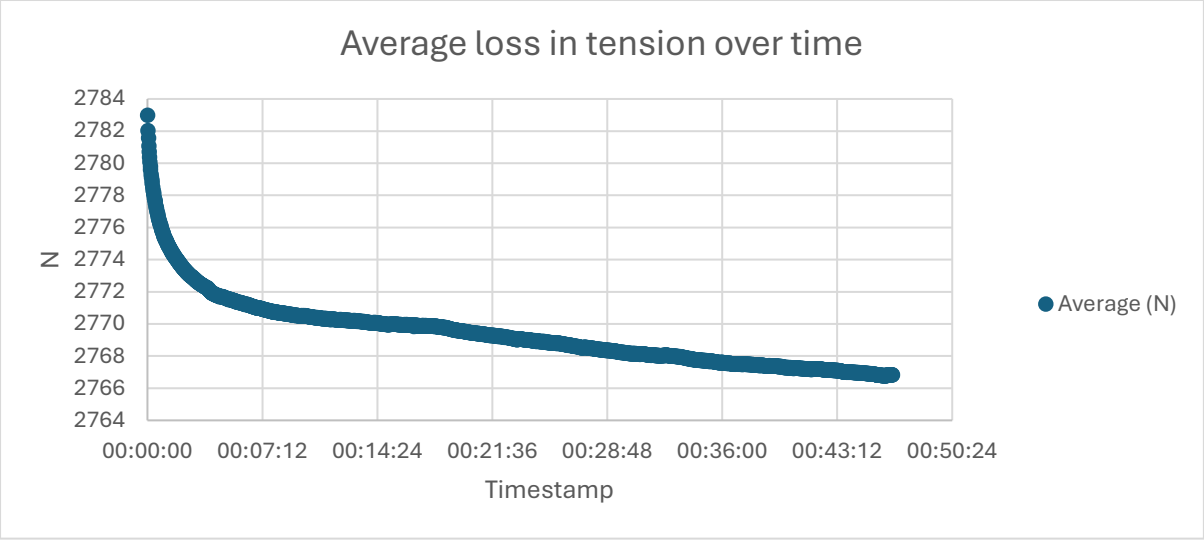

Figure 91: Average loss in tension in the load cells over time

Depth meters

The final step in the assembly involved installing the depth gauges, or more precisely, their custom holders. Four Mitutoyo Absolute Depth Gauges were borrowed from the faculty, each with a 12.7 mm measurement range and a resolution of ±0.0025 mm, providing more than adequate accuracy for the intended tests.

To mount the gauges around the inner frame, four custom holders were fabricated from 18 mm MDF plates. Each holder was equipped with three feet to ensure stability and prevent wobbling on the table surface (Figure 92).

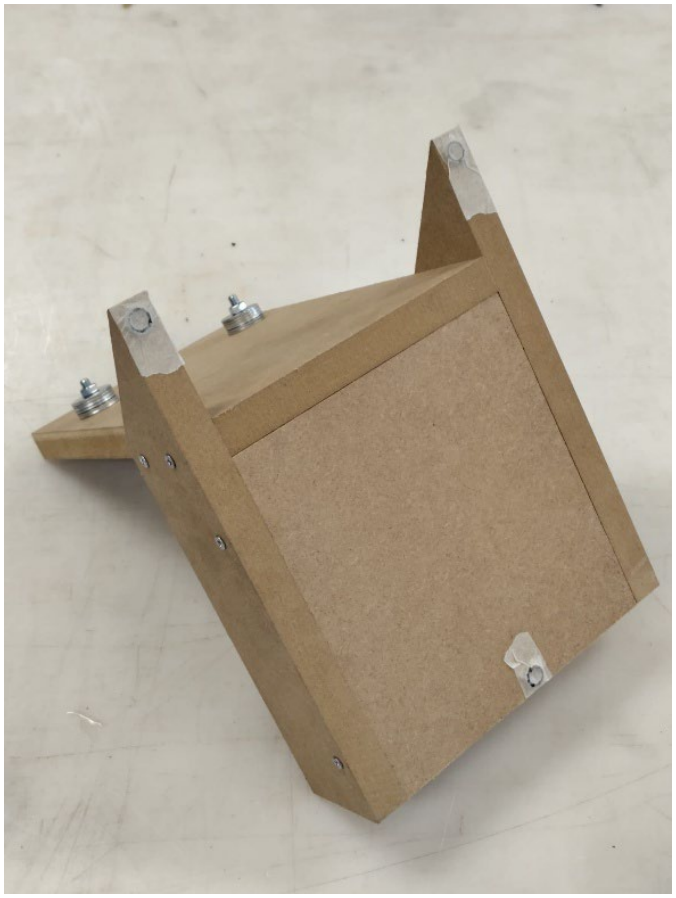

Figure 92: Feet placement on depth gauge holders

To further secure them, heavy steel offcuts from previous projects were added as ballast, effectively eliminating any unintended movement (Figure 93).

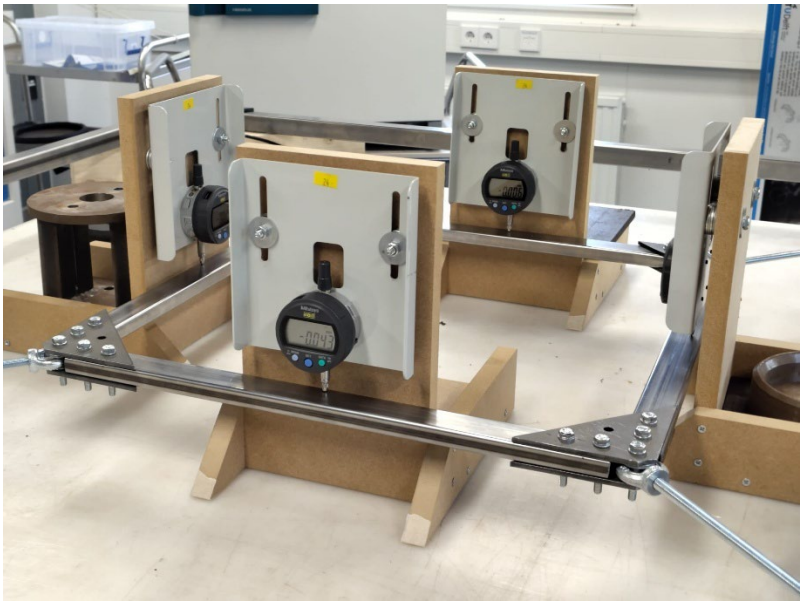

Figure 93: Setup for the depth gauges

During setup, the zeroing of the gauges remained stable over time, with no variation observed unless the frame or table was physically disturbed. Even in such cases, the gauges consistently returned to within ±0,01 mm of their original position, confirming that the holders were sufficiently rigid and reliable for the duration of testing.

To ensure accurate correlation between the physical prototype and the digital model, alignment markings were made at the midpoint of each inner frame strut. The depth gauges were then precisely aligned with these reference points, allowing for consistent and repeatable measurement throughout all tests (Figure 94).

Figure 94: Depth gauge marking alignment

Weights and load steps

The model was loaded using its self-weight and additional calibrated weights sourced from dumbbell sets. Each weight was individually checked and paired with others to achieve the most uniform distribution possible, for example, a weight that was 50 grams lighter could be balanced by combining it with two weights that were 20 grams and 30 grams heavier, minimizing discrepancies in the applied loads.

Weights	[g]
A1	2512
A2	3022
A1 + A2	5534
B1	2456
B2	3091
B1 + B2	5547
C1	2529
C2	2066
C3	980
C2 + C3	3046
C1 + C2 + C3	5575
D1	2467
D2	2052
D3	1008
D2 + D3	3060
D1 + D2 + D3	5527

Each setup consisted of three load steps:

- Step 1: No additional weights applied (self-weight only),
- Step 2: Low applied weights,
- Step 3: High applied weights.

In the symmetrical setup, this corresponded to applied weights of 0 g, ≈2500 g, and ≈5500 g at each corner, respectively.

For the asymmetrical configurations, the applied weights were adjusted to simulate higher wind loads on the areas with greater surface exposure, and lower weights on the opposing sides with smaller exposed areas, mimicking the expected real-world pressure distributions.

Additionally, the loading and unloading process was carried out over multiple cycles. This approach provided more data points and allowed for monitoring whether any slippage

occurred in the system, which could lead to a reduction in cable pretension during the loading of the inner frame and therefore cause inaccuracies in the measured deformation levels.

Design of the fourth out of plane configuration

The fourth and final setup tested a configuration in which the cables initially included an out-of-plane component. Specifically, at each corner, the cables were positioned 50 mm away from the frame's centreline, introducing a predefined spatial offset. In this setup, all force gauges were installed on one side of the frame, enabling the measurement of the differences in tension between the inward- and outward-facing cables (Figure 95).

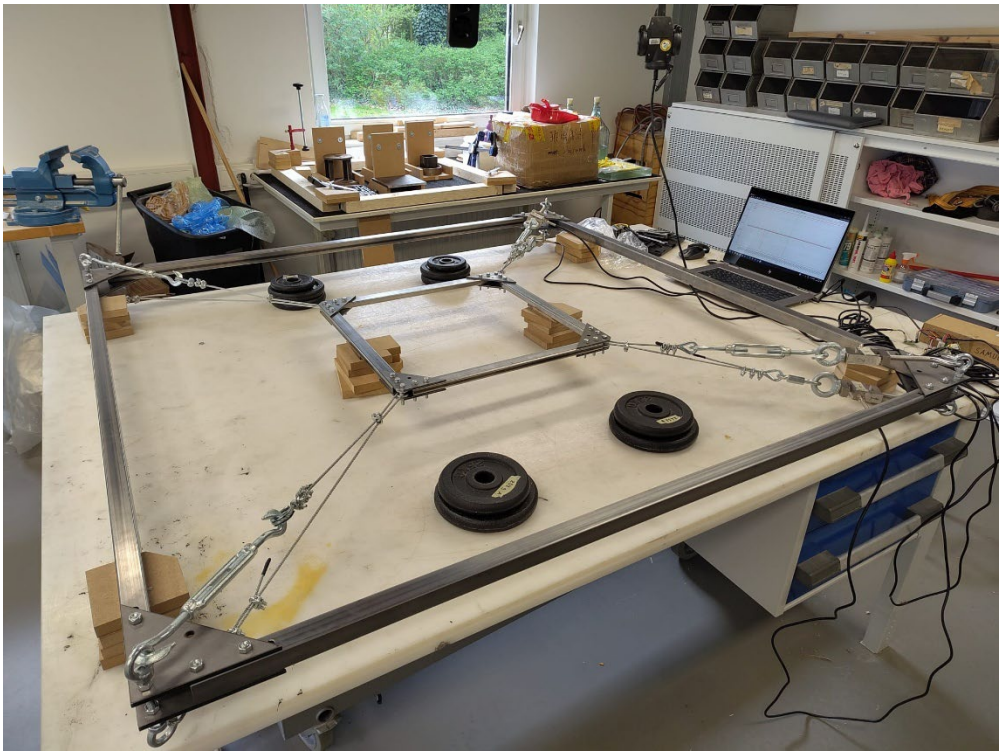

Figure 95: Fourth test setup with 8 out of plane cables, spaced 50mm apart at each corner

Additionally, this setup made use of distancing blocks to ensure that the inner frame was perfectly aligned in-plane with the outer frame during the initial pretensioning. This step was crucial, as without alignment, it would have been impossible to accurately predict the required pretension difference between the inward- and outward-facing cables. By using the distancing blocks, the cables could be tensioned and equalized under controlled, symmetric conditions (Figure 96). Only once the desired pretension was achieved and balanced, the spacer blocks could be removed.

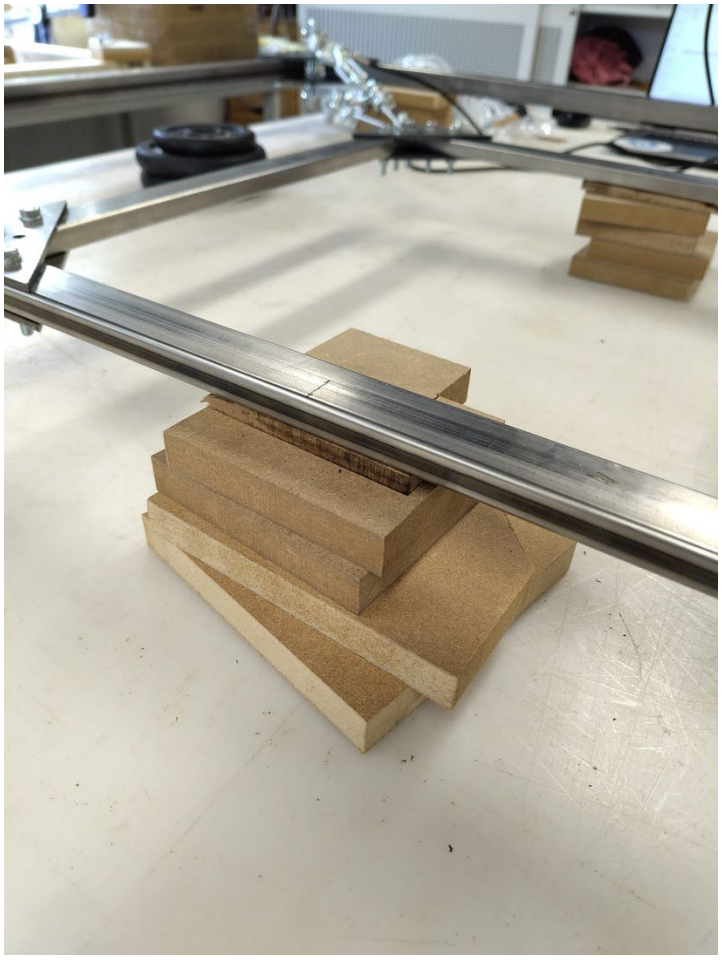

Figure 96: Spacer blocks used to ensure the frames were in the same plane when applying a pretension

To ensure balanced pretension on the opposite side of the frame, where pretension forces could not be directly measured due to the limit of four force gauges, a custom corner detail was devised to allow the cables to slip freely during the initial pretensioning phase. This setup involved wrapping the cable around an M8 bolt, with a 12 x 1 mm aluminium ring placed around the bolt to prevent cable damage from friction during tensioning. Additional M8 washers were used to keep the cable in position while the load was applied.

Once the desired pretension was reached, a clamp was installed around the corner, preventing the cable from rotating around the bolt and thereby locking the connection in place. To monitor any unintended movement during loading, reference markings were added to the cable and fixture, enabling visual checks for slippage throughout the testing phases (Figure 97).

Figure 97: Corner detail of the inner frame in the 3D setup

Although not perfect, the corner detail performed relatively well. The same setup was used on the opposite side of the frame, with tensioners placed in identical locations (Figure 95). During tensioning, a consistent increase in cable force was observed across both the top and bottom cables, with measured values matching within approximately 10–20%. The top cable where the tensioner was located exhibited a slightly higher pretension than the bottom, likely due to friction in the corner.

For the cables equipped with force gauges, final adjustments were made by tightening the eyebolts around the gauges. This allowed the pretension to be precisely equalized, ensuring perfect symmetry between the top and bottom cables on the measured side of the frame.

5.2 Prototype Results

In the first setup, the inner frame was positioned perfectly centrally, with less than 1 mm difference measured between all corresponding inner and outer struts. As expected, this resulted in the pretension forces in the cables being closely matched across all points, confirming the uniformity of the setup (Figure 98).

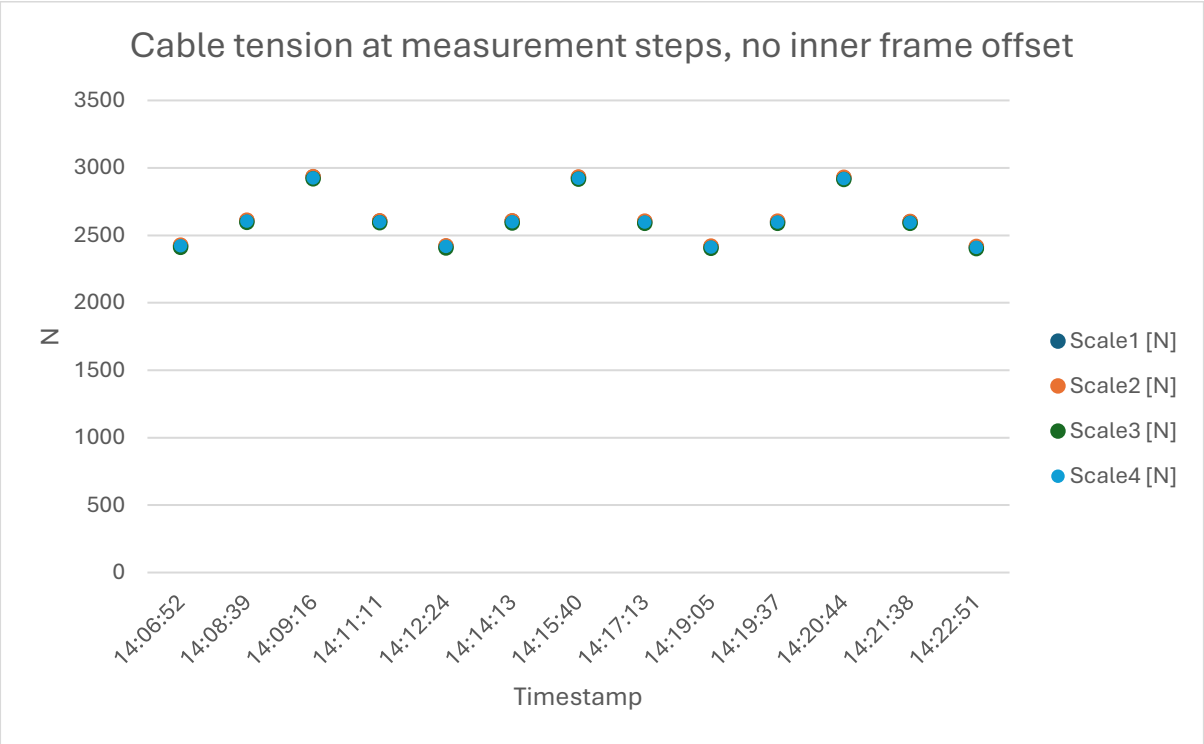

Figure 98: Pretension at measurement steps, no inner frame offset

Similarly, the deformation levels across the inner frame were consistent, and when plotting the four-point average over each loading cycle, no significant increase or decrease in deformation levels was observed. This indicates that no noticeable relaxation or slippage occurred during the loading and unloading cycles. The labels p, q, r & s refer to the points where the inner frames were measured, which was at the centre of each inner frame strut (Figure 99).

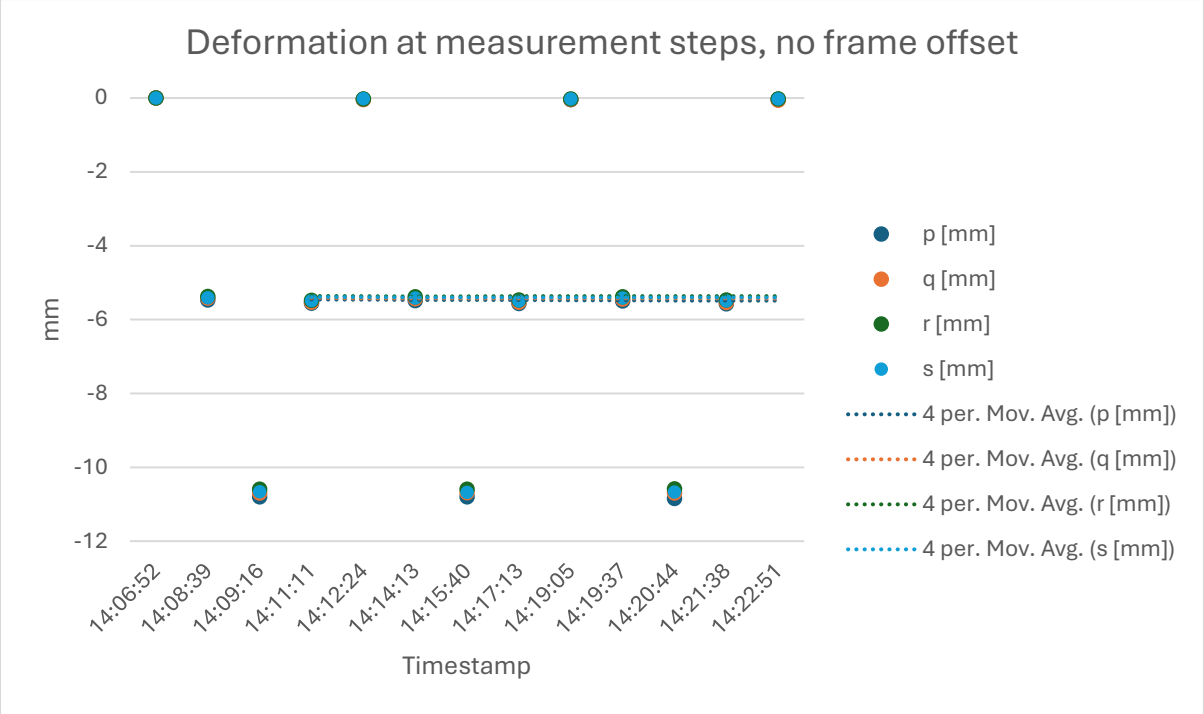

Figure 99: Deformation at measurement steps, no frame offset

In the second setup, the inner frame was moved 72mm off-centre and was also slightly shifted by 3 mm to one side. Given the practical challenges of precisely repositioning the frame during the tensioning sequence, this small deviation was considered acceptable for the purposes of the experiment.

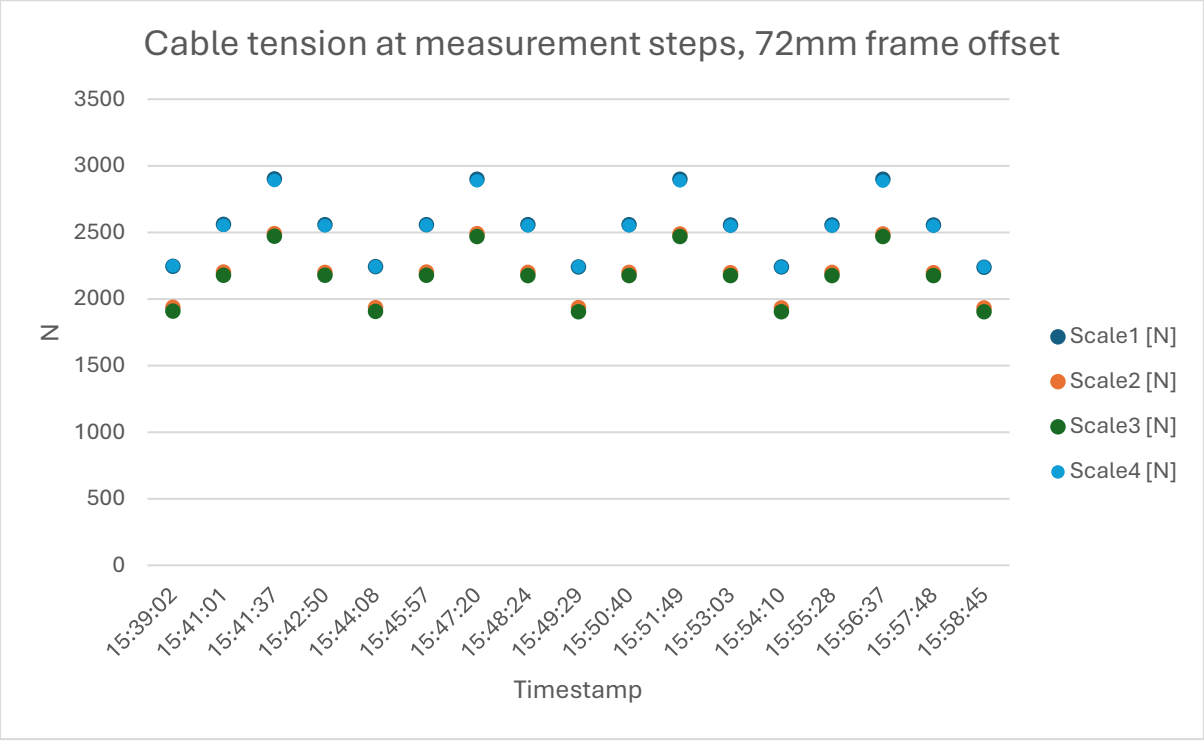

Figure 100: Pretension at measurement steps, 72mm frame offset

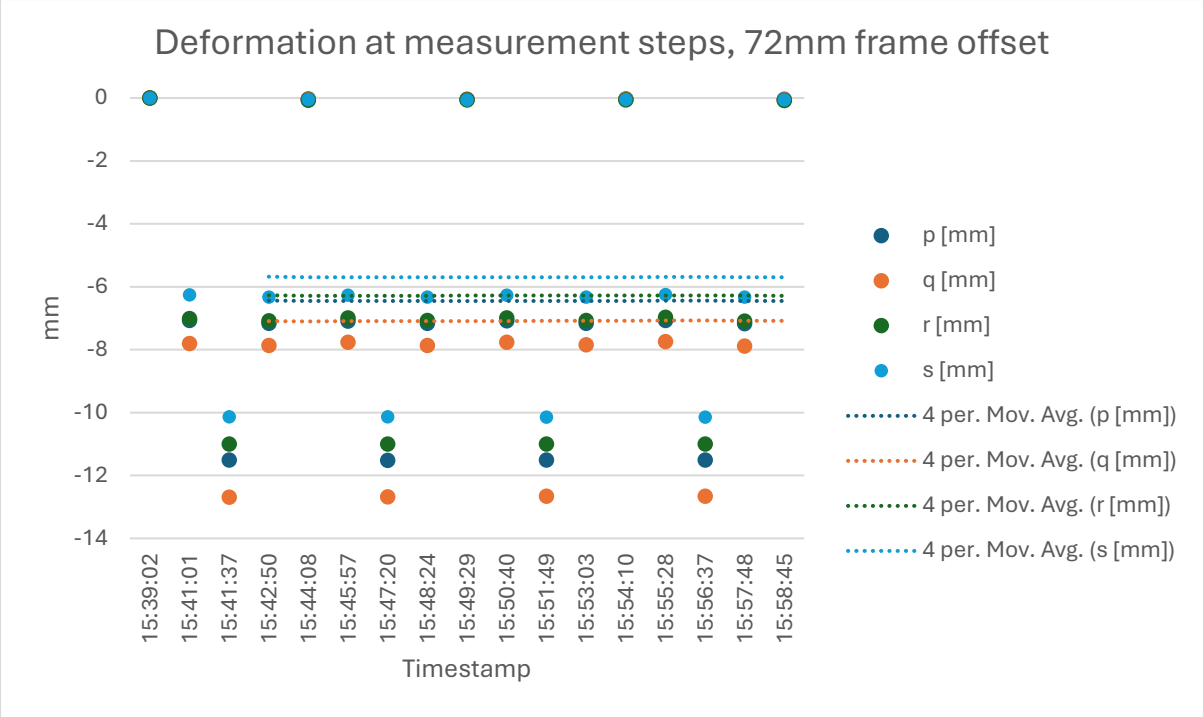

Figure 101: Deformation at measurement steps, 72mm frame offset

In the third setup, the inner frame was moved 123mm off-centre, with a lateral shift of 1 mm. Once again, the recorded data, including cable tensions and frame deformations, showed consistent measurements across the load cycles (Figure 102 & Figure 103).

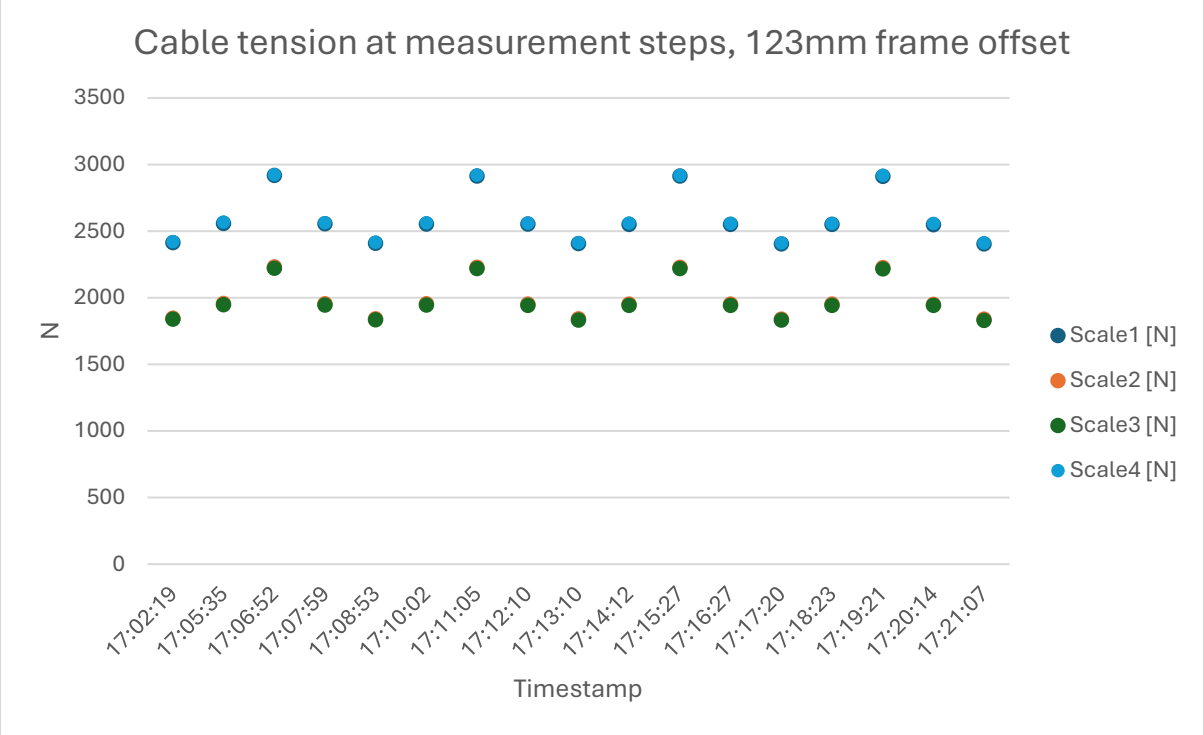

Figure 102: Cable tension at measurement steps, 123mm frame offset

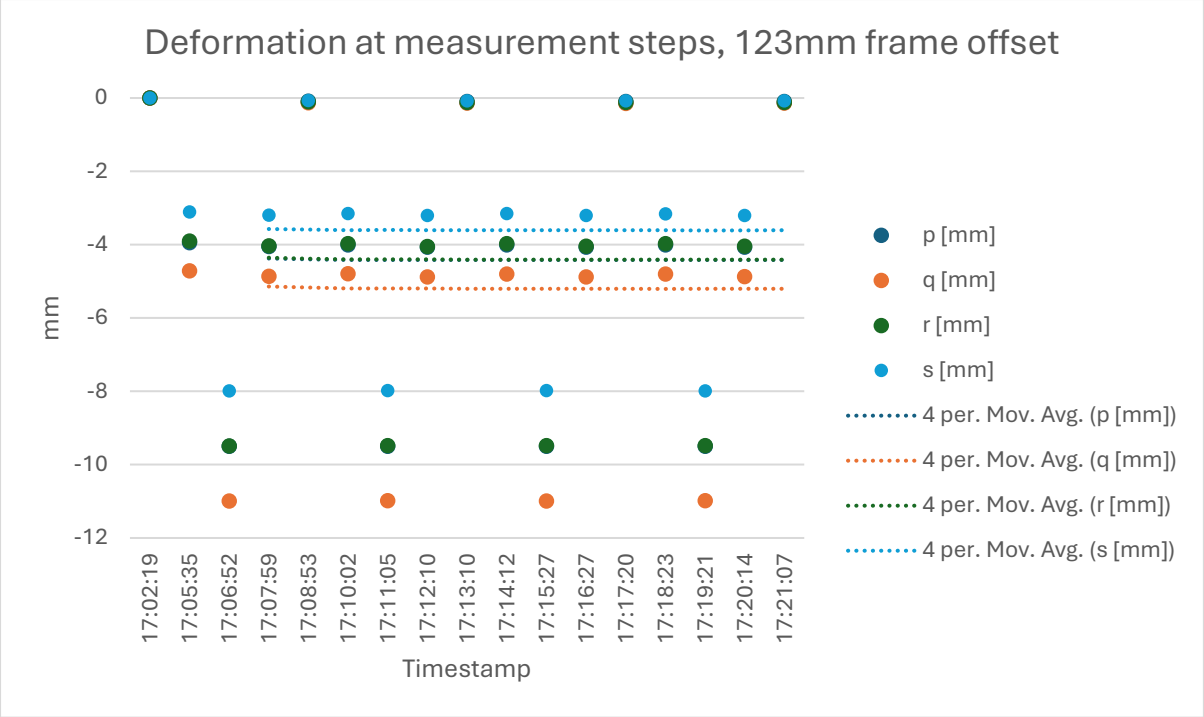

Figure 103: Deformation at measurement steps, 123mm frame offset

In the fourth and final configuration, the frame was connected using eight cables positioned 50 mm out of plane. The inner frame was placed centrally, though with a relatively large misalignment of 5 mm. Given the particular difficulty in repositioning the frame in this setup, this deviation was deemed acceptable. Despite the offset, the system was successfully tensioned, and the following tension and deformation levels were recorded (Figure 104 & Figure 105).

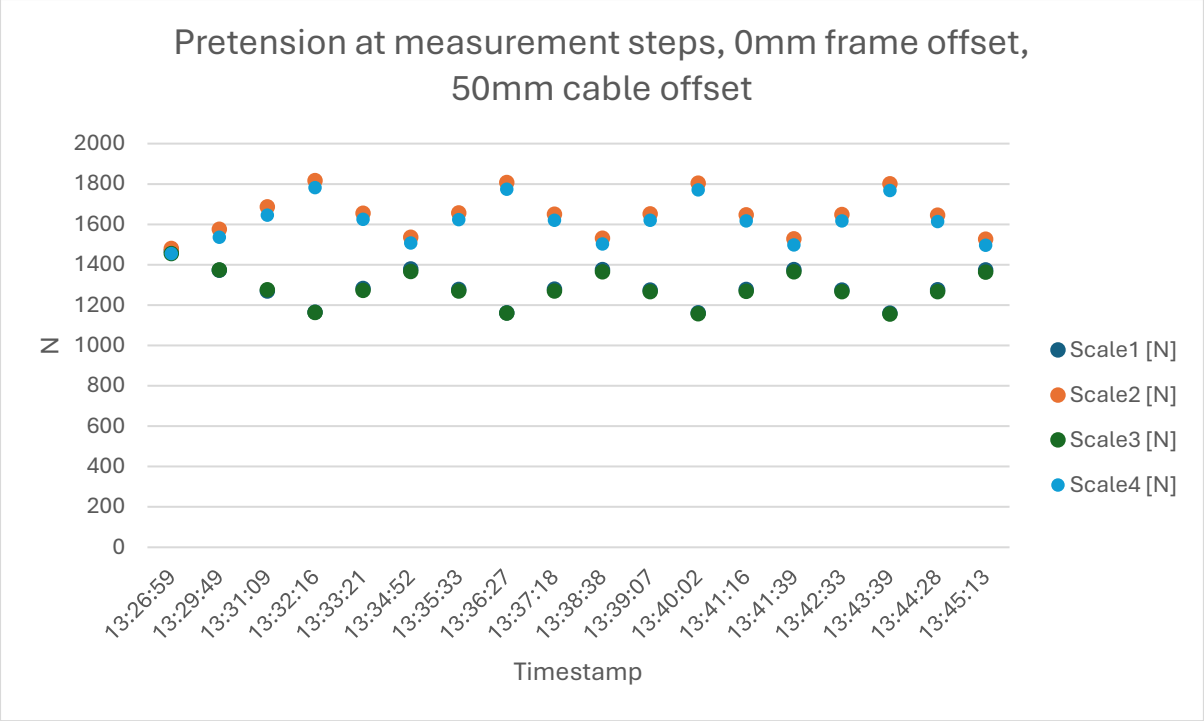

Figure 104: Pretension at measurement steps, 0mm frame offset, 50mm cable offset

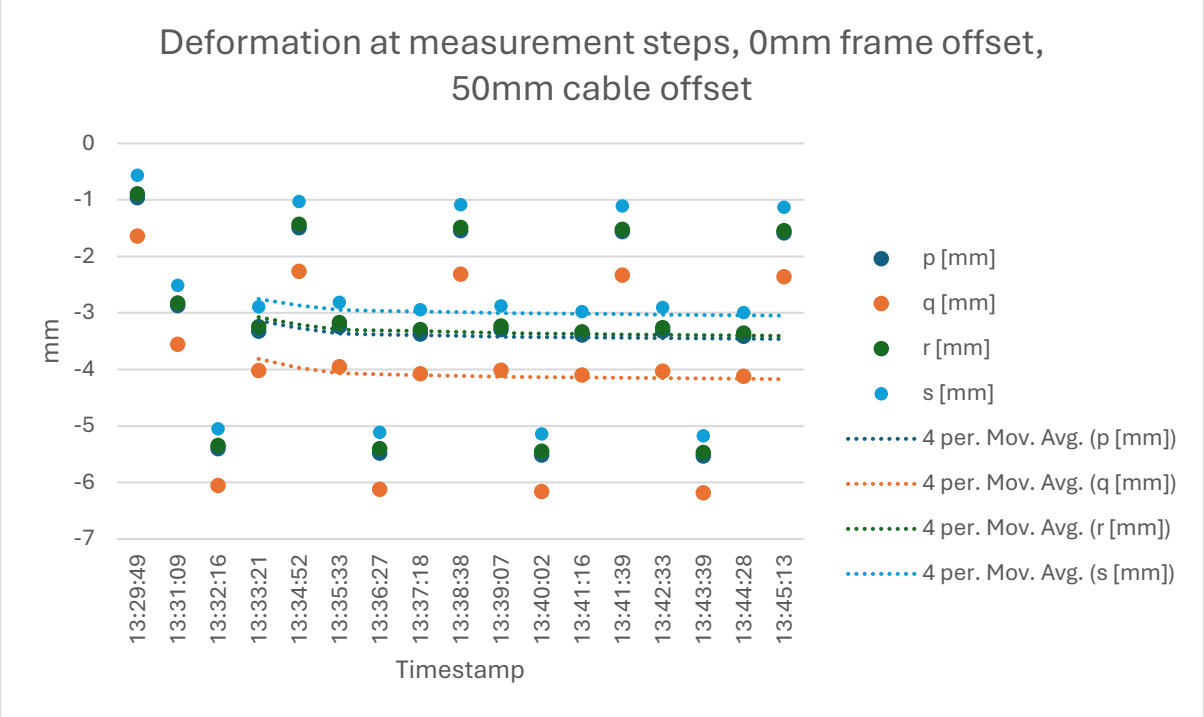

Figure 105: Deformation at measurement steps, 0mm frame offset, 50mm cable offset

In this configuration however, noticeable slippage occurred, and repeating the experiment did not resolve the issue. While the results indicated that the cables were inherently prone to slipping in this setup, visual inspection of the connection joints showed no clear signs of movement (Figure 97). However, slippage appeared to occur

gradually over time, with a noticeable increase in movement observed at the measuring gauges. To mitigate this effect, the first force measurements were taken within the first minute of loading, before significant slippage could develop. This approach allowed for the capture of potentially more accurate values for the first load cycle.

5.3 Result validation

To validate the experimental results, twin digital models were developed in Ansys Mechanical 2024. These models incorporated the self-weight of the components, which was applied as additional loads to the subdivided cable elements. This method was necessary because the FEA software did not support applying continuous line loads directly to cables. Instead, the loads were distributed across the cable segments to approximate a uniform load distribution and ensure realistic simulation of the physical setup. Additionally, the outer frame was omitted from the simulation, and the axial contraction that would have occurred in the physical frame was instead compensated for by modelling the cables with slightly reduced stiffness, speeding up the simulation process. This was later verified by modelling one of the three in plane configurations with outer struts and yielded identical results.

The following figures illustrate the support conditions and how the individual loads were applied to the cables.

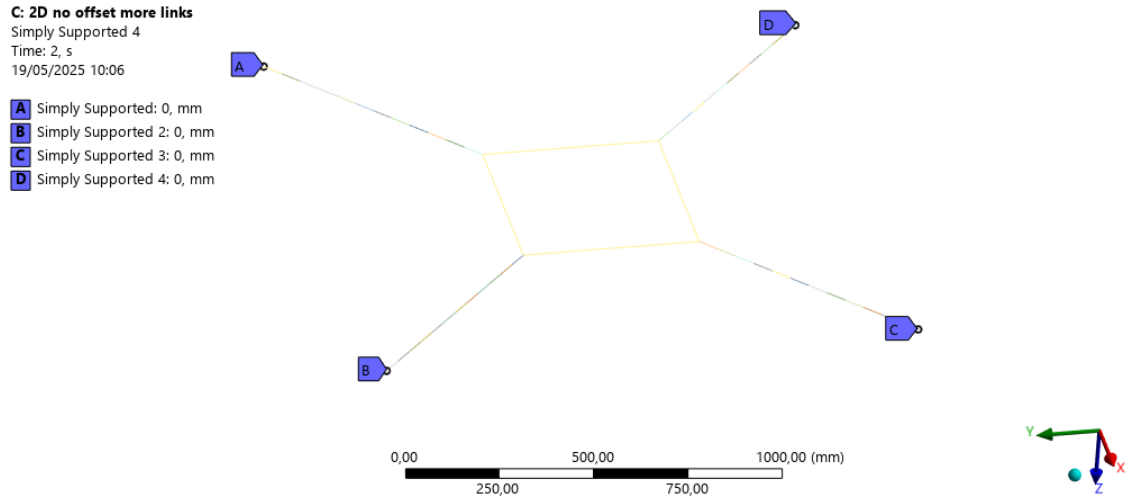

Figure 106: FEA model of the 2D symmetrical setup, support conditions

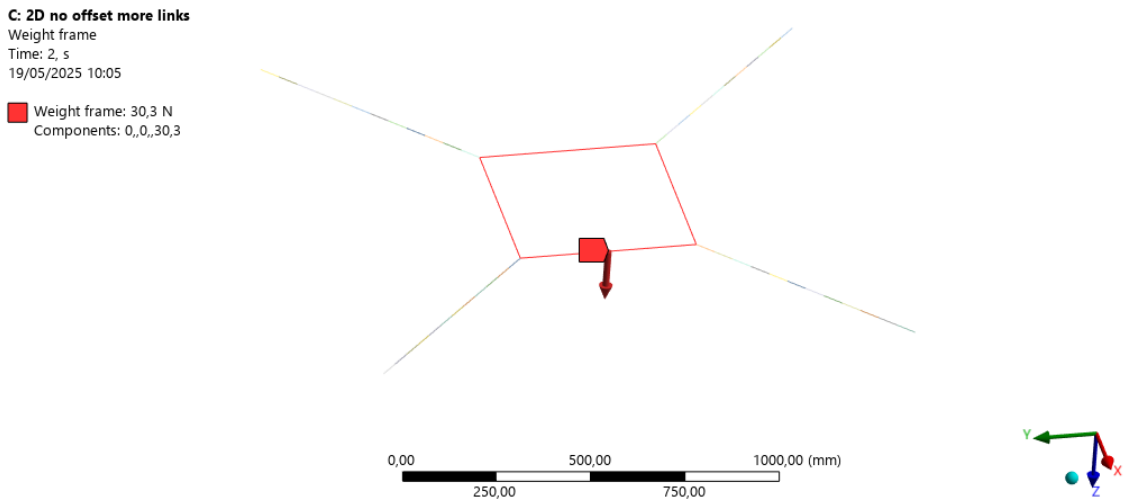

Figure 107: FEA model of the 2D symmetrical setup, frame weight

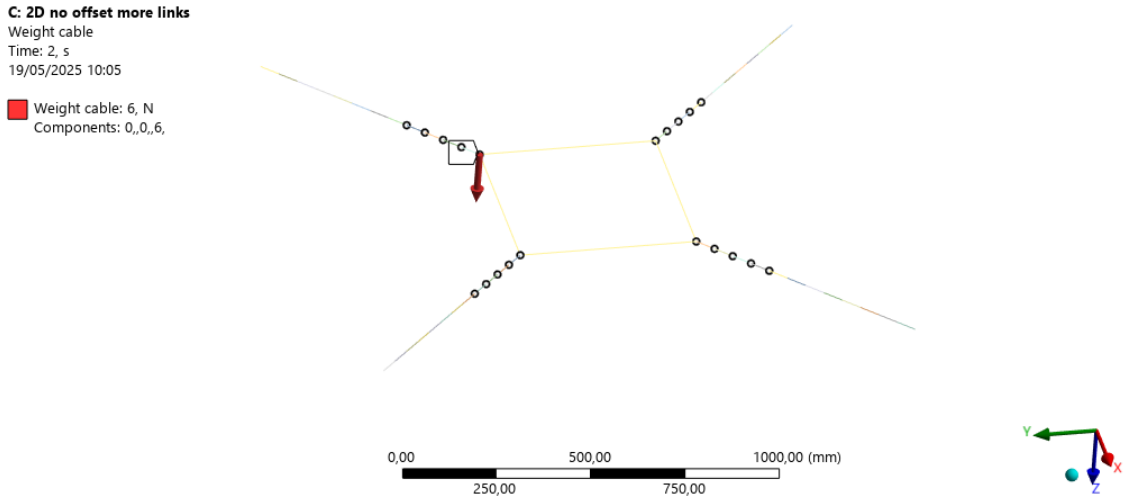

Figure 108: FEA model of the 2D symmetrical setup, weight of the threaded rods

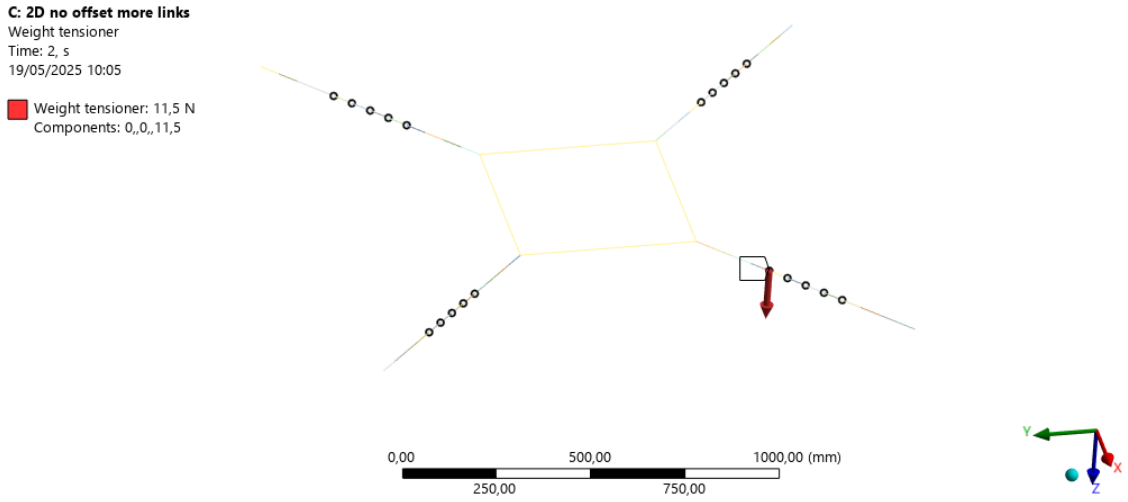

Figure 109: FEA model of the 2D symmetrical setup, weight of the tensioners

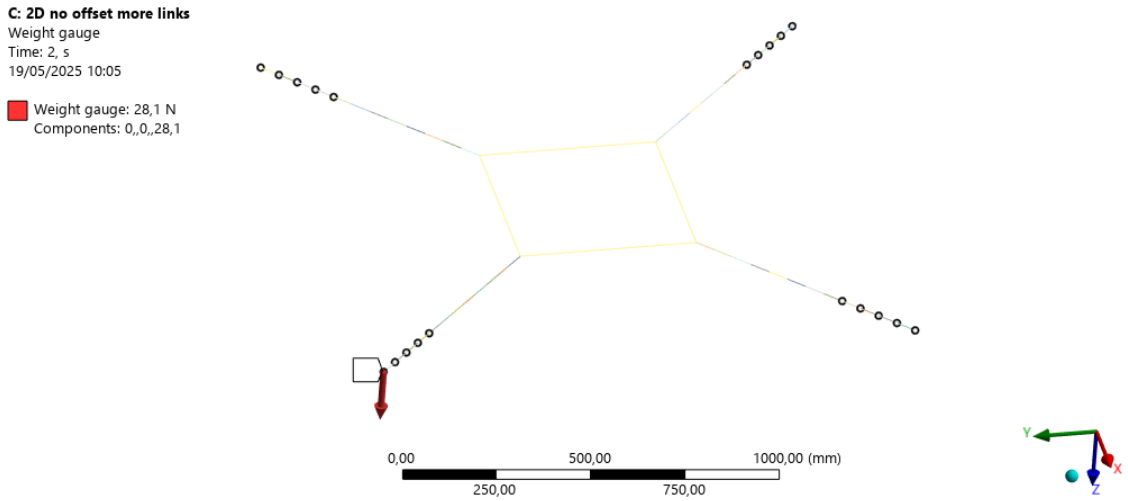

Figure 110: FEA model of the 2D symmetrical setup, weight of the force gauges

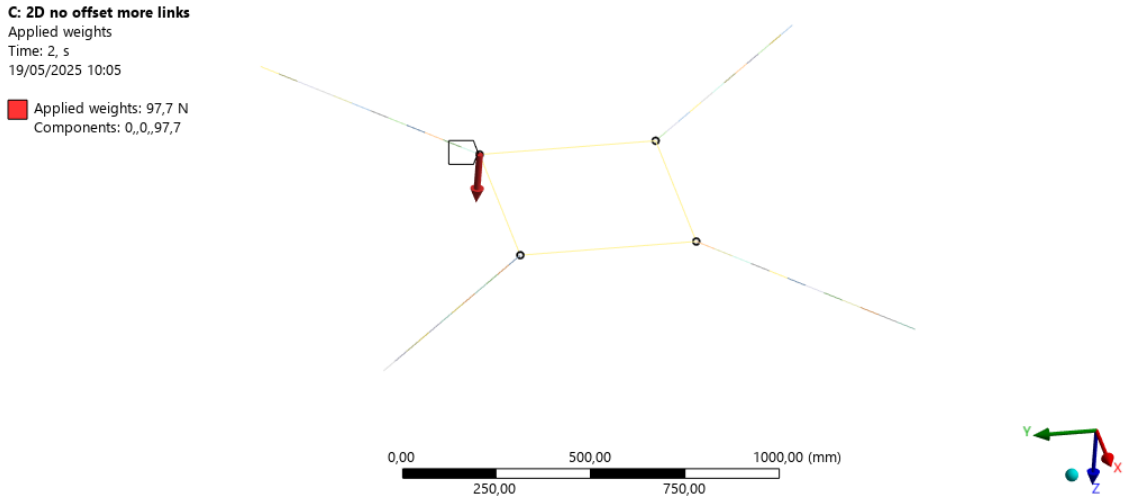

Figure 111: FEA model of the 2D symmetrical setup, applied weights

To ensure alignment with the real-world test results, the cable stiffness and pretension values were incrementally adjusted within the simulation. This iterative process continued until an almost perfect match with the experimental measurements was achieved. As shown in Figure 112, the simulation and physical test data closely overlap, with the two curves forming a near-identical match, validating the accuracy of the digital model. The values for the measured pretension and deformation were taken as the average of all the cyclic load steps.

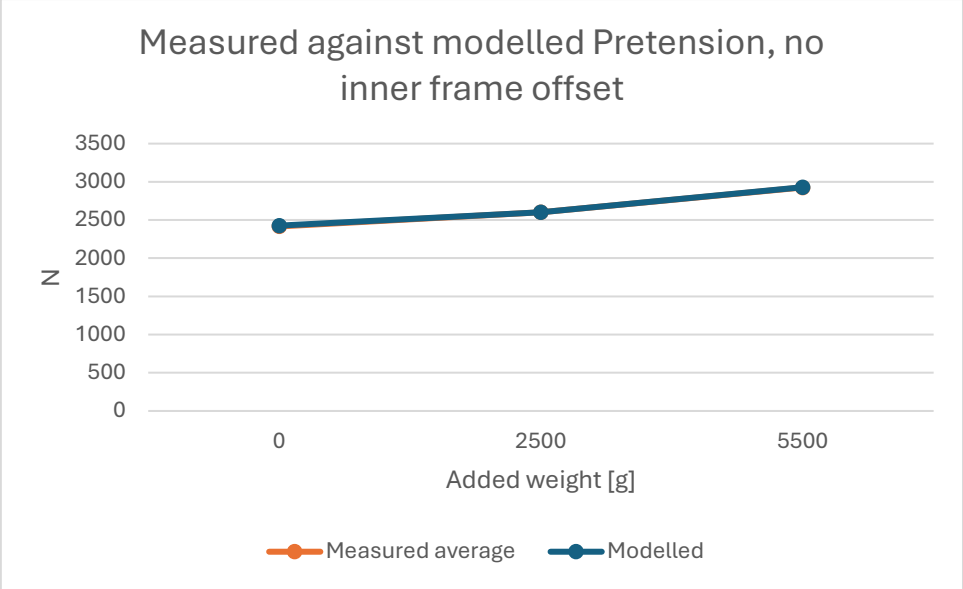

Figure 112: Measured against modelled Pretension, no inner frame offset

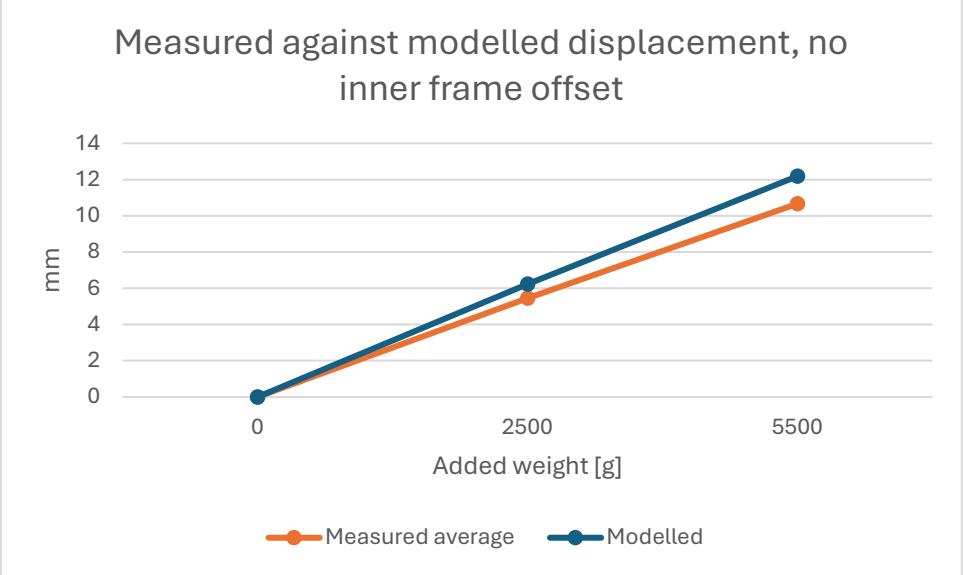

Figure 113: Measured against modelled displacement, no inner frame offset

However, when comparing the deformation levels side by side, a 14% variation was observed between the simulated and real-world results, with the real-world system exhibiting greater stiffness than the FEA model (Figure 113). Interestingly, this variation remained consistent across the two additional in-plane, off-centre configurations, with the real-world setups consistently 10–15% stiffer than their simulated counterparts. This trend is illustrated in the following figures, where "back" refers to the side with shorter cables, resulting from the off-centre placement of the inner frame, and "front" refers to the side with longer cables.

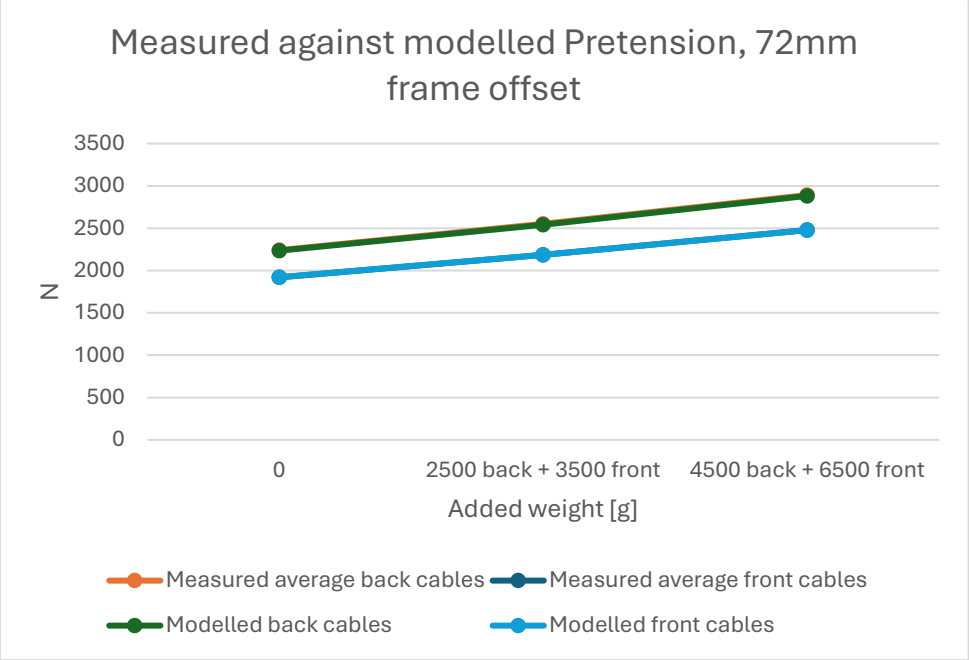

Figure 114: Measured against modelled Pretension, 72mm frame offset

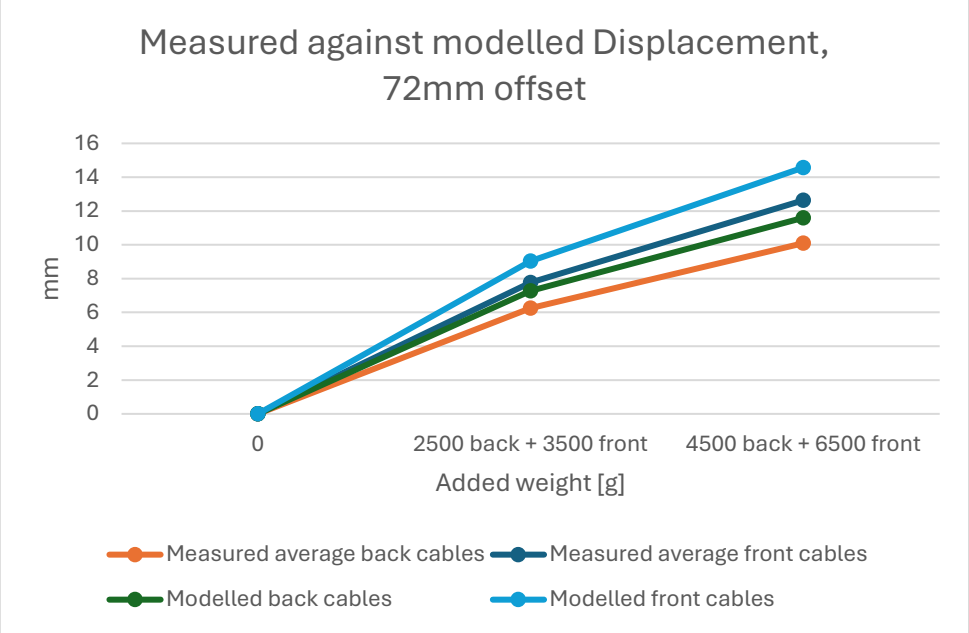

Figure 115: Measured against modelled Displacement, 72mm frame offset

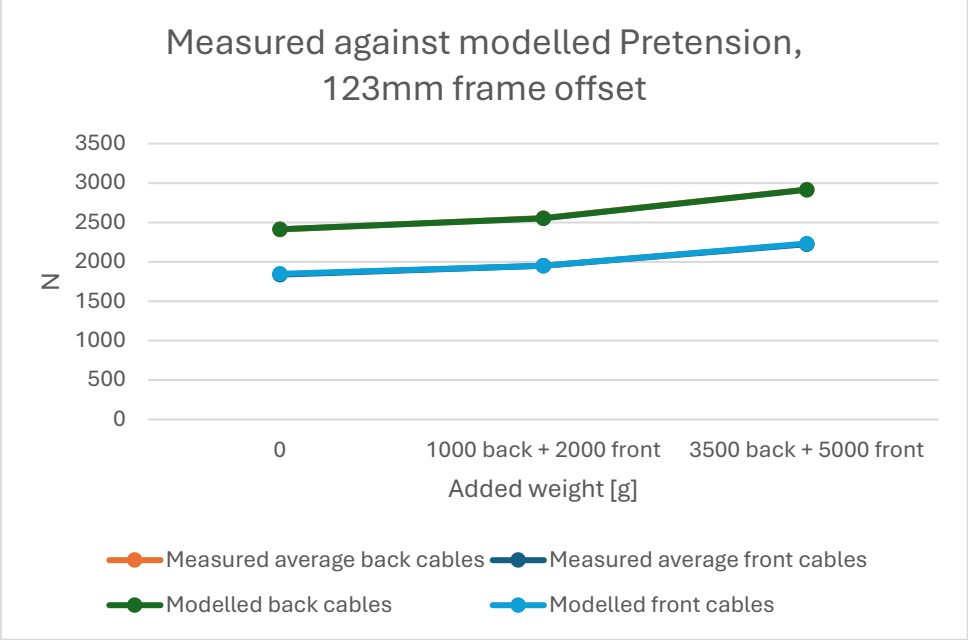

Figure 116: Measured against modelled Pretension, 123mm frame offset

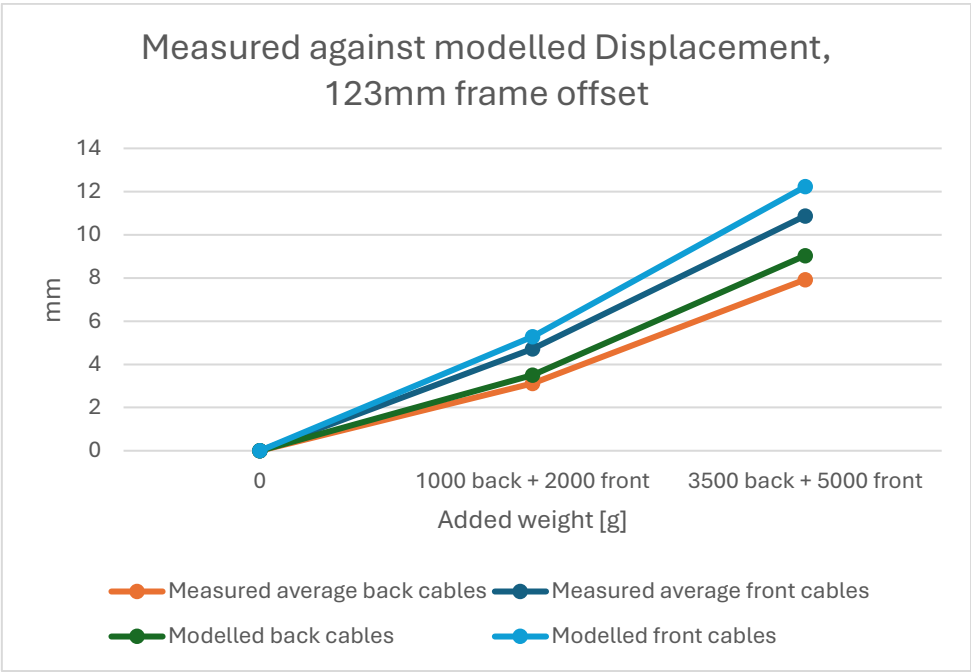

Figure 117: Measured against modelled Displacement, 123mm frame offset

Due to the consistent 10–15% discrepancy observed in the first three prototypes; a brief sensitivity analysis was conducted to assess whether any degree of out-of-planeness in the outer frame could have significantly influenced these results. In this analysis, four frames were modelled using the first symmetrical prototype configuration under comparable loading conditions, this time including the outer frames for completeness. Each outer frame differed only in the out-of-plane displacement of two opposing corners. To prevent any initial movement during cable tensioning, the inner frame was raised by

half the offset distance. From left to right, the corner offsets were 0, 1, 3, and 10 mm, with the 10 mm case representing an extreme scenario (Figure 118 & Figure 119). All frames were subjected to identical force and pretension conditions.

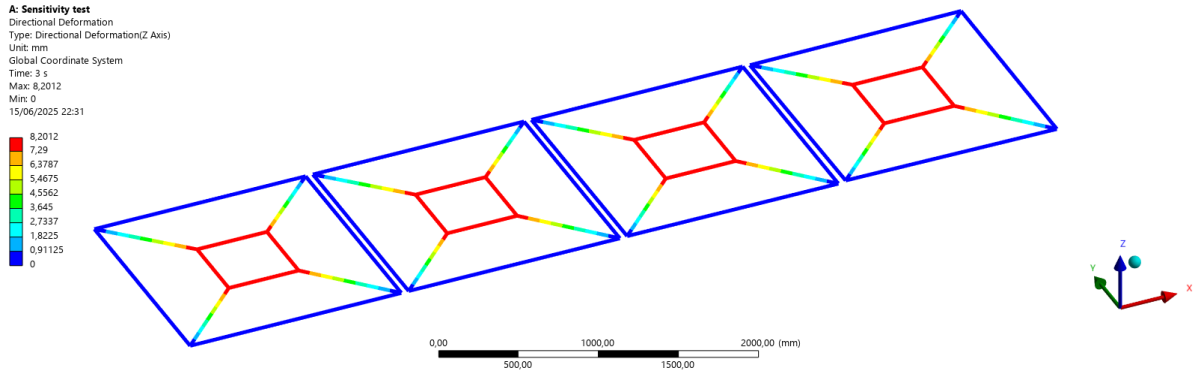

Figure 118: Full out of plane deflections of the sensitivity analysis

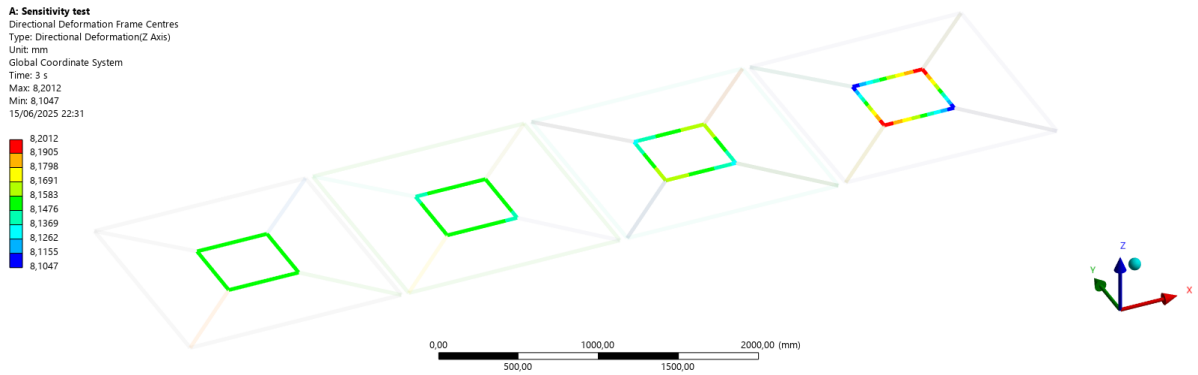

Figure 119: Out of plane deflections of the inner frames of the sensitivity analysis

The results indicate no significant average change in deflection due to slight initial out-of-plane geometries in the outer frame. Minor deflection differences were observed in the corners of the 10 mm out-of-plane configuration, which exhibited slight asymmetrical deformation. This outcome is expected, as the inner frame begins to conform to the deformed geometry of the outer frame under the influence of the cable tensions. However, such asymmetry would not have been captured in the physical prototypes, as measurements were taken at the midpoint of each strut.

Therefore, the 10–15% discrepancy is likely attributable to factors such as unmodeled friction or joint stiffness that increased the observed rigidity of the physical prototype. For instance, at the interface between the eyebolts, hooks, and the bolts in the inner and outer frames, short aluminium tubes were added around the bolts to serve as a softer interface and prevent damage to the bolt threads. After loading, indentations were observed on these aluminium tubes, suggesting that the connections were no longer

perfectly pinned and may have permitted some moment transfer. Although not perfect, this discrepancy was accepted, and it was assumed that the subsequent FEA models of planar cable configurations were sufficiently accurate to support conclusions about the system's performance.

In the fourth tested configuration, this time including out-of-plane cables, the previous 10–15% discrepancy between simulation and real-world results no longer held, with a larger and now negative variation in deformation observed.

As in the physical setup, the weight of the force gauges caused the inner frame to deform asymmetrically in the simulation. To maintain consistency and ensure a fair comparison, the average deformation of the inner frame was used as the reference in both the simulated and real-world scenarios. This averaging approach aimed to mitigate the influence of localized distortions and provided a more representative view of the system's global behaviour (Figure 120).

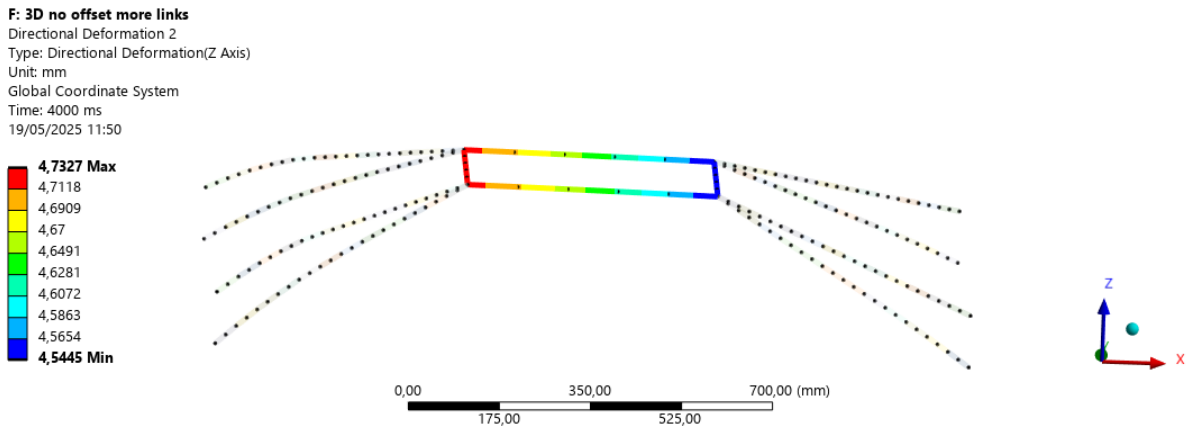

Figure 120: Asymmetrical deformation of the inner frame due to the weight of the force gauges (left)

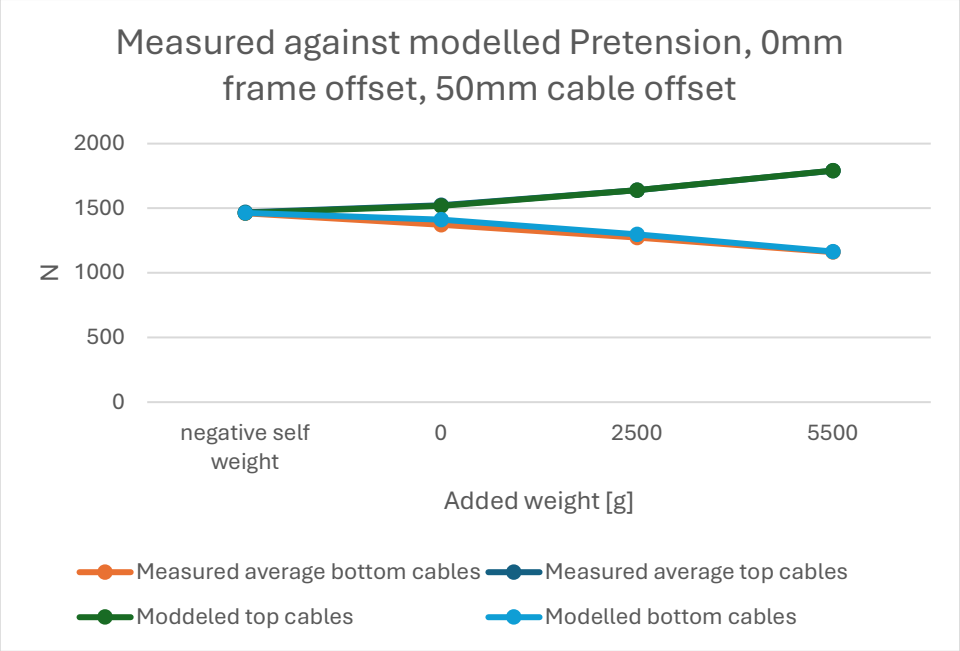

Figure 121: Measured against modelled Pretension, 0mm frame offset, 50mm cable offset

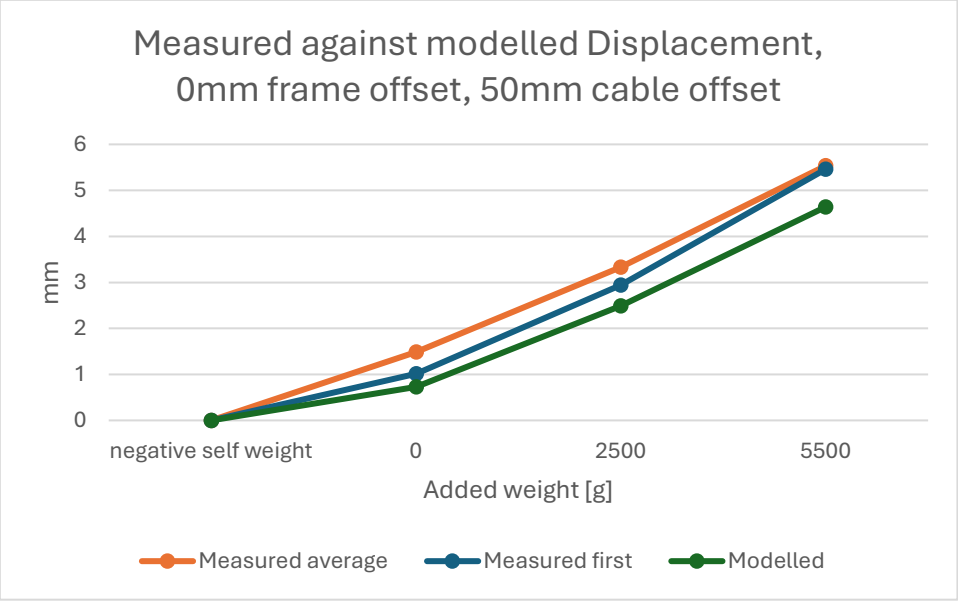

Figure 122: Measured against modelled Displacement, 0mm frame offset, 50mm cable offset

For the displacement curves seen in Figure 122, an additional curve is plotted based only on the first measured deformation levels, mitigating the effect of cable relaxation as best as possible. This increases the accuracy; however, a large discrepancy can still be observed, particularly at the first load step when the self-weight (-SW) of the frame is deforming the system (Table 4).

Table 4: Displacement levels of the 50mm offset system, comparing first and average displacement levels

Added weight [g]	- SW Frame	0	2500	5500
Average displacement modelled [mm]	0,00	0,73	2,49	4,64
Average displacement measured [mm]	0,00	1,49	3,33	5,53
First displacement measured [mm]	0,00	1,01	2,94	5,46
Difference average displacement measured	0%	51,0%	25,3%	16,2%
Difference first displacement measured	0%	27,7%	15,3%	15,0%

This likely indicates that there was significant slack in the connection joints especially noticeable during the initial loading of the system. However, as the system is gradually loaded further, this slack is taken out of the system, and it starts to more closely match the modelled scenario.

However, even in the scenario with the highest applied weights, and removing the observed slack, the real-world setup still exhibited greater deformation than the FEA model. This persistent discrepancy highlighted the limitations of the simplified simulation approach and prompted the development of a second, FEA model, this time including the outer frame.

By explicitly modelling the full frame, it became evident that a secondary mechanism was contributing to the reduced out-of-plane stiffness of the inner frame: the asymmetric movement or rotation of the connection points. As the opposing cables increased and decreased in tension, the threaded rods experienced varying degrees of bending, and a moment was simultaneously transferred to the outer frame, causing it to rotate slightly (Figure 123).

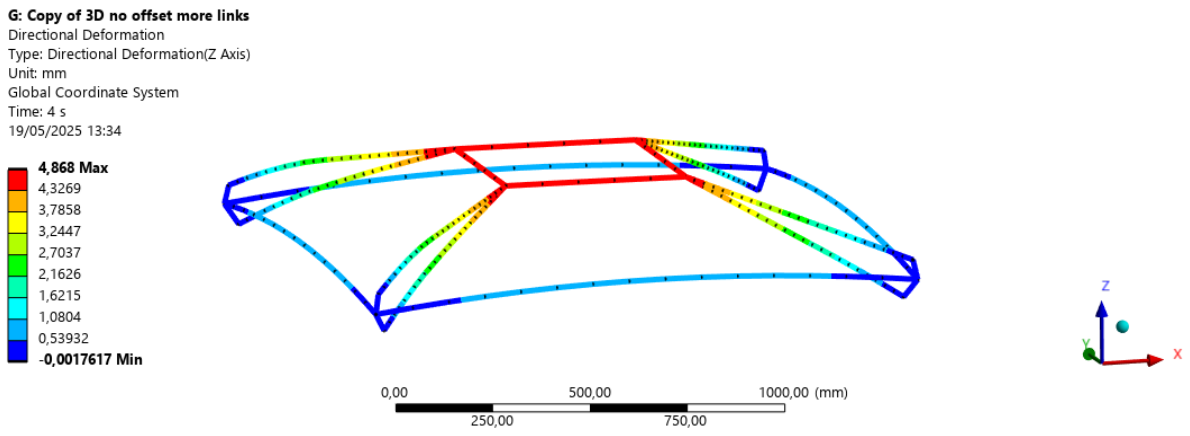

Figure 123: Increased deformation due to the rotation of the connection points of the outer frame

This rotation, combined with the asymmetric bending of the threaded rods, altered the relative positioning of the cable anchor points, resulting in one connection point shifting further inward compared to its opposing counterpart. This in turn leads to a change in cable tension balance between the inner and outer facing cables, hurting system performance (Figure 124).

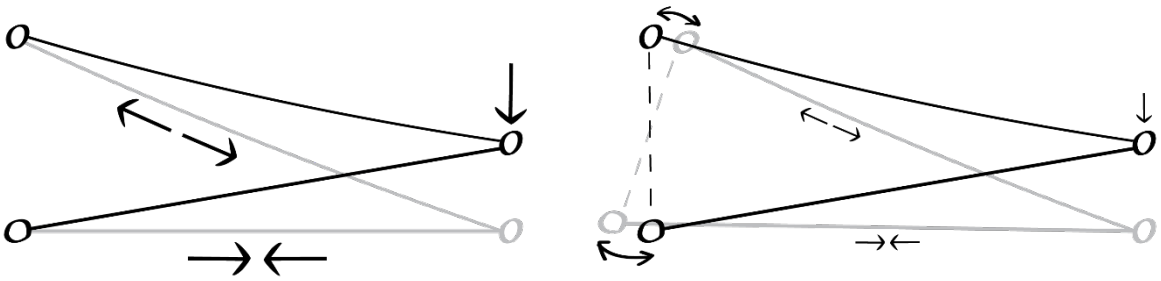

Figure 124: How rotation of the connection points hurts system out of plane resistance

Table 5: Displacement levels of the 50mm offset system with outer frame, comparing first and average displacement levels

Added weight [g]	**- SF**	**0**	**2500**	**5500**
Average displacement modelled [mm]	0,00	0,95	2,65	4,87
Average displacement measured [mm]	0,00	1,49	3,33	5,53
First displacement measured [mm]	0,00	1,01	2,94	5,46
Difference average displacement measured	0,0%	36,2%	20,4%	12,0%
Difference first displacement measured	0,0%	5,8%	9,7%	10,8%

This updated model more closely matched the experimental results, indicating that the movement of the connection points can be a significant contributing factor to the overall stiffness of the system (Table 5). This effect becomes more pronounced when the outer struts are able to rotate, or when the connecting rods are more prone to bending.

With that in mind, when considering the overall deformation levels, a significant reduction can still be observed. Comparing the two practical cases in which the inner frame was centrally positioned, the configuration where the struts lay in-plane with the outer frame exhibited a deformation of approximately 10.7 mm, with a calculated compressive force of around 2.1 kN in the outer struts, determined by solving the equilibrium equations for the rest of the frame.

In contrast, in the configuration where the cables were positioned 50 mm out of plane, the deformation was reduced to approximately 5.5 mm, while the compressive force in the outer frame remained similar, at roughly 2.1 kN.

This indicates that introducing an out-of-plane cable geometry contributes to a notable stiffening effect. In this particular scenario, it effectively halved the deformation without increasing the compressive loads in the outer struts, even in the presence of significant slack in the connecting joints. This highlights a promising strategy for enhancing structural performance without adding additional mass. The effectiveness of this approach increases significantly when the connection points are more effectively restrained from moving, further improving the system's overall stiffness and stability.

6. Design Integration

6.1 Comparing cross-sectional configurations

Integrating the model results into the design led to the development of various cross-sectional configurations, each differing in terms of cable planarity and the potential placement of the thermal line. In total, nine configurations were considered. Throughout this process, numerous simulations were conducted to assess the feasibility and performance of each design. A summary of the key findings is provided for each configuration group.

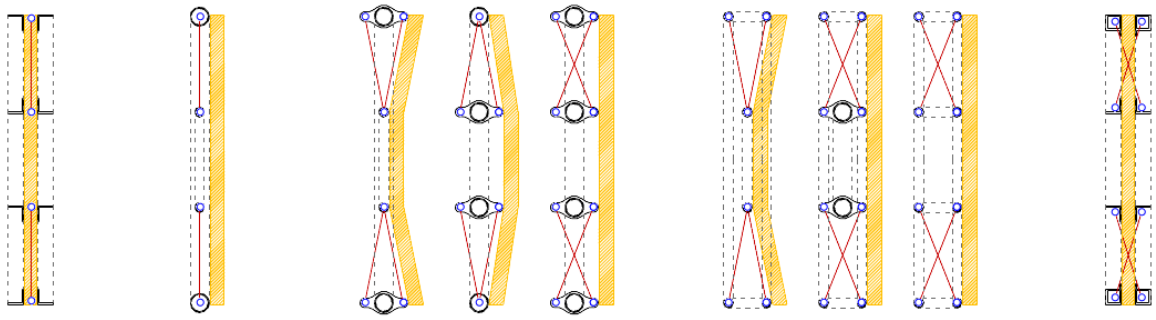

Figure 125: Cross-sectional configurations of tensile façade systems, illustrating variations in cable geometry and thermal line placement across the evaluated design groups.

The leftmost configuration represents the system in its most traditional form, featuring planar cables with the thermal line located centrally within the panel. Similar to cable net facades, this configuration requires relatively large deformations to develop significant out-of-plane resistance, unless compensated by substantially increasing the pretension in the cables.

For example, approximate values for this setup to resist a 1 kPa wind load on a 3 x 3 m panel with a 1 x 1 m inner frame and 100mm^2 cable cross-sectional area (with a Young's modulus of 210 GPa) are provided below (Table 6). These estimates are based on the Excel model previously discussed:

Table 6: Tensions in the cables at varying deformation levels of a 3x3m panel with a 1x1m inner frame and 1kPa wind loads

Maximum level of out of plane deflection	Applied cable pretension [kN]	Tension in cables at maximum deflection [kN]	Compressive force in outer struts at maximum deflection [kN]
1/500	236	236	167
1/250	117	117	83
1/100	43	48	34
1/50	5	24	17

The thermally broken configuration of this setup is particularly vulnerable to stability issues, primarily due to the low torsional rigidity of the profiles. As cable tension increases, this lack of stiffness causes the frame to warp, compromising the system's stability. As a result, this façade panel can feasibly only be pretensioned after installation, when it is restrained from out-of-plane deformations.

The second configuration is similar to the first in terms of out-of-plane resistance, but it employs single hollow sections with significantly greater torsional rigidity (Figure 125). This can effectively resolve frame stability issues and allows the frame to be pretensioned in the factory, eliminating the need for on-site tensioning. Additionally, the frame no longer needs to be rigidly connected to the substructure, an advantage in terms of accommodating movement between the frame and the substructure.

However, in this configuration, the thermal line is positioned outside the structural line, which introduces new challenges. Specifically, any structural deformation would require greater movement tolerances within the insulation layer, compromising thermal and acoustic performance due to the larger gaps required.

The third group of configurations introduces an out-of-plane component to the system and utilizes a torsionally rigid, singular strut for the outer frame (Figure 125). As with the second configuration, the thermal line must be placed outside the structural line. However, in this case, it is aimed for the structure to deform less, reducing the need for large gaps in the insulation layers, an advantage for both thermal and acoustic performance.

The trade-off, however, is that the assembly becomes wider and more complex to manufacture, potentially impacting fabrication efficiency and material usage.

The fourth group of configurations is similar to the third; however, instead of relying on torsionally rigid frames and connection rods that resist bending, these setups utilize a double-frame system (Figure 125). In this configuration, when an out-of-plane load is applied, the forces are transferred to double struts, one experiencing an increase in compression, while the other decreases. This approach can potentially result in stiffer connection points and, as a result, makes more effective use of the out-of-plane components of the cable system.

The last and rightmost configuration is again similar to the fourth group, with the only variation being the placement of the thermal line (Figure 125). In this case, due to the out-of-plane component of the cables, the compressive forces in the initial prestressed configuration can be significantly reduced, even when strict deformation limits are imposed. This suggests that only limited torsional rigidity would be required for the system to remain stable, potentially allowing it to maintain structural stability during manufacturing without relying on heavily reinforced elements.

6.2 Simulating the most promising cross-sectional configurations

To assess the structural performance of the systems, three types of configurations were modelled using Ansys Mechanical 2024. These are based on structural similarity, and are as follows:

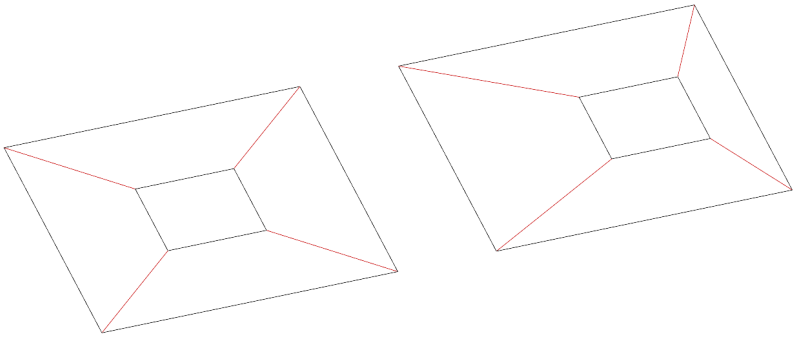

Figure 126: A fully planar configuration, potentially using thermally broken struts

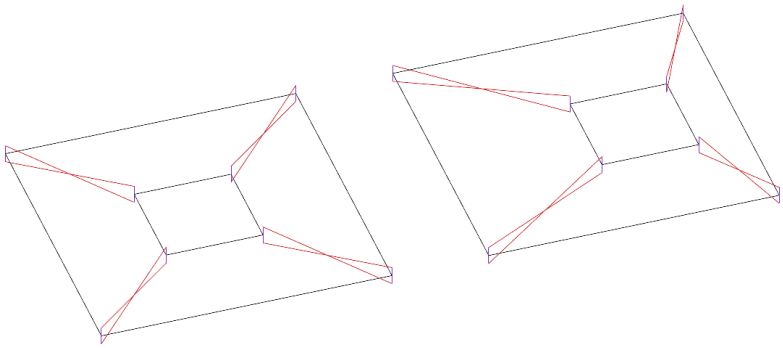

Figure 127: An out-of-plane cable configuration attached to single struts with high torsional and bending resistance

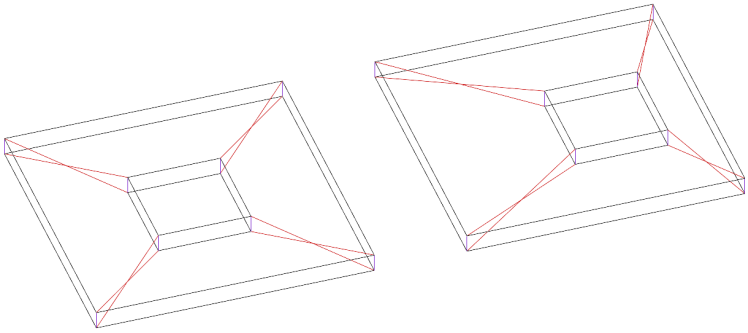

Figure 128: An out-of-plane cable configuration with doubled struts one increasing in compression and one decreasing in compression when loaded

Other configurations where the cables are placed out of plane on only one side were excluded from the analysis, as they would consistently underperform compared to systems with out-of-plane cable placement on both ends (Figure 129).

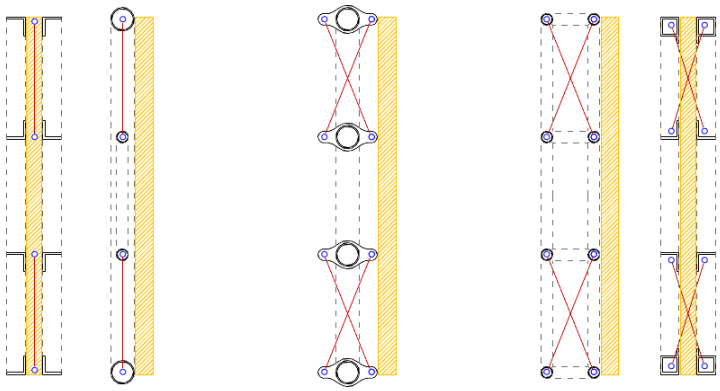

Figure 129: The remaining cross-sectional configurations simulated in Ansys Mechanical 2024

What follows is a summarized list of all of the most relevant simulation parameters:

- For all simulations, SHS (square hollow section) profiles were used for all struts. This choice was made to minimize complex deformations, prevent LTB and to provide approximate values for relatively optimized cross-sectional shapes.
- In the second configuration, all rods connecting the cable connection points to the single SHS profile were modelled as solid sections with an arbitrarily high radius of 100 mm, ensuring that no significant bending occurred. In this setup, any movement of the connection points was solely due to the rotation of the SHS frames itself.
- For the third configuration, no composite behaviour was modelled between the doubled cross-sections along the length of the profiles. The profiles were only coupled at their ends using similar r=100mm rods.
- All loads applied to the frame configurations were based on a wind load of 1 kPa and were applied directly to the struts in a way that induced pure bending.
- The geometric configuration of the frame measured 3 x 3 meters, with an inner frame opening of 1 x 1 meter placed symmetrically.
- In addition, supplementary simulations were conducted with the inner frame offset by 0,5 meters and are specifically mentioned.
- All components are materialized with the standard structural steel material properties Ansys Mechanical 2024 ships with; this includes a Young's modulus of 210GPa.
- All frame corner supports were restricted from out-of-plane deflection; however, in-plane movement of the support points was not constrained, and rotation at all points was permitted.
- All of the simulations were run with large deflections turned on and weak springs turned off.

The initial configurations tested were symmetrical, with the inner frame positioned perfectly centrally to ensure optimal system performance (Figure 130 & Figure 131). Please note that the y-axis of the following graphs does not use a linear scale for deflections. Instead, it represents the inverse deflection limit (1/x). This approach was chosen to provide a more detailed comparison of stiffer systems, which would otherwise appear compressed into a narrow band of low deflections. It also allows for a more direct comparison with the deflection limits typically used to rate and assess façade systems.

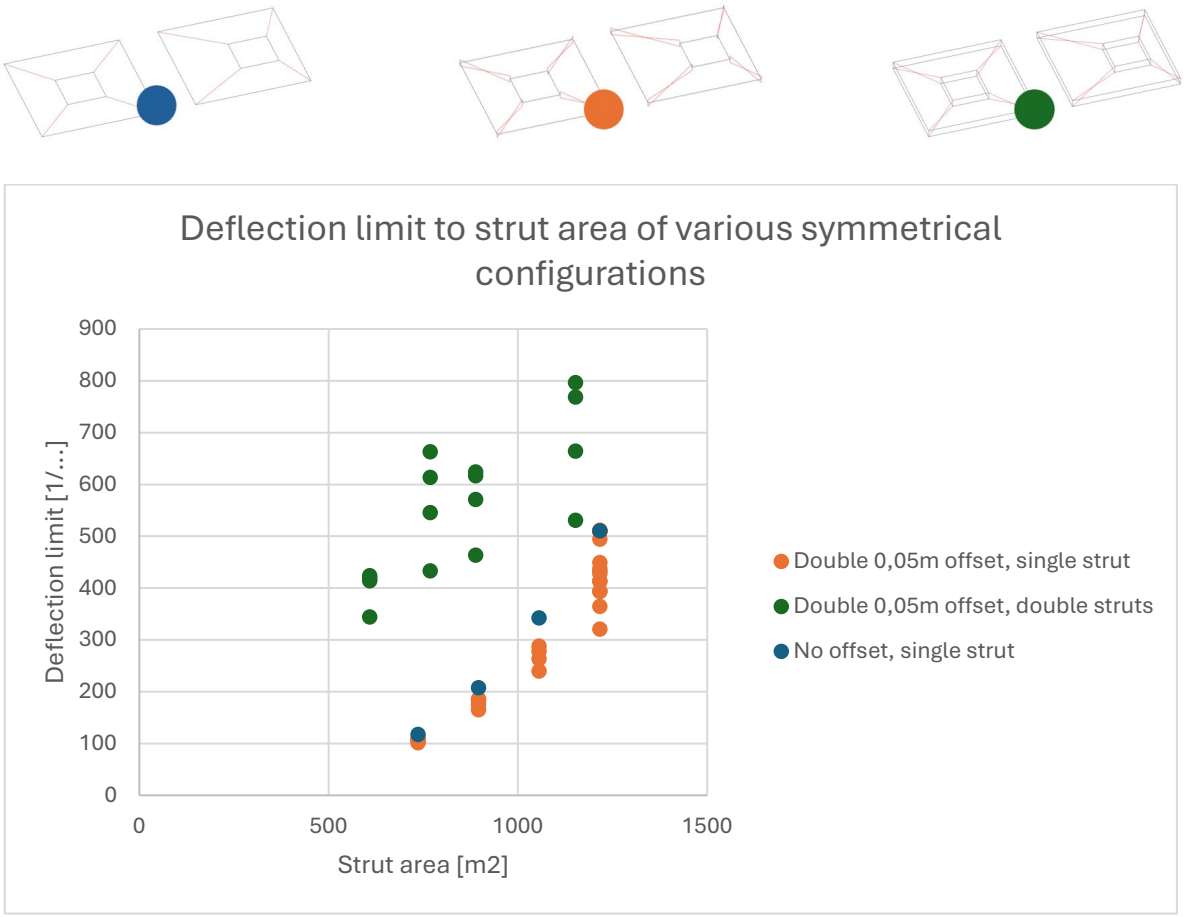

Figure 130: Deflection limit to strut area of various symmetrical configurations

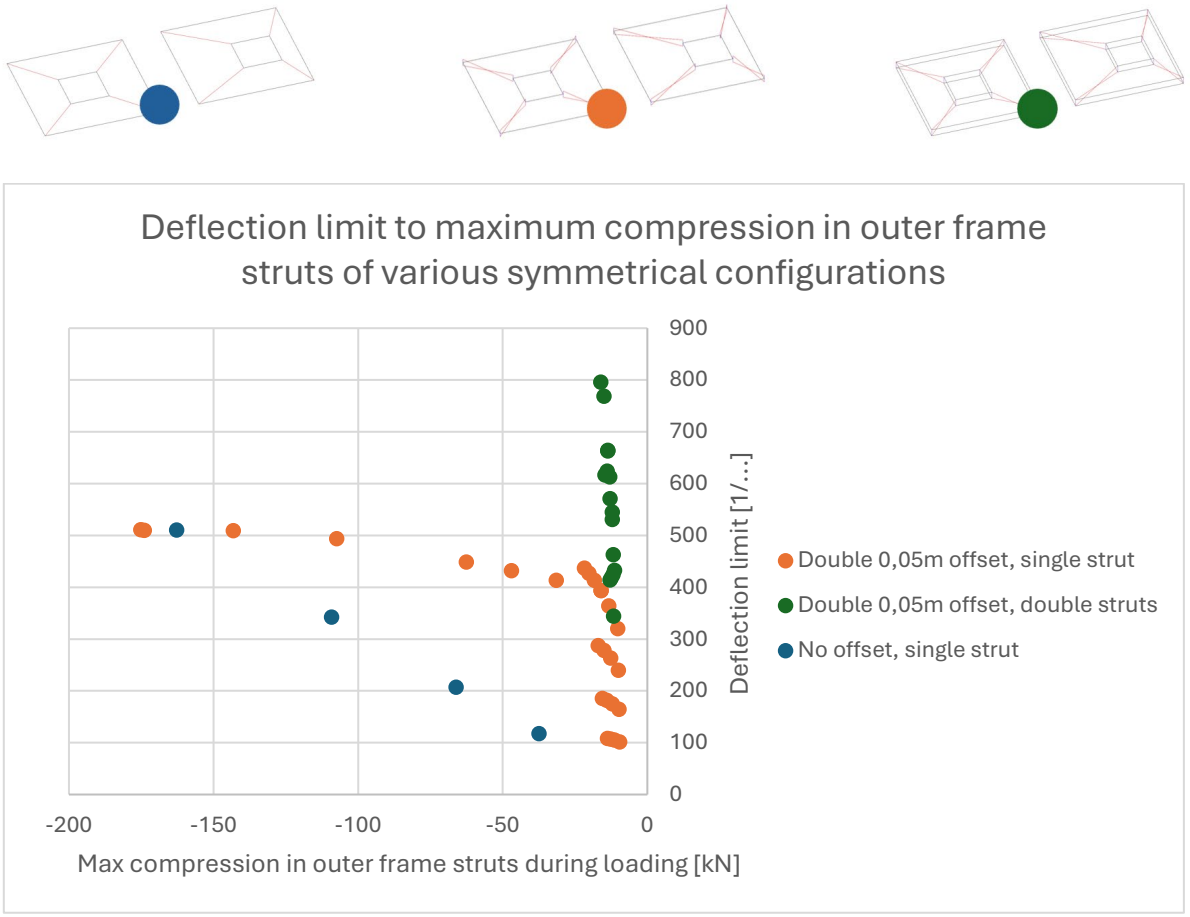

Figure 131: Deflection limit to maximum compression in outer frame struts of various symmetrical configurations

Interestingly, in terms of profile area, the planar configuration appears to outperform the offset variant with single torsionally resistant outer struts in the symmetrical case (Figure 130). This occurs because, at high pretension levels, in the offset configuration the inner and outer frame rotate significantly, even with profiles with high torsional resistance.

The geometric advantage of the offset system becomes apparent only when deflection is plotted against the maximum compressive stress in the outer strut (Figure 131). However, as pretension increases, both systems begin to converge, with the initially offset configuration gradually aligning with the behaviour of the planar configuration. This occurs because the rotation of the frames prevents an effective tension differential from developing between the opposing crossing cables; instead, the frames rotate to equalize tension on both sides. As a result, the system begins to behave increasingly like a single, planar cable (Figure 132).

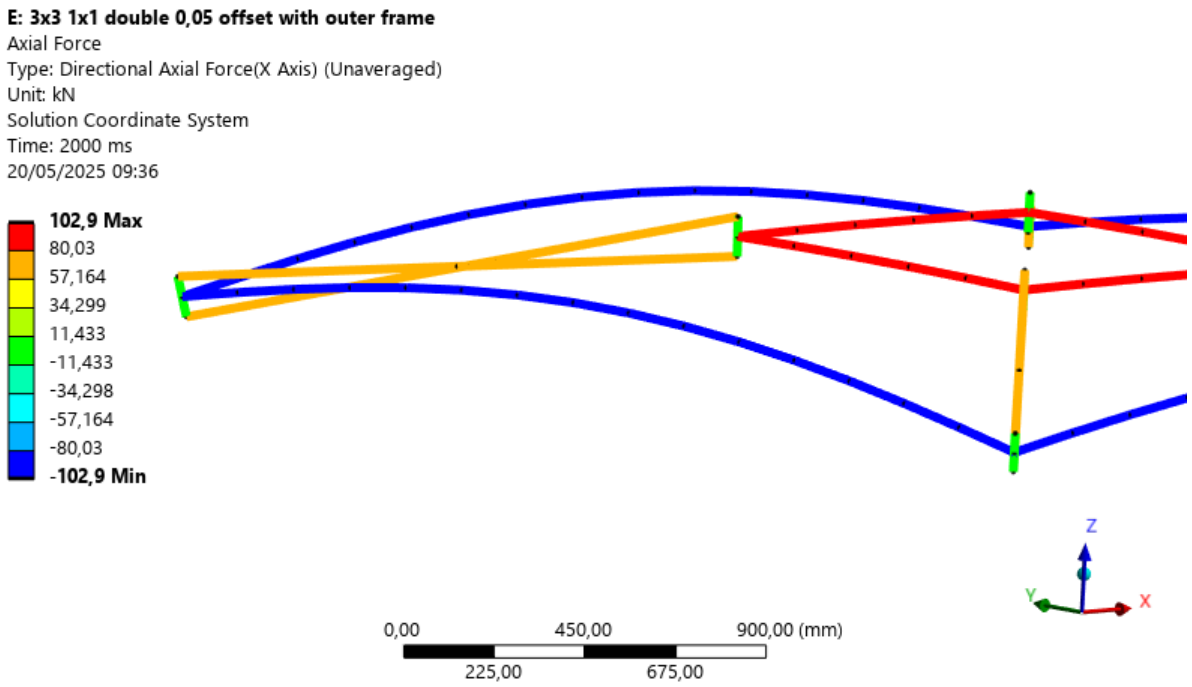

Figure 132: Significant rotation occurring in the connection points of the out-of-plane configuration attached to single struts, causing the cables to equalize in tension.

In contrast, the variant with separate struts outperforms both other configurations. It proves more effective at preventing movement at the cable connection points, allowing tension in opposing cables to rise and fall more significantly. This results in a greater out-of-plane force component being generated at lower deflection levels, making the system much stiffer.

A second noticeable performance improvement in limiting deflections becomes evident when examining asymmetrical configurations in both systems that utilize out-of-plane cables (Figure 133 & Figure 134).

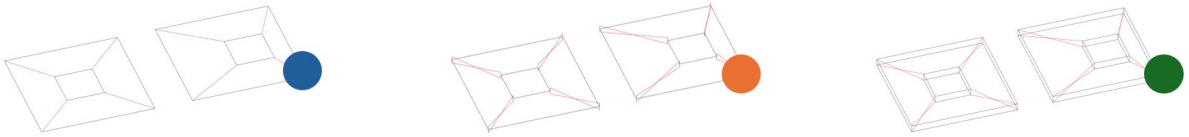

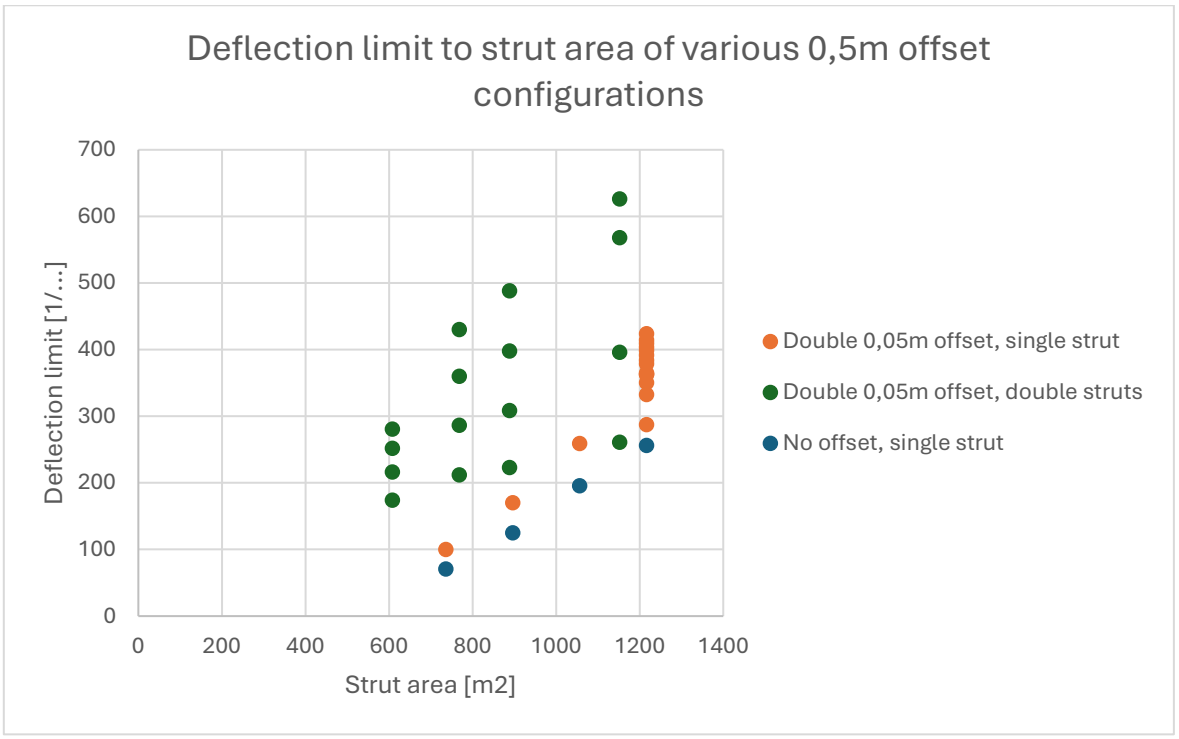

Figure 133: Deflection limit to strut area of various 0,5m offset configurations

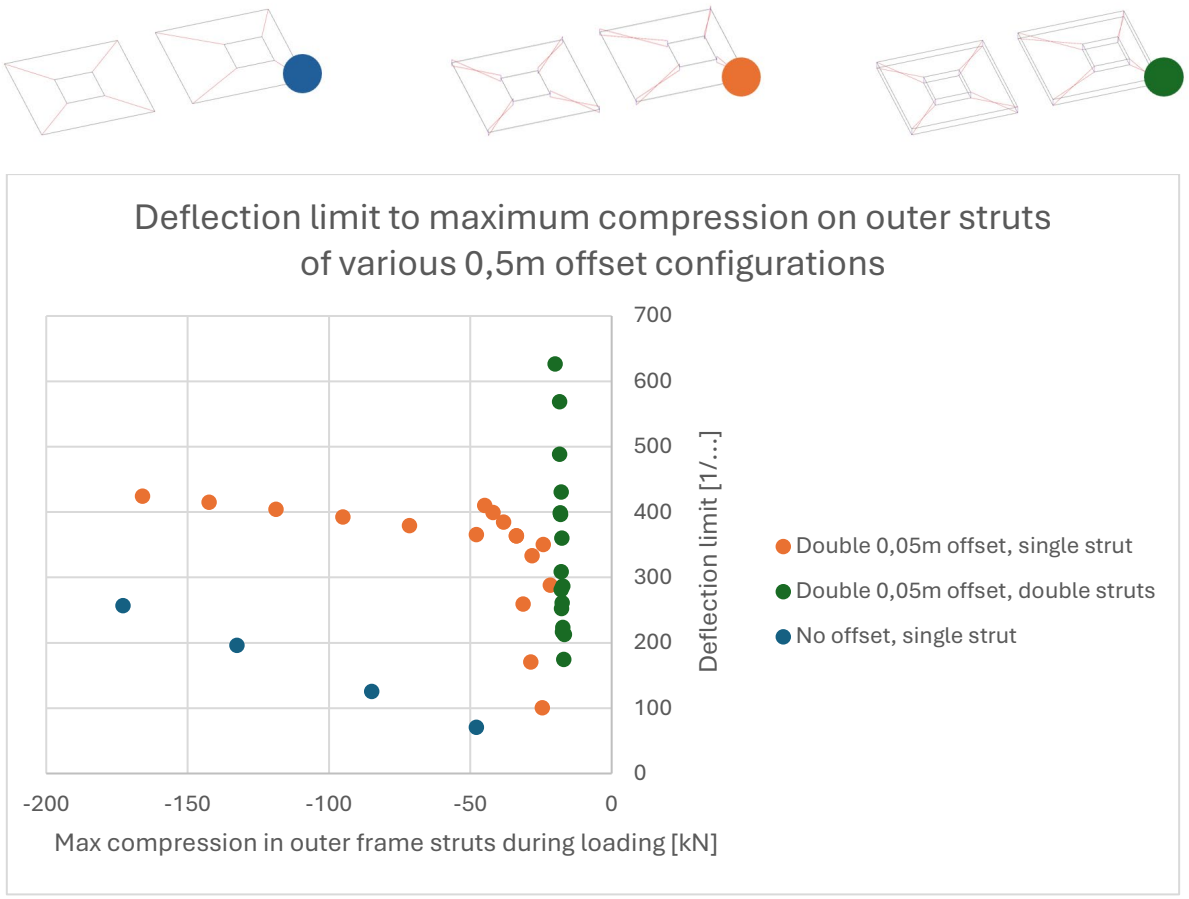

Figure 134: Deflection limit to strut area of various 0,5m offset configurations

In this case, the asymmetry is largely counteracted by the increasing tension differential in the cables on the far end of the system, represented by the green and orange pair in Figure 135. As the inner frame deforms and rotates, the cable experiencing increased tension elongates more than its opposing counterpart contracts. This growing tension differential generates a greater out-of-plane resistance compared to the planar configuration, thereby offering superior stiffness (Figure 135).

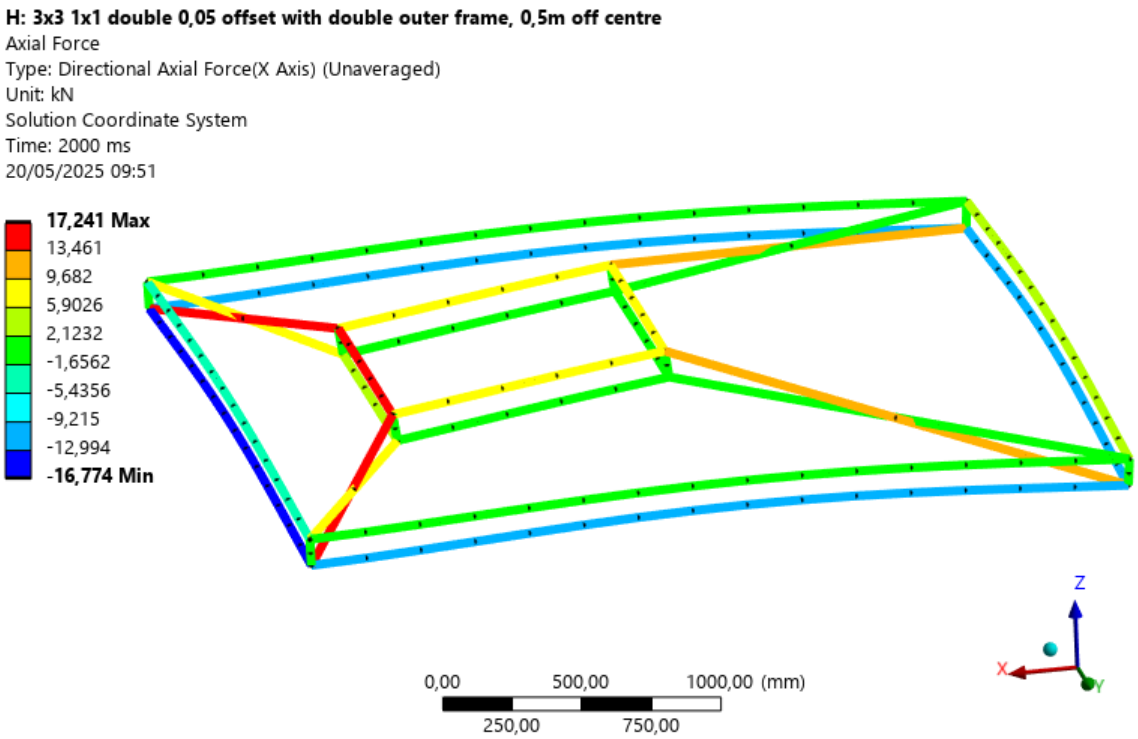

Figure 135: Out-of-plane configuration with doubled outer struts and the inner frame positioned 0.5 m off-centre, showing deformation and axial forces after loading.

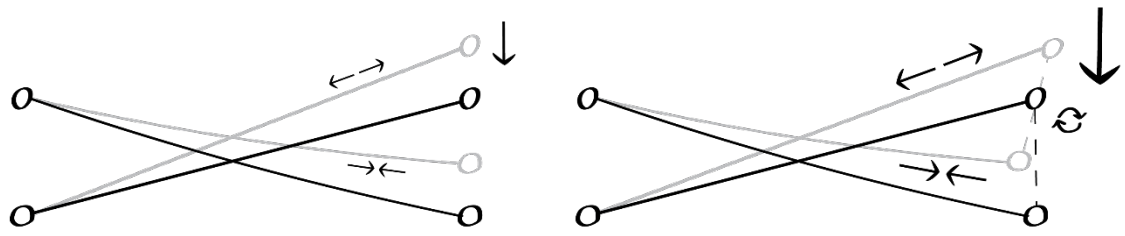

Figure 136: How rotation of the inner frame is in this case preferential for the out of plane resistance of the system.

Plotting these results together provides an overview of system performance and highlights the decline in effectiveness as the frame is positioned more asymmetrically (Figure 137). It also demonstrates that, in terms of material efficiency, the double strut system significantly outperforms the other two configurations, provided it can be manufactured as intended.

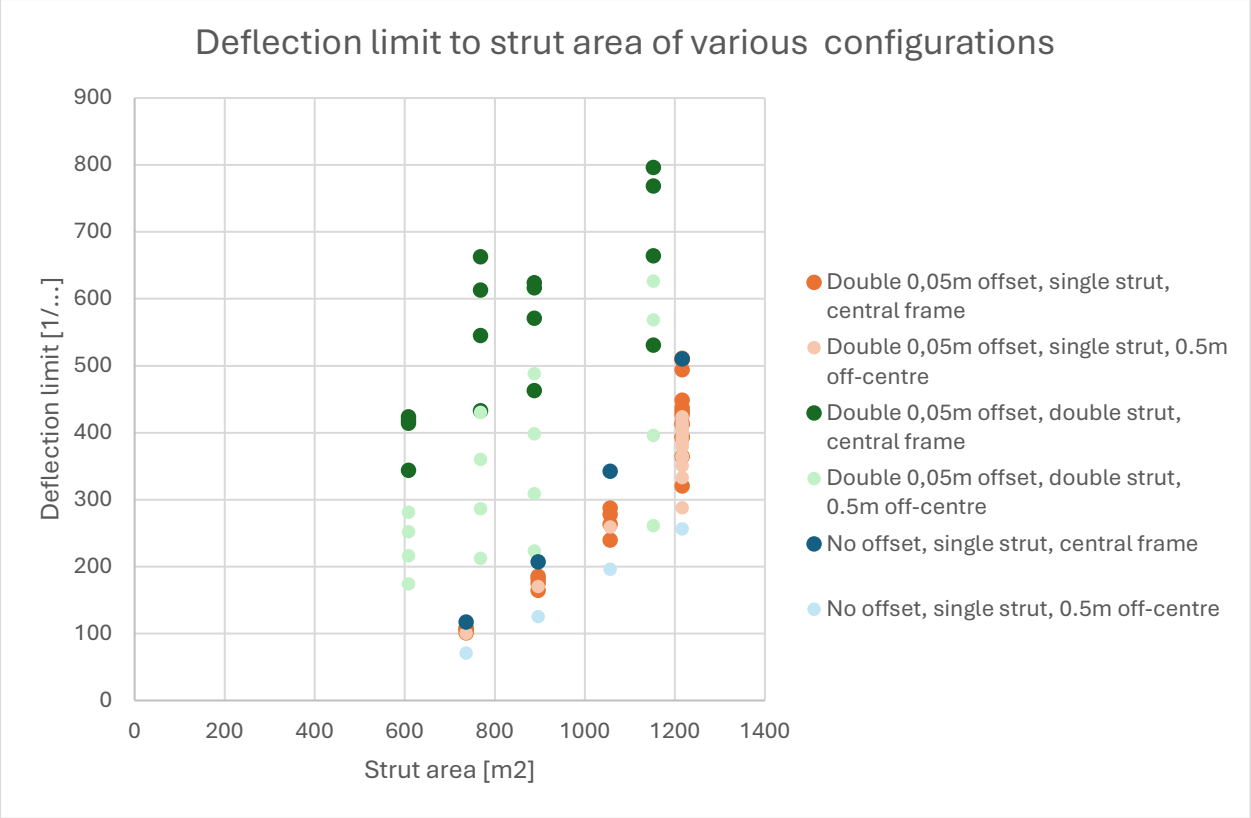

Figure 137: Deflection limit to strut area of various configurations

It is also worth noting that increasing the cable offset in the non-planar configurations leads to a clear and significant improvement in performance. However, for these simulations, a double offset of 0.05 m was selected, as it would remain feasible to implement within the constraints of a relatively slim façade panel, aligned with the original intent of the system.

6.3 Detailing of promising structural configurations

Based on the findings, two strategies can be best adopted for designing a materially efficient tensile-based facade panel (Figure 138).

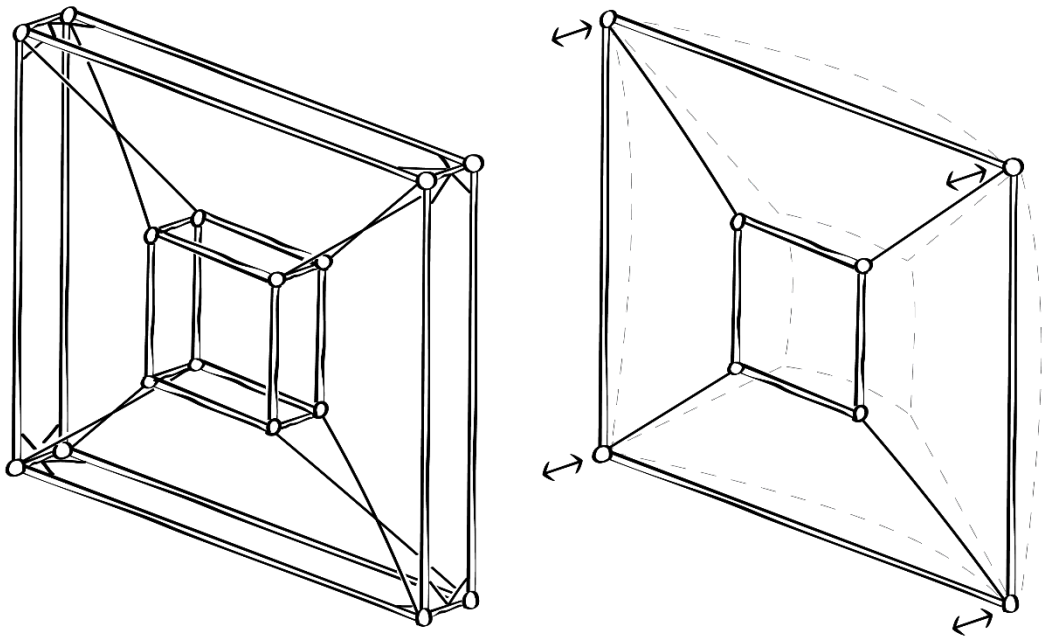

Figure 138: Potential structural strategies

The first approach involves creating a sufficiently stiff panel, using doubled frames and crossing cables, to limit deflections within acceptable ranges. This method allows for the use of brittle finishes and reduces or eliminates the need for expansion gaps. Depending on the cable offset, the system can be integrated within a façade panel. Also noteworthy, in this configuration, stability can be achieved more easily, as only the outer frame requires joints that maintain right angles on each side as depicted in the figure.

The second strategy embraces the inherent flexibility of the planar tensile-based system, detailing the facade to accommodate movement using large expansion joints or highly flexible materials.

Based these strategies, two preliminary detailing attempts were made, one for each strategy. These are conceptual designs, intended to illustrate potential solution spaces rather than provide finalized detailing. No further simulations or checks have been conducted to verify their structural, thermal, fire resistance, or acoustic performance after detailing was completed.

6.3.1 Designing for large deflections

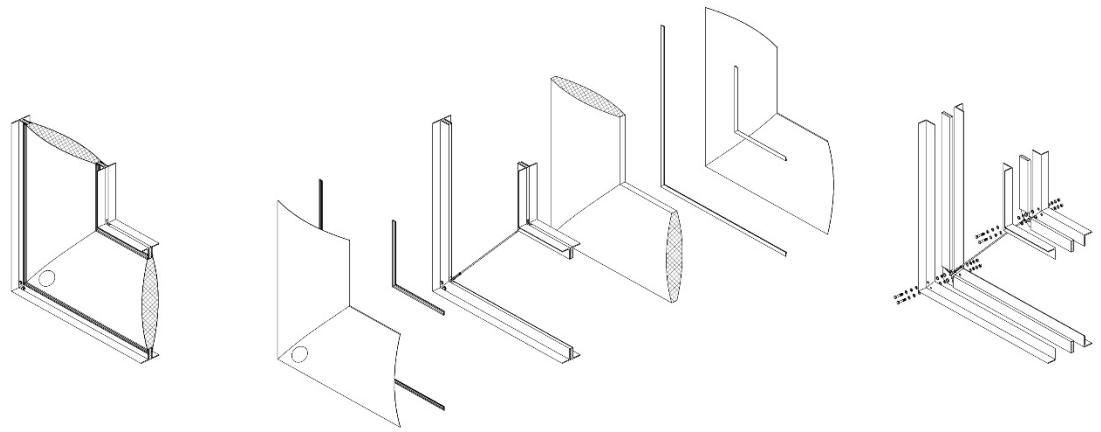

Figure 139: Axonometric view of the first design option, illustrating a system that can accommodates large deflections and integrates flexible insulation materials.

The first design alteration is structurally based on the images of the patented system and represents a simple continuation that embraces large deformations. It maintains the thermal break between two of the profiles and incorporates a membrane on either side of the structure. When designed to tolerate deflections of up to 1/50 under a 1 kPa wind load, within a 3x3 m frame and a 1x1 m symmetrically placed opening, the required cable pretension is only around 5 kN.

This low pretension requirement allows the panel to potentially resist the frame's stability issues during manufacturing. Even when using two opposing thermally broken L-profiles, provided they are sufficiently connected along the length of the struts, ensuring some composite action. Tension forces will however increase under actual wind loads, so the panel should at that point be connected to the surrounding building preventing out of plane movement of the outer frame.

The high deflection tolerance of the inner frame, combined with the high rigidity of the outer frame, results in significant relative movement between the two. To accommodate this, a potential finish could consist of two membranes filled with cellulose flakes or a similar loose-fill material. This approach allows the membrane to bulge, developing sufficient surface tension to maintain form and function even during wind loading.

Depending on whether the façade panel is intended to be permanent or temporary, it may be necessary to include access points to allow for periodic pretensioning checks and adjustments. Fortunately, due to the loose-fill nature of the flaked insulation, these access points would remain relatively easy to reach without compromising the overall system.

This system should be relatively easy to manufacture at scale, and depending on the opening configuration, only the membranes may need to be replaced or remanufactured, provided the loose-fill insulation material remains in acceptable condition.

A significant drawback of this system remains the potentially high deformations under load. Additionally, depending on the weight of the element placed within the inner frame, the overall system is likely to exhibit a very low natural frequency. A quick modal analysis of the inner frame and cables, assuming a fully rigid outer frame, already shows that the first four modes fall below 5 Hz, even when considering the weight of the cables and a double L80x80x8 frame profile. Although not conclusive, this suggests possible challenges with wind-induced vibrations.

The vibration issue can however be mitigated by increasing the cable pretension, or using more lightweight profiles, which would raise the system's natural frequency, and decrease the likelihood of wind induced vibrations. However, doing so would make full prefabrication in the factory impossible, as the higher pretension levels would introduce stability risks during manufacturing. As a result, additional on-site tensioning would be required after installation to achieve the desired structural performance.

Taken together, these factors suggest that this configuration may be better suited for component-based prefabrication, allowing for more compact transportation of the struts, cables, membranes, and loose-fill insulation, that might even be sourced locally.

This approach could enable a simple and reusable solution for temporary shelter, offering greater thermal insulation performance than a conventional tent, while remaining lightweight and adaptable. Taking a leap, this system could, for instance, be applied in arctic regions with sufficient snow coverage, where the membranes could be filled with snow to serve as an insulation material.

6.3.2 Designing for low deflections

The second scenario focuses on ensuring sufficient stiffness to withstand high wind loads, particularly in the context of potential high-rise applications.

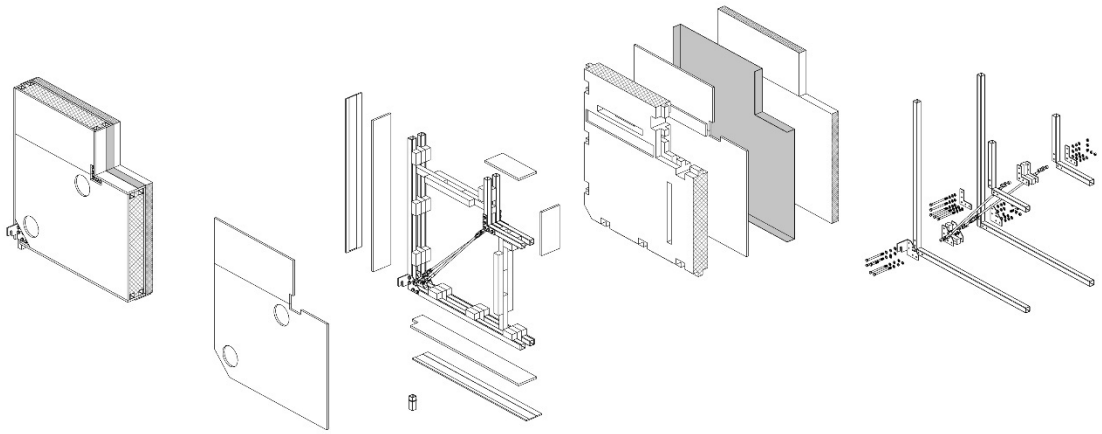

Figure 140: Axonometric view of the second design option, illustrating a stiff structural system that utilizes doubled crossing struts and a doubled frame for enhanced rigidity and reduced deformation.

In this scenario, the frame is modelled to limit deflection levels to manageable thresholds, such as 1/360 or even 1/500 for heavier systems, enabling the use of a much wider range of cladding options. The design is based on a doubled frame, which prevents significant movement at the connection points of the tensile elements, more likely threaded rods in this case, resulting in a much stiffer system.

Additionally, the system could be fully prefabricated, as the required pretension forces can remain relatively low and stability issues can be resolved more easily, only requiring connections in the outer frame that resist bending. The completed frame could then be suspended from the façade at just two connection points, as no significant out-of-plane restraints would be needed, even under high wind loads. A simple connector between the inner and outer frames could then be used to ensure vertical alignment.

Over the lifespan of the system, tension losses may occur, making access points necessary for monitoring and adjusting cable pretension. To accommodate this, a loose-fill insulation solution could again be utilized. This type of insulation is also easier to integrate within the central cavity of the element, between the inner and outer frame, which may contain more complex shaped internal beams. These beams could be specifically designed to support potential reconfiguration of the inner frame, lengthening or shortening when needed.

Depending on the effectiveness of the thermal break, it is likely that the vapour line would still be positioned within the loose-fill insulation layer. To prevent moisture issues, an

additional layer of vapour-closed insulation should be added. This would also enhance the system's overall thermal performance, which is likely necessary for building compliance. Fortunately, this outer layer could be easily installed, particularly if a rigid panel is used to cover the loose-fill insulation.

The joints in this system are however challenging to resolve, primarily because opposing tensile rods must be able to move independently. As opposing rods cannot be placed in the exact same plane, some degree of eccentricity will inevitably arise within the joints. Especially for narrower panel widths this would be problematic, as cable thickness would need to be significant to ensure proper stability. These eccentricities can lead to unwanted bending moments, which would need to be thoroughly analysed and carefully addressed during the detailed design phase.

The question remains whether this system holds practical potential. As it stands, it is complex to manufacture, and precisely balancing the pretension in the rods would be difficult, especially if re-tensioning is required on-site, which would necessitate opening up the wall assembly. Although the frame might have a higher reuse potential, not every component can be reused. These factors could pose significant challenges to its feasibility and long-term maintainability.

6.4 Material performance compared to a LGSF wall element

To assess the system's feasibility, a simplified comparison can made using a 3x3 m façade panel constructed from light gauge steel sections, which represent the most comparable conventional prefabricated panelised system in terms of material usage. For the analysis the LGSF is based on typical Metsec Metframe configurations (Figure 141).

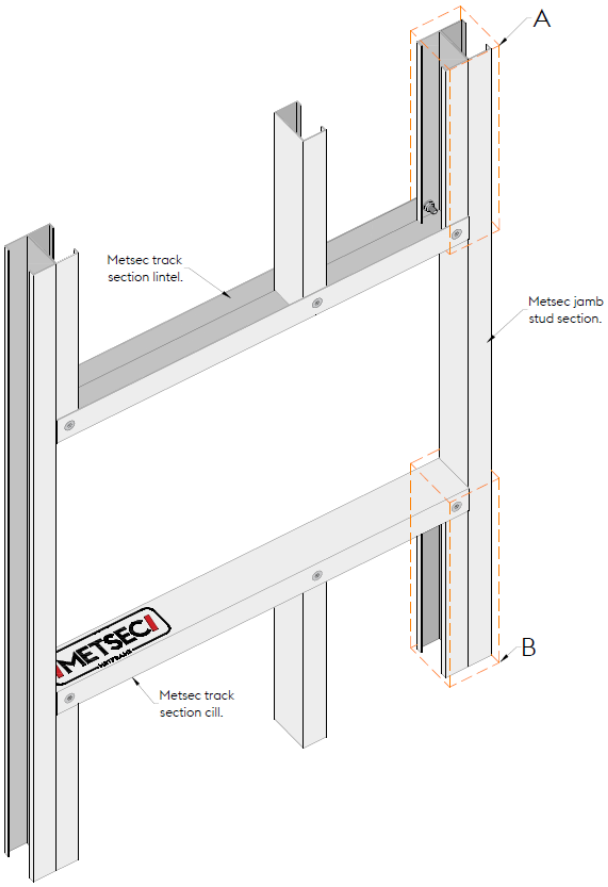

Figure 141: Metsec Metframe window configuration ("METFRAME INSTALLATION GUIDE," July 2023)

For both the tensile façade and the LGSF system, two configurations were developed and their corresponding required profile and cable lengths determined (Figure 142). Specifically, the cable length varies for the tensile system, depending on if the setup used single layer or double layer cables.

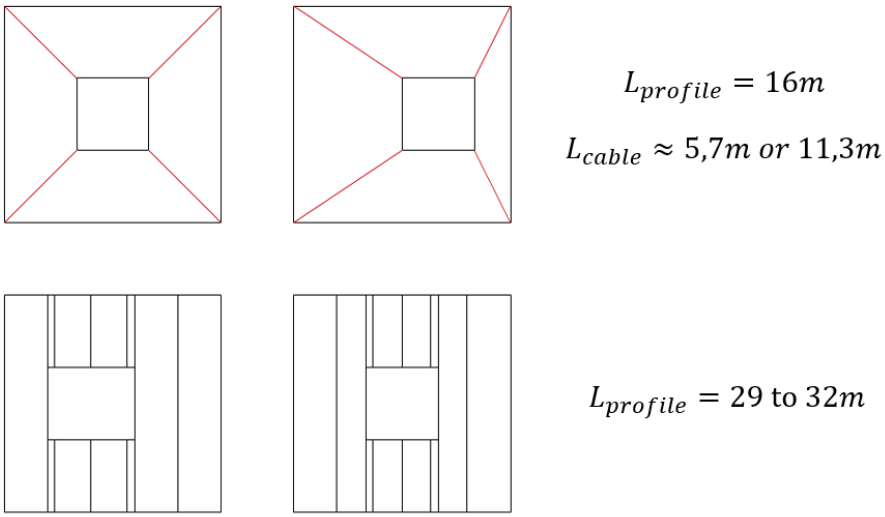

Figure 142: Profile lengths of the tensile and Metframe system

Although the manufacturer does not specify deflection limits for the Metframe system, it does provide guidance for Metsec infill walling at various wind pressure values. Based on these design guidelines, six potential framing options were analysed and compared for wind loads of 1kPa. In addition, separate FEA models were developed to verify the manufacturer's claims (Figure 143 & Table 7).

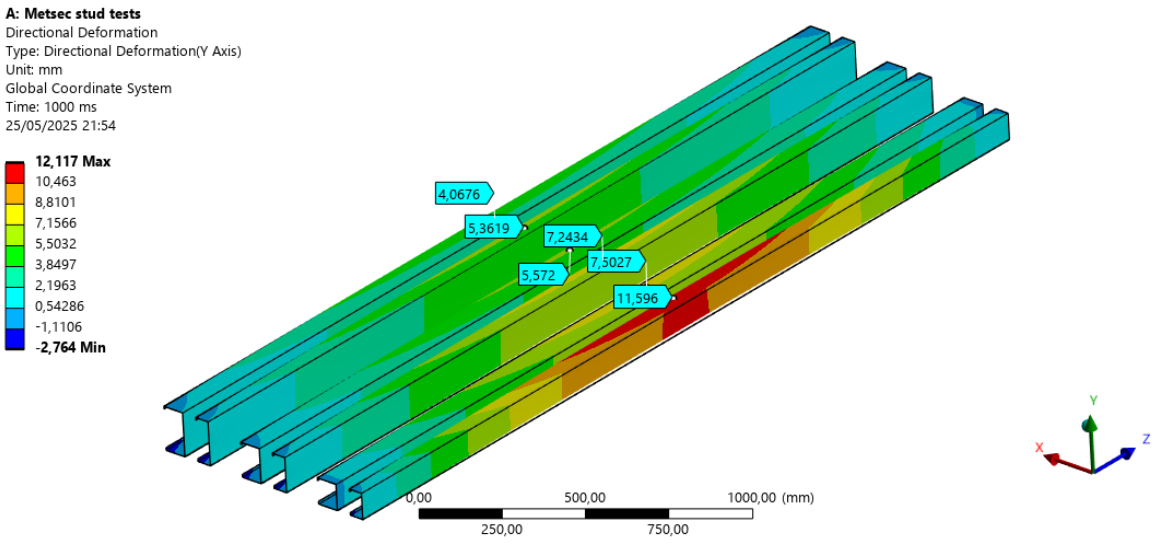

Figure 143: LGSF deflection verification

The table below presents the deflection limits for the various profiles. Two columns contain FEA model results, and another contains the manufacturers specifications:

LTBR-1: Lateral-torsional buckling is restricted on one side of the profile.

LTBR-2: Lateral-torsional buckling is restricted on both sides of the profile.

Metsec: Reflects the deflection limits specified in the manufacturer's documentation.

Table 7: Deflection limits of various Light Gauge Steel Framing (LGSF) profiles, as determined by FEA simulations and compared with the manufacturer's specifications.

		Deflection limit 1/...		
Profile	**Area [mm2]**	**LTBR - 1**	**LTBR - 2**	**Metsec**
090M12-50	246	259	291	250
090M16-75	406	400	508	500
120M12-50	282	417	500	500
120M16-75	454	536	811	500
150M12-50	318	556	714	500
150M16-75	502	732	1034	500

From this data, a rough material comparison can be made for all three systems. This involves interpolating the results from the tensile systems and calculating the total volume and weight of steel used, based on the profile areas and spanning lengths of the components, and comparing them to the LGSF. The results are shown in the figures below.

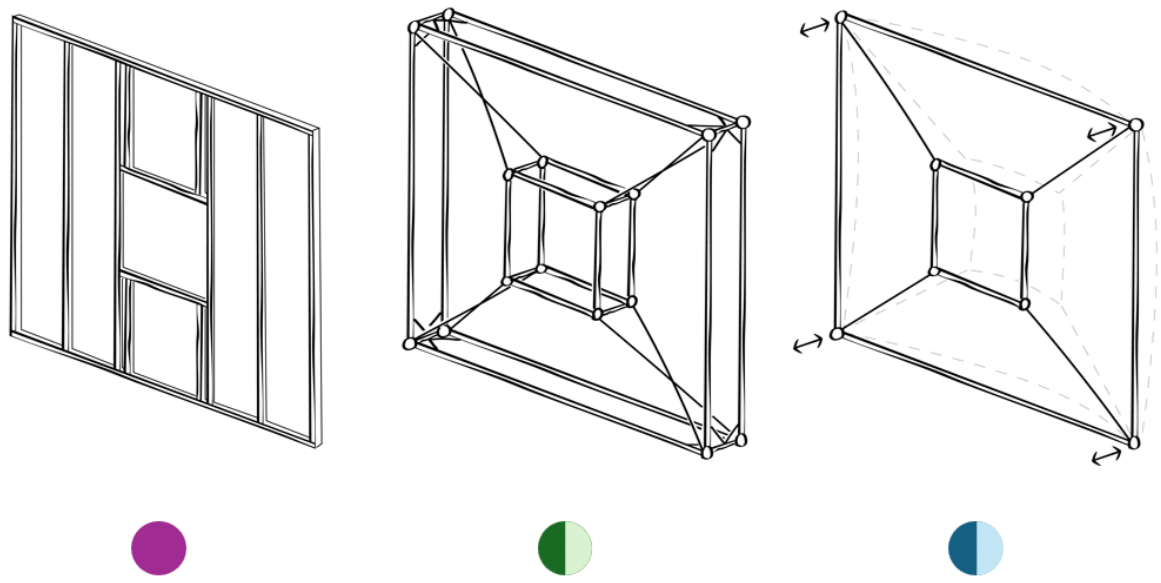

Figure 144: Colour coding for each of the facade systems

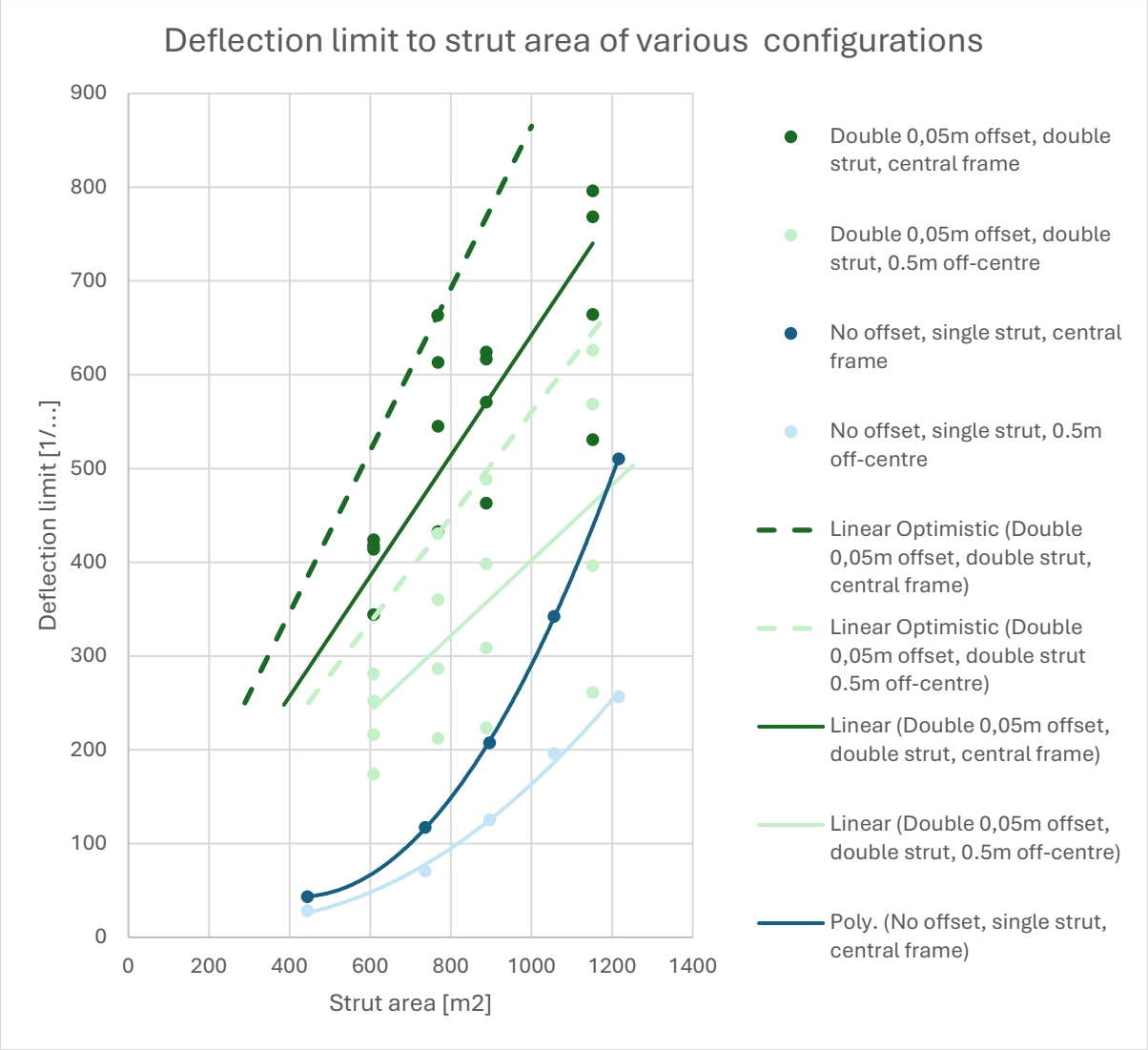

Figure 145: Interpolating the deflection limit to strut area of various facade configurations

The data interpolation has been conducted presenting optimistic performance outcomes (Figure 145). In the simulations, the blue and light blue systems were relatively straightforward to optimize, as they involved a single optimization step: finding the highest pretension level at which both the cables and outer struts experienced equal deflection. This approach globally minimized deflections based on the SHS (Square Hollow Section) profile. As a result, the blue lines represent the upper performance limit of the system when using SHS sections.

In contrast, the green configurations were more complex to optimize and exhibit a broader range of results. In these systems, variations in cable diameters also significantly influenced total system deflection. For each configuration, steel cables with radii of 8, 10, 12, and 14 mm were tested. All cables were pretensioned such that a minimal level of tension remained in all cables even after deformation under load, just enough to

prevent them from going slack. This ensured the maximum possible force differential between the cables while minimizing the force transmitted to the outer struts.

In general, for configurations with larger strut areas, cables with radii of 12 mm and 14 mm produced the stiffest results. However, in setups with smaller strut areas, such as the case of doubled SHS 40×40×2 profiles, with a total strut area of A = 608 mm^2, even cables with radii of 10 mm were sufficient to transfer enough force to the outer frames that they began to bend more than the inner frame was displaced. This suggests that further increasing the cable area was unnecessary, as the system's performance had become fully constrained by the structural capacity of the outer frame.

Due to the greater variability in the green systems, a linear approximation, rather than a polynomial, is used, intersecting the origin (0,0). While the actual relationship is likely not perfectly linear, especially given the graph's non-linear y-axis (1/deflection), the linear trendline serves as a reasonable simplification for making rough estimates. A visual inspection of the data points suggests that plausible solutions could lie along or near this line, particularly as it approaches the origin. Conceptually, the reasoning is straightforward: a system requiring no material would exhibit infinite deflections (1/0).

This linear approximation provides a useful baseline but does not capture the full potential for complete system optimization. As many data points still lie above this line, it becomes necessary to define an upper bound. To do so, two additional dashed curves are plotted, also intersecting the origin, for the same conceptual reasons as before. These lines intersect the data points representing the highest stiffness achieved with the lowest strut area, offering an estimate of the system's highest optimization potential (Figure 145).

To estimate the likely weight values for the green systems at deflection limits of L/500 and L/250, the intersection points of the linear and optimistic linear curves are examined. For example, in the case of the symmetrical system with a deflection limit of L/500, the total strut area is likely to fall between 580 mm^2 and 780 mm^2. A roughly estimated value is then selected one-third of the way between the lower and upper linear bounds, leaning toward the lighter (more efficient) side. In this case, the estimated value is calculated as:

(Upper bound − Lower bound) × 1⁄3 + Lower bound

(780 − 580) × 1⁄3 + 580 = 646.7 mm^2

Additionally, variation bars are included to represent the upper and lower limits of the range, depicting the potential spread in system performance (Figure 146 & Figure 148).

The steel weight of the panel can then be further approximated by accounting for the contribution of the cables, which is particularly significant in the green configurations (Figure 147). In these cases, stiffer systems typically require thicker cables, which are

now also used in pairs. Although no cable configurations were explicitly optimized to meet deflection limits of L/250 and L/500, sufficient simulation data is available to make reasonable estimates. By identifying configurations that reached these deflection thresholds, the corresponding cable radii were inferred.

For both 0.5 m offset systems, the thinnest cables that met the deflection limits of L/250 and L/500 had radii of at least 12 mm, so this value was used. In the case of the symmetrical system, available data only covered the region around the L/500 deflection limit, which was achieved using cables with a radius of 10 mm or more.

No direct cable thickness data was available for the symmetrical system around the L/250 deflection limit, but a cable radius of 6 mm was selected based on overall trends observed across the simulations. For reference, an 8 mm cable was already sufficient to achieve a deflection level of L/344 (approximately 8.7 mm), suggesting that a smaller diameter cable could reasonably meet the more relaxed L/250 limit of 12mm.

For the blue planar configurations, cable radii were selected instead based on ultimate limit state criteria. Assuming high-strength steel with a UTS of approximately 1800 MPa and applying a safety factor of 5, the required cable radii were determined as follows: approximately 5 mm for the L/50 centred configuration, 7 mm for the L/50 with a 0.5 m offset, and 6 mm and 8 mm for the centred and 0.5 m offset L/100 configurations, respectively.

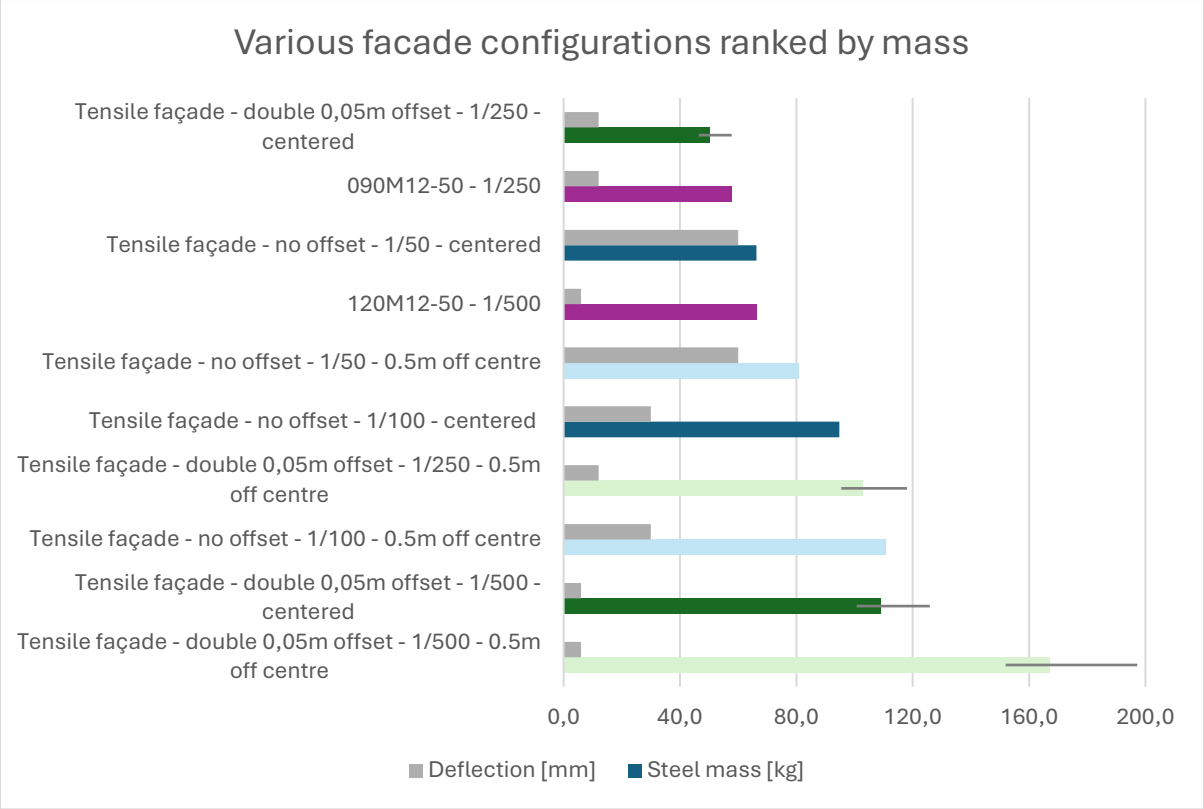

Figure 146: Various facade configurations ranked by mass

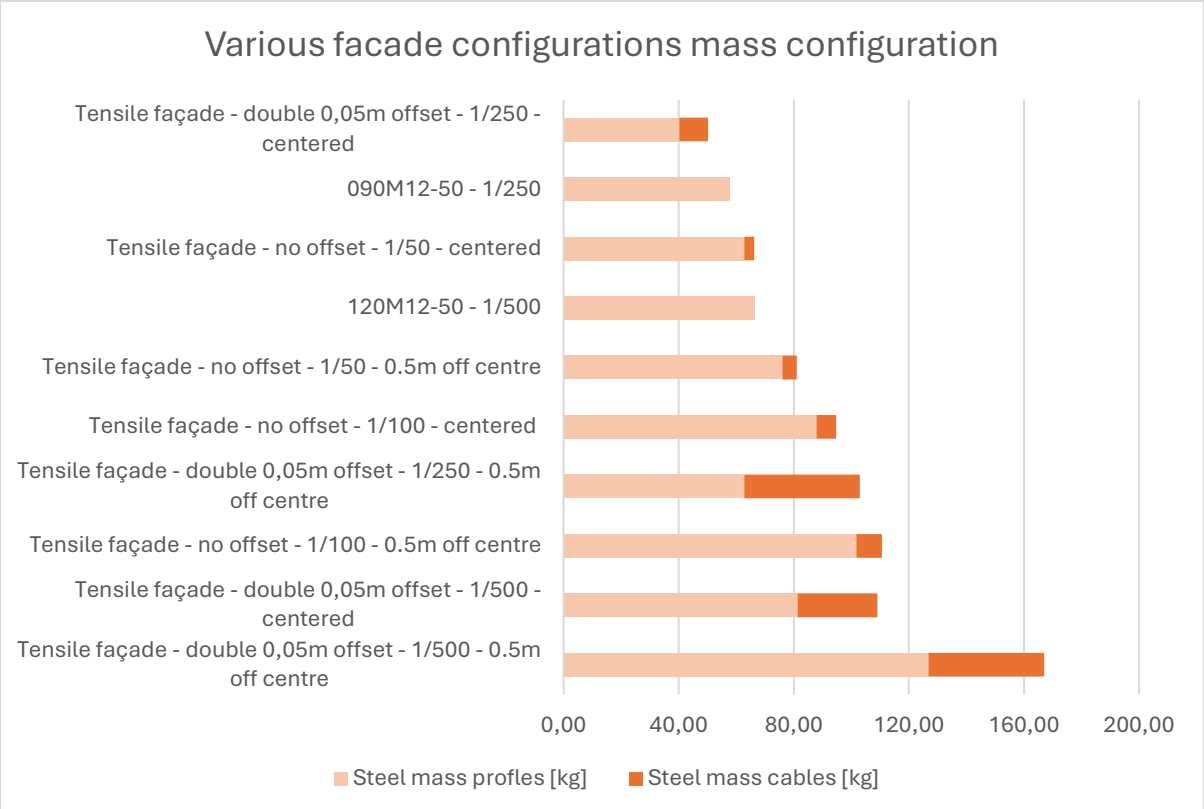

Figure 147: Various facade configurations mass configuration

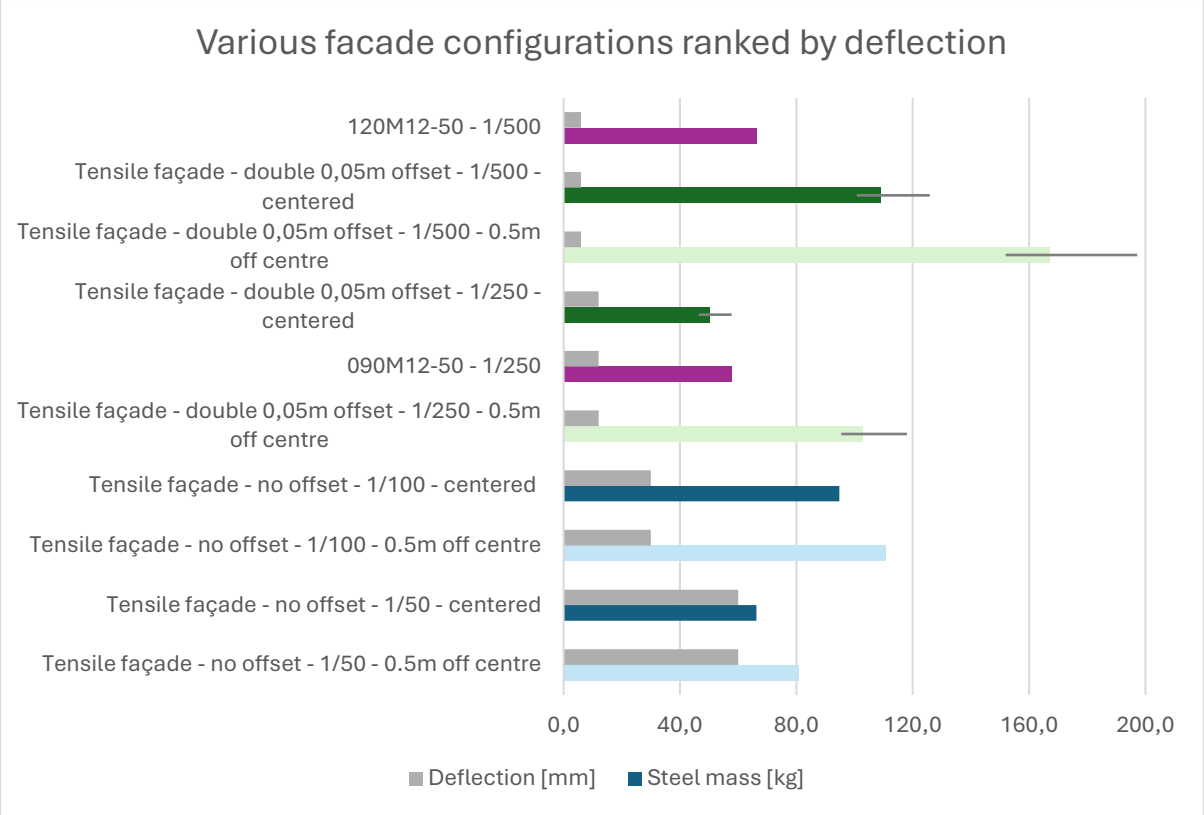

Figure 148: Various facade configurations ranked by deflection

It becomes evident that, in low-deflection conditions, the LGSF system generally outperforms the tensile configurations in terms of material efficiency. The blue tensile configuration may approach the material efficiency of the LGSF system, but this is only achievable if a lenient deflection limit of L/50 is accepted and the frame is positioned centrally. To exceed the material efficiency of the LGSF system, even more relaxed deflection limits would be required.

The green tensile configuration generally underperforms compared to the LGSF system, particularly around the stricter L/500 deflection limit and especially when the inner frame is not placed perfectly centrally.

While the configuration with a centrally placed inner frame could likely outperform the LGSF system at the L/250 deflection limit, it already comes with a notable trade-off: increased system thickness. This L/250 configuration would likely be wider than its 90 mm LGSF counterpart. The closest simulated green system uses a double 50 mm offset paired with SHS 40x40x2 profiles, resulting in a total system thickness of 140 mm, excluding joint connections, which would further increase the overall depth.

The tensile system could, of course, be made significantly more efficient by further increasing its structural depth. However, this does not align with the original design intent

of creating a stiff and thin facade system. Additionally, increasing this offset would require substantial connection hardware to connect the inner and outer frames.

It is generally worth noting that connection hardware, such as bolts and screws, has been omitted from the material comparison across all systems. While not conclusive, including connection hardware in the comparison would likely further favour the LGSF system, as it relies on smaller, simpler connections designed to handle significantly lower forces.

Considering that the tensile system is significantly more complex to manufacture and maintain and, in most configurations, less material-efficient, it becomes difficult to justify its reconfigurability, particularly since any off-centre placement of the inner frame negatively impacts system performance.

An intuitive example of why the LGSF system offers much better material efficiency can also be seen by examining the actual span that the structural elements must cover. In the LGSF system, the struts span a straightforward 3 m. In contrast, the tensile system increases this span to approximately $3 \times \sqrt{2}$, or about 4.3 m, due to the diagonal cable arrangement (Figure 149).

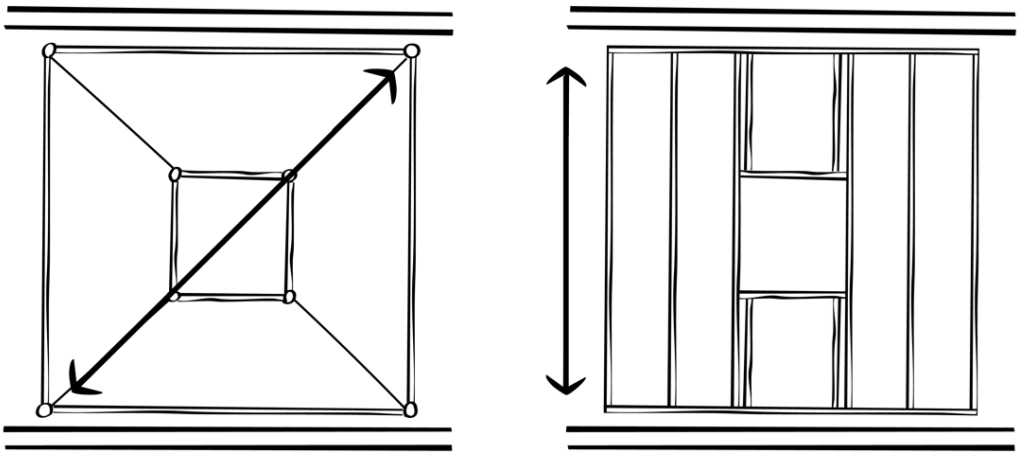

Figure 149: Spanning length of the tensile and LGSF panels

While a comparison with LGSF struts spanning 4.3 m could be made and would cast the tensile system in a more favourable light, it is not particularly relevant in most practical applications, where facades can be supported by intermediate floors. A more insightful approach may be to explore alternative applications for the tensile system, particularly in scenarios where limiting connection points to the corners provides a distinct advantage.

7. Expert Evaluation and Feedback

Recognizing the value of practical experience, two forms of expert interviews were held with specialists in architecture, façade systems, and structural engineering.

The first type involved three interviews providing minimal background information, aimed at gathering initial impressions and evaluating the patented concept in comparison to other prefabricated penalized facade systems discussed in section 2.2.2.

The second type consisted of eleven interviews, which included a condensed version of the research findings and examples of potentially more promising applications. The purpose of which was to gather expert opinions on the most viable directions for future development of the system.

7.1 Interview type 1; comparing the tensile based system to conventional prefabricated façade panels

In the first interview, experts were shown only two images of the façade panel (Figure 150). Based on these images, they were asked to provide initial feedback on the façade concept, as well as how they might approach detailing the panel.

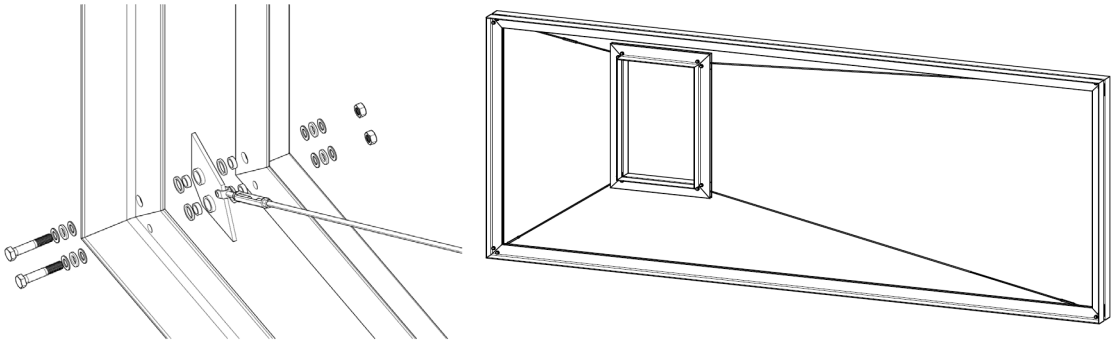

Figure 150: Figures used for the first interviews

Additionally, they were asked to rate other types of prefabricated façades based on a broader range of performance criteria, using a scale from 1 to 5, where 1 indicates poor performance and 5 indicates good performance. The average results are shown in Table 8.

Table 8: Table used during the first interviews

Prefabricated Façade Solutions	 Precast Concrete Sandwich Panel (PCSP)	 Cross Laminated Timber (CLT)	 Structural Insulated Panel (SIP)	 Lightweight Timber framing Panel (LTFP)	 (Unitized) Curtain Wall Systems	 Light Gauge Steel Framing Panel (LSFP)	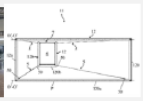 Steel-Tensile
Architectural design freedom	4,33	2,33	3,00	2,33	4,00	2,50	-
Thermal performance	4,67	3,33	5,00	3,67	3,67	2,67	-
Acoustic performance	5,00	2,67	4,50	2,67	3,67	2,67	-
Fire resistance	4,67	2,00	2,50	2,00	3,67	3,33	-
Installation speed	4,17	3,17	3,25	2,83	4,67	2,17	-
Durability	4,67	2,83	2,75	2,83	3,33	3,50	-
Environmental Impact	2,17	4,83	4,75	4,50	2,50	3,17	-
Cost	2,83	2,83	3,50	3,83	1,67	3,67	-

The ratings for the SIP panel are based on feedback from only two experts, as one of the three interviewers refused reviewing this system stating it was a poor choice for a building method. Additionally, two of the three experts emphasized that the environmental impact ratings for the LTFP and LSFP panels are highly dependent on the final surface finish.

While the table ratings do not provide definitive conclusions, they served as a valuable starting point during the interviews for discussing how the steel tensile system might compare to other prefabricated façade solutions, and whether it could occupy its own distinct set of advantages and disadvantages.

The interviews ultimately revealed two key insights: first, they confirmed many of the initial research findings; and second, they uncovered a high degree of scepticism among the three experts regarding the feasibility of the steel tensile system in comparison to the conventional prefabricated façade systems.

Some specific highlights were:

Structural Stiffness

All three experts emphasized or recognised the panel's lack of structural stiffness and the need for system symmetry. Expert 1 described the system as inherently prone do deformations without substantial pretensioning, noting that even with incredible tension, the panel would remain prone to "wobble," posing a risk to rigid cladding components. Similarly, Expert 2 pointed out that any rigid infills must be designed to accommodate the cable net's movement, warning that incompatibility between the cables and outer frames

would likely lead to material failure. Expert 3 extended this argument by noting that users would find visible facade movement disconcerting, particularly in standard building types.

Compatibility of Materials

The interviewees also questioned the integration of flexible load-bearing systems with rigid materials. Expert 1 and Expert 2 both cited precedents where excessive movement in cable-based facades caused cladding breakage. Expert 2 suggested that, unless designed as a fully integrated cable-net system, the proposed concept would result in performance failures due to incompatibility between movement of the rigid outer frame and infill materials.

Installation and Maintenance

Each expert highlighted significant installation and operational challenges. Expert 1 noted the difficulty in achieving equal cable tension across asymmetric geometries, questioning the configurability of the panel. Expert 2 and Expert 3 raised concerns about how the system would be assembled and maintained on-site. Expert 3, in particular, pointed out that cable-stayed systems typically require ongoing maintenance, such as retensioning, that is uncommon in conventional unitized systems. Which as he stated could undermine long-term reliability and market acceptance.

Thermal Bridging

Despite built-in thermal breaks, all experts expressed doubts about the panel's ability to reach good thermal and moisture performance. Expert 1 noted that the edge detailing would likely still cause excessive thermal bridging in mid to northern European climates, while Expert 2 warned of insulation discontinuities due to joint movement. Expert 3 echoed these concerns, emphasizing that tensioned cables crossing thermal zones introduce both thermal and structural trade-offs that are difficult to reconcile.

Adaptability and Reusability

While the panel was presented as offering adaptability and reusability, its practical value was called into question. Expert 1 expressed doubt that these intended benefits could justify the mechanical and thermal complications introduced by the concept. Expert 2 acknowledged the panel's conceptual innovation but emphasized that critical trade-offs across structural, thermal, and acoustic domains remained unresolved, particularly the need for large expansion joints between rigid infill elements if substantial deflections were to be accommodated. Such joints, they noted, would negatively impact both thermal insulation and acoustic performance. Expert 3 similarly concluded that the system offered no clear advantage over conventional prefabricated façade systems, stating that "the system is creating more problems than it's solving," and anticipated strong resistance from manufacturers due to the concept's departure from established fabrication and installation practices.

Recommendations

All three experts proposed potential design revisions. Expert 1 and Expert 3 supported the idea of integrating crossing out-of-plane cables to improve stiffness, although Expert 3 maintained that even with such improvements, the overall concept might still remain impractical. Expert 2 recommended simplifying the structure by changing the cable directions from the corners to a more grid-like pattern, more in line with traditional cable-net facades. Additionally, both Expert 1 and Expert 3 suggested rethinking the system entirely, potentially shifting toward rigid panel approaches that eliminate the use of cables altogether. These alternatives, they argued, could better preserve the intended goals of adaptability and reusability while reducing excessive deflections.

In conclusion, when comparing the tensile-based panel to other unitized systems, the experts acknowledged the originality of the concept and its ambition to rethink prefabricated façade design. However, they consistently emphasized that the current design suffers from significant technical and practical limitations. They remained sceptical that the system could realistically replace existing prefabricated façade solutions.

7.2 Interview type 2; finding alternative applications for the tensile based façade panel

Due to the perceived negativity in the first three interviews, which primarily focused on comparisons with traditional prefabricated façades, a second type of interview was conducted. This revised approach began with an explanation of the system's objectives, followed by a presentation of research findings related to its structural boundary conditions and potential material use. The corresponding slides can be found in the appendix.

Participants were then asked whether, based on these boundary conditions, they could identify applications suited to the system's design characteristics. After this discussion, they were presented with five potential applications for future development:

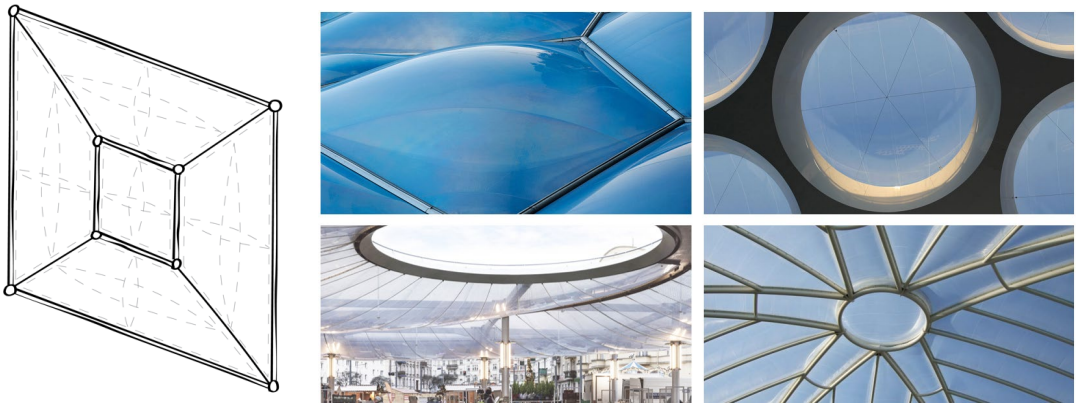

Figure 151: (1) Integration with ETFE panels. These panels are typically expensive to install on site and have inherent flexibility, making them potentially well-suited for prefabrication and to accommodate the high deformations of the tensile based panel.

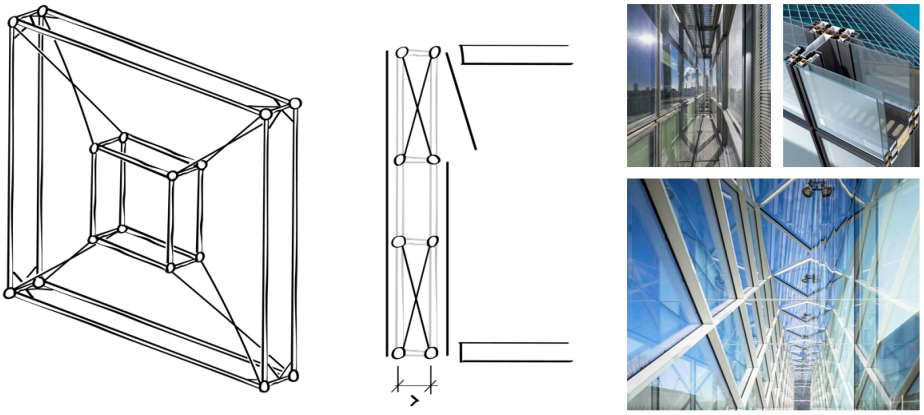

Figure 152: (2) Integration with double-skin façades. The crossing cable configuration becomes significantly more material efficient as its width increases.

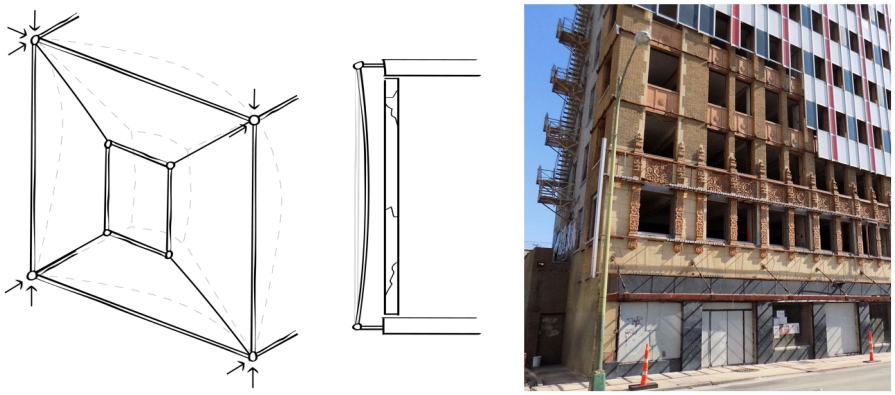

Figure 153: (3) Overcladding of (historical) façades. The system requires only four connection points, preserving most of the underlying surface. An additional benefit is that the original façade remains intact, minimizing discomfort to occupants despite the large deflections of the exterior façade.

Figure 154: (4) Integration with structural cross-bracing. The system could benefit from larger structural elements, enabling higher cable pretensions. Buckling of the outer compression members would be less problematic.

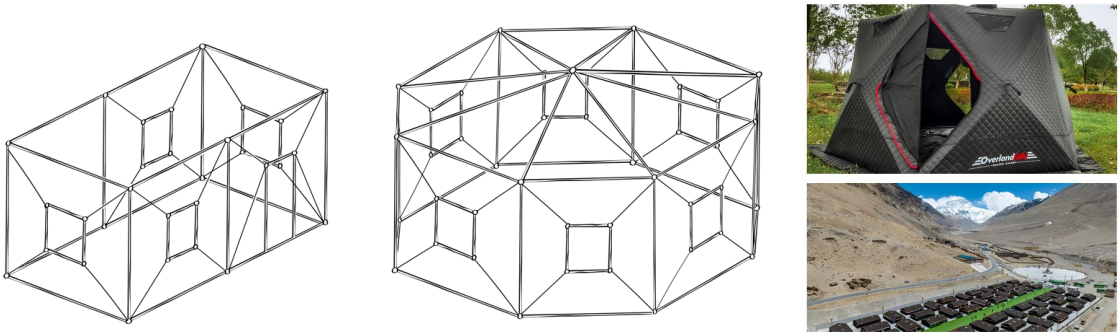

Figure 155: (5) Use in modular, tent-like systems. These could offer improved insulation compared to traditional tents.

At the end, participants were asked whether the process had inspired any new ideas and what they considered the most promising direction for the system's future development. The primary aim of this interview format was to provide contextual information to stimulate creative thinking and uncover novel, potentially relevant applications for the system.

7.2.1 General Remarks

Compared to the first interview, Experts 4 through 14 generally provided more nuanced feedback on the tensile-based façade panel concept. While most appreciated its innovation and potential in lightweight applications, general concerns were also consistently raised about:

- *Deflection Control*: Noted by Experts 4, 6, 8, 11, and 14, who emphasized the need for managing deformations to avoid durability issues and user discomfort.
- *Material Compatibility:* Raised by all experts, particularly in relation to integrating flexible structures with rigid panels or infills. Flexible membranes were generally

preferred as infill materials. Expert 10 also noted potential issues with using galvanized mild steel in exterior applications, recommending more specialized, corrosion-resistant materials to ensure durability and reduce maintenance.

- *Fire Safety*: Particularly highlighted by Experts 10, 12, and 14, who questioned the system's compliance with fire codes and the risks posed by membrane like materials such as ETFE.
- *Acoustic Performance*: Expressed by Experts 8, 9, and 12, concerned about resonance and sound insulation in lightweight or flexible configurations.
- *Thermal Bridging*: Identified by Experts 5, 6, 10 & 14, who mentioned issues with cable continuity through insulation zones and the impact on thermal efficiency.
- *Buildability*: Noted by Experts 4, 8, 10, 11, and 12, referencing complexity in assembly, tensioning, and sealing.
- *Architectural distinctiveness*: Noted by experts 9 and 10, as both a drawback and a benefit, as the system may primarily appeal to specific architects, distinctly selecting it for its unique aesthetic.
- *Maintenance*: Raised by Experts 10, and 12, citing concerns over long-term upkeep, particularly retensioning and panel replacement logistics.

The system was generally seen as unsuitable for standard building typologies like commercial or residential façades. Instead, experts supported the idea of seeking applications that align more closely with the system's inherent strengths.

7.2.2 Feedback on the five application cases

Experts also provided feedback on the five proposed application cases. Below is a summary of the most notable findings and observations:

1. ETFE Panels

- Experts 4, 5, 6, 7, 8, 9, 10, & 11 highlighted ETFE's ability to accommodate large deformations, its lightweight nature, and alignment with the tensile panel's behaviour.
- Expert 5 & 6 suggested using a singular large cushion, instead of the 4 trapezoidal cushions depicted in the given image.
- Expert 5 & 6 also suggested potentially using rigid temporary frames to support the tensioned panels during construction and installation, circumventing the inherent stability issues.
- Expert 12 & 14 cautioned about detailing around the sharp corners of the trapezoidal compartments and emphasized the need for robust edge profiles beyond just cables to ensure a good pressure seal of the ETFE cushions.

- Experts 9, 10, & 14 raised concerns about the fire safety of ETFE membranes. However, Expert 9 also identified an intriguing opportunity: the use of membranes with varying fire resistance levels, including specific sacrificial membranes designed to aid in effective smoke dissipation.
- Expert 8 highlighted the potential for significant cost reductions without compromising engineering performance, noting that ETFE cushion façades, typically expensive to install on-site, could benefit greatly from prefabrication.
- Expert 10 & 14 mentioned the potential application in larger spanning structures particularly in stadiums or airports for instance.

2. Double-Skin Façades

- Experts 5, 7, 13, and 14 appreciated the added structural depth offered by this solution, seeing it to enhance overall system efficiency.
- Experts 8, 9, 10 and 12 raised concerns about practical challenges of the crossing cables, including difficulties integrating shading systems, limited cleaning access, and the complexity of managing condensation within the enclosed space.
- Expert 9 additionally highlighted the system's low thermal mass as a potential performance drawback, noting the risk of rapid internal temperature fluctuations.
- Expert 6 acknowledged the potential of double-skin façades but along with 8, 9, and 12 emphasized that this system must demonstrate clear, measurable advantages over conventional mullion systems to be considered viable. Expert 11 was more sceptical, arguing that a traditional mullion-based façade would outperform this approach in both simplicity and efficiency.
- After reviewing, Experts 4 and 8 proposed a prefabricated closed cavity façade (CCF) configuration in which only the outer planar glazing would be replaced with a tensioned membrane. Both citing references where a double skin facade was internally glazed and externally cladded with a membrane. This alternative, they suggested, could improve structural efficiency while preserving the cavity's functional purpose and maintaining acoustic and fire performance through a traditional glazed inner layer.

3. Overcladding of (historical) facades

- Experts 4, 5, 8, 9, and 13 valued the minimal anchoring requirement and non-intrusiveness.
- Expert 8 highlighted a potential scenario where the inner frames could be oriented around existing windows and the tensile panel itself would be kept open at those locations. Limiting visual deflections of the occupants.
- Expert 9 mentioned the potential advantage this system would have for uneven or protruding facades (e.g. balconies).
- Expert 10 mentioned the systems distinct visual characteristics making the application range potentially limited for existing facades.

- Expert 11 rejected this use case due to its unnecessary complexity, stating that even when limiting to 4 connection nodes a simple stick-based system would be structurally preferable.
- Experts 7 and 12 emphasized the need for careful sealing and weatherproofing.

4. Integration with Structural Cross-Bracing

- Experts 4, 5, 6, 8, 11, and 12 deemed it too niche or structurally mismatched to be viable.
- Expert 7 pointed out this application would severely limit the systems aimed benefits of disassembly and reconfigurability.
- Expert 10 noted it could work if used to infill exposed bracing zones, though this remains a limited use case.
- Expert 14 supported this idea only in large-scale buildings (e.g., data centres), provided higher pre-stress can be achieved.

5. Tent-Like or Modular Structures

- Experts 5, 6, 7, 10, 11, and 14 emphasized the system's potential modularity, rapid assembly, and adaptability, particularly for temporary or semi-permanent architectural applications.
- Experts 5 and 6 also noted the system's potential for enhanced structural synergy. They suggested that if the cables could be interconnected, they might help share each others opposing tensile loads across the system, thereby reducing stress on the compressive struts, a benefit that would also be valuable for large-scale façades such as stadiums.
- Expert 8 pointed out a distinct advantage this system may have over traditional tent-like structures: the ability to integrate real windows and doors.
- In the context of temporary use, Expert 8 also underscored the importance of ease of installation, suggesting that such a structure should be designed for assembly by no more than two people.
- Expert 9 mentioned the incorporation of building services in the facade to be impractical, stating it is unsuitable for direct attachment or conduit routing.

7.2.3 Conclusions and Expert Preferences

Looking at all interviews, enthusiasm for the proposed applications can be ranked from most to least promising:

ETFE Integration was the most widely endorsed application. Most Experts highlighted its strong compatibility with the tensile-based system, especially due to ETFE's inherent flexibility, lightweight properties, and tolerance for large deformations. It was frequently described as a natural fit, although fire safety and detailing were flagged as requiring further attention.

Tent-like modular systems received substantial support. Experts generally emphasized the facade's suitability for temporary, semi-permanent, or deployable structures, particularly in humanitarian or event-based contexts. However, for such applications to be successful, the system would need to be easy to assemble and offer clear advantages over traditional tents, especially in terms of insulation, deployment speed, and occupant comfort. That said, several experts acknowledged that their support was based more on intuitive appeal than technical validation, and none indicated having actual experience in designing tent-like temporary structures.

Overcladding of (historical) facades was regarded as a high-potential niche application. Experts 4, 5, 8, 9, 12, and 13 appreciated the system's potential lightweight nature and minimal anchoring, especially for retrofit contexts where intrusion must be limited. Still, Experts 7, 10 and 11 remained sceptical, mentioning hurdles with sealing, architectural distinctiveness and structural overcomplication.

Double-skin façades received mixed feedback. Experts 4, 5, 6, 7, 8, 13, and 14 acknowledged the concept's potential, occasionally offering design suggestions. However, Experts 8, 9, 11, and 12 raised significant concerns, particularly related to buildability, integration of shading systems, maintenance challenges, and overall unnecessary complexity compared to conventional mullion-based systems.

Cross-Bracing Integration was the least supported application. Experts 4, 5, 8, 11, and 12 regarded it as too niche or unwise to integrate the load bearing structure into a facade in this way. Expert 10 viewed it as feasible only for highly specific use cases such as infill within exposed exoskeletons. Expert 14 accepted it in large-scale buildings, conditional on high pre-stress and specialized coordination.

Experts broadly supported the development of the system for membrane-based and lightweight applications, with its low weight identified as the primary advantage. In addition to the proposed use cases, experts also suggested large-scale buildings such as stadiums, data centres, and airports as suitable contexts. However, significant concerns regarding deflection control, fire safety, and acoustic performance led to strong caution against applying the system in residential or office environments.

8. Conclusions and Recommendations

With the help of the interviews, some insight can be gained into the potential future of the prefabricated tensile façade panel. However, it is important to first revisit the original aim of the tensile system and the key research findings in order to address the central research question:

'*How can the principle of a tensile based system be utilized to create a more effective prefabricated facade solution?*'

Reviewing the original design

The original tensile system was intended to deliver a stiff, highly prefabricated façade solution that is highly reconfigurable, simple to remanufacture, lightweight, and thermally efficient within a thin profile.

Addressing the primary challenge: the out of plane *stiffness* of the panel. Although it is possible to design a planar tensile system that achieves stiffness comparable to other prefabricated façades, the required pretensions would become enormous and likely unsafe to handle. This system is inherently better suited to accommodate large deflections, as these deflections are necessary for the system to develop meaningful out-of-plane resistance. Accepting deflection limits of around l/50 is necessary to achieve acceptable material efficiency, or alternatively, a different configuration should be adopted in which the cables already possess an out-of-plane geometry.

Secondly, addressing the promise of *reconfigurability*: This research has shown that although the façade panels can indeed be reconfigured, the range of possible configurations is limited when trying to maintain adequate performance with respect to out-of-plane deflections. Any asymmetry in the panel configuration directly contributes to increased wind-induced deflections. This also implies that the use of rectangular panels is suboptimal when aiming for a material-efficient design. Furthermore, while the steel substructure of the façade panel may be reconfigurable, the cladding and infill materials might not be, rendering this proposed advantage less appealing and less feasible.

Next, regarding *remanufacturability*: depending on the final detailing of the system, it could still be easily remanufactured. If standardized components are used, the fact that the panel could consist of relatively few parts remains a key advantage. However, this remains a significant uncertainty, as proper detailing has yet to be completed.

Then, the *level of prefabrication*: Positioning and tensioning the inner frame proved to be a time-consuming and challenging task to execute precisely, and no effective solution has yet been found to simplify this process. Performing this step in a factory and shipping

the panels fully assembled would eliminate the need for this complex task on site, while also aligning with the general benefits of a high level of prefabrication. However, since the frame suffers from stability issues, it would likely still require additional tensioning during installation, which may be difficult to manage on site and significantly add to the installation time. The pretensioning challenge could also be addressed by using single hollow steel sections with greater torsional resistance, but this would contradict the original design intent and negatively impact thermal performance.

Regarding *thermal performance*: Although no explicit thermal analyses were conducted, many of the interviewed experts expressed concerns about the potential for thermal bridging between the steel outer frames, especially if the two opposing profiles require additional connections to enable composite action for increased torsional resistance. The system would likely require an additional external insulation layer to shift the vapor line outside the structural layer, particularly in configurations incorporating crossing cables. However, these issues can potentially still be mitigated through proper detailing. While this will present certain challenges, it remains possible for the panel to achieve relatively good thermal performance within a thin profile, though further research is needed to confirm this.

Turning to the *material efficiency* of the system: compared to Light Gauge Steel Framing (LGSF), the tensile-based solution demonstrated that, for a 3 x 3 m panel subjected to 1 kPa wind loads, deflection limits greater than l/50 would be required to achieve comparable material efficiency to LGSF systems designed for significantly stricter deflection limits of l/250 and l/500. Additionally, the crossing cable configuration, intended to provide similar stiffness, proved to be much less material efficient for a panel of the same thickness as the LGSF, as it required large cable diameters to achieve adequate stiffness. This configuration would only become competitive in terms of material usage with significantly thicker panels.

Additionally, tensile systems like this may be *challenging to maintain*, as adequate pretension in the cables is critical to ensuring sufficient stiffness. However, tensile systems are prone to relaxation over time, making planned inspections likely necessary. At a minimum, a strategy should be developed to address this issue, such as over tensioning during assembly or incorporating softer spring elements, to compensate for the expected tension loss over time. This aspect also requires further investigation, depending on the final application and design.

Comparing this system to traditional prefabricated façade solutions for residential or office applications appears unproductive, as it is highly unlikely to offer a more effective alternative. Experts interviewed were also highly sceptical that such a system could compete with established solutions such as PCSP, SIP, CLT, LTF, LGSF, or UCW. The

tensile-based system would likely either lack sufficient stiffness, be materially inefficient and difficult to manufacture and install, or result in panels that are overly thick and complex to produce, all of which also likely requiring more intensive maintenance.

Recommendations for future design explorations

This does not imply that the tensile system lacks potential; rather, its effectiveness depends on identifying applications where its unique aesthetic and design features align with specific performance and architectural requirements. When exploring alternative use cases, several promising opportunities arise. For example, the system can achieve good material efficiency if larger deflections are acceptable. The panel also offers strong shear resistance when out-of-plane warping of the frame is adequately controlled. Additionally, the visually unobtrusive cables can contribute to a highly transparent façade solution. With only four connection points required, the system is well suited for situations with limited structural attachment options and potentially for larger spans, provided that dynamic challenges such as wind-induced resonance are properly managed.

The interviews suggested that integrating the tensile system with ETFE cushions presents a promising design opportunity. Due to its flexible nature, ETFE may be particularly well-suited to complement the flexibility of the tensile system. Introducing prefabrication into ETFE systems could also potentially yield significant cost savings.

Moreover, ETFE offers high transparency and some potential for thermal insulation, making it a potentially attractive option for overcladding historical façades (Figure 156).

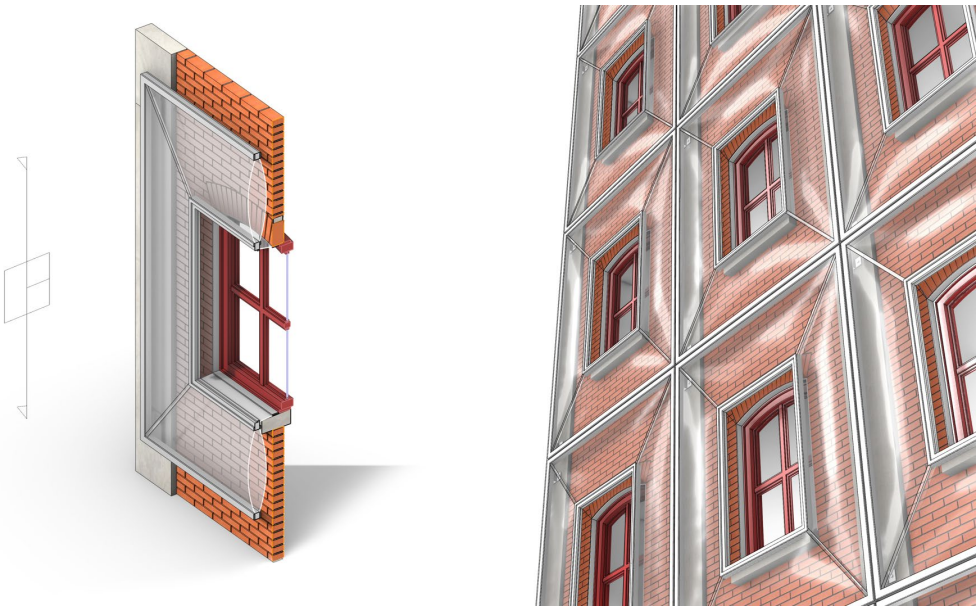

Figure 156: Architectural impression of the tensile façade system integrating ETFE cushions, overcladding existing façades.

This approach preserves the visual connection to the underlying structure while juxtaposing it with a high-tech aesthetic. Enhancing thermal performance, essentially wrapping the building in a large-scale, transparent "bubble wrap." Additionally, overcladding would shield occupants from direct exposure to the potentially discomforting movements of the panels, addressing another major concern associated with the system.

The possibility of implementing the system within a double-skin façade was also discussed. While this was not generally identified as a high-potential application, one configuration stood out during the interviews: the integration of a tensile membrane as the exterior layer of a Closed Cavity Façade (CCF) (Figure 157).

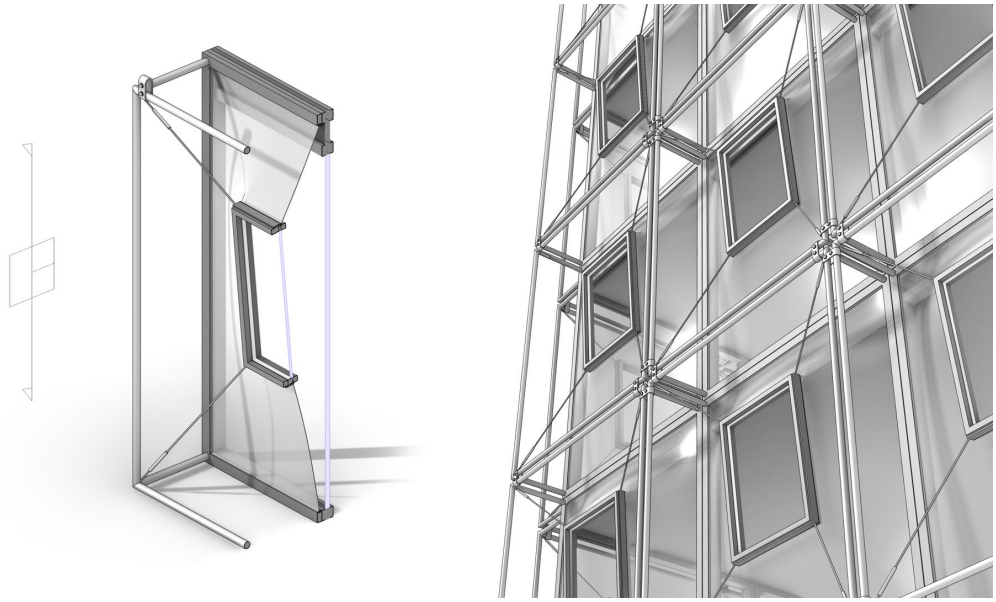

Figure 157: Architectural impression of the tensile façade system integrated with a CCF.

This system presents an architecturally interesting solution, offering significant design flexibility in the configuration of the inner frame. By utilizing traditional glazing for the inner façade of the Closed Cavity Façade (CCF), concerns related to acoustics and fire safety can be effectively addressed. Rather than relying on a heavier and more costly outer glazing layer, a tensioned membrane would serve as the exterior layer. This membrane also already introduces a slight out-of-plane deformation, which enhances resistance to wind loads. Additionally, the open cavity between the membrane and glazing is free of cables allows for the integration of blinds. Taken together, these features could make the system a promising candidate for further exploration.

Finally, thanks to its inherent shear resistance, the system shows promise for standalone insulated tent-like structures. If the panels are lightweight and easy to install, they could

offer greater comfort than traditional tents, including the integration of higher-quality doors and windows. Interconnected cable configurations might also improve structural synergy between panels. However, careful detailing is needed to address stability issues, and adding thermal breaks would likely require extra tensioning during assembly to prevent warping, making further research into these designs essential.

In summary, although the current tensile-based prefabricated façade system faces notable challenges compared to established solutions in office or residential applications, it offers a unique aesthetic and characteristics, such as flexibility, minimal connection points, and lightness, that make it promising for niche uses. These opportunities call for dedicated future research to further explore and develop these potential designs.

Appendix

Explainer: how to use the load cells and provided code

To read out the load cell data using a laptop or desktop computer, follow the steps below. If you only want to monitor the values and do not need to record data, everything can be done directly inside Arduino IDE. If you do want to record the data, a Python script is provided, which is explained in later steps.

1. Connect the force gauges (load cells) to the Arduino board. Make sure each load cell is connected to the correct HX711 amplifier module. Be especially careful to connect the red wire (VCC) to the correct pin. Refer to the image for guidance:

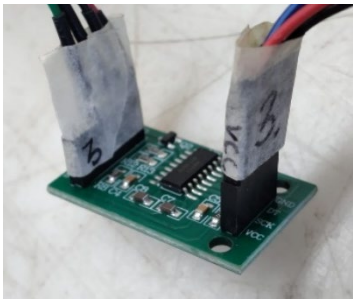

2. Open the file HX711_setup_4x.ino using the Arduino IDE (version 2.3.4 was used for testing).

3. In the Arduino IDE, go to Tools → Serial Monitor.

4. Connect the Arduino board to the laptop by plugging in the USB cable. After 5–10 seconds, you should see the following messages in the Serial Monitor:

   “HX711 modules ready.
   Using Arduino IDE, press 's' to start, 'x' to stop, and 't' to tare scales.
   Scale1 Scale2 Scale3 Scale4”

5. Make sure the load cells are not under any load (no compression or tension).
   Press ‘t’ in the Serial Monitor. You should see the message:
   “Scales tared.”
   Press ‘s’ to begin streaming data. You should now see values for each load cell, typically ranging between -0.15 to +0.15. These values are calibrated in Newtons.

```
-0.01   0.03    0.00    0.10
-0.01   0.10    0.00    0.06
-0.01   0.15    -0.00   0.02
0.00    0.15    0.03    0.01
```

6. If the values are inaccurate, you can adjust the scale factors in line 8 of the Arduino code. The following worked well in testing:
   const float SCALE_FACTORS[4] = {1482, 1498, 1479, 1503}
   Note: These values scale linearly, but inverse (as in 1/x), so modifying them requires some calculations on your end.

7. In the Arduino IDE, go to Tools → Serial Plotter. If data is being streamed, you will see real-time force graphs for each load cell:

8. To record the data, open the script 20250328_ArduinoToCSV.py in a python interpreter to your liking.
   This script was made in Python 3.12.9.
   Make sure the following packages are installed in your Python environment:
   - Matplotlib (for plotting)
   - Pyserial (for communication with Arduino)

9. Run the script, a window should now appear displaying live data (make sure to start the measurements):

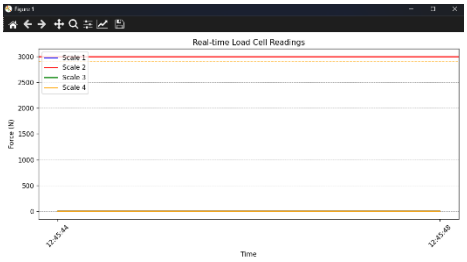

   If you see this error:

   'Failed to connect to COM5: could not open port 'COM5': PermissionError(13, 'Access is denied.', None, 5)'

   Make sure to close Arduino IDE, then unplug and reconnect the USB cable.
   Run the python script again without opening Arduino IDE. If this still does not work, test the COM5 connection in Arduino IDE and troubleshoot there.

10. While the python script is running, you can control it with the following commands:

start	→	begin data stream (device)
record	→	start recording to CSV
‘spacebar’	→	make a marker at next data point
stop	→	stop recording
tare	→	zero the scales
exit	→	quit program

Additionally, during recording, a red dot will appear in the corner to indicate that data is being saved. You can also press the spacebar to insert a marker at a specific timestamp, which can later be viewed using a CSV interpreter like Excel. Red and orange lines are also plotted on the graph to warn you not to exceed certain force thresholds, as the load cells are rated for a maximum load of 300 kg.

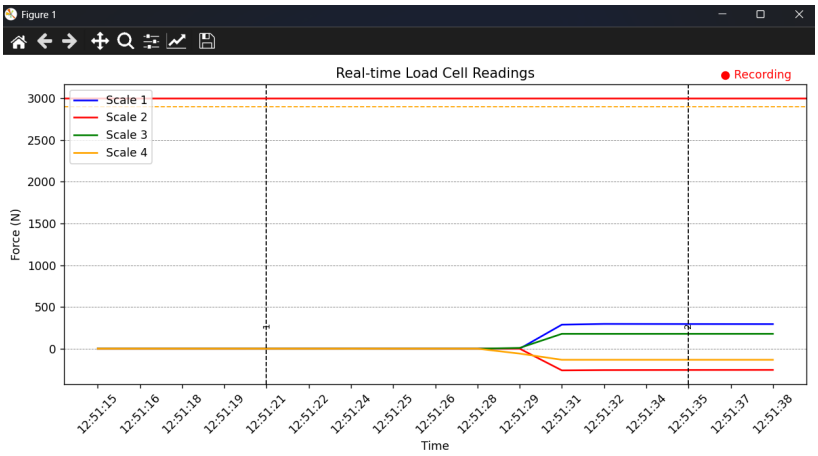

11. The files will be saved to the same directory from which the Python script is run. The .csv files can be opened with any CSV interpreter; Excel is recommended. Use the Text to Columns feature in Excel to format the data. Then it can be formatted as a table, at that point the data can be easily filtered or graphed based on specific timestamps.

Good luck measuring!

Interview summaries

Feedback from Expert 1 (Interview type 1)

Concerns:

1. **Deformation and Instability:**
    - Without pretension, cables provide no stiffness and cannot resist out-of-plane forces.
    - Significant pretension is required to control deformation—likened to tuning a guitar string.
    - Even when pretensioned, the panel would still experience instability and "wobble."
    - A rigid cladding attached to such a system would be at risk of cracking, especially near edges.
2. **Precedents Highlighting Risks:**
    - Mentioned a past cable-net facade project where rigid glass components repeatedly broke due to excessive deformation.
    - Stressed that flexible structures and stiff materials (like glass or rigid insulation) perform poorly when directly integrated.
3. **Installation Complexity:**
    - Different cable lengths and angles introduce significant installation and tuning challenges.
    - Achieving balanced pretension across all cables is difficult due to material elasticity and geometric asymmetry.
    - Recommended looking into advanced cable tensioning hardware from specialized manufacturers.
4. **Edge Thermal Bridges:**
    - Despite internal thermal breaks, edge detailing may still cause thermal bridging.
    - Additional insulation at the panel edges would likely be required.
5. **Doubts on Functional Advantage:**
    - The supposed benefit, adaptability and reusability, was seen as insufficient to justify the mechanical and thermal complications.
    - Raised concerns about whether the modular nested-frame concept adds real value compared to more straightforward alternatives.

Suggestions for Redesign:

1. **Structural Reconsideration:**
    - Proposed abandoning the tensile cable concept in favour of simpler systems.
    - Agreed implementing crossing cables could improve out-of-plane behaviour and reduce cladding deformation problems.
2. **Different Corner profiles and only straight sections:**
    - Encouraged using modular corner joints and simple beams to simplify installation and keeping the goal of adaptability and modularity.

Conclusion:

- Concluded that the current concept suffers from major structural and building physics drawbacks.
- Believed that these issues outweigh the potential benefits in adaptability and reusability.
- Strongly advised a fundamental redesign of the system.

Feedback from Expert 2 (Interview type 1)

Concerns:

1. **Movement vs. Infill Compatibility:**
    - Noted that rigid infills (e.g., glass or solid panels) will be subjected to the same movement as the cables, which can result in breakage or failure.
    - Suggested that if movement is expected, infills must be designed as part of the cable net system to ensure integrated movement, like existing large-scale cable-net facades.
2. **Comparison to Cable-Net Systems:**
    - Cited an example of a known cable-net facade system that deflects up to 1.5 meters under wind. The proposed panel is expected to deflect 5–6 cm, which is less, but still presents design challenges for rigid elements.
    - Emphasized that the cable net and its cladding must be compatible in movement behaviour; otherwise, mechanical failure is likely.
3. **Panel Movement and Geometry:**
    - Expressed concern about how the joints and internal components (e.g., insulation) will behave during deformation.
    - Emphasized that the panel's movement under pressure/suction will cause compression and tension that must be accommodated through specialized joint design.
    - Pointed out that rectangular panels inherently span longer diagonals, worsening deflection and load paths.

Suggestions for Redesign:

1. **Consider Cable-Net Simplification:**
    - Advised simplifying the concept by using horizontal and vertical cables only, reducing deformation complexity.
    - Stated that this could improve structural predictability and eliminate unnecessary complexity in load paths.
2. **Modular Frame Reconfiguration:**
    - Acknowledged the intended adaptability and modularity of the system, including reusing internal frames in new configurations.
    - Noted that while this is feasible, varying cable lengths and required joint tolerances will impose design and installation complications.

3. **Structural Anchoring Needs:**
    - Referenced precedents where large cable-net facades require massive anchor blocks to transfer tensile forces.
    - Indicated that this principle applies to the tensile panel as well, anchor points must be structurally substantial.
4. **Thermal and Moisture Considerations:**
    - Expressed concern about integrating cables through thermal breaks, which can lead to condensation or thermal bridging.
    - Recommended detailed diagrams showing the panel in its neutral (no-load) and deformed (under wind load) states to analyse how thermal continuity, joints, and insulation are affected.
5. **Insulation and Joint Detailing:**
    - Highlighted the risk of discontinuous insulation when panels move, necessitating visible joints or gaps in insulation layers.
    - Explained that expansion gaps can compromise thermal, air, water, and acoustic performance unless joints are carefully designed.

Conclusion:

- Acknowledged that the concept is innovative but technically complex, particularly when rigid infills are combined with a flexible load-bearing structure.
- Recommended early-stage elimination of infeasible options to focus on viable redesigns.
- Encouraged developing simple, clear diagrams and mechanical sketches to anticipate physical behaviour under wind loads.
- Advised refining the concept to anticipate the full range of building physics challenges, structural, thermal, moisture, and acoustical and consider trade-offs across these domains.
- Stressed that a good facade design anticipates multi-domain performance early in development, not just structural or visual goals.

Feedback from Expert 3 (Interview type 1)

Concerns:

1. **Stiffness and Stability Issues:**
    - Noted that traditional systems use a steel plate or rear element to provide stiffness and vapor control, which is missing in the concept.
    - Stated that without such rigidity, the panel would deform excessively.
2. **Load Distribution Problems:**
    - Recognised a major issue: asymmetrical cable forces can lead to large uneven deformation.
    - Highlighted the impracticality of achieving low deformations without excessive material use.
3. **Thermal Break Complications:**
    - Emphasized that integrating pretensioned cables across a thermal break undermines both thermal performance and mechanical stability.
    - Agreed that the two-part frame (inner and outer) would be prone to stability issues, unless designed as a hollow cross-section.
4. **On-Site Installation Challenges:**
    - Installing and tensioning cables on-site is problematic because the panels would already need to be fixed to the structural frame, creating additional concerns with building movement, thermal expansion, and seismic response.
    - Cautioned against adding unnecessary complexity to an already solved problem.
5. **Maintenance Requirements:**
    - Highlighted that all cable-stayed facades require regular retensioning and inspection, adding a long-term maintenance burden not typical of unitized systems.
6. **Lack of Clear Advantage:**
    - Could not identify a convincing benefit over existing unitized systems.
    - Argued that unitized systems already provide structural integrity, vapor control, and prefabrication efficiency.
    - Suggested that the reconfigurability benefit of the tensile system is marginal and still requires significant remanufacturing for each new layout.
7. **Industry Resistance:**

- Noted that manufacturers have well-established processes for current facade types.
- Unlikely they would adopt a novel system requiring a complete overhaul of production, engineering, and testing routines.

8. **User Perception Issues:**
    - Expressed concern that visible facade movement (5 cm+) would undermine user confidence, especially in residential or commercial contexts.
    - Considered the system possibly suitable only for experimental projects or academic case studies, not standard real-world buildings.

Suggestions for Redesign:

1. **Diagonal Cable Configuration:**
    - Supported the idea of using crossing out of plane cables (instead of planar) to reduce pretension requirements and improve stiffness.
    - Acknowledged this significantly improves mechanical performance but likely still does not resolve the cost-benefit imbalance.
2. **Return to Stiff Panel System:**
    - Suggested that a better approach might be to use standard unitized panels with replaceable panel infill elements, based on bending.
    - Proposed a concept where the outer frame remains constant, and pre-glazed or solid panels can be inserted or reconfigured as needed.
    - Stated this would offer higher reusability, simpler logistics, and more freedom of infill design without the drawbacks of tension-based deformation.

Conclusion:

- Did not recommend pursuing the current tensile facade concept for practical architectural applications.
- Argued that it introduces more problems than it solves, including excessive complexity, reduced performance, higher maintenance, and no meaningful environmental or cost benefit.
- Acknowledged the intellectual value of exploring the concept, but maintained that simpler, well-established systems provide better performance with fewer trade-offs.

Feedback from Expert 4 (Interview type 2)

General Feedback on the System

The expert considered the system an interesting exploration of pre-stressed facade elements but cautioned that its material savings and practical benefits remain unproven. A key concern was the complexity of closing the surface between the inner and outer frame, a task made more difficult by the system's inherent movement. The interviewee questioned whether the use of cables and pre-compression meaningfully reduces material use, noting that standard lightweight timber stud systems already achieve efficient spans. In their view, the concept might only find application if combined with membrane or fabric-based materials that accommodate movement and require minimal fixings.

Feedback on Proposed Systems

1. ETFE Panels

- Considered one of the most suitable applications.
- The system's flexibility and need for lightweight, tension-compatible cladding makes it a good fit for ETFE cushions.
- Expert affirmed that this would be a logical and direct application for the tensile frame concept.

2. Double Skin Facades

- Seen as plausible, but practical execution was questioned.
- The expert pointed out that even if the cavity depth increases, the glass still needs to span a large distance, which poses challenges in terms of glass thickness and performance.
- The expert proposed an interesting variation: using cables on one side of the system to pull the membrane out of plane on the other side, thereby introducing pre-stress and curvature. This could create a structurally more efficient form that leverages the system's strengths in tension, particularly when paired with lightweight foil or membrane materials.
- Encouraged referencing specific case studies (e.g., Hamburg project using ETFE as external skin and glass as internal skin) for inspiration.

3. Overcladding of Heritage Buildings

- Identified as potentially valuable, especially due to the limited number of connection points required (four corners).
- Could enable refurbishment without major disruption to the existing façade.
- Expert agreed that reduced anchorage was advantageous but emphasized the need to resolve how to effectively seal the surface (e.g., if using fabrics, tensioning is needed).

4. Cross Bracing Systems

- Regarded as too niche.
- Such applications are limited to very specific areas of a building and are not scalable across entire facades.
- The expert dismissed this option as lacking general relevance.

5. Tent-Like Systems

- Seen as a good conceptual match, especially if membranes or foils are used for cladding.
- Acknowledged that this use aligns with the system's natural movement and structural behaviour.
- Highlighted acoustic limitations of fabric systems but affirmed their feasibility for lightweight or temporary applications.

Conclusions and Recommendations

- The expert recommended that the system focus on fabric or foil-based applications, where its movement tolerance and low anchorage needs offer meaningful advantages.
- Strongly advised against pairing the system with rigid panels (e.g., timber or glass) due to likely mechanical failure at fixings under deformation.
- Of the proposed applications, ETFE systems and tent-like structures were deemed the most promising.
- Double skin facades and overcladding were conditionally viable if the sealing and cladding strategy is carefully designed around system flexibility.
- The expert concluded that the tensile frame panel is not suited to general facade replacement but may be developed into a specialized system within a membrane-based or inflatable architectural niche.

Feedback from experts 5 & 6 (Interview type 2)

General Feedback on the System

The experts appreciated the innovative nature of the proposed tensile facade panel system. They acknowledged its potential and noted that while the system is a “solution in search of a problem,” it holds promise, particularly in settings where structural and geometric flexibility are valuable. The system's reuse potential, structural uniqueness, and adaptability to various forms were highlighted as distinguishing features. They cautioned, however, that its benefits over traditional systems (e.g., light-gauge steel framing) need more justification, especially in terms of cost & complexity. A core theme was the balance between rigidity and flexibility: the experts questioned whether the system's increased complexity and inherent flexibility truly offered sufficient functional advantages to justify adoption.

Feedback on Proposed Systems

1. ETFE Panels

- Regarded as a fitting application, particularly due to ETFE's flexibility and adaptability to deformation.
- Suggested using membranes not only for peripheral zones but potentially for the full panel, unless structural backing provides a necessary function.
- Raised the question: why not just use a full ETFE cushion directly, unless the tensile frame adds clear value?

2. Double Skin Facades

- Seen as the most promising application due to built-in depth allowing better structural efficiency and thermal breaks.
- Experts noted potential for meaningful performance in this use case, especially with thicker cavity walls and potential for walkable zones. Although the cross bracing would get in the way.

3. Overcladding of Heritage Buildings

- Considered viable; a lightweight external cladding system with only a few anchoring points was seen as advantageous.
- Could provide added insulation and weather protection without imposing on existing façades structurally or visually.
- Experts highlighted that thermal and acoustic performance would still need to be supplemented by other layers.

4. Cross Bracing Systems

- Deemed structurally interesting but potentially niche due to the limited number of buildings with exposed or usable cross-bracing.

- Recognized as an example where the system could be integrated with existing load-bearing frameworks, although practical adoption may be limited.

5. Tent-Like Systems

- The experts responded positively to this idea; the integration of pre-tensioned elements within a tent structure was considered a strong potential use case.
- Emphasis placed on structural synergy: if cables could contribute not just to forming the geometry but also to bearing loads together, potentially cancelling each other out, the application becomes more compelling.
- Noted potential in combining with structurally optimized forms.

Conclusions and Recommendations

- The experts found double-skin facades to offer the most tangible opportunity, particularly if structural behaviour, thermal performance, and form-driven load balance are optimized.
- ETFE/membrane integration was a close second, especially for applications prioritizing lightness, curvature, and ease of prefabrication.
- They emphasized the importance of identifying a clear performance or cost advantage over conventional solutions. Without a well-defined problem the system uniquely solves, uptake is unlikely.
- Suggested further exploration of alternative geometries or aggregated panel systems where internal forces might balance out (e.g., multi-story stacking with shared nodes).

Feedback from Expert 7 (Interview type 2)

General Feedback on the System

The interviewee described the concept as “exciting” and promising from a circularity and architectural freedom perspective. The potential for disassembly, reconfiguration, and the minimized material palette were seen as valuable innovations. However, they raised key concerns about stability, deflections and especially watertightness, a challenge typically well-resolved in standard systems. They noted that the introduction of cables alters conventional load-sharing mechanisms and questioned whether dry or wet sealing methods would remain viable under large deflections. Ultimately, they thought the system’s unique value proposition lies in its potential for disassembly and reusability, which should be the focus in identifying application areas.

Feedback on Proposed Systems

1. ETFE Panels

- Seen as a very natural and promising fit.
- Aligned well with the system’s flexible, lightweight character.
- Provides maximum transparency and minimal framing, consistent with ETFE design goals.
- The expert called this the closest and most direct application of the system, architecturally speaking.

2. Double Skin Facades

- Considered an interesting scenario due to its structural depth and potential for prefabrication.
- Questions were raised about expected thermal and acoustic performance, ventilation strategy, and depth-to-weight ratio.
- While structurally viable, more study needed on integration details, especially how it compares thermally to other ventilated systems.

3. Overcladding of Heritage Buildings

- Viewed as promising but technically underdeveloped.
- Concerns focused on sealing strategies and how cladding would interface with existing buildings.
- The expert emphasized the importance of defining the load-sharing mechanism and how water and wind loads are distributed between from external to internal layers.
- Encouraged attention to connection and sealing methods (e.g., silicone, dry gasket, structural sealant).

4. Cross Bracing Systems

- Technically possible but questioned the added value in this case.
- Pointed out that such applications wouldn't benefit significantly from disassembly or reconfigurability.
- Emphasized staying aligned with the system's primary strength: ease of disassembly, which this scenario lacks.

5. Tent-Like Systems

- Seen as feasible and potentially innovative.
- Would depend heavily on the effectiveness of the thermal break to ensure adequate insulation.
- Could be suited for semi-permanent or deployable architecture, although thermal and airtight performance would need validation.

Conclusions and Recommendations

- The expert reiterated that the main driver for this system should be ease of disassembly and reusability.
- Recommended prioritizing application areas where this benefit is clearly superior to existing solutions.
- Among the five options, ETFE integration was favoured due to its simplicity, transparency, and material alignment.
- Overcladding and tent applications were also promising but would require careful attention to sealing and insulation.

Feedback from Expert 8 (Interview type 2)

General Feedback on the System

The interviewee acknowledged the conceptual novelty of the tensile panel but emphasized the difficulty of competing with standard steel frame systems (SFS) on cost and simplicity. The magnitude of deflections posed key challenges, particularly with interior finish quality and perception. The expert highlighted that plasterboard or other rigid materials would crack, requiring large expansion gaps or dual-layer facades, which undermines the system's economic advantage. Without a compelling niche, they found it difficult to justify the complexity introduced by tensioning, asymmetric loading, and deflection control.

Feedback on Proposed Systems

1. ETFE Panels

- Identified as the most promising application.
- Integration with ETFE membranes seen as logical since ETFE already uses cables and tolerates movement.
- The panelised system could lower cost and complexity compared to existing bespoke ETFE solutions.
- Strong potential for cost reduction while maintaining engineering quality.

2. Double Skin Facades

- Considered possible but complex.
- Cleaning, cavity access, and solar shading integration would be problematic due to cable interference.
- For openable cavities, custom openings would offset savings.
- A closed cavity facade (CCF) may work but would be highly specialized and still run into problems with blinds but deemed the most likely to gain significant advantages of prefabrication.

3. Overcladding of Heritage Buildings

- Seen as a viable and potentially cost-effective application.
- Useful where traditional solutions are hard to implement due to limited connection points or structural sensitivity.
- Could provide continuous insulation with minimal penetrations, unlike typical rain screens which require dense sub-framing.
- Integration with existing windows would be promising, keeping the original window frames that limit deflections substantially. This would however require careful consideration in terms of detailing.

4. Cross Bracing Systems

- Technically feasible but too complex and niche for broad application.
- Requires dismantling and reengineering existing bracing, which is expensive and limited to specific use cases.

5. Tent-Like Systems

- Seen as promising for temporary buildings.
- Could support real windows and doors, unlike typical fabric tents, making it more liveable and functional.
- Emphasis on ease of deployment (two-person operation) could make it competitive in high-end temporary or disaster relief markets.
- Lacked certainty about the market size but saw architectural and functional merit.

Conclusions and Recommendations

- ETFE integration was identified as the strongest opportunity due to alignment with current system needs and cost-reduction potential.
- Heritage overcladding was second but would require case-by-case comparisons with traditional rain screens.
- Tent-like systems ranked third, with promise but uncertain market clarity.
- The expert recommended avoiding comparison with SFS systems due to their overwhelming cost advantage and unsuitability for high-deflection solutions.
- Overall, the system's success depends on targeting niche, high-value contexts where movement is acceptable or beneficial and standard systems fall short.

Feedback from Expert 9 (Interview type 2)

General Feedback on the System

The interviewee found the facade panel concept innovative and potentially lightweight, with potential in applications requiring rapid assembly, flexibility, and reusability. They appreciated the architectural opportunities offered by modularity and fabric materialization but highlighted significant concerns regarding the system's behaviour under environmental stress. Key areas identified for further development include pressure equalization (both external and internal, not just from wind), acoustic performance due to its lightweight and flexible nature, fire safety, humidity management in cavities, and service integration. Overall, the system shows promise in specific use cases but needs careful technical refinement before broader implementation.

Feedback on Proposed Systems

1. ETFE Panels

- The interviewee agreed the system could pair well with ETFE cushions due to similar deformation tolerance and low weight.
- However, integration complexity was noted, especially regarding the window modules and sharp corner angle of the proposed configuration.
- Particular attention must be paid to corner details and transitions between transparent and structural components.

2. Double Skin Facades

- The expert acknowledged this application's potential, especially with crossing cables for improved stiffness.
- They raised maintenance concerns, including cleaning, dust accumulation, and humidity control within the cavity.
- Rapid temperature shifts due to low thermal mass were identified as a performance risk, as well as difficulty in integrating solar shading.
- Placement of sun protection (outside or inside) would need to be resolved due to cable interference.

3. Overcladding of Heritage Buildings

- Seen as one of the most promising applications due to minimal anchoring and non-intrusive installation.
- Allows internal occupancy to continue during retrofit and speeds up the construction process.
- Suitability for uneven or protruding facades (e.g., balconies) was mentioned, with resulting out of plane components potentially becoming a beneficial design aspect.

4. Cross Bracing Systems

- Considered viable where the panel integrates within an exposed structural system.
- Emphasized need to accommodate thermal expansion and allow movement at connection points with steel structures.
- Preserving visual transparency of structural framing was seen as an architectural benefit.

5. Tent-Like Systems

- Highly suitable for emergency or temporary buildings due to speed, lightness, and thermal/acoustic performance.
- Cited as a strong candidate for standalone systems or deployable shelters.
- Integration of building services must be internal, as the facade is unsuitable for direct attachment or conduit routing.

Conclusions and Recommendations

- The panel system offers strong potential in applications emphasizing speed, modularity, and architectural flexibility, particularly for heritage overcladding, temporary tents, and integration with exposed structural systems.
- The ETFE panel and tent-like applications are promising due to compatibility with lightweight structures.
- Double skin facades are technically possible but currently the most complex, requiring deeper study of thermal, moisture, and shading strategies.
- Noise, resonance, and acoustic comfort might be problematic for such a system.
- Fire-safe materials and strategies should be considered, potentially allowing for controlled smoke release making use of sacrificial membranes.
- Focus on fabric-based solutions where low weight and aesthetics are key.

Feedback from Expert 10 (Interview type 2)

General Feedback on the System

The expert described the concept as interesting and potentially valuable, especially in the context of prefabrication, temporary accommodation, and non-standard applications. They appreciated the goals of the system but highlighted several critical concerns. The use of galvanized mild steel was seen as problematic for long-term external use due to the risk of chipping and rusting during installation. From a façade engineering perspective, the thermal bridging posed by the cables was seen as a major issue. The expert emphasized the importance of weathertightness, condensation risk mitigation, and safe, accessible connections to the primary structure, particularly regarding slab edge deflections and installation logistics. They viewed the system as aesthetically specific, which may limit its application range.

Feedback on Proposed Systems

1. ETFE Panels

- Viewed as one of the strongest candidates for application.
- The system's lightweight and flexible nature complements ETFE, especially for large-scale roofs or stadium cladding.
- Cautioned about fire safety of ETFE and suggested consulting providers (e.g., Novum) to assess compatibility, especially in corners where stress concentration may occur.
- Mentioned the potential for integrating transparent photovoltaics (e.g., ClearVue) as an innovative extension.

2. Double Skin Facades

- Feasible but only if justified by environmental performance (e.g., thermal, acoustic, solar gain control).
- Stressed the importance of understanding ventilation strategy and blind placement, especially in closed cavity facades.
- Warned that if not functionally necessary, the use of additional materials would be difficult to justify.
- Suggested this could be suited for airports or buildings with strict performance criteria.

3. Overcladding of Heritage Buildings

- Seen as promising and innovative, especially due to the system's potential for minimal anchorage (four points).
- Noted its likely lightweight construction, which is beneficial in refurbishment contexts.
- Emphasized the need to carefully consider additional horizontal loads and weatherproofing between modules.

- Mentioned the system's distinct visual identity, which may not suit all buildings without additional “dressing up.”

4. Cross Bracing Systems

- Regarded as a logical extension, particularly for areas with higher pre-stress requirements.
- Appreciated the idea of using the system to fill existing bracing zones with modular infill panels.
- Advised that materials used here may need to be flexible and fire-rated, depending on context.

5. Tent-Like Systems

- Seen as a very strong candidate, especially for emergency or temporary housing.
- Noted advantages over traditional tents, such as modularity, insulation, and robust window/door integration.
- Highlighted potential use in humanitarian settings (e.g., post-disaster shelters or refugee camps) and festival or pop-up architecture.

Conclusions and Recommendations

- ETFE-based roofing systems were viewed as the most promising application, particularly in stadia, large-span roofs, or structures requiring quick, repetitive installation.
- Tent-like systems also showed high potential for temporary, modular construction with enhanced performance.
- Overcladding was considered a viable but niche application, contingent on architectural acceptance and technical resolution of connections and thermal issues.
- Double skins and cross-bracing scenarios were conditionally supported, provided they were grounded in specific functional needs (e.g. solar shading).
- The expert emphasized the need for in-depth structural collaboration with the mechanical engineering team of the substructure, particularly around deflection management of floor slabs & slab connection design
- Additionally, the expert highlighted careful attention was needed to ensure weatherproofing detailing between panels. They referenced a project of similar SFS panels that faced great difficulty in ensuring this weatherproofing.
- Aesthetic limitations were seen as a constraint for widespread adoption, suggesting it will appeal to a specific architectural vision or typology.

Feedback from Expert 11 (Interview type 2)

General Feedback on the System

The expert described the concept as structurally innovative but practically questionable, especially in standard facade applications. While the theoretical adaptability and configurability of the panel was acknowledged, they questioned the realistic use cases for repositioning window modules. They emphasized the need for high-frequency reconfiguration to justify the complexity. The expert was also sceptical about the structural performance, particularly regarding deflection limits (L/50) and the required stiffness of the framing, which could negate the intended material savings. Concerns were also raised around detailing, vapor control, and feasibility of tensioned cables in real-world building envelopes. Overall, they appreciated the conceptual exploration but found few viable use cases in standard façade engineering practice.

Feedback on Proposed Systems

1. ETFE Panels

- Seen as an interesting and fitting application, primarily due to ETFE's high deformability.
- The flexibility of ETFE makes the L/50 deflection tolerance acceptable.
- Warned that detailing at connection points and long-term performance under deformation (e.g., seal durability) need careful evaluation.
- Considered appropriate if both the inner and outer layers of the panel are ETFE membranes.

2. Double Skin Facades

- Viewed as one of the few structurally viable adaptations of the concept.
- Expert stressed that using the full cavity depth structurally (as constructive depth) makes sense and improves performance.
- However, noted a key limitation: the system only works in central configurations. When offset, it becomes highly asymmetric and loses efficiency.
- Warned that despite the depth, the structural behaviour of the cables remains problematic and standard framing may still outperform in many cases.

3. Overcladding of Heritage Buildings

- Initially promising due to minimal attachment points (four corners).
- Ultimately rejected by the expert, citing that the potential for reconfiguration is unnecessary in this context.
- Emphasized that any advantage gained in lightness is likely offset by complexity and inefficiency of the diagonal cable layout and additional prestresses.
- Suggested standard stud framing remains a more efficient and practical solution.

4. Cross Bracing Systems

- The expert was unconvinced about structural feasibility in this use case.
- Pointed out that to act as actual bracing, the diagonals would need to pass continuously through multiple modules, which the system does not support.
- Without that continuity, the frame must resist moments and forces it wasn't designed for or would become large and inefficient.
- Declared the system structurally inefficient and not viable for bracing purposes.

5. Tent-Like Systems

- Identified as the most promising application.
- Agreed that this could work at smaller scales where the panel behaves like a fabric module.
- Supported the idea of using the cables to pre-tension membrane infill, with the frame acting as a holder for flexible materials and lightweight doors/windows.
- Preferred a fabric-based system over rigid glazing due to better integration with the system's inherent movement and tolerances.

Conclusions and Recommendations

- The expert emphasized that the concept does not outperform traditional systems in typical façade applications and lacks clear justification unless very specific needs are met.
- Recommends tent-like applications as the most fitting scenario, especially where lightness, modularity, and flexible infill are prioritized.
- ETFE-based facades are viable if detailing is optimized and deformation is acceptable.
- Double-skin facades may work structurally, but practical challenges like asymmetric load paths and cladding detail complexity remain.
- Strongly advised against use in heritage overcladding or bracing systems, citing better conventional solutions.
- Overall, the expert viewed the concept as architecturally imaginative but structurally and functionally limited, only worth pursuing in niche or experimental applications.

Feedback from Expert 12 (Interview type 2)

General Feedback on the System

The expert found the core concept intriguing, especially due to its lightweight and prefabricated nature. However, they emphasized that for the system to be viable, cost-efficiency and simplicity in design are crucial. They raised early concerns about constructability, detailing, and membrane attachment, noting that the system would need additional profiles (not just cables) to support tensioned membranes effectively. Furthermore, they questioned structural robustness under perpendicular loads (e.g., wind, maintenance impact) and emphasized the need for proper edge detailing to ensure watertightness and durability. Despite some technical reservations, the expert was positive about niche applications and shared potential references from previous experience in tensile structures.

Feedback on Proposed Systems

1. ETFE Panels

- Viewed as a theoretically fitting application, given the flexibility of ETFE and the large deformation tolerance of the system.
- Stressed that diagonal cables alone would be insufficient to support ETFE membranes, structural perimeter profiles are required.
- Raised concerns about ETFE's pressure sensitivity and performance under loss of internal pressure (ballooning or collapse).
- Suggested design should allow for membrane attachment on four sides with proper support to handle multidirectional tension.

2. Double Skin Facades

- Sceptical about this use case due to complexity of achieving watertightness and detailing with many intersecting layers.
- Mentioned the potential of integrating a "fancy" (non-load bearing) outer skin but advised to first research existing products (e.g., Schüco's "FACID Façade").
- Highlighted that glass placement (centre and surroundings) would require precise structural coordination and sufficient support.
- Preferred membrane-based outer layers for flexibility and simplicity.

3. Overcladding of Existing Facades

- Identified as the most suitable application.
- Appreciated the minimal attachment points (four), which would allow installation without disrupting the existing façade.

- Valued the system for being lightweight, potentially cost-effective, and flexible in implementation.
- Recommended detailed design development for the connection between the facade panel and the underlying structure, this is where challenges and opportunities lie.
- Suggested potential to integrate into unitized systems as a secondary cladding element.

4. Cross Bracing Systems

- Rejected this application due to structural mismatch.
- Strongly recommended separating load-bearing structure from the cladding system.
- Noted that bracing functions should remain within the core building structure; attempting to combine with a cladding panel would introduce risks and inefficiencies.
- Warned about the high deformation levels that could occur, which lightweight cladding cannot tolerate.

5. Tent-Like or Event Structures

- Found this to be the second most promising application, especially in temporary or flexible structures.
- Mentioned companies like Nussli that specialize in lightweight, modular setups for events, expos, and pavilions.
- Liked the idea for its ease of installation, low cost, and potential reusability.
- Suggested exploring bamboo or stick-based frameworks as structural inspiration for low-impact architecture.

Conclusions and Recommendations

- Overcladding is the most promising application, especially where minimal contact points and light weight are essential.
- Temporary tensile architecture is another strong fit, where the facade system's flexibility and simplicity can shine.
- ETFE integration could work but requires more robust structural detailing and edge profiles—cables alone are insufficient.
- Double skin facades and structural bracing are not recommended due to performance, cost, and complexity concerns.
- Emphasized the importance of keeping structure and cladding separate for structural integrity.
- Recommended focusing on ease of fabrication, simplified connections, and market feasibility (e.g., compatibility with existing systems).

Feedback from Expert 13 (Interview type 2)

General Feedback on the System

The expert expressed appreciation for the conceptual framework of the tensile-based prefabricated panel, particularly its potential material efficiency. The panel's flexibility and structural behaviour were seen as both a challenge and an opportunity. While the expert questioned how much framing was needed to manage out-of-plane forces, they emphasized the potential for minimizing substructure and optimizing Life Cycle Assessment (LCA) performance. The expert suggested future research could investigate frame reduction strategies and better understanding of maximum panel sizing and modularity in relation to building typologies.

Feedback on Proposed Systems

1. ETFE Panels

- Cautiously positive, particularly in terms of cost-saving through prefabrication.
- Expressed concern that the panel geometry may not suit pneumatic ETFE cushions (double/triple layers).
- Suggested single-layer ETFE membranes or a hybrid system where the middle section holds a cushion while outer triangles use single ETFE layers.
- Warned that combining glass and membrane may introduce connection complexity and weight management issues.

2. Double Skin Facades

- Seen as a very promising direction, especially when cavity depth is used structurally.
- Recommended limiting membranes to two layers rather than three (to avoid over-complication).
- Proposed a setup where a single outer membrane is tensioned across a singular inner frame, instead of a double one, combining visual quality and structural simplicity.
- Emphasized the possibility of creating dynamic and lightweight geometries with reduced material use.

3. Overcladding of Heritage Buildings

- Identified as a high-potential application.
- Aligns with the expert's own PhD research into textile solutions for façade retrofitting.
- Applauded the system’s lightweight nature, minimal attachment points, and aesthetic non-intrusiveness when using transparent membranes, making it ideal for preserving existing facades.

- Strongly encouraged continued development for retrofitting applications, ensuring low structural demand on host buildings.

4. Cross Bracing Systems

- Regarded as structurally feasible, but design intensive.
- Applicable only if careful coordination is achieved between architecture and structural engineering.
- Warned against standard cross-bracing where slabs are disrupted, mid-span positioning must be delicately handled.
- Considered less promising than other solutions due to complexity.

5. Tent-Like or Modular Structures

- Viewed as very applicable, especially for emergency architecture or temporary shelters.
- Highlighted system benefits: fast assembly, modularity, reusability, and the ability to create multiple spatial configurations.
- Mentioned similarity to existing research projects, which prioritize speed and ease of construction.
- Noted that this system could differentiate itself by offering more enclosed, room-like modules compared to open pavilion setups.

Conclusions and Recommendations

- Most promising applications identified:
  1. Overcladding of existing buildings
  2. Double-skin facades
  3. Modular tent-like structures (with reservations about market demand)
- Suggested avoiding cross-bracing and ETFE systems in the current form due to complexity and impracticality of integration.
- Recommended exploring:
    - Frame simplification, possibly merging or reducing the number of structural elements.
    - All-membrane solutions (e.g., ETFE/PTFE composites) instead of glass, to maintain low weight and simple detailing.
    - Panel scaling and modularity to match architectural layouts (e.g., fitting larger office spans).
- Strongly encouraged continued research into LCA performance and substructure reduction as differentiating factors in both retrofitting and new construction.

Feedback from Expert 14 (Interview type 2)

General Feedback on the System

The expert expressed appreciation for the lightweight, prefabricated, and potentially modular nature of the proposed panel system. They emphasized that controlling deflection is critical, particularly in buildings where users are near the facade (e.g., residential or office). A key concern was ensuring perceived and actual structural stability, as visible movement might create discomfort. They highlighted that while the minimal deflection variant of the system using crossing cables could be suitable for a broader range of applications, the large-deflection version might only be appropriate in low-occupancy or industrial settings where visible movement is acceptable.

Feedback on Proposed Systems

1. ETFE Panels

- Seen as interesting, particularly due to the potential for cost reduction through prefabrication.
- The expert raised concerns about:
    - Fire safety, especially within UK regulations.
    - Acoustic and thermal performance, which need further definition.
    - Buildability and detailing, especially with unknowns about cavity interruption due to the cables.
- Cited the U.S. Embassy in London as a reference project that used similar rain screen approaches with transparency.
- Concluded ETFE applications might only be suitable in non-residential or non-occupied envelopes, such as theatres, airports, or data centres.

2. Double Skin Facades

- Identified key benefits: lightweight, transparent, and great use of prefabrication.
- Mentioned tensile membranes to be particularly applicable as the outer skin in double skinned facade systems.
- Fire remained the primary concern but was considered more manageable in a configuration where only the outer skin was made using a tensile membrane.
- Speed of construction and reduced carbon footprint were noted as competitive advantages that need to be assessed and ensured.
- Referred again to the American Embassy in London as a model for such layered transparent facades.

3. Overcladding of Heritage Buildings

- Acknowledged the potential for retrofitting older or non-performant facades with minimal intervention.
- Praised the panel's lightness and limited attachment requirements, making it ideal for structures with restricted load-bearing capabilities.
- Cautioned that cleaning and maintenance of internal cavities would need thoughtful detailing, especially if transparency is retained.

4. Cross Bracing Systems

- Seen as a naturally fitting niche for the system.
- If existing buildings include structural exoskeletons, the system could integrate efficiently, benefiting from higher pre-stress capacity.
- Applications could include large-scale envelopes such as those for airports, industrial buildings, and data centres, where aesthetics and high-performance cladding are desirable.
- Fire, again, was flagged as a problem to address.

5. Tent-Like or Modular Structures

- Regarded as a strong application, building on existing architectural typologies.
- Highlighted the advantage of modularity: panels could be reassembled and reconfigured, unlike traditional one-piece tents.
- Saw potential for commercial use, where standardized components enable flexibility across different settings.
- Found this concept well-aligned with reusability and scalability in temporary or semi-permanent architecture.

Conclusions and Recommendations

- Most promising applications identified:
  1. Industrial-scale buildings (e.g., airports, power stations, data centres)
  2. Double skin facade integration using the outer skin as a tensile membrane.
  3. Modular temporary tentlike structures
- Recommended avoidance of:
  - Residential or office contexts requiring tight deflection tolerances.
  - Applications where fire or acoustic performance is heavily regulated without clear mitigation strategies.
- Design criteria to prioritize moving forward:
  - Fire compliance (especially in UK/EU)
  - Ease of cleaning for transparent layered systems

    - Improving buildability (e.g., integrating fire stops, acoustic barriers, connections to the substructure)
    - Clear demonstration of performance-to-cost advantages over traditional prefab panels (like SFS systems)
- Emphasized that the system could become commercially competitive if it meets performance and price expectations in the specialized infrastructure and industrial building market.

Slides shown during the second interview

Interview - Prefabricated Tensile Façade Design and Prototyping

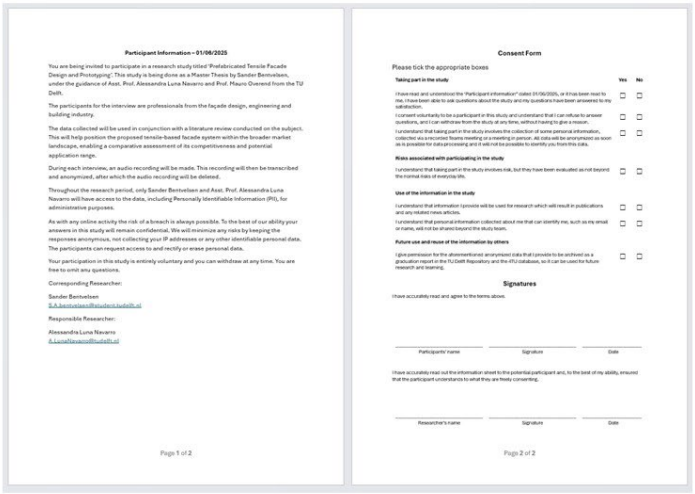

Participant Information – 01/08/2025

You are being invited to participate in a research study titled 'Prefabricated Tensile Facade Design and Prototyping'. This study is being done as a Master Thesis by Sander Bentvelsen, under the guidance of Asst. Prof. Alessandra Luna Navarro and Prof. Mauro Overend from the TU Delft.

The participants for the interview are professionals from the façade design, engineering and building industry.

The data collected will be used in conjunction with a literature review conducted on the subject. This will help position the proposed tensile-based facade system within the broader market landscape, enabling a comparative assessment of its competitiveness and potential application range.

During each interview, an audio recording will be made. This recording will then be transcribed and anonymized, after which the audio recording will be deleted.

Throughout the research period, only Sander Bentvelsen and Asst. Prof. Alessandra Luna Navarro will have access to the data, including Personally Identifiable Information (PII), for administrative purposes.

As with any online activity the risk of a breach is always possible. To the best of our ability your answers in this study will remain confidential. We will minimize any risks by keeping the responses anonymous, not collecting your IP addresses or any other identifiable personal data. The participants can request access to and rectify or erase personal data.

Your participation in this study is entirely voluntary and you can withdraw at any time. You are free to omit any questions.

Corresponding Researcher:

Sander Bentvelsen
S.A.bentvelsen@student.tudelft.nl

Responsible Researcher:

Alessandra Luna Navarro
A.LunaNavarro@tudelft.nl

Page 1 of 2

Consent Form

Please tick the appropriate boxes

	Yes	No
Taking part in the study		
I have read and understood the "Participant information" dated 01/08/2025, or it has been read to me. I have been able to ask questions about the study and my questions have been answered to my satisfaction.	☐	☐
I consent voluntarily to be a participant in this study and understand that I can refuse to answer questions, and I can withdraw from the study at any time, without having to give a reason.	☐	☐
I understand that taking part in the study involves the collection of some personal information, collected via a recorded Teams meeting or a meeting in person. All data will be anonymized as soon as is possible for data processing and it will not be possible to identify you from this data.	☐	☐
Risks associated with participating in the study		
I understand that taking part in the study involves risk, but they have been evaluated as not beyond the normal risks of everyday life.	☐	☐
Use of the information in the study		
I understand that information I provide will be used for research which will result in publications and any related news articles.	☐	☐
I understand that personal information collected about me that can identify me, such as my email or name, will not be shared beyond the study team.	☐	☐
Future use and reuse of the information by others		
I give permission for the aforementioned anonymized data that I provide to be archived as a graduation report in the TU Delft Repository and the 4TU database, so it can be used for future research and learning.	☐	☐

Signatures

I have accurately read and agree to the terms above.

Participants' name | Signature | Date

I have accurately read out the information sheet to the potential participant and, to the best of my ability, ensured that the participant understands to what they are freely consenting.

Researcher's name | Signature | Date

Page 2 of 2

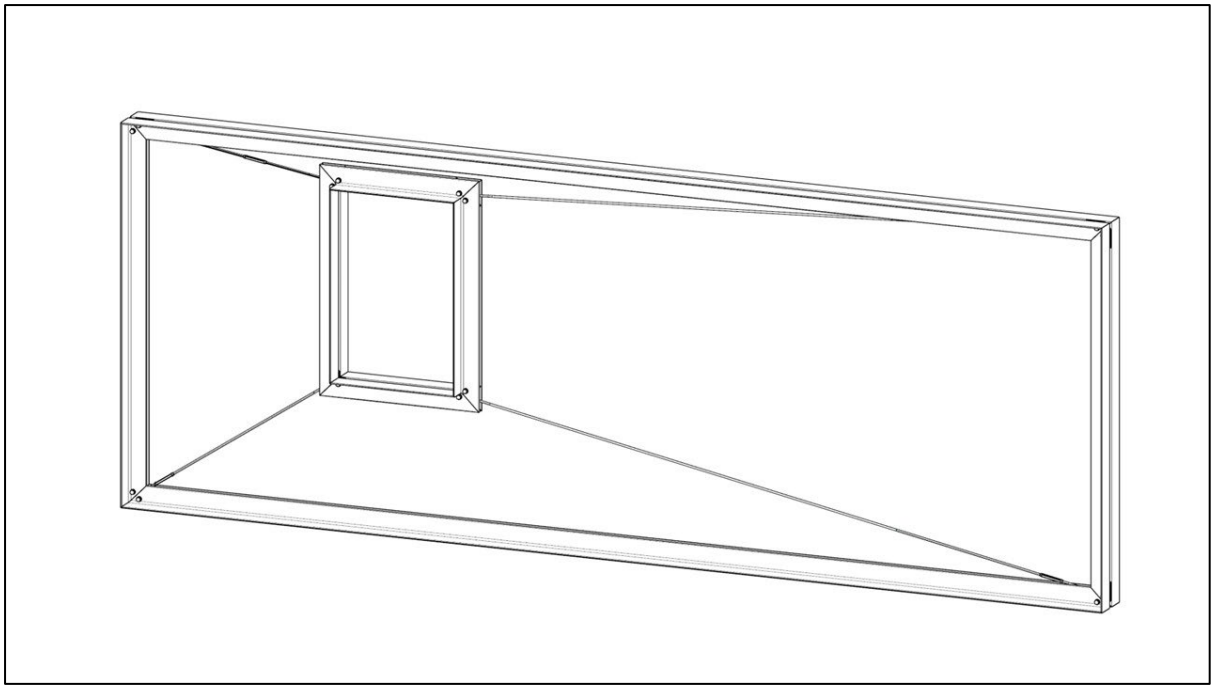

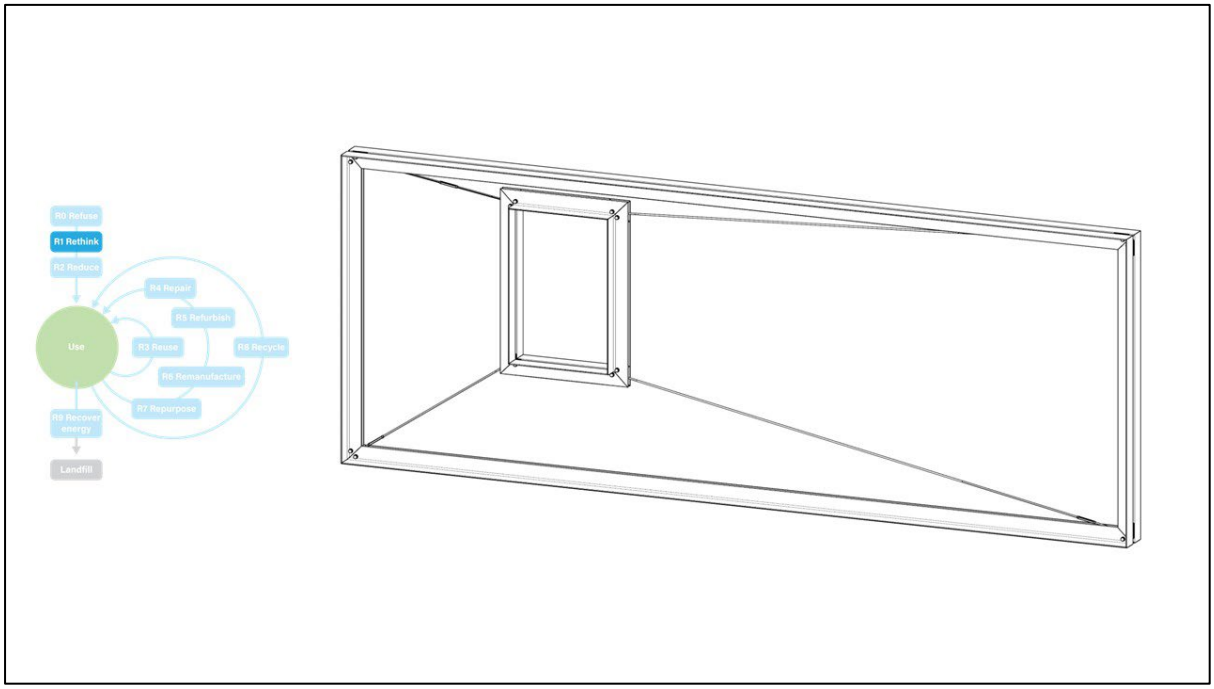
R0 Refuse
R1 Rethink
R2 Reduce
R4 Repair
R5 Refurbish
Use
R3 Reuse
R8 Recycle
R6 Remanufacture
R7 Repurpose
R9 Recover energy
Landfill

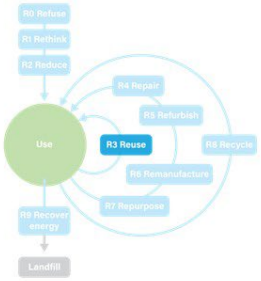
R0 Refuse
R1 Rethink
R2 Reduce
R4 Repair
R5 Refurbish
Use
R3 Reuse
R8 Recycle
R6 Remanufacture
R7 Repurpose
R9 Recover energy
Landfill

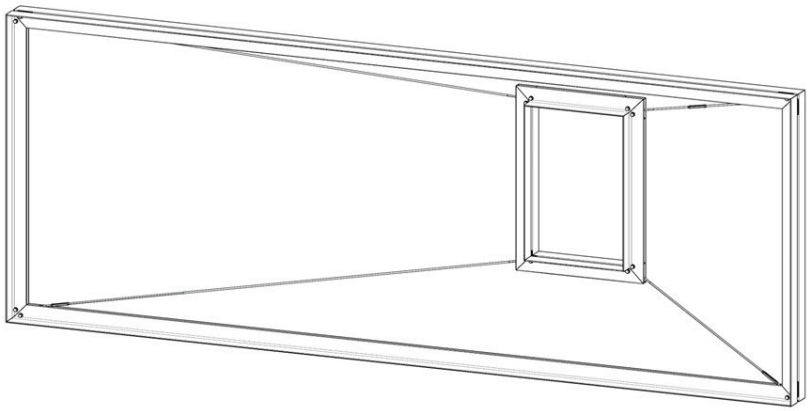

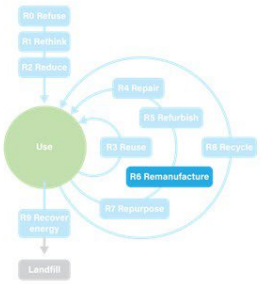
R0 Refuse
R1 Rethink
R2 Reduce
R4 Repair
R5 Refurbish
Use
R3 Reuse
R8 Recycle
R6 Remanufacture
R7 Repurpose
R9 Recover energy
Landfill

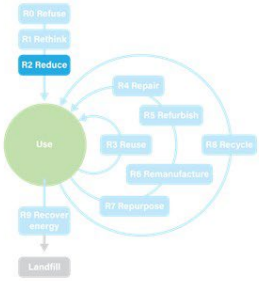

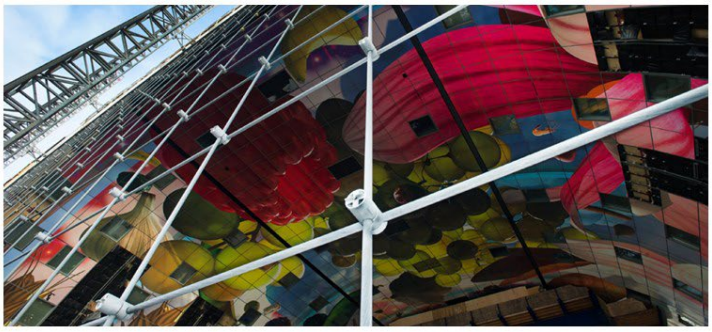

"The combination of the structural principle in which pure tension occurs in the cables with high-quality prestressing steel leads to a weight of the cable net including the knots of only **9 kg/m2**, with a span of 34x42 m. More traditional facade systems would require a steel use of **25 to 35 kg/m2**."

Nationale staalprijs: Markthal (https://www.nationalestaalprijs.nl/project/gevel-winkel-en-appartementengebouw-markthal)

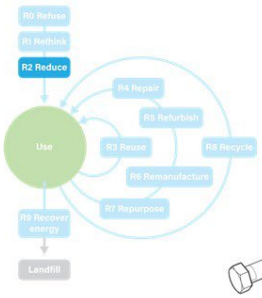

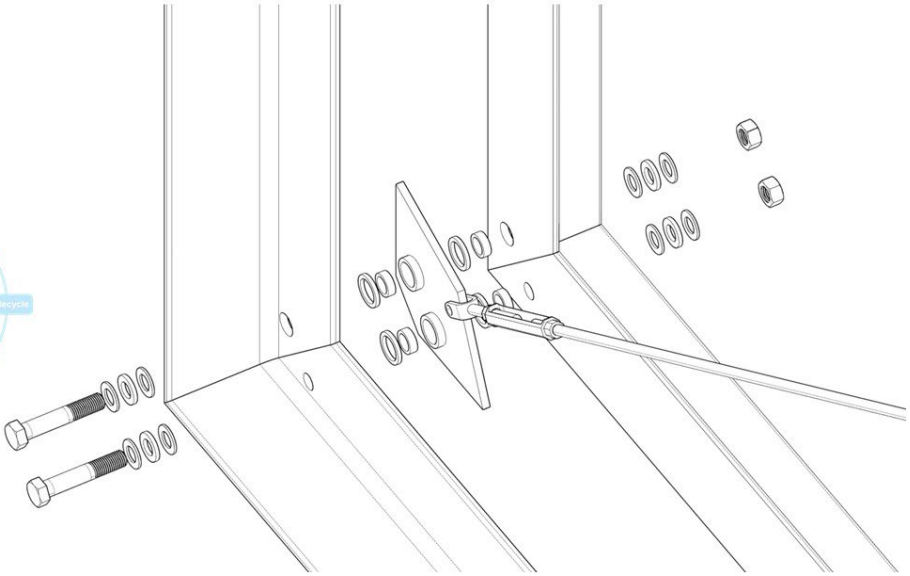

RQ: ‘How can the principle of a tensile based system be utilized to create a more effective prefabricated facade solution?’

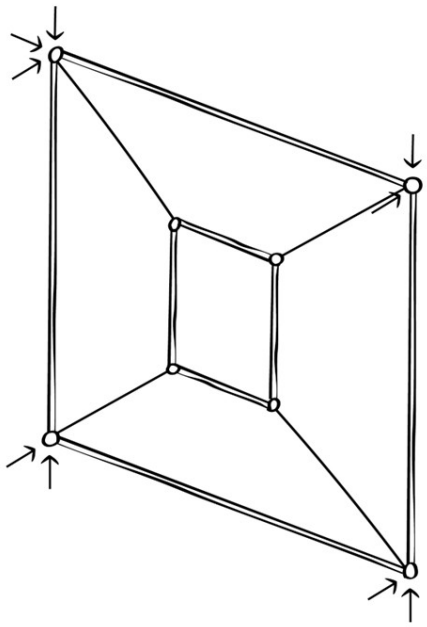

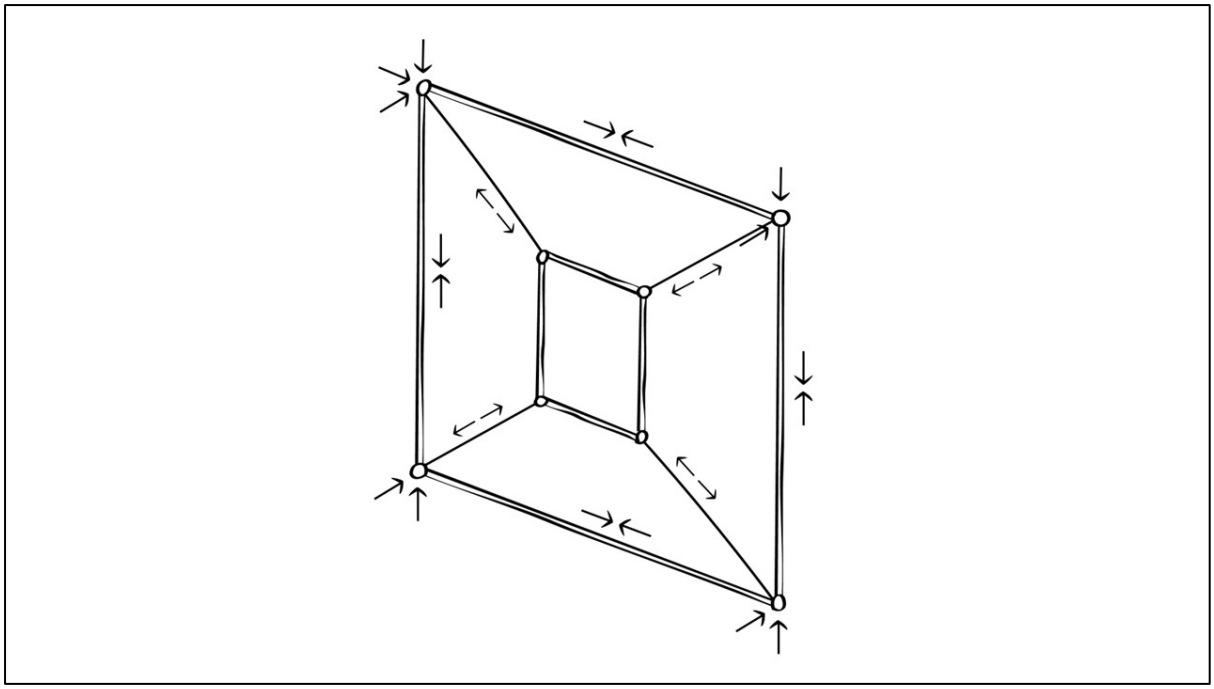

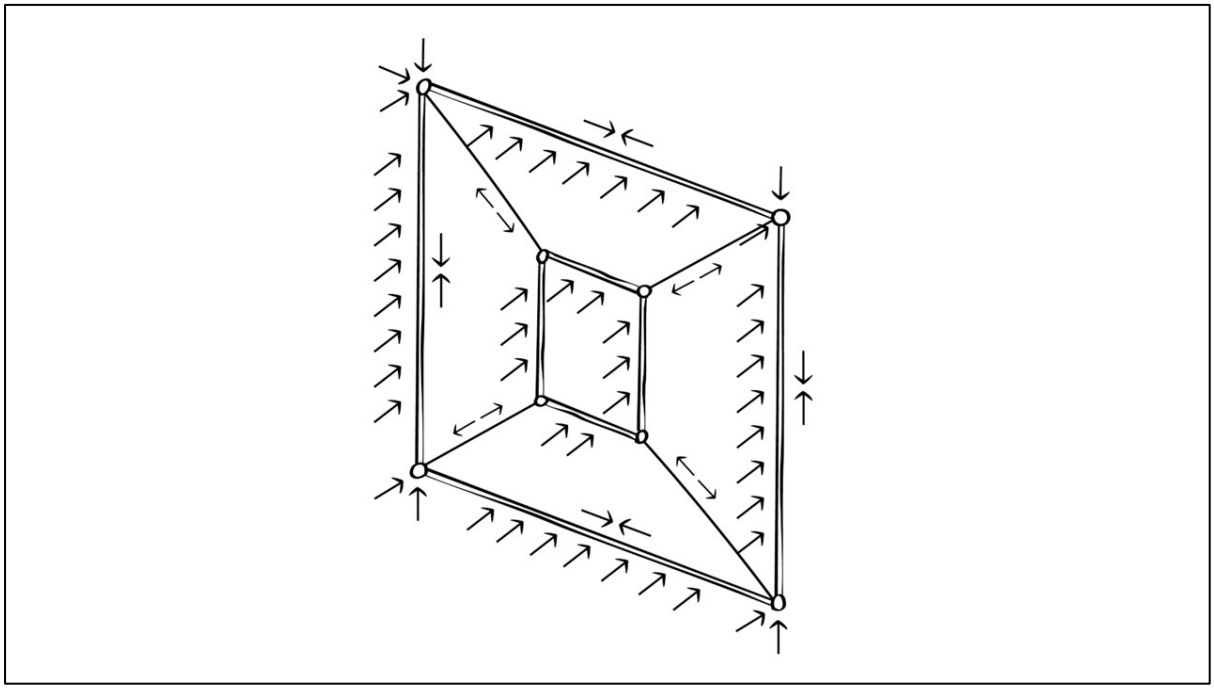

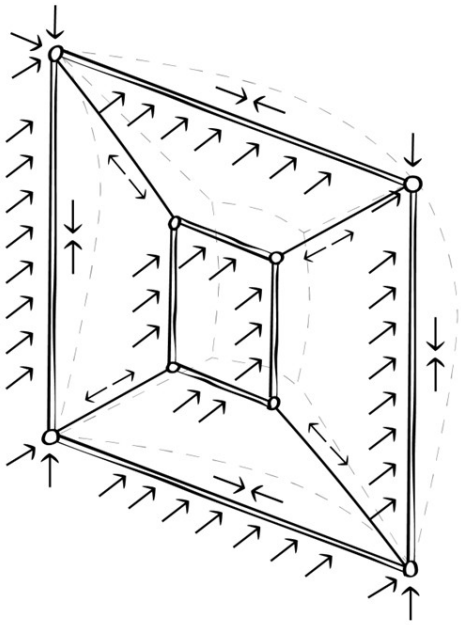

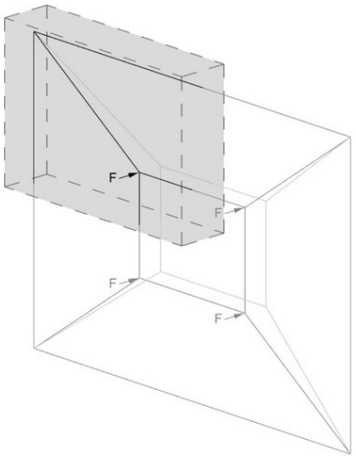

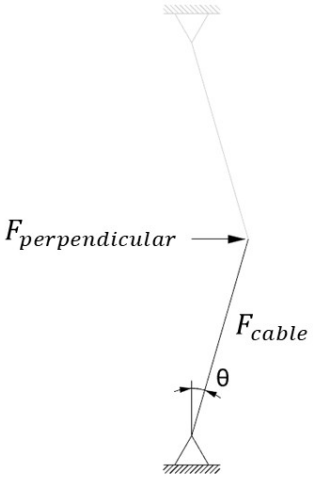

$$F_{perpendicular} = \sin\theta \cdot F_{cable}$$

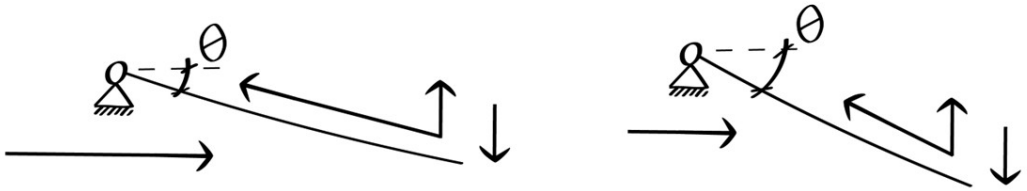
θ
θ

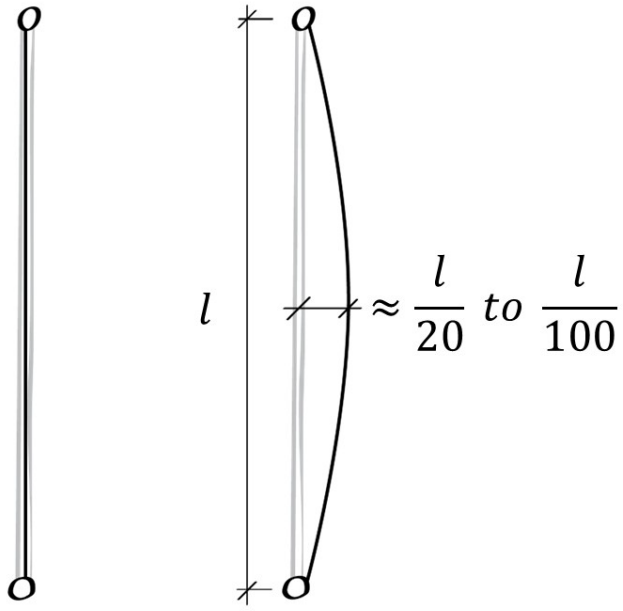
l
≈ l/20 to l/100

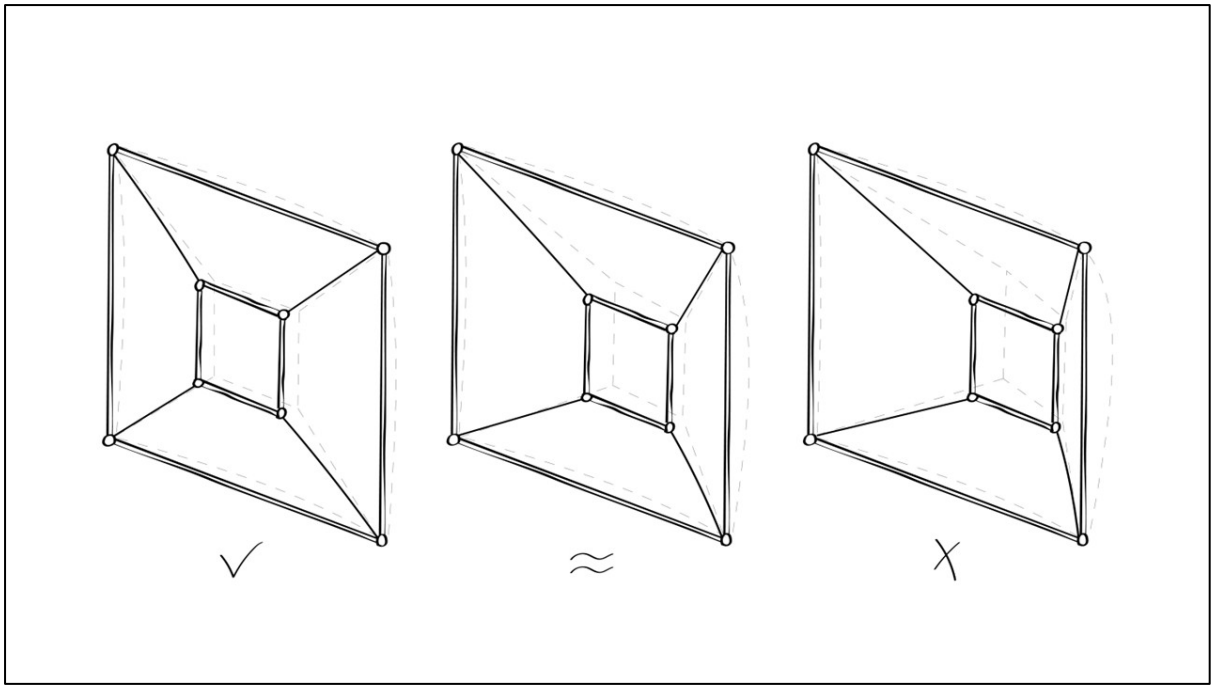

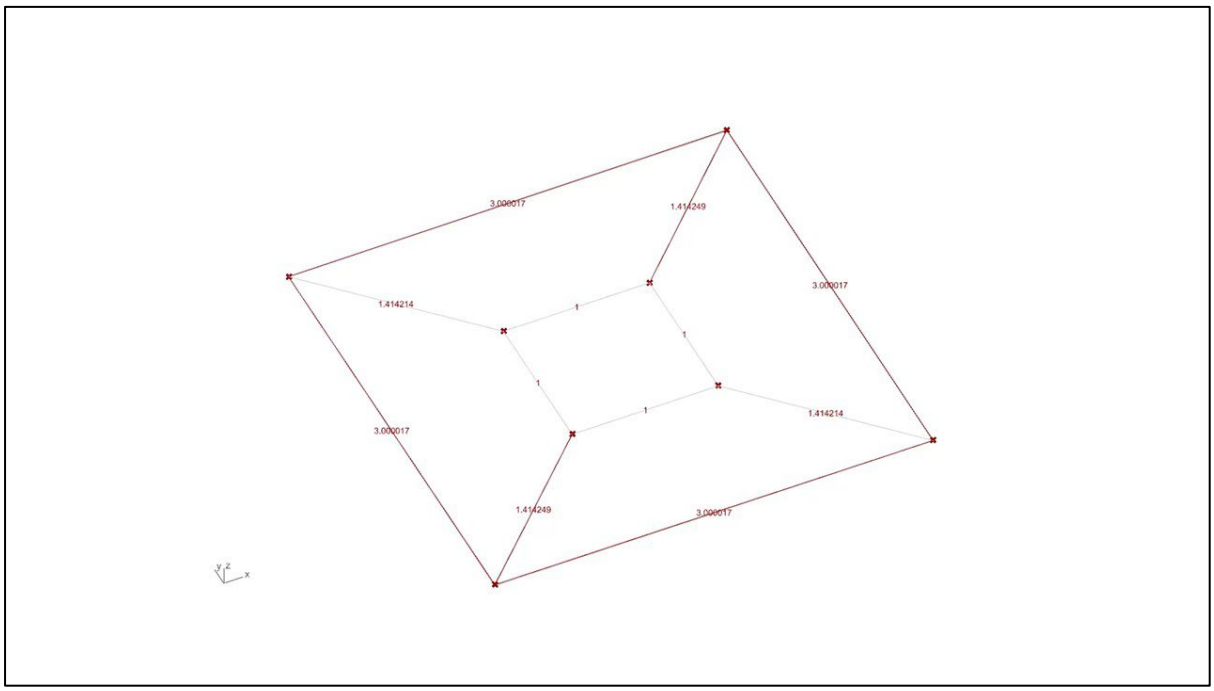

**Video showing system instability*

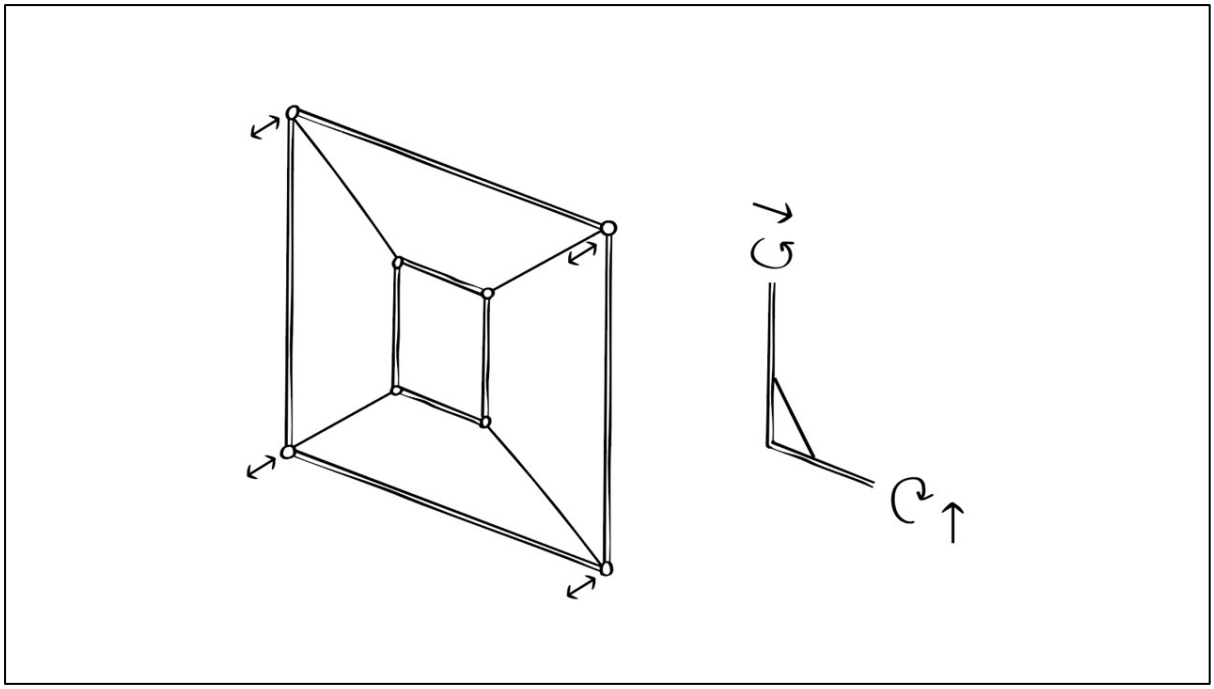

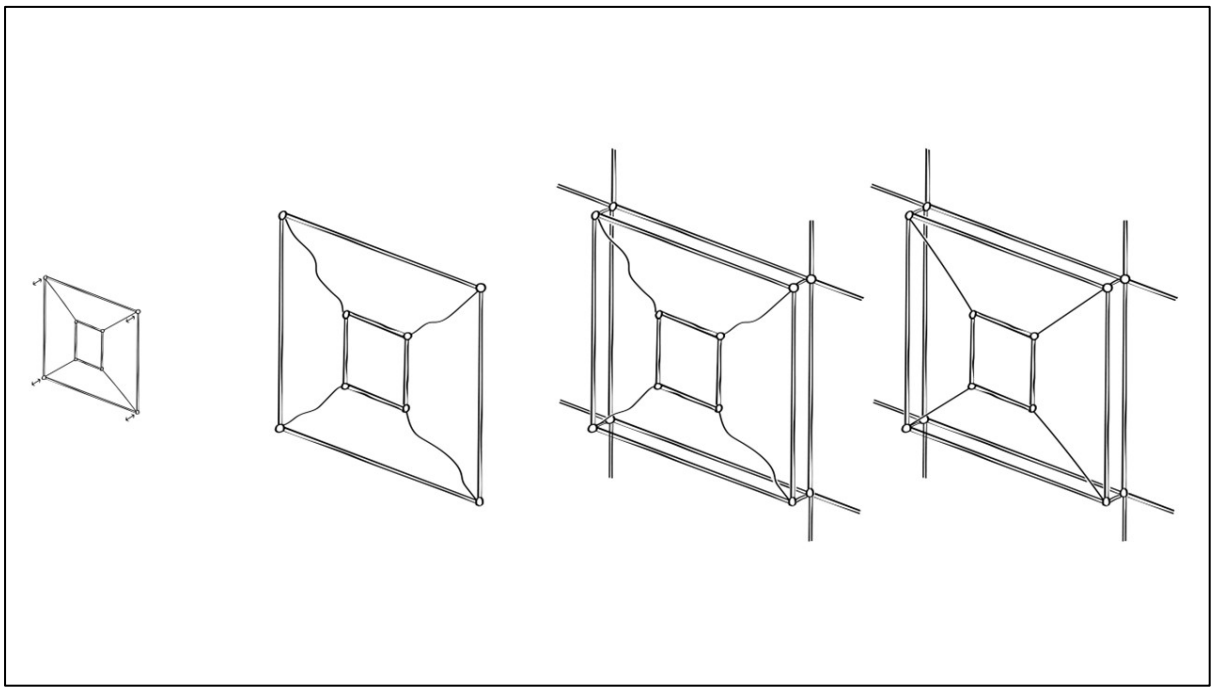

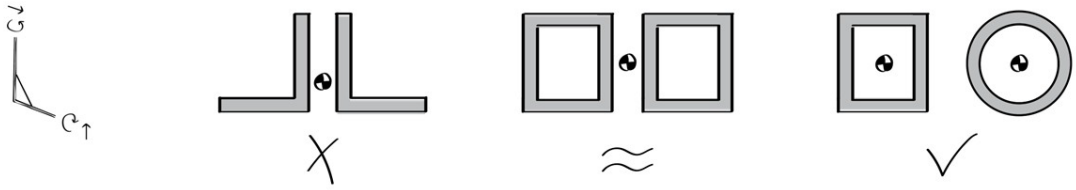

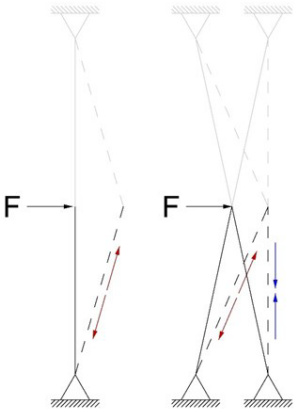

$$F_{perpendicular} = \sin\theta_{cable_1} \cdot F_{cable_1} - \sin\theta_{cable_2} \cdot F_{cable_2}$$

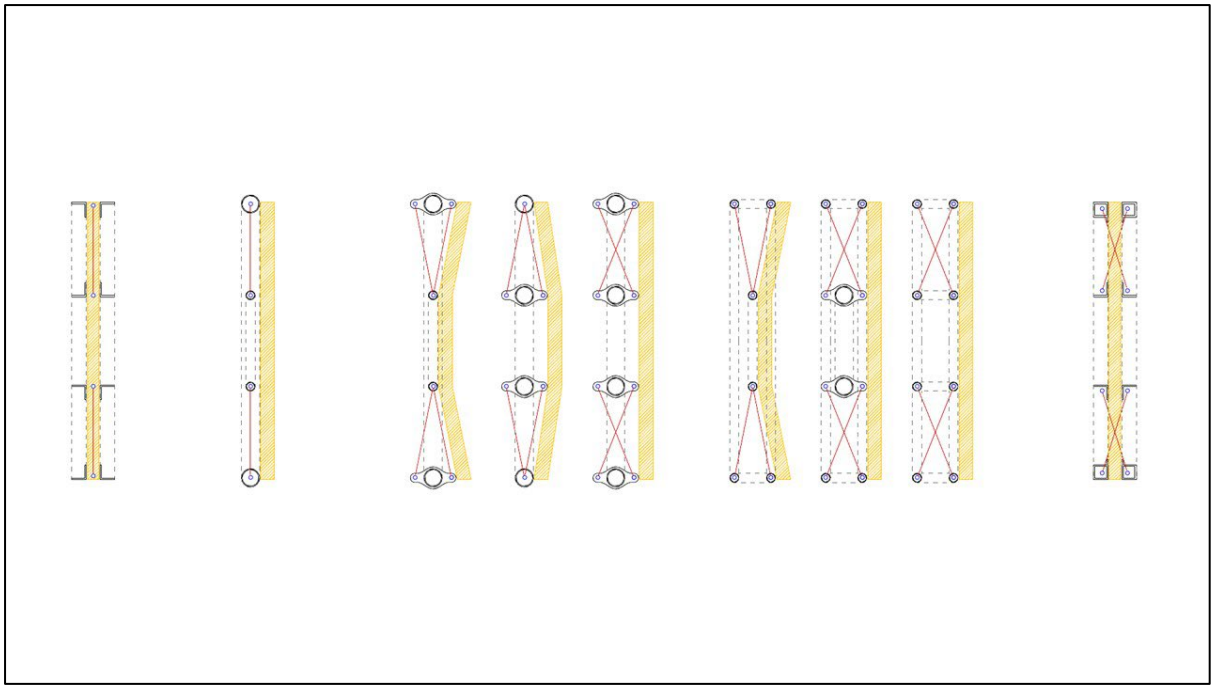

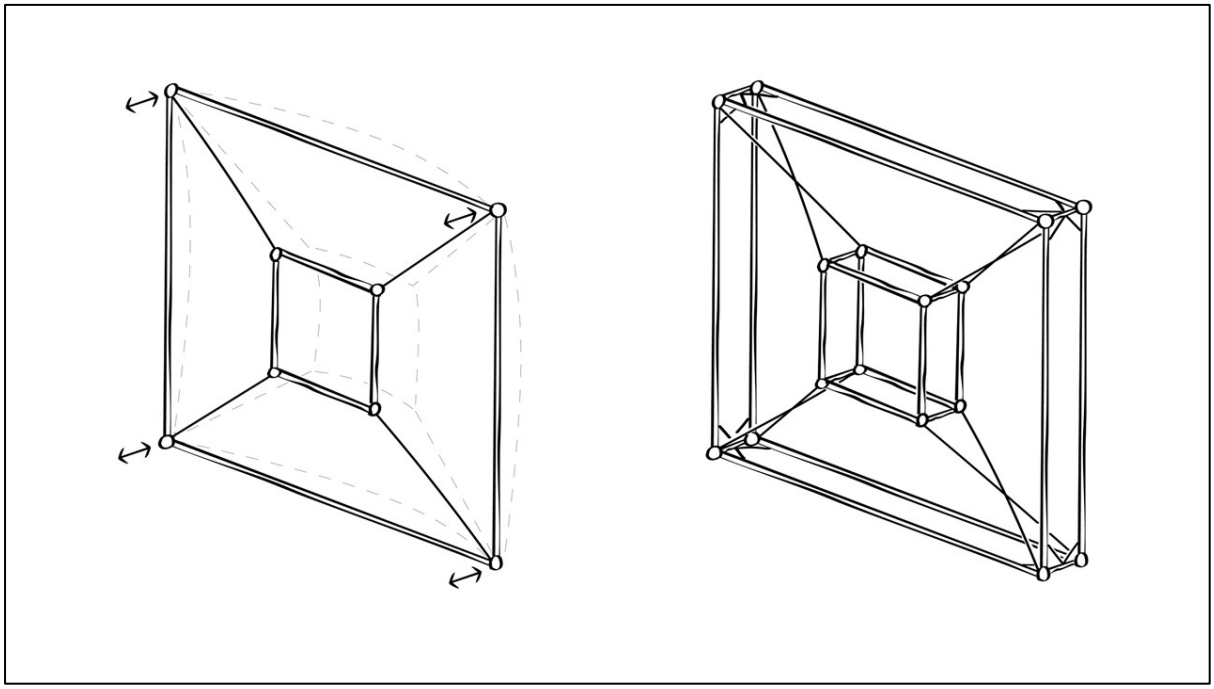

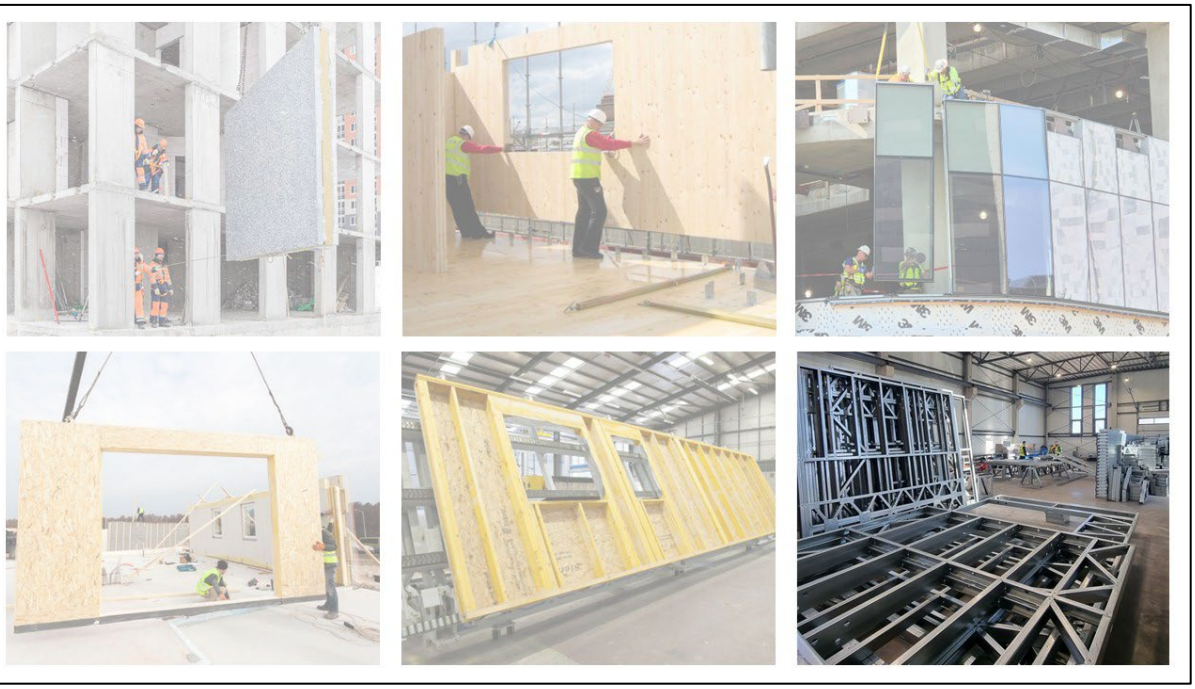

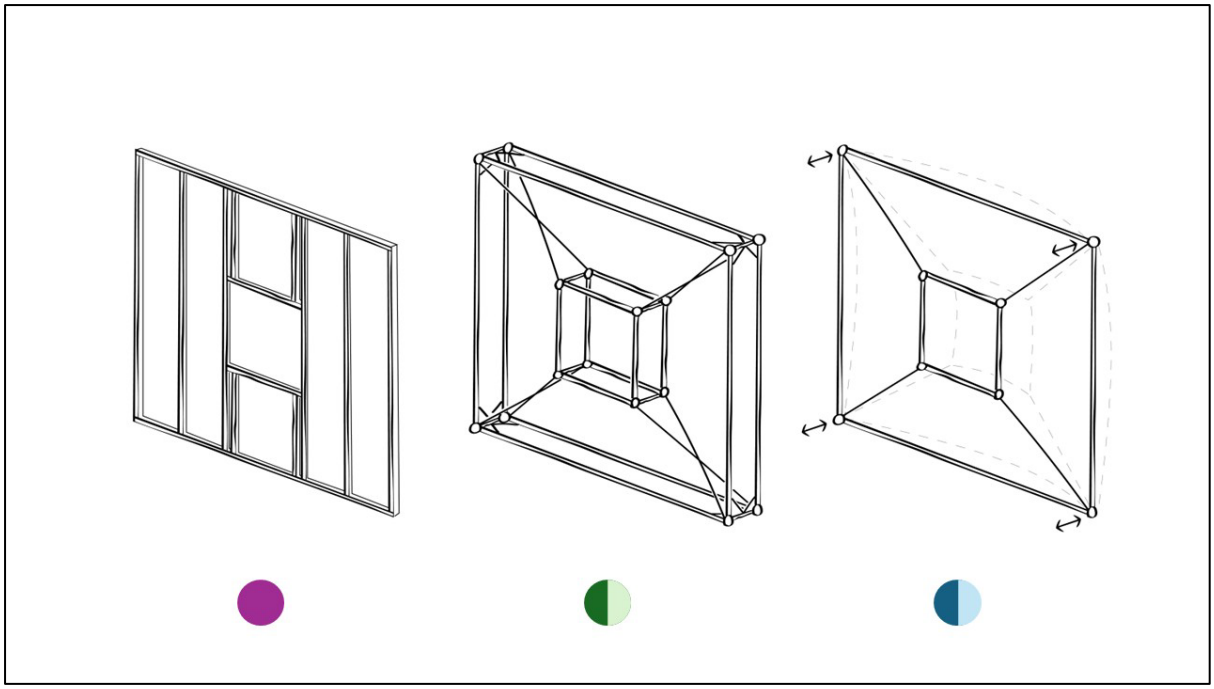

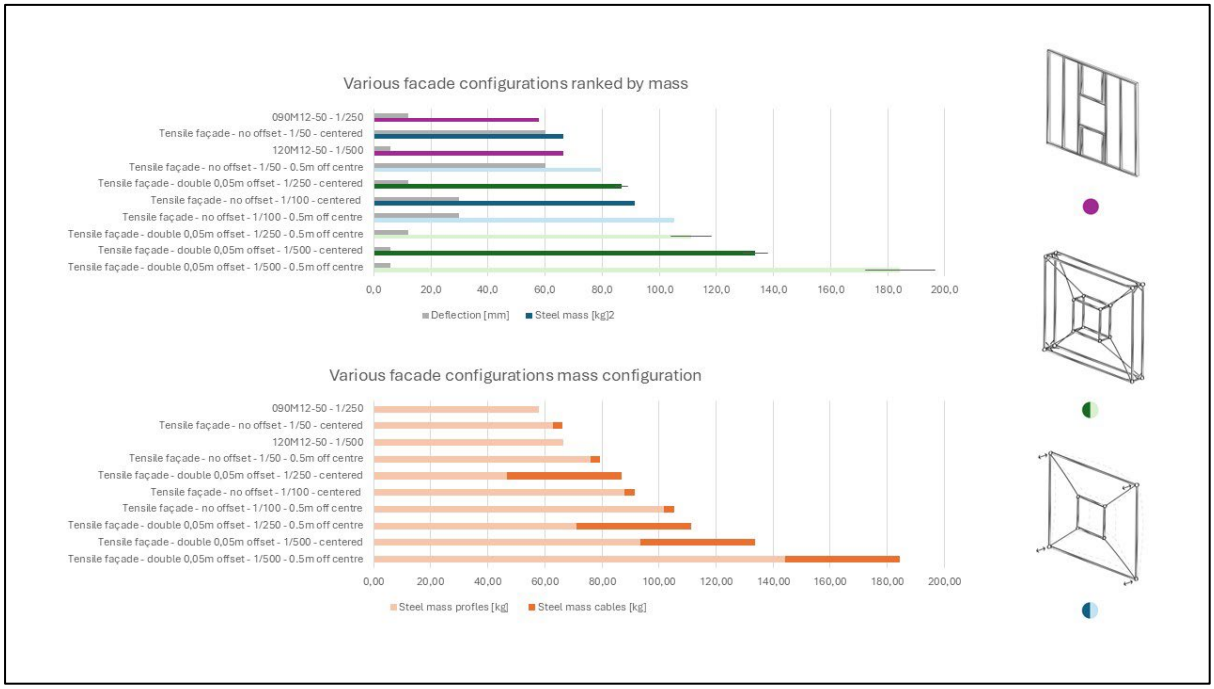
Various facade configurations ranked by mass
090M12-50 - 1/250
Tensile façade - no offset - 1/50 - centered
120M12-50 - 1/500
Tensile façade - no offset - 1/50 - 0.5m off centre
Tensile façade - double 0,05m offset - 1/250 - centered
Tensile façade - no offset - 1/100 - centered
Tensile façade - no offset - 1/100 - 0.5m off centre
Tensile façade - double 0,05m offset - 1/250 - 0.5m off centre
Tensile façade - double 0,05m offset - 1/500 - centered
Tensile façade - double 0,05m offset - 1/500 - 0.5m off centre
0,0 20,0 40,0 60,0 80,0 100,0 120,0 140,0 160,0 180,0 200,0
Deflection [mm]
Steel mass [kg]2
Various facade configurations mass configuration
090M12-50 - 1/250
Tensile façade - no offset - 1/50 - centered
120M12-50 - 1/500
Tensile façade - no offset - 1/50 - 0.5m off centre
Tensile façade - double 0,05m offset - 1/250 - centered
Tensile façade - no offset - 1/100 - centered
Tensile façade - no offset - 1/100 - 0.5m off centre
Tensile façade - double 0,05m offset - 1/250 - 0.5m off centre
Tensile façade - double 0,05m offset - 1/500 - centered
Tensile façade - double 0,05m offset - 1/500 - 0.5m off centre
0,00 20,00 40,00 60,00 80,00 100,00 120,00 140,00 160,00 180,00 200,00
Steel mass profiles [kg]
Steel mass cables [kg]

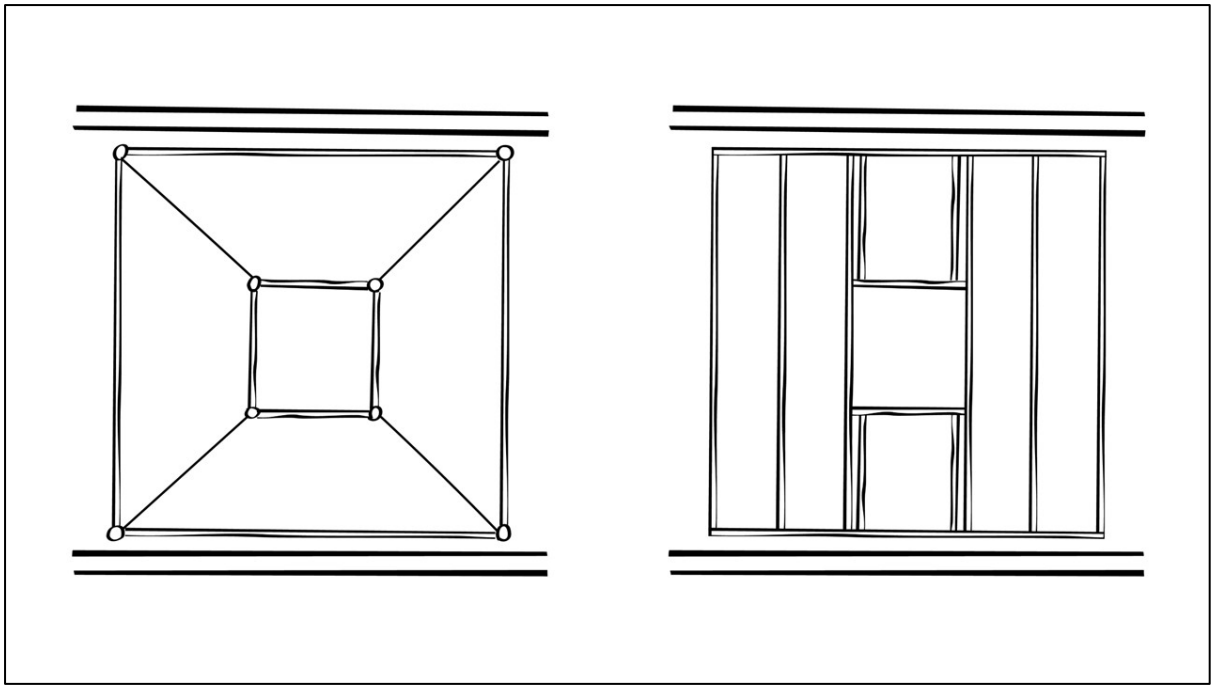

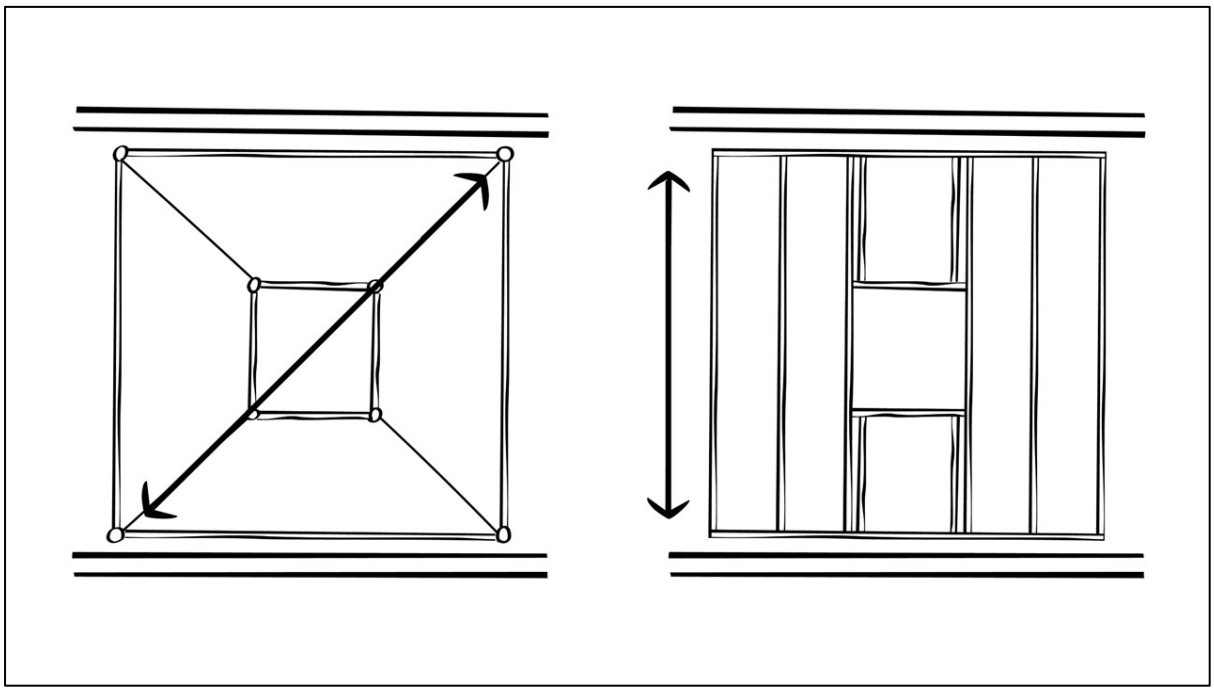

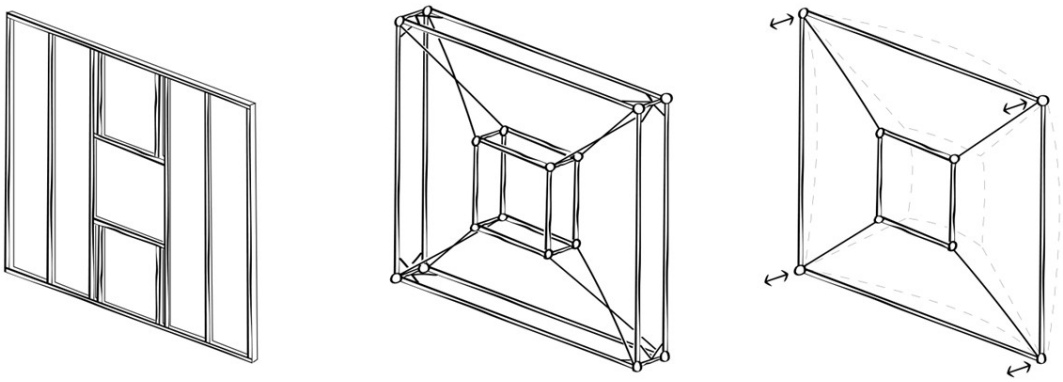

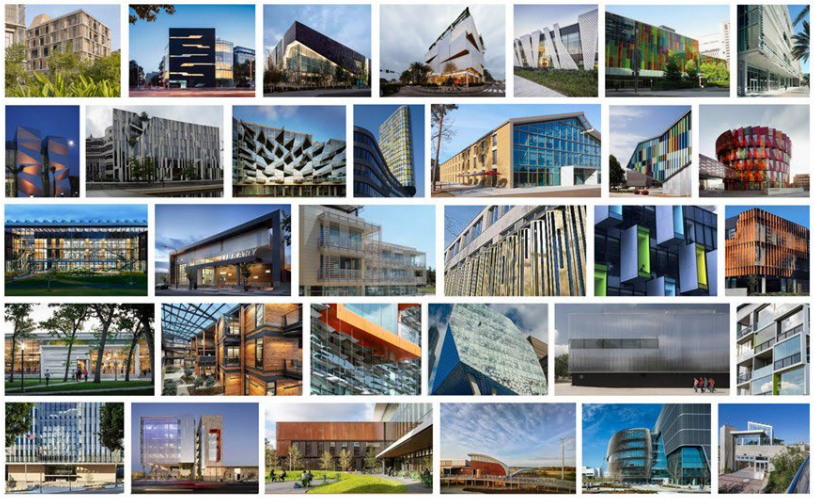

Facade Case Studies Interactive Map (https://cbe.berkeley.edu/research/map-facade-case-studies/)

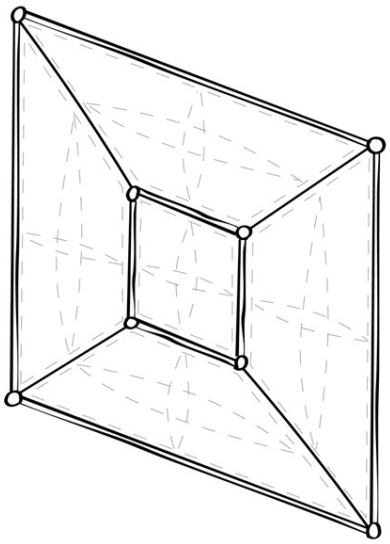

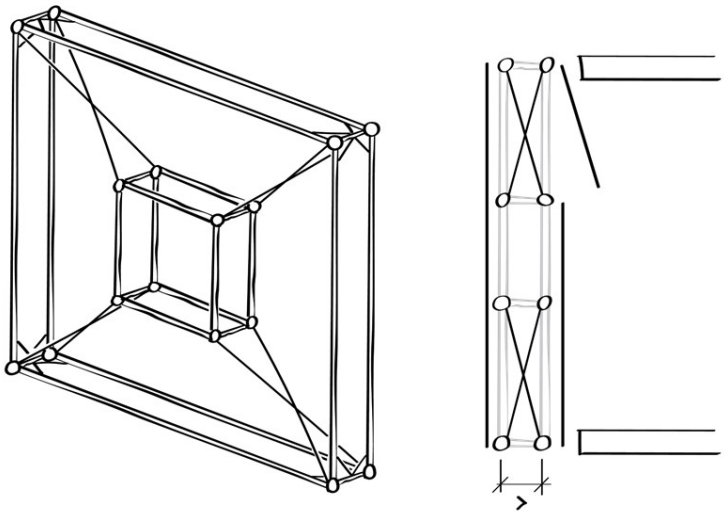

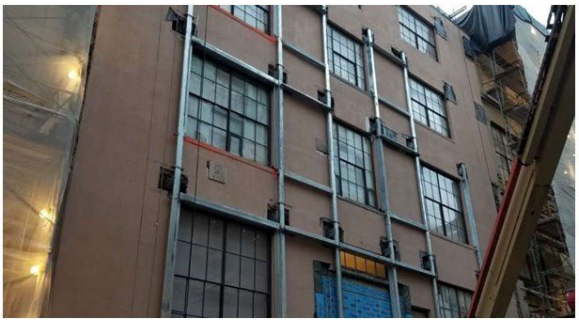

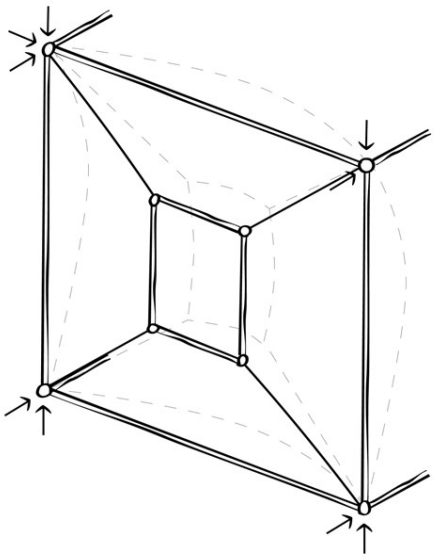

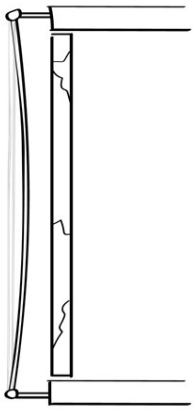

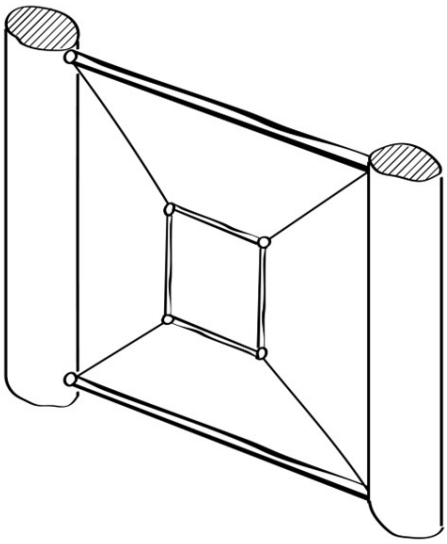


Overlandish
BASE CAMP

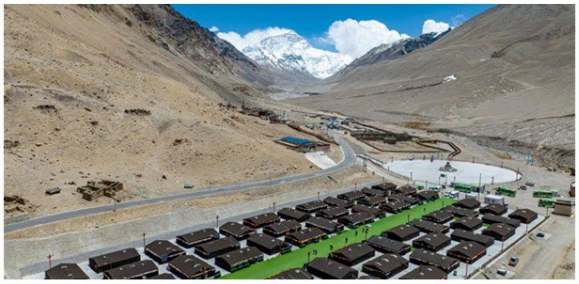

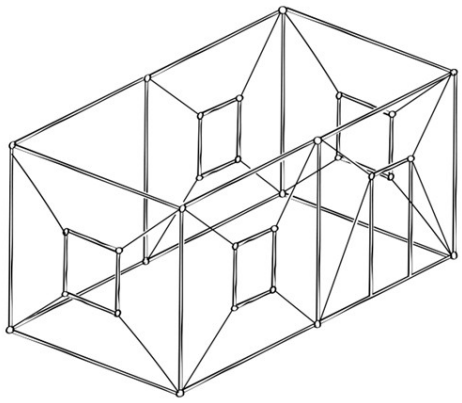

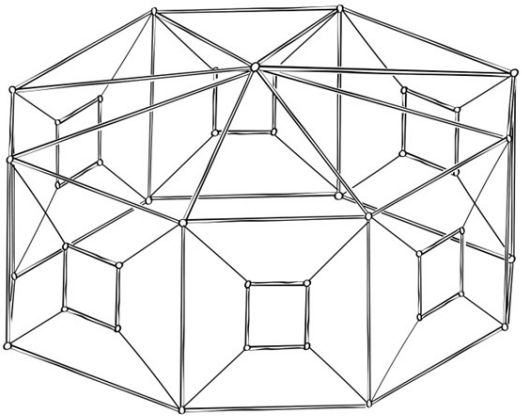

Design compression resistance calculations

SHS-CF 30x30x2x2380 SHS-CF

	Value	Unit
Material properties		
Modulus of Elasticity (E)	210	GPa
Modulus of Elasticity (E)	2,10E+11	Pa
Yield Strength (sigma_y)	2,35E+02	MPa
Yield Strength (sigma_y)	2,35E+08	Pa
Cross-sectional Area (A)	214	mm2
Cross-sectional Area (A)	0,000214	m2
Column Geometry		
Length (L)	2,38	m
Effective length factor (K)	1	
Effective length (KL)	2,38	m
Moment of inertia (I)	2,72E+04	mm4
Moment of inertia (I)	2,72E-08	m4
Radius of Gyration (r)	0,011273988	m
Radius of Gyration (r)	11,3	mm
Extreme fibre Distance (y)	15	mm
r/y	0,752	
Slenderness Ratio (Lambda)	211,1	
Slenderness Ratio 0 (Lambda0)	93,9	
Relative slenderness (Lambda roof)	2,25	
Euler's critical loads		
Ideal Critical load (Pcr)	9,95E+03	N
Ideal Critical load (Pcr)	9,95	kN
Yield load (Pyield)	5,03E+04	N
Yield load (Pyield)	50,29	kN
Governing load (slenderness </> 100)	9,95	kN
Design compression resistance according to strut capacity curves		
Buckling reduction factor (X)	0,18	
Safety factor (ym1)	1,5	
Design compression resistance (NRd)	6,03	kN
Design compression resistance (NRd)	615,17	kg

SHS-CF 30x30x2x1430 SHS-CF profile

	Value	Unit
Material properties		
Modulus of Elasticity (E)	210	GPa
Modulus of Elasticity (E)	2,10E+11	Pa
Yield Strength (sigma_y)	2,35E+02	MPa
Yield Strength (sigma_y)	2,35E+08	Pa
Cross-sectional Area (A)	214	mm2
Cross-sectional Area (A)	0,000214	m2
Column Geometry		
Length (L)	1,43	m
Effective length factor (K)	1	
Effective length (KL)	1,43	m
Moment of inertia (I)	2,72E+04	mm4
Moment of inertia (I)	2,72E-08	m4
Radius of Gyration (r)	0,011273988	m
Radius of Gyration (r)	11,3	mm
Extreme fibre Distance (y)	15	mm
r/y	0,752	
Slenderness Ratio (Lambda)	126,8	
Slenderness Ratio 0 (Lambda0)	93,9	
Relative slenderness (Lambda roof)	1,35	
Euler's critical loads		
Ideal Critical load (Pcr)	2,76E+04	N
Ideal Critical load (Pcr)	27,57	kN
Yield load (Pyield)	5,03E+04	N
Yield load (Pyield)	50,29	kN
Governing load (slenderness </> 100)	27,57	kN
Design compression resistance according to strut capacity curves		
Buckling reduction factor (X)	0,45	
Safety factor (ym1)	1,5	
Design compression resistance (NRd)	15,09	kN
Design compression resistance (NRd)	1537,92	kg

References

2018 International Building Code (IBC), (2018). https://codes.iccsafe.org/content/IBC2018/chapter-16-structural-design

Abdelmohsen, S., & Hassab, A. (2020). *A Computational Approach for the Mass Customization of Materially Informed Double Curved Façade Panels*. https://doi.org/10.52842/conf.caadria.2020.1.163

Cao, Q., Jiang, H., & Wang, H. (2015). Shear Behavior of Corrugated Steel Webs in H Shape Bridge Girders. *Mathematical Problems in Engineering*, *2015*, 1-15. https://doi.org/10.1155/2015/796786

Domaracka, L., Matuskova, S., Tausova, M., Senova, A., & Kowal, B. (2022). Efficient Use of Critical Raw Materials for Optimal Resource Management in EU Countries. *Sustainability*, *14*(11).

Dr. Minas E. Lemonis, P. (2024). *Column buckling calculator*. Calc Resource. https://calcresource.com/statics-buckling-load.html

Drahtseile24. (2021). *Prüfbericht: 4mm Drahtseil mit Drahtseilklemmen 3/16“ DIN 741*. https://www.staalkabels24.nl/media/pdf/5b/62/38/Pruefbericht-4mm_Drahtseilklemmen.pdf

Eurocode 1: Actions on structures - Part 1-4: General actions - Wind loads, (2012).

Gedeon, M. (December 2009). Stress Relaxation and Creep. *Technical Tidbits*(12).

Granello, G., & Palermo, A. (2019). Creep in Timber: Research Overview and Comparison between Code Provisions. *27*, 6-22.

Greminger, M. (March 12, 2023). Calculating the Natural Frequency of a String Under Tension. *The Official EngineeringPaper.xyz Blog*. https://blog.engineeringpaper.xyz/calculating-the-natural-frequency-of-a-string-under-tension

Hancock, G. J. (1997). Design for distortional buckling of flexural members. *Thin-Walled Structures*, *27*(1), 3-12. https://doi.org/https://doi.org/10.1016/0263-8231(96)00020-1

HILTI. (July 2019). *WHAT’S BEHIND THE CURTAIN? AN OVERVIEW OF FAÇADE DESIGN FOR ARCHITECTS*. https://files-ask.hilti.com/original/dm/dmyznxrp9c.pdf

Hsiao, J.-k. K. (Jan 2017). Prestress Loss Distributions along Simply Supported Pretensioned Concrete Beams. *Electronic Journal of Structural Engineering*, *16*, 18-25.

Intro to Nonlinear Solver — Lesson 2. Ansys. https://innovationspace.ansys.com/courses/courses/computational-resource-considerations-recommended/lessons/intro-to-nonlinear-solver-lesson-2/

Iturralde, K., Feucht, M., Illner, D., Hu, R., Pan, W., Linner, T., Bock, T., Eskudero, I., Rodriguez, M., Gorrotxategi, J., Izard, J. B., Astudillo, J., Cavalcanti Santos, J., Gouttefarde, M., Fabritius, M., Martin, C., Henninge, T., Nornes, S. M., Jacobsen, Y.,...Elia, L. (2022). Cable-driven parallel robot for curtain wall module installation. *Automation in Construction*, *138*, 104235. https://doi.org/https://doi.org/10.1016/j.autcon.2022.104235

Iturralde, K., Linner, T., & Bock, T. (2016). Development and preliminary Evaluation of a concept for a Modular End-Effector for automated/robotic Facade Panel Installation in Building Renovation.

Jafari, M., & Alipour, A. (2021). Methodologies to mitigate wind-induced vibration of tall buildings: A state-of-the-art review. *Journal of Building Engineering*, *33*, 101582. https://doi.org/https://doi.org/10.1016/j.jobe.2020.101582
JRC. (2008). THE ROLE OF EN 1990: THE KEY HEAD EUROCODE In.
Karamba3D. (2024). *AnalyzeThII*. https://manual.karamba3d.com/3-in-depth-component-reference/3.5-algorithms/3.5.2-analyzethii
Knaack, U. (2007). *Façades : principles of construction*. Birkhäuser.
Linear Thermal Expansion Coefficients of Materials. Engineering Toolbox. https://www.engineeringtoolbox.com/linear-expansion-coefficients-d_95.html
Loh, P., Leggett, D., & Prohasky, D. (2019). *Robotic Fabrication of Doubly Curved FaA§ade System - Constructing intelligence in the digital fabrication workflow*. https://doi.org/10.52842/conf.caadria.2019.2.521
Mendis, P., Ngo, T., Haritos, N., Hira, A., Samali, B., & Cheung, J. (2007). Wind Loading on Tall Buildings. *Electronic Journal of Structural Engineering*, *Volume 7*, 41-54. https://doi.org/10.56748/ejse.641
METFRAME INSTALLATION GUIDE. (July 2023). (2).
Moeinadini, A., Ziyaeifar, M., & Nekooei, M. (2023). Facade isolation in seismic design of tall buildings. *Structures*, *58*, 105416. https://doi.org/https://doi.org/10.1016/j.istruc.2023.105416
Mon, T. Y., Selvam, J., & Candidate, P. (2023). Numerical Investigation on Buckling Behavior of Cold-Formed Steel Built-up Box Slender Columns. *10*, 2456-1304.
Montali, J. (2021). *A frame for a prefabricated element for a builing* (Italy Patent No. A. S.r.l. https://data.epo.org/publication-server/pdf-document?pn=4095335&ki=B1&cc=EP&pd=20240131
Obinna, U. (2024). *Comparison of the Force and Displacement Methods of Structural Analysis*. Structville. https://structville.com/force-and-displacement-methods-of-structural-analysis
Octatube. *DE KABELNETGEVELS VAN DE MARKTHAL IN ROTTERDAM*. https://www.joostdevree.nl/bouwkunde2/jpgk/kabelnetgevel_8_markthal_rotterdam_projectdocumentatie_www_octatube_nl.pdf
Piker, D. (2024). *Kangaroo3d*. http://kangaroo3d.com/
Precast Cladding Design Guide. (2012). In: Explore Manufacturing by Laing O'Rourke.
PUSHTON. *PSD-S1 Load Cell*. Retrieved 23-04-2025 from http://www.pushton.com/?m=home&c=View&a=index&aid=122
Rammig, L., Zani, A., Murphy, T., Paparo, I., Hildebrand, L., Abbring, S., Kopreck, D., Wu, C., Lee, J., & Turpin, K. (2023). Prefab Facades – From Prototype to Product? : The Kit-of-Parts approach to a facade design. *Journal of Facade Design and Engineering*, *11*(1), 61-75. https://doi.org/10.47982/jfde.2023.1.04
RNSI. (2014). NEN 2608. In.
RNSI. (2019). NEN-EN 1990+A1+A1/C2/NB. In.
Sah, T. P., Lacey, A. W., Hao, H., & Chen, W. (2024). Prefabricated concrete sandwich and other lightweight wall panels for sustainable building construction: State-of-the-art review. *Journal of Building Engineering*, *89*, 109391. https://doi.org/https://doi.org/10.1016/j.jobe.2024.109391
Saidani, M., Shevchenko, T., Esfandabadi, Z. S., Ranjbari, M., Mesa, J. A., Yannou, B., & Cluzel, F. (2024). The future of circular economy metrics: Expert visions.

Resources, Conservation and Recycling, *205*, 107565. https://doi.org/https://doi.org/10.1016/j.resconrec.2024.107565
Saidani, M., Yannou, B., Leroy, Y., Cluzel, F., & Kendall, A. (2019). A taxonomy of circular economy indicators. *Journal of Cleaner Production*, *207*, 542-559. https://doi.org/https://doi.org/10.1016/j.jclepro.2018.10.014
Samuel, J. (2019). *Hydrodynamics of an Oscillating Water Column Device Integrated with Breakwaters John Ashlin Samuel*
Santhosh, N., Un, U. N. K., Sajjan, G., & Gowda, A. (2017). Fatigue Behaviour of Silicon Carbide and Fly Ash Dispersion Strengthened High Performance Hybrid Al 5083 Metal Matrix Composites. *Journal of Minerals and Materials Characterization and Engineering*, *05*, 274-287. https://doi.org/10.4236/jmmce.2017.55023
Schlaich, J., Schober, H., & Moschner, T. (2005). Prestressed Cable-Net Facades. *Structural Engineering International*, *15*(1), 36-36. https://doi.org/10.2749/101686605777963332
Shamass, R. (2020). Plastic Buckling Paradox: An Updated Review. *Frontiers in Built Environment*, *6*. https://doi.org/10.3389/fbuil.2020.00035
SIMSCALE. (2023). *What is Fatigue Analysis?* https://www.simscale.com/docs/simwiki/fea-finite-element-analysis/what-is-fatigue-analysis/
Sobek, W., Feirabend, S., Blandini, L., & Tarazi, F. (2010). Cable-stayed glass façades - 15 years of innovation at the cutting edge.
Spathis, G., & Kontou, E. (2012). Creep failure time prediction of polymers and polymer composites. *Composites Science and Technology*, *72*, 959–964. https://doi.org/10.1016/j.compscitech.2012.03.018
Spjuth, G., & Åkesson, L. (2016). *WIND-INDUCED TRANSMISSION OF LOW FREQUENCY VIBRATIONS FOR A TALL MULTI-STOREY WOOD BUILDING* Lund University].
Tam, V. W. Y., Le, K. N., & Wang, J. Y. (2018). Cost Implication of Implementing External Facade Systems for Commercial Buildings. *Sustainability*, *10*(6).
Tish, D., King, N., & Cote, N. (2020). Highly accessible platform technologies for vision-guided, closed-loop robotic assembly of unitized enclosure systems. *Construction Robotics*, *4*(1), 19-29. https://doi.org/10.1007/s41693-020-00030-z
Vandamme, M., & Ulm, F.-J. (2009). Nanogranular origin of concrete creep. *Proceedings of the National Academy of Sciences*, *106*(26), 10552-10557. https://doi.org/10.1073/pnas.0901033106
Walter Podolny, J. (October 1969). Understanding The Losses In Prestressing. *PCI Journal*.
Wang, W., Yan, S., & Kodur, V. (2016). Temperature Induced Creep in Low-Alloy Structural Q345 Steel. *Journal of Materials in Civil Engineering*, *28*(6), 06016003. https://doi.org/10.1061/(ASCE)MT.1943-5533.0001519
Xin, Q. (2013). 2 - Durability and reliability in diesel engine system design. In Q. Xin (Ed.), *Diesel Engine System Design* (pp. 113-202). Woodhead Publishing. https://doi.org/https://doi.org/10.1533/9780857090836.1.113